Studies on Human Protoporphyrinogen Oxidase

Mbulelo H Maneli

BSc (Hons) (Biochem) (UCT)

Thesis Presented for the Degree of

Doctor of Philosophy

in the Department of Medicine

University of Cape Town

September 2002

ACKNOWLEDGEMENTS

I would like to thank:

- **Prof. Ralph Kirsch** for accepting me into his research laboratory, and for his enthusiasm and guidance throughout this study.
- **Prof. Peter Meissner and Dr Anne Corrigall** for their supervision, help and encouragement in both the research and writing of this dissertation.
- **Prof. Harry Dailey (Department of Microbiology, University of Georgia, Athens, Georgia, USA)** for providing us with the pHPPOX vector and the R168C mutant.
- **Prof. Horst Klump (Molecular and Cell Biology, University of Cape Town)** for allowing me to perform the UV melting and CD studies in his laboratory and for his help in the writing of chapter 7.
- **Madhu Chauhan** for her technical assistance in running the CD spectra.
- **Prof. Richard Hift** for his help in writing the literature review.
- **Dr Kwanele Siziba, Leslie Martin and Christopher Jacobs** for helping with the PPOX assays.
- **Lester Davids** for helping with the creation of the PPOX mutants.
- **Leslie Frith and Mr M Wells** for their technical assistance.
- **Lavinia Petersen** for helping with formatting and printing of this document.
- **The secretarial staff of the Department of Medicine** for their administrative assistance.
- **My colleagues and friends in the Liver Research Centre** for their encouragement and provision of a happy working environment.
- **My parents, brothers ("Tasko" and "Phumphum") and friends** for their support.
- **The Wellcome Trust** for their financial assistance under their International Senior Research Fellowship program (in which Prof. Peter Meissner is a recipient).
- **The Medical Research Council** for financial assistance.

ABSTRACT

STUDIES ON HUMAN PROTOPORHYRINOGEN OXIDASE

This study examines the effects of various protoporphyrinogen oxidase mutations responsible for variegate porphyria, the role of the arginine-59 residue, and the glycines in the conserved flavin binding site, in catalysis and/or cofactor binding. Wild type recombinant human protoporphyrinogen oxidase and a selection of both naturally occurring and self-designed mutants were generated, expressed and purified. The self designed mutants included a conservative and two non-conservative arginine-59 replacements, and subsititution of glycine residues at positions 9, 11, and 14 by alanine.

The expression and purification for all protoporphyrinogen oxidases was optimised, enabling their purification to homogeneity by single step metal affinity chromatography. Partial characterisation of these enzymes included investigation of cofactor composition, kinetic behaviour, inhibitor profiles and physicochemical properties by circular dichroism spectroscopy and thermal denaturation (T_m).

All mutations resulted in reduced protoporphyrinogen oxidase activity to varying degrees. However, the activity data did not correlate with the ability/inability to bind flavin. The comparative results suggest that the positive charge at arginine-59 is directly involved in catalysis and not flavin-cofactor binding. The K_ms for the arginine-59 mutants imply that there is more likely a substrate binding problem than a mechanistic one. Studies investigating the effect of temperature on activity ($T_{1/2}$) showed that arginine-59 is required for the integrity of the active site. The secondary structure of protoporphyrinogen oxidase showed a dominant α-helical content, which was decreased in the mutants. The degree of α-helix did not correlate linearly with $T_{1/2}$ nor T_m values, supporting the assumption that arginine-59 is important for catalysis at the active site.

Examination of the conserved dinucleotide-binding sequence showed that substitution of glycine in codon 14 was less disruptive than substitutions in codons 9 and 11.

Ultraviolet melting curves generally showed a two-state transition suggesting formation of a multi-domain structure. Generally all mutants studied were more stable to thermal denaturation compared to wild type, except for R168C.

In comparative inhibitor studies, the aciflurofen inhibitor parameters measured did not parallel the observed kinetic activities, suggesting that the inhibitor binds near, rather than at, the active site.

This work illustrates the use of studying expressed, purified mutant protoporphyrinogen oxidases in elucidating the importance of specific amino acid residues in the study of variegate porphyria and protoporphyrinogen oxidase structure-function studies, and identifies a role for arginine 59 in catalysis rather than dinucleotide binding alone.

16 September 2002

ABBREVIATIONS AND SYMBOLS

General

ΔA	change in absorbance
°C	degrees centigrade
µg	micrograms
ΔG	change in free energy
ΔH	change in enthalpy
µl	microlitre
µM	micromolar
ΔS	change in entropy
[I]	inhibitor concentration
[S]	substrate concentration
Å	angstrom
bp	base pairs
BSA	bovine serum albumin
CHO	Chinese hamster ovary cells
Da	daltons
DMSO	dimethylsulfoxide
EDTA	Ethylenediaminetetraacetic acid
GFP	green fluorescence protein
g	centrifugal force
h	hour
HIV	Human immunodeficiency virus
HPLC	high performance liquid chromatography
His	histidine
IMAC	immobilised metal affinity chromatography
IPTG	*n*-isopropyl-β-D-galactopyranoside
kb	kilobases
L	litre
LB	Luria-Bertani
MEL	murine erythroleukemia
mg	milligram
min	minutes
ml	millilitre
mM	millimolar
MOPS	(3-[N-Morpholino]propanesulfonic acid)
M_r	relative molecular weight
M	Molar (moles/litre)
ng	nanogram
Ni-NTA	nickel-(nitrilo-tri-acetic acid)
nm	nanometre
nmol	nanomole

OD	optical density
PAGE	polyacrylamide gel electrophoresis
PCR	polymerase chain reaction
pmol	picomole
PMSF	Phenylmethylsulfonylfluoride
QSAR	quantitative structure-activity
rpm	revolutions per minute
RFU	relative fluorescent unit
s	second
SD	standard deviation
SDS	sodium dodecyl sulphate
SDS-PAGE	sodium dodecyl sulphate polyacrylamide gel electrophoresis
Tris	Tris(hydroxymethyl)methylamine
TCA	trichloroacetic acid
TE	Tris/ EDTA
TBE	Tris/borate/EDTA
THP	tetrahydrophthalimide
TLC	thin layer chromatography
UTR	untranslated region
UV	Ultraviolet
V	volts
VIS	visible

Amino acids

A	alanine
C	cysteine
D	aspartic acid
E	glutamic acid
F	phenylalanine
G	glycine
H	histidine
I	isoleucine
K	lysine
L	leucine
M	methionine
N	asparagine
P	proline
Q	glutamine
R	arginine
S	serine
T	threonine
V	valine
W	tryptophan
Y	tyrosine

CD spectrum and UV melting

T_m	melting temperature
CD	circular dichroism
H_{vH}	Vant Hoff enthalpy
K	Kelvin
kcal	kilocalories
Mut	mutant
∂	change
n	molecularity
T	Absolute temperature
Wt	wild type

Cofactors

NAD	nucleotide adenine dinucleotide
FAD	flavin adenine dinucleotide
FMN	flavin mononucleotide
NADP	nucleotide adenine dinucleotide phosphate
PFP	pyridoxal 5'-phosphate
Rb	riboflavin

DNA nucleotide base

A	adenine
C	cytosine
G	guanine
T	thymine

Enzymes of the haem biosynthetic pathway

CPOX	Coproporphyrinogen oxidase
ALAS	5-aminolevulinic acid synthase
ALAD	5-aminolevulinic acid dehydratase
PBG deaminase	porphobilinogen deaminase
PPOX	Protoporphyrinogen oxidase
UROSIII	Uroporphyrinogen III synthase

Enzyme kinetics

V_{max}	maximum velocity
ES	enzyme substrate
k_{cat}	catalytic constant
K_m	Michaelis constant

Enzyme substrates

ALA	aminolevulinic acid
Succinyl coenzyme A	succinyl CoA
PBG	porphobilinogen

Inhibitors

AF	Acifluorfen
BR	Bilirubin
BV	Biliverdin
DPE	diphenyl ether
DPI	diphenyleneiodonium
MeAF	Methyl acifluorfen

Porphyrias, clinical involvement and pattern of inheritance

EPP	erythropoietic protoporphyria
ALA	5-aminolevulinic acid
AA	acute attack
PS	photosensitivity
VP	variegate porphyria
AD	autosomal dominant
AIP	acute intermittent porphyria
ALADP	5-ALA dehydratase porphyria
AR	autosomal recessive
CEP	congenital erythropoietic porphyria
FC	ferrochelatase
HEP	hepatoerythropoietic porphyria
HCP	hereditary coproporphyria
HCV	hepatitis C virus
PCT	porphyria cutanea tarda
HVP	homozygous variegate porphyria

Symbols

Δ	change
α	alpha
β	beta
γ	gamma
δ	delta
ε	epsilon
θ	theta
μ	micro

TABLE OF CONTENTS

Acknowledgements i

Abstract ii

Abbreviations and symbols iii

CHAPTER 1: THE HAEM BIOSYNTHETIC PATHWAY AND THE PORPHYRIAS: LITERATURE REVIEW 1

Introduction 1

Porphyrins 1

Structure and chemistry 1

Properties 2

Haem biosynthetic pathway 3

The porphyrias 3

Historical perspective of porphyrins, the porphyrias and the Haem Biosynthetic Pathway 4

Discovery of porphyrins 4

Discovery of the porphyrias 4

Elucidation of haem biosynthetic pathway 5

Detailed Description of the Haem Biosynthetic Pathway 7

Formation of the pyrrole 7

Biosynthesis of 5-Aminolevulinic Acid by ALAS (EC 2.3.1.37) 7

Biosynthesis of Porphobilinogen by 5-ALA Dehydratase (EC 4.2.1.24) 9

Assembly of the tetrapyrrolic (porphyrinogen) macrocycle 12

Biosynthesis of Hydroxymethylbilane by PBG deaminase (EC 4.3.1.8) 12

Closure of the Tetrapyrrole ring by Uroporphyrinogen III Synthase (EC4.2.1.75) 14

Modification of the peripheral side chains of the tetrapyrrole 15

Biosynthesis of Coproporphyrinogen III by Uroporphyrinogen Decarboxylase (EC4.1.1.37) 15

Biosynthesis of Protoporphyrinogen IX by Coproporphyrinogen Oxidase (EC1.3.3.3) 18

Oxidation of protoporphyrinogen IX and insertion of iron 20

Oxidation of Protoporphyrinogen IX to Protoporphyrin IX by Protoporphyrinogen Oxidase (EC1.3.3.) 20

Insertion of Iron by Ferrochelatase (EC4.99.1.1) 20

Haem Regulation in Erythroid and Non-erythroid tissues 23
Non-Erythroid tissues 23
Erythroid tissues 24

The Porphyrias 24
The specific syndromes of porphyria 27
ALA Dehydratase deficiency 27
PBG Deaminase deficiency 27
Uroporphyrinogen III Synthase deficiency 28
Uroporphyrinogen Decarboxylase deficiency 29
Coproporphyrinogen Oxidase deficiency 31
Protoporphyrinogen Oxidase deficiency 32
Ferrochelatase deficiency 32
ALA synthase deficiency 33

CHAPTER 2: PROTOPORPHYRINOGEN OXIDASE AND VARIEGATE PORPHYRIA: LITERATURE REVIEW 2

Protoporphyrinogen Oxidase 35
Enzymic oxidation of protoporphyrinogen IX to protoporphyrin IX 35
Substrate specificity 36
pH optima 37
Subcellular localisation 37
PPOX destribution in the cell 37
Subfractionation studies 38
PPOX labelling studies 38
PPOX localisation in the light of its protein and gene sequence 38
Enzyme purification 40
Molecular size and subunit composition 40
Cofactor composition in PPOX 41
Flavoproteins and flavins in nature 43
Spectrophotometric analysis of flavins 43
Fluorometric analysis 43
Determination of non covalently bound flavins 44
PPOX inhibition 44
Inhibitors 44
Mode of inhibition 45
Inhibition by diphenyl ether herbicides 46

Effect of DPE on plants 46
Effect of DPE on animals 47
PPOX resistance to DPE 47
Inhibition by haem and its metabolic products 49
Inhibition by diphenyleneiodonium 50
PPOX gene 51
Identification of the gene 51
Gene sequence 51
Assignment of the gene to chromosome 1q22–23 51

Variegate Porphyria 52
Historical perspective 52
Prevalence 53
Clinical features 54
Skin disease 54
Acute attack 55
Biochemical features and diagnosis 55
Stool 56
Urine 56
Plasma 56
PPOX activity 56
Genetic diagnosis 57
PPOX gene mutation responsible for VP 57
Mutations in South Africa 58
Correlation between mutation and clinical presentation 58
Homozygous variegate porphyria 58
Clinical features 59
Molecular biology 59

CHAPTER 3: STUDIES ON HUMAN PROTOPORPHYRINOGEN OXIDASE: DEVELOPMENT OF THIS THESIS

Introduction 67
Previous studies on human mutant PPOX 67
This study 68

CHAPTER 4: PRODUCTION OF HUMAN WILD TYPE AND MUTANT PROTOPORPHYRINOGEN OXIDASES, THEIR EXPRESSION AND PURIFICATION

Introduction 69

Objectives 69

Methods 70

Transformation of wild type PPOX 70

Site-directed mutagenesis 70

Principle 71

Procedure 71

Transformation of BMH 71-18 mutS competent cells 72

Plasmid DNA purification 72

Transformation into JM 109 cells 72

Mutational analysis 73

Expression of PPOX 73

Effect of culture time and temperature on expression 73

Effect of IPTG induction on PPOX expression 73

Purification of wild type and mutant PPOX 74

Principle 74

Procedure 74

Results 75

Engineering of mutants 75

Expression of protoporphyrinogen oxidase 80

Purification 78

Discussion 83

Conclusion 85

CHAPTER 5: PARTIAL CHARACTERISATION AND KINETICS OF WILD TYPE AND MUTANT PROTOPORPHYRINOGEN OXIDASE

Introduction 87

Objectives 87

Methods 87

Protoporphyrinogen oxidase activity assay 87

pH optima 88

Derivation of kinetic constants 88

Fluorimetric analysis of cofactor from purified PPOX 88
Spectrophotometric analysis of purified PPOX and FAD binding 88

Results 89
pH optima 89
PPOX kinetics 90
Fluorimetric identification of cofactor 94
UV/VIS spectra of FAD cofactor 95
Effect of FAD on catalytic activity 96

Discussion 96
PPOX kinetics 96
FAD cofactor 97
The FAD binding motif 98

Conclusions 99

CHAPTER 6: INHIBITION STUDIES ON HUMAN WILD TYPE AND MUTANT PROTOPORPHYRINOGEN OXIDASE

Introduction 101

Objectives 101

Methods 102
Inhibition studies and determination of kinetic data 102

Results 103
IC_{50}s 103
Kinetic parameters (K_i, K_s and α) and mode of inhibition 104

Discussion 106

Conclusions 106

CHAPTER 7: PHYSICOCHEMICAL CHARACTERISATION OF HUMAN WILD TYPE AND MUTANT PROTOPORPHYRINOGEN OXIDASE

Introduction 107
Protein folding 107
Thermodynamics of protein folding 108
Thermal denaturation 109
Protein circular dichroism spectrum 110

Objectives 112

Methods 112
Protein preparation 112
Effect of temperature on PPOX activity 112
Temperature induced denaturation 112
CD spectrum 113

Results 113
Effect of temperature on PPOX activity 113
Thermal unfolding of PPOX 114
Thermal equilibrium studies 116
Effect of AF on T_m of PPOX 118
Secondary structure 120

Discussion 121
Effect of temperature on PPOX activity ($T_{1/2}$) 122
Effect of temperature on PPOX folding (T_m) 122
Thermal equilibrium studies 123
Effect of FAD/AF ligand binding on PPOX stability 123
Secondary structural analysis of PPOX 124
Physicochemical analysis of R59 residue 124

Conclusions 125

CHAPTER 8: OVERVIEW, IMPLICATIONS AND FUTURE DIRECTIONS

Overview and implications 127

Future work 128

BIBLIOGRAPHY 131

APPENDICES 171

LIST OF APPENDICES

1. Transformation of *E.coli* JM 109 cells with human PPOX recombinant plasmid 171
2. Expression of wild type PPOX 173
3. DNA purification 175
4. Human PPOX cDNA sequence 177
5. Site-directed mutagenesis 179
6. Mutational analysis 187
7. Restriction analysis 191
8. Agarose gel electrophoresis 197
9. Qiaex II agarose gel extraction protocol 199
10. Optimisation of PPOX expression 201
11. Native purification of wild type and mutant PPOX by metal affinity chromatography (Talon resin) 203
12. Sodium dodecyl sulphate polyacrylamide gel electrophoresis (SDS-PAGE) 205
13. Protoporphyrinogen oxidase assay 209
14. Protein concentration determination by Microassay procedure 215
15. Analysis of flavin cofactor 217
16. Inhibition of PPOX 219
17. Effect of temperature on PPOX activity and stability 221
18. Circular dichroism (CD) spectroscopy 225
19. UV melting curves 227
20. CD scans 229
21. Observed data for determination of means and standard deviations 235

CHAPTER 1

THE HAEM BIOSYNTHETIC PATHWAY AND THE PORPHYRIAS

LITERATURE REVIEW 1

Introduction

Haem is an iron-containing complex of protoporphyrin IX, which associates with numerous proteins and is central to many biological oxidations throughout nature. For example, haem is the prosthetic group in haemoglobin, myoglobin, microsomal cytochromes, catalase, tryptophan oxygenase and nitric oxide synthase. In all living organisms haem is synthesised via a specific pathway involving a series of chemical reactions and modifications of various porphyrin intermediates. While this thesis undertakes a detailed study of the penultimate enzyme of haem biosynthesis, protoporphyrinogen oxidase (PPOX) and various mutant PPOXs, this chapter reviews porphyrins, haem biosynthesis and the porphyrias in general terms, giving it a broader context. The focus of this work, PPOX and variegate porphyria (VP) is reviewed in detail in Chapter 2.

Porphyrins

Structure and chemistry

Porphyrins are rigid planar structures consisting of a macrocycle of four pyrrole rings linked by four methene bridges (Figure 1.1A) (Falk et al., 1961; Falk, 1964; Marks, 1969; Adler, 1973; Smith, 1975; Dolphin, 1979; Bissell and Schmid, 1987; Bloomer and Straka, 1988; Kappas et al., 1989; Wyckoff and Kushner, 1994; McDonagh and Bissell, 1998). Eight side chains can be attached at positions 1 to 8 in the Fischer nomenclature. The type of side chains determines the physical characteristic of the porphyrin and typically consists of methyl, ethyl, vinyl, acetate, and propionate substituents. The four pyrrole rings are designated A, B, C, and D and the four methene bridges α, β, γ, and δ. Varying arrangements of side chain substituents around the porphyrin ring allow the porphyrin structure to form a number of isomers. The III-isomer series (eg. uroporphyrinogen III and coproporphyrinogen III) occur in nature and are the biologically active isomers; uroporphyrinogen I and coproporphyrinogen I isomers are produced non-enzymatically and are not utilised biologically.

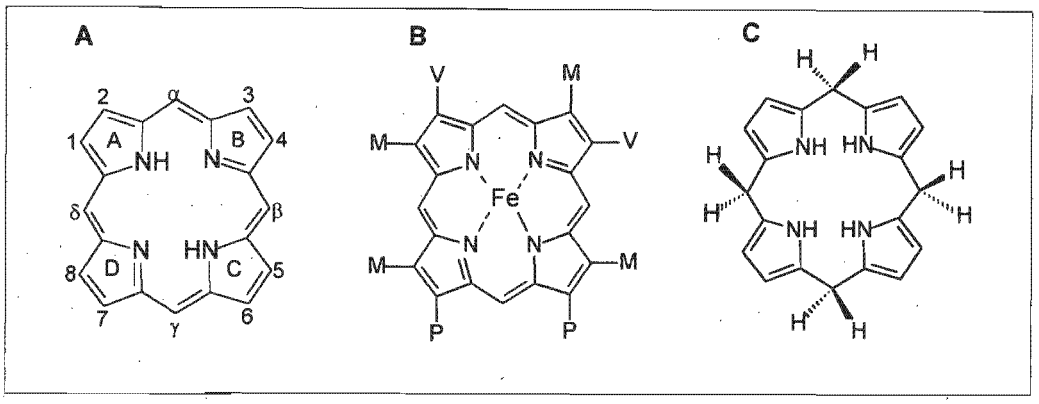

Figure 1.1 **A: Tetrapyrrole structures showing four pyrrole rings of porphyrin joined by methene bridges**

B: Haem structure

C: Tetrapyrrole structures showing four pyrrole rings of porphyrinogen joined by methylene bridges

Properties

The porphyrin ring structure is capable of binding metals such as iron and magnesium within. The iron-containing complex, haem (figure 1.1B) binds to various proteins and is central to many biological oxidation reactions and to oxygen transport. Magnesium-porphyrin compounds constitute the chlorophylls and are central to solar energy utilisation in the biosphere. Most naturally occurring porphyrins have ampholytic properties, by virtue of the fact that they have carboxylic-acid side chains and basic nitrogen atoms making them soluble in both aqueous acid and aqueous alkali. Porphyrins with a high number of carboxyl groups (8 – 4) are hydrophilic and are excreted in the urine, whereas those with fewer carboxylic groups (2 – 4) are lipophilic and are excreted through the hepatobiliary route. Both types of porphyrins bind to various proteins and phospholipids in plasma.

Porphyrins are highly conjugated structures of bright colour that fluoresce red in the near ultraviolet (UV) (± 400nm). The absorption spectra of porphyrins show absorption in the visible (VIS) regions of the electromagnetic spectrum with a major band in the region of 400nm called the Soret band (Soret, 1883). The main absorption bands have very high extinction coefficients (up to 4 x 10^5 M). The porphyrinogens (Figure 1.1C) (in which the methene bridges are reduced to methylene bridges) are colourless and do not fluoresce. They are unstable and can easily oxidise to the corresponding porphyrins when exposed to air. Thus, the haem pathway intermediates are generally in the porphyrinogen form except for protoporphyrin IX, which is used as the substrate during the insertion of iron by ferrochelatase (FC) (Bonkovsky et al., 1975; Dailey, 1990, 1996).

Haem biosynthetic pathway

The haem biosynthetic pathway is a well-defined pathway in mammals starting in the mitochondrial matrix with the condensation of succinyl-coenzyme A (succinyl CoA) (from the citric acid cycle) and the amino acid glycine to form 5-aminolevulinic acid (ALA). The pathway continues in the cytosol and ultimately returns to the mitochondrion when protoporphyrinogen IX is synthesised. Briefly, the process starts by condensation of glycine and succinyl CoA to form ALA. The mitochondrial enzyme ALA synthase (ALAS) catalyses this reaction. Thereafter, a series of cytosolic enzymes are involved, starting with the conversion of ALA to porphobilinogen (PBG) through the condensation of two ALA molecules. The enzyme ALA dehydratase (ALAD) catalyses this reaction. The next step involves condensation of four pyrrole rings, resulting in the conversion of PBG to hydroxymethylbilane. This reaction is catalysed by PBG deaminase PBGD. Uroporphyrinogen III synthase (UROSIII) then catalyses the ring closure and intramolecular rearrangement of the pyrrole ring D, to form uroporphyrinogen III. Uroporphyrinogen decarboxylase (UROD) catalyses the conversion of uroporphyrinogen III to coproporphyrinogen III by stepwise decarboxylation of four acetate side chains. At this stage, the pathway re-enters the mitochondria with the conversion of coproporphyrinogen III to protoporphyrinogen IX. The enzyme coproporphyrinogen oxidase (CPOX) catalyses this step through oxidative decarboxylation of two propionate groups of rings A and B to vinyl groups. Considering the reducing environment present in the mitochondrion, an enzyme is required to oxidise protoporphyrinogen IX to protoporphyrin IX. PPOX catalyses this oxidation. Haem synthesis is completed by the insertion of iron into protoporphyrin IX by FC. Despite the fact that porphyrins are often described as intermediates of the haem biosynthetic pathway, it is important to recognise that it is their reduced porphyrinogen forms that are the true haem intermediates.

Generally the rate of the haem production is regulated by a complex system of negative feed back control on ALAS activity, primarily by haem. It is further complicated by the fact that erythropoietic and "housekeeping" (hepatic) haem synthesis appears to be regulated via different mechanisms.

The porphyrias

Inborn metabolic disorders of haem biosynthesis in which specific patterns of overproduction of haem intermediates are associated with characteristic clinical features. This group of diseases is referred to as the porphyrias. The specific syndromes of the porphyrias will be considered in more detail in a later section. Most are inherited as Mendelian autosomal dominant conditions, some are recessive and one form is acquired.

Historical perspective of porphyrins, the porphyrias and the haem biosynthetic pathway

Discovery of the porphyrins

Scherer (1841) first alluded to porphyrin pigments. To demonstrate that the red colour of blood was not due to iron, he added concentrated sulphuric acid to dried powdered blood, and washed the precipitate free of iron. He then treated the iron-free residue with alcohol and applied heat. The end result was a residue that was blood-red in colour. Similar experiments were conducted by other scientists (Lecanu, 1837; Berzelius, 1840; Mulder, 1844). Mulder called the purple-red fluid "iron-free haematin", and Thudicum (1867) called the red substance "cruentine" based on the fluorescence of this material with a splendid blood-red colour. Hoppe-Seyler (1871) renamed the substance haematoporphyrin after the Greek "*porphuros*" meaning purple.

Discovery of the porphyrias

The first case of porphyria was recorded by Schultz (1874). A numbers of case reports describing porphyria resulting from sulphonal drug administration followed (Kast, 1888; Stokvis, 1889; Harley, 1890; Ranking and Pardington, 1890; McCall-Anderson, 1898). In all these reports the common feature was the excretion of dark red urine containing haematoporphyrin and was associated with skin photosensitivity and sometimes, acute symptoms. The photosensitising property of porphyrin was tested by Meyer-Betz (1913) by injecting 200mg of hematoporphyrin into his own veins. On his exposure to sunlight, he observed marked photosensitivity on his exposed skin. In addition to sulphonal, several other drugs that were capable of provoking patients with porphyria into an acute form were noted. These drugs were identified through recognition of their effect by clinical observation and by experimental animal studies.

Fischer, (1916) showed that porphyrin excreted in urine following sulphonal administration was actually quite discrete from hematoporphyrin. Nencki and Sieber (1888) showed that hematoporphyrin was a dicarboxylic porphyrin and both carboxyl groups could be esterified. They named this mesoporphyrin (Zaleski, 1903). Saillet, (1896) prepared "urospectrine" from urine. Later this was named coproporphyrin by Fischer and Zerweck, (1924). They also showed a colourless chromogen compound in urine, coproporphyrinogen III. Protoporphyrin IX was prepared by Laidlaw (1904). The structure of haem was proposed by Küster, (1912) but others rejected it because they had doubts about the stability of such a large ring structure. Fischer, (1915) and others differentiated between natural haem and hematoporphyrin, which was correctly named protoporphyrin IX. In 1937 the term "porphyrias" came to be associated with diseases of porphyrin

metabolism (Waldenström, 1937) rather than the previously used "hematoporphyria" originally introduced by Günther, (1911).

Elucidation of the haem biosynthetic pathway

Isolation of crystalline porphobilinogen from the urine of acute intermittent porphyria (AIP) patients was an important milestone towards the understanding of the haem pathway (Westall, 1952). The elucidation of the monopyrrole structure of PBG followed (Cookson and Rimington, 1954). PBG was demonstrated to be enzymatically converted into uroporphyrinogen when the enzyme was incubated with chicken red cell haemolysate (Falk et al., 1953).

The study of the haem biosynthetic pathway (Figure 1.2) was carried out on suitable animal models and based on the incorporation of radiolabelled precursors (such as [^{15}N]glycine and [^{14}C]succinate) at different steps of the pathway, during the formation of haem (Shemin and Rittenberg, 1946; Grinstein et al., 1949; Muir and Neuberger, 1950; Shemin and Wittenberg, 1951; Gray, 1952; Shemin et al., 1955). Radiolabelled [^{14}C]acetate (Shemin and Wittenberg, 1951) and *in vitro* experiments in avian erythrocytes established that the 4-carbon starting compound was succinyl CoA from the tricarboxylic acid cycle, and that this compound provided some of the carbon atoms in the haem macrocycle (Gibson et al., 1958). Shemin and Russell, (1953), and Neuberger and Scott, (1953) showed that ALA formation leads to the synthesis of all porphyrin intermediates. Falk et al. (1953) also showed that PBG is the monopyrrole precursor for all the tetrapyrrole synthesis in this pathway. Subsequently, Granick (1958, 1966), Gibson et al. (1958), Kikuchi et al. (1958a,b), and Granick and Sassa, (1971) showed that ALA was formed by the action of ALAS, and was therefore important as a potential controlling point of the biosynthetic pathway. Thus, the porphyrin biosynthetic pathway was established by the mid 50's and was shown to be virtually the same as that proposed earlier by Lemberg and Legge (1949). Eventually all eight enzymes of the biosynthetic pathway were described. PPOX was the last enzyme of the sequence to be described (Jackson et al., 1974; Poulson and Polglase, 1975).

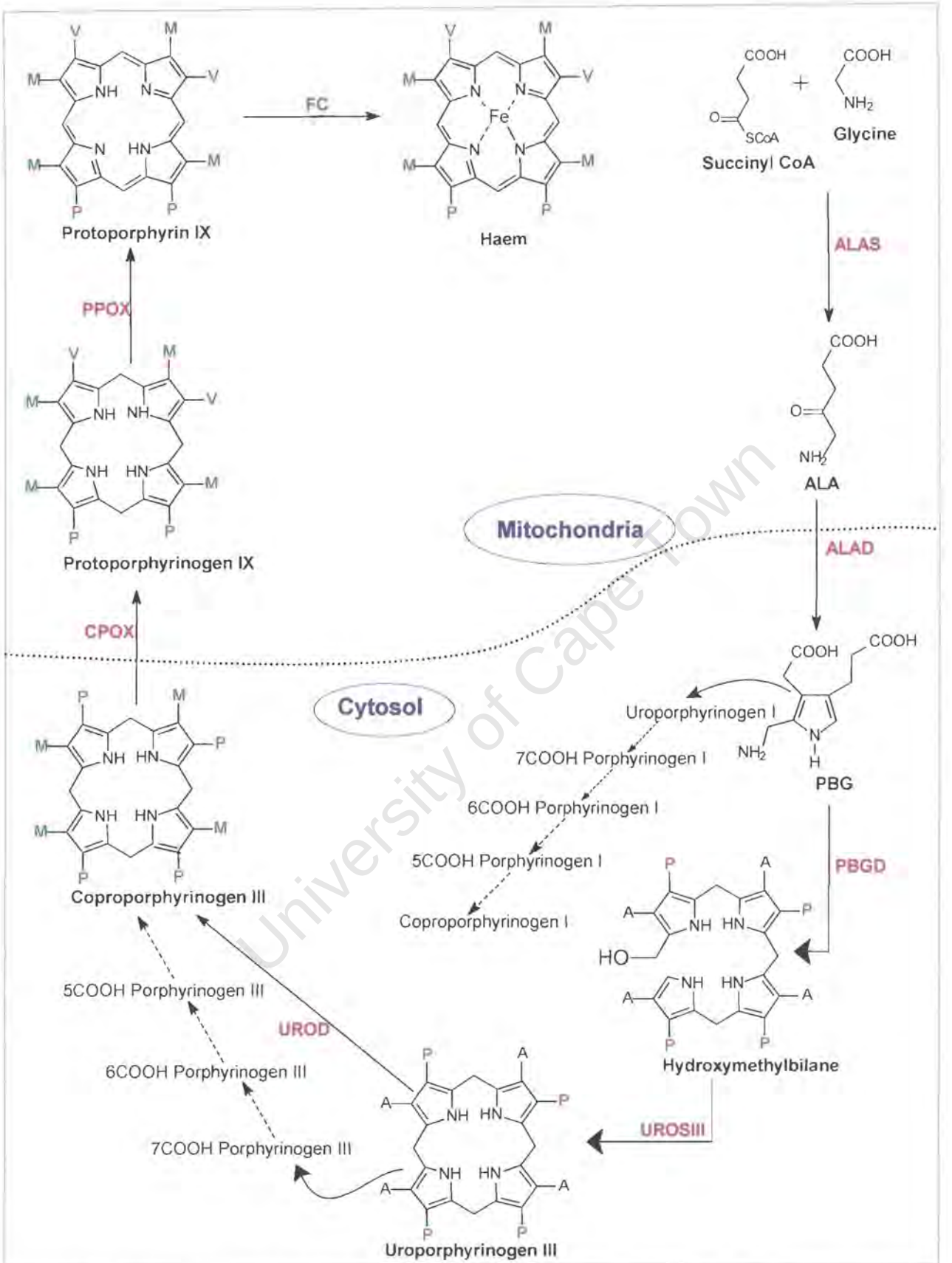

Figure1.2: Haem biosynthetic pathway involving eight enzyme catalysed "pyrrolic" reactions which are located sequentially in the mitochondria, cytosol and finally mitochondria. M = methyl ($-CH_3$), V = vinyl ($-CH=CH_2$), P = propionate ($-CH_2CH_2COOH$), A = acetate ($-OCH_3$).

Detailed Description of the Haem Biosynthetic Pathway

Formation of the pyrrole

Biosynthesis of 5-Aminolevulinic Acid by ALAS (EC 2.3.1.37)

Reaction and Mechanism: ALAS catalyses the first committed step of the haem biosynthetic pathway. In non-plant eukaryotes, and the alpha subdivision of purple bacteria, catalysis involves the condensation of glycine and succinyl CoA (derived from the tricarboxylic acid cycle) to yield ALA, CoA and carbon dioxide (Figure 1.3) (Jordan 1991; May et al 1995; Ferreira and Gong, 1995). Glycine is bound through an essential pyridoxal cofactor as a stable Schiff-base carbanion on the enzyme surface, which can react with the electrophilic carbonyl group of succinyl CoA to produce an α-amino-β-ketoadipic acid with the release of CoA. The carboxyl carbon of glycine is then decarboxylated enzymatically to yield ALA.

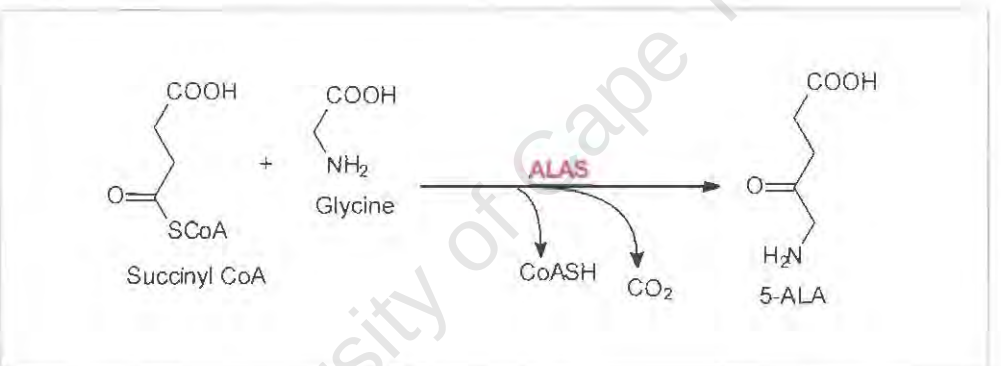

Figure 1.3: Biosynthesis of ALA from glycine and succinyl CoA by ALAS.

Enzyme assay: ALAS activity is determined by quantifying the conversion of glycine and succinyl CoA to ALA. The ALA concentration is measured colourimetrically by Ehrlich's reagent (paradimethylaminobenzaldehyde in acid) after condensation to a pyrrole. Alternatively ALA is measured fluorimetrically after enzymatic conversion of the product to uroporphyrin (Li-Fen and Beattie, 1982; Bishop et al., 1982). A radiochemical method that is reportedly more sensitive and specific has been described (Brooker et al., 1982).

Enzyme structure: Cloning, expression and detailed characterisation of mouse ALAS have demonstrated a conserved active site ε-amino group of a lysine residue (murine ALAS Lys 313) attached to the pyridoxal 5'–phosphate (PFP) cofactor in the active site (Yoshimura et al., 1992; Lu et al., 1993; Rege et al., 1996) in the absence of the substrate. This lysine residue was identified by Ferreira et al., (1993) as a Schiff base

linkage. The Lys-313 is essential for catalysis but not for binding cofactor *per se* (Ferreira et al., 1995). A conserved tyrosine residue (murine Tyr-121) is now thought to play that role (Tan et al., 1998). The electron sink function of the PFP cofactor may be enhanced by the presence of an aspartate residue (murine ALAS Asp-279), and Arg-439 in the mouse is suggested as playing an essential role in substrate binding (Tan et al., 1998; Gong et al., 1998).

A conserved glycine-rich sequence (GAGAGG) has been identified in the sequence alignment of all known ALAS sequences. There is a similar sequence motif (GXGXXG) for some PFP dependent enzymes (Marceau et al., 1988; Hyde et al., 1988). This motif has also been identified in many nucleotide-binding proteins (Saraste et al., 1990; Pai et al., 1990; Branden and Tooze, 1991; Swindells, 1993).

Subcellular location and translocation: Studies on the subcellular location of the mitochondrial enzyme showed that ALAS is loosely bound to the inner mitochondrial membrane but generally available within the mitochondrial matrix (McKay et al., 1969; Scott et al., 1983). The presence of ALAS in the mitochondrial matrix was demonstrated on rat enzyme using specific enzyme markers (Scott et al., 1983). Initially, studies demonstrated that small amounts of newly synthesised enzyme are found in the cytosol and are then imported into mitochondria (Hayashi et al., 1969; Patton and Beattie, 1973). ALAS protein is encoded by nuclear DNA and synthesised in the cytoplasmic ribosomes as a larger precursor protein prior to insertion into the mitochondrial membrane where it functions as a smaller mature protein. (Hayashi et al., 1970, 1976, 1983; Whiting and Elliot, 1972; Yamauchi et al., 1980; Borthwick et al., 1985; Urban-Grimal et al., 1986).

Purification and molecular sizes: Purification of ALAS has been described in *Rhodobacter sphaeroides* (*R. sphaeroides*) (Warnick and Burnham, 1971), rat liver (Ohashi and Kikuchi, 1978), *Euglena gracilis* (*E. gracilis*) (Dzelzkalns et al., 1982), chicken liver (Borthwick et al., 1983), yeast (Volland and Felix, 1984) and *Escherichia coli (E. coli)* (Ferreira and Dailey, 1993). Two isoforms of the enzyme are known to exist and share a 50% amino acid identity (ALA-S1 and ALA-S2). ALA-S1 is a "house keeping" gene and is expressed in all tissues (Riddle et al., 1989; Bishop et al., 1990; May et al., 1995). ALA-S2 is predominantly expressed in primitive erythroid cells (Riddle et al., 1989; Bishop et al., 1990). ALA-S1 and ALA–S2 appear to be regulated by different mechanisms in which haem is involved, to different degrees.

The human ALAS gene encodes a 640 amino acid protein with molecular weight of approximately 70000 Da. The N-terminal is 56 amino acids long, and constitutes the "presequence", which is cleaved on translocation of protein into mitochondria. The mature

mitochondrial enzyme isoforms of human ALA-S1 and ALA-S2 have molecular weights of 64 600 and 59 500 Da, respectively (Bishop, 1990; Cox et al., 1991).

Gene sequence: The gene for ALA-S2 has been cloned and mapped to the X-chromosome (Xp11.21) (Cox et al., 1990; Bishop et al., 1990; Cox et al., 1991), and the distinct house keeping isoform ALA-S1 encoded by separate gene on chromosome 3 (3p21) (Sutherland et al., 1988; Bishop et al., 1990). ALA-S1 is the only ALAS gene expressed in liver and other non-erythroid tissue. Its activity is decreased during differentiation of erythroid cells. The gene for ALA-S2 is induced during erythropoiesis and its product becomes the dominant form of ALAS (Riddle et al., 1989; Fujita et al., 1991). The human ALA-S2 gene spans approximately 22kb and contains 11 exons. The C-terminal portion (comprising exons 5 – 11) has 73% sequence identity with ALA-S1 and contains a catalytic domain. Exons 2 – 4 of the ALA-S2 gene encode the N-terminal signal sequence for mitochondrial import (Conboy et al., 1992). The 5'-flanking region of the gene spans an erythroid-specific promoter element including a GATA-1 binding site (Cox et al., 1991). This site interacts with GATA-1 transcription factor (Tsai et al., 1989) to restrict expression in erythroid cells.

Biosynthesis of Porphobilinogen by ALA Dehydratase (EC4.2.1.24)

Reaction and Mechanism: In the second step of the haem biosynthetic pathway a multisubunit cytosolic enzyme ALAD catalyses the condensation of two molecules of ALA to form a monopyrrole, PBG (Figure 1.4) (Shemin, 1976; Tsukamoto et al., 1979; Neier, 1996). ALAD requires an intact sulfhydryl group and a zinc atom per subunit for its full activity (Abdulla and Haeger-Aronsen, 1971; Meredith and Moore, 1978; Sassa, 1982). The reaction involves a series of intermediate stages with an aldol condensation and formation of Schiff base and is accompanied by the elimination of two water molecules. ALAD has two different active sites, the P- and the A-site (Shoolingin-Jordan et al., 1996; 1997; 1998). The P-site contributes the propionate side chain and pyrrolic nitrogen. The A-site forms the acetic acid and amino-methyl side chain of PBG (Neier, 1996).

The formation of the Schiff base between enzyme and substrate at the P-site has been investigated (Jordan and Seehra, 1980; Gibbs and Jordan, 1986; Spencer and Jordan, 1995; Erskine et al., 1997a). There is an ordered binding in which the keto group of the ALA contributing the propionate side chain forms a transient covalent bond with a conserved lysine (human Lys-252) in the P-site first. Once it is bound to substrate at the P-site with an available 5-amino group, a second ALA molecule binds at the A-site. The amino-nitrogen is then incorporated into the pyrrole ring of PBG. The presence of a divalent metal ion is essential for binding of the second substrate at the A-site (Shoolingin-

Jordan, 1998). Typically, the required metals are Zn^{2+} or Mg^{2+}. Thus an ALAD octamer can bind up to a maximum of 8 Zn^{2+} ions, 4 being required for catalysis at the A-site.

Enzyme assay: ALAD activity is monitored by quantifying PBG production using Ehrlich's reagent (Sassa, 1982). The enzyme is relatively unstable at room temperature but can maintain its activity for approximately 24 hours. At 4°C and at -20°C it is degraded much more slowly.

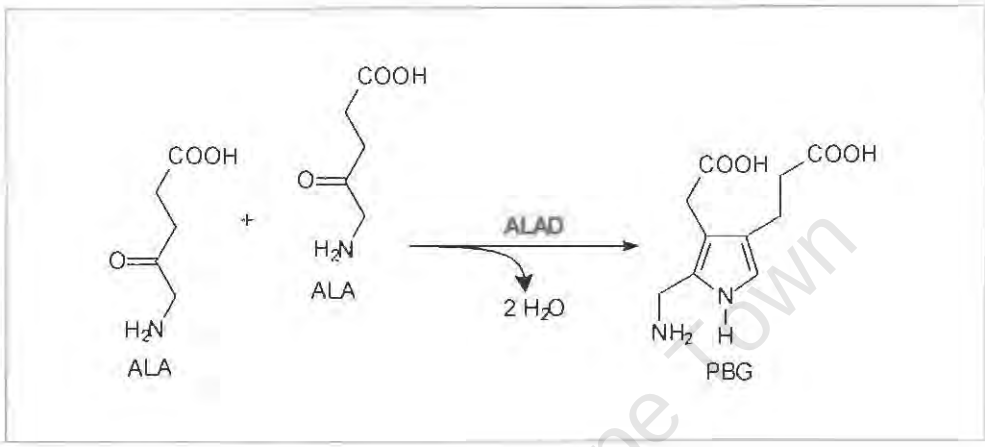

Figure 1.4: Biosynthesis of PBG from ALA by ALAD.

Enzyme structure: Cloning of ALAD has allowed the development of expression systems for various forms. Ultra-pure preparations of recombinant enzyme have yielded a crystal structure suitable for x-ray characterisation (Senior et al., 1996, 1997). The crystallisation and initial x-ray characterisation of the ALAD from *E. coli* and *Saccharomyces cerevisiae* (*S. cerevisiae*) of around 2 Å have been reported (Erskine et al., 1997a,b) with more detailed structure for *Pseudomonas aeruginosa* (*P. aeruginosa*) ALAD (1.67 Å) (Frankenberg et al., 1999). In all cases the best crystals were obtained when these proteins were covalently bound to ALA. The x-ray structures confirmed the structure of ALAD as a homo-octomer. Each of the subunits was adopting a "TIM" (*t*riosephosphate isomerase) barrel fold with an N-terminal arm of 30 amino acid residues (Jordan and Warren, 1987). The monomers formed asymmetric dimers with their "arms" wrapped around each other. Four of these dimers interact to form octomers with their active sites located on the surface.

In *E. coli* ALAD, Lys-247 (equivalent to the essential Lys-252 at the P-site in human ALAD) forms a Schiff-base link with the bound levulinic acid at the active site. In yeast ALAD x-ray analysis shows the formation of a Schiff base with Lys-263 that is also equivalent to human Lys-252 (Jordan and Warren, 1987). Structural analysis of *P.*

aeruginosa ALAD showed differences in the monomers of each dimer (in that one had a "closed" and the other an "opened" active site pocket). A single well-defined and highly hydrated Mg^{2+} was identified in the active site of both monomers. A structure-based mechanism of action involving Mg^{2+} allosteric binding at the active site and rate enhancement has been proposed, based on this information (Frankenberg et al., 1999).

Purification and molecular sizes: ALAD purification has been reported from yeast (De Barreiro, 1967), *R. sphaeroides* (Nandi et al., 1968), human erythrocytes (Anderson and Desnick, 1979; Gibbs et al., 1985), bovine liver (Bevan et al., 1980; Jordan and Seehra, 1986), and spinach (Liedgens et al., 1983).

Human ALAD is a homo-octamer with subunits of 36 274 Da (Wetmur et al., 1986). This is identical to *E. coli* ALAD, which presented identical subunits of 36544 Da (Spencer and Jordan, 1993). ALAD from unicellular green algae, *Scenedesmus obliqus* had a molecular weight of 282000 Da with six subunits of 42000 Da arranged in a ring (Stoltz and Dornemann, 1996). It appears therefore, that generally ALAD exist as an octamer with a molecular weight of approximately 280000 Da with identical units of approximately 35000 Da each (Jordan, 1990).

Gene sequence: The gene has been sequenced from various sources including human (Witmur et al., 1986), mouse (Bishop et al., 1996), *E. coli* (Echelard et al., 1988), pea (*Pisum sativum L.*) (Boese et al., 1991), *Bradyrhizobium japonicum (B. japonicum)* (Chauhan and O' Brian, 1993), soyabean (Kaczor et al., 1994), *Chlamydomonas reinhardtii* (*C. reinhardtii*) (Matters and Beale, 1995), and *P. aeruginosa* (Frankenberg et al., 1998). The enzyme is present in all organisms that require the biosynthesis of tetrapyrroles (Jordan, 1991; Chadwick and Ackrill, 1994). Human ALAD is encoded by a gene localised at chromosome 9q34 (Wetmur et al., 1986). The human ALAD gene contains two promoter regions in a single gene that generates housekeeping and erythroid-specific transcripts by alternate splicing (Kaya et al., 1994; Bishop et al., 1996). The expression of these erythroid-specific transcripts is to ensure sufficient haem biosynthesis for the high level tissue-specific production of haemoglobin (Kaya et al., 1994).

Enzyme inhibition: Several ALAD inhibitors have clinical significance. The enzyme is inhibited by lead (Moore and Goldberg, 1985; Duydu et al., 2001), alcohol (Moore et al., 1984), and succinyl acetone, a structural analogue of ALA (Lindblad et al., 1977; Tschudy et al., 1981; Kappas et al., 1995; Erskine et al., 2001).

The effect of inhibitors on the study of enzyme structural mechanism has been studied (Cheung et al., 1997). Succinyl acetone may be overproduced in patients suffering from

hereditary tyrosinemia (Lindblad et al., 1977). The patients suffer from a functional ALAD deficiency and may experience acute porphyric-like symptoms (Rank et al., 1991). Many 4-ketoacids such as 4-ketopentanoic acid interact with ALAD to form a Schiff-base. Many inhibitors derived from such compounds has been synthesised and act as competitive inhibitors by forming a Schiff-base at the PFP-site (Neier, 1996) and can be linked irreversibly to the enzyme (Spencer and Jordan, 1995; Cheung et al., 1997). Irreversible enzyme inhibition has also been reported in styrene and bromobenzene poisoning (Akagi et al., 1992).

Assembly of the tetrapyrrolic (porphyrinogen) macrocycle

Biosynthesis of hydroxymethylbilane by PBG deaminase (EC4.3.1.8)

Reaction and Mechanism: The PBG deaminase enzyme performs its catalysis at the active site by deamination and polymerisation of four PBG molecules (Figure 1.5) (Awan et al., 1997). PBG deaminase is unique in that it is covalently attached to a dipyrromethane cofactor at the active site that binds substrate molecules during sequential assembly of the linear tetrapyrrole molecule (Jordan and Warren, 1987). The structure of the dipyrromethane cofactor and its site of attachment to the enzyme have been characterised. The dipyrrole is covalently linked to the enzyme through a conserved cysteine via a thioether linkage (*E. coli*, Cys-242) (Miller et al., 1988; Louie et al., 1996). The dipyrrolic cofactor then acts as a primer, and is elongated in a stepwise mechanism one PBG unit at a time, through enzyme-substrate (ES) intermediate complexes, ES (with one PBG attached); ES_2 (two PBGs attached); ES_3 (three PBGs attached); and finally ES_4 (four PBGs attached) to form the tetrapyrrolic product, hydroxymethylbilane. The product is then released by hydrolytic cleavage, regenerating the enzyme-dipyrromethane intact (McNeill and Shoolingin-Jordan, 1998). Consequently the two proximal PBGs (i.e., the dipyrromethane cofactor) remain covalently linked to the enzyme and are not turned over.

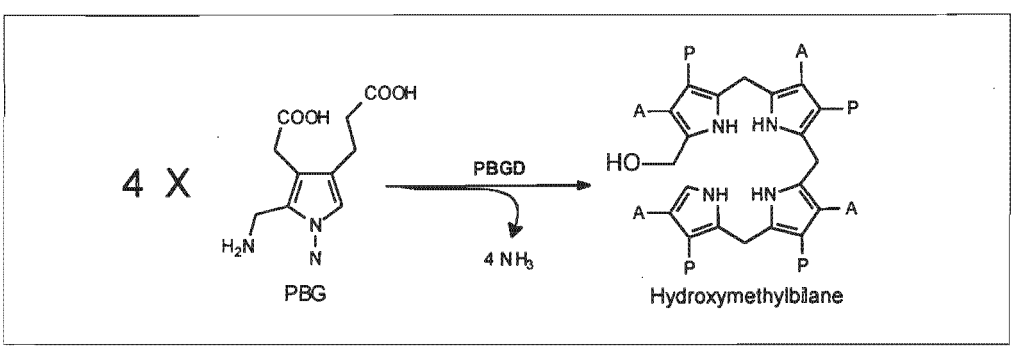

Figure 1.5: **Biosynthesis of hydroxymethylbilane from PBG by PBGD. A = acetate, P = propionate.**

Enzyme assay: PBG deaminase activity is measured (typically in erythrocytes) by spectrophotometry or fluorimetry to detect the production of uroporphyrin by enzyme using PBG as substrate (Ford et al., 1980; Anderson and Desnick, 1982).

Enzyme structure: x-ray crystallographic studies at 1.76 Å resolution (Jordan et al., 1992) was performed on the cloned and expressed PBGD from *E. coli* (Grandchamp et al., 1987). The resolution revealed protein folded into three α/β domains of approximately 100 amino acids each, linked to one another by flexible strands (Shoolingin-Jordan 1998; Louie et al., 1996). Domains 1 and 2, which have similar overall topology, form a cleft at their interface. The dipyrromethane cofactor is bound by extensive contacts, including salt bridges and hydrogen bonds between these two domains in this cleft. Several of these salt bridges between arginine, pyrrole acetates and propionates were demonstrated by site-directed mutagenesis, as important for enzymatic activity (Jordan and Woodcock, 1991; Lander et al., 1991). Domain 3 is an open-faced antiparallel sheet of three strands containing cysteine. The cofactor is covalently bound to it and is situated deep within the cleft between domains 1 and 2. This is the point where deamination of PBG and formation of the methene bridges takes place. Consequently, domain 3 is considered as containing the single catalytic site. The crystal structure shows flexible boundaries between the three domains, which are important in allowing conformational changes that accommodate each added PBG pyrrole during synthesis of the tetrapyrrole.

Purification and molecular sizes: PBG deaminase has been purified from various sources and is frequently complexed to the next enzyme in the pathway UROSIII (Sancovich et al., 1969; Llambias and Batlle, 1970; Frydman and Fenstein, 1974). The enzyme has been purified in both eukaryotes and prokaryotes including spinach (Higuchi and Bogorad, 1975), *R. spheroides* (Jordan and Shemin, 1973; Davies and Neuberger, 1973), *E. coli* and *E. gracilis* (Hart and Battersby, 1985), and human erythrocytes (Anderson and Desnick, 1980; Corrigall et al., 1991). It appears to exist as a monomer with molecular weight of 35000 – 44000 dalton (Jordan, 1990).

Gene sequence and its product: Genes for various PBG deaminases including plant, animals and bacterial enzymes have been cloned, and overexpressed from recombinant bacterial strains (Shoolingin-Jordan, 1995). In humans there are two forms of PBG deaminase that are encoded by a single gene transcribed from separate erythroid-specific and housekeeping promoters (Grandchamp et al., 1987; Chretien et al., 1988). The two enzyme isoforms are encoded by a 10kb long gene with 15 exons of two overlapping transcription units in chromosome 11q24.1–24.2 (Wang et al., 1981; Raich et al., 1986; Namba et al., 1991). The erythroid promoter lies in intron 1 with initiation of transcription starting 5' to exon 2 and translation of mRNA starting at exon 3. The erythroid isoenzyme

is therefore encoded by sequences of the 3' section of exon 3 and exons 4 – 15. The housekeeping isoenzyme transcribed from the promoter 5' to exons 1 and 2, is then excluded by splicing. Translation of mRNA continues from the start of exon 1 resulting in the housekeeping isoenzyme 17 amino acids longer at the N-terminus than erythroid isoenzyme (Lannfelt et al., 1989).

Closure of the Tetrapyrrole Ring by Uroporphyrinogen III Synthase (EC4.2.1.75)

Mechanism and reaction: UROSIII, also known as uroporphyrinogen III cosynthase or hydroxymethylbilane hydrolase, catalyses the conversion of hydroxymethylbilane to uroporphyrinogen III (Figure 1.6). It has been established experimentally that this catalysis involves intramolecular inversion of the terminal D ring of hydroxymethylbilane (Leeper, 1994, Shoolingin-Jordan, 1995; Battersby and Leeper, 1998) with the key intermediate being a chiral *spiro* intermediate (Spivey et al., 1996) giving rise to uroporphyrinogen III after cyclisation.

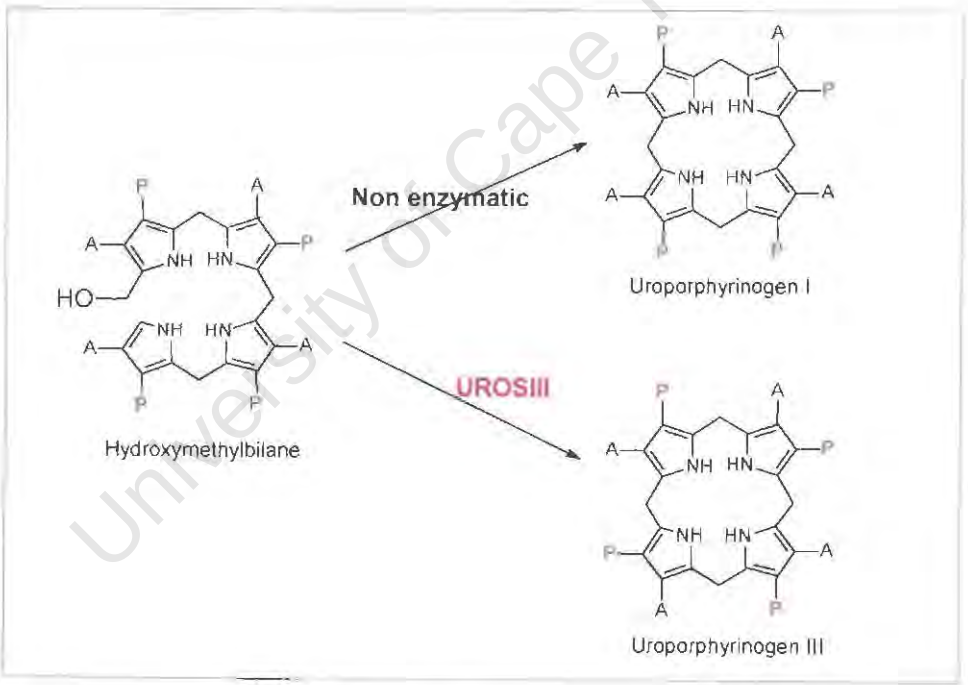

Figure 1.6: Closure of the tetrapyrrole ring by UROSIII. A = acetate, P = propionate.

Enzyme assay: Enzyme activity is assayed by measuring the formation of uroporphyrinogen III from PBG in the presence of excess PBG deaminase. Alternatively, activity can be measured using hydroxymethylbilane as a substrate (Jordan, 1982; Hart and Battersby, 1985).

Purification and molecular sizes: UROSIII has been cloned, expressed and purified from various sources (Higuchi and Bogorad, 1975; Kohashi et al., 1984; Hart and Battersby, 1985; Smythe and Williams, 1988; Alwan and Jordan, 1988; Alwan et al., 1989; Leeper, 1994, Shoolingin-Jordan, 1995; Battersby and Leeper, 1998) including human erythrocytes (Tsai et al, 1987).

Most forms of the protein exist as monomeric subunits of molecular weight approximately 30000 Da (Jordan, 1990). The protein is thermolabile and is thus poorly characterised. There is no evidence for a cofactor. This enzyme is present in excess over PBG deaminase, favouring synthesis of uroporphyrinogen III over uroporphyrinogen I (Tsai et al., 1987; Desnick et al., 1998).

Gene sequence: The gene that encodes UROSIII has been isolated from various sources including animals and bacteria (Jordan et al., 1988; Tsai et al., 1988; Stamford et al., 1995; Amillet and Labbe-Bois, 1995; Xu et al., 1995). The full-length cDNA encoding human UROSIII has been isolated, sequenced, and expressed in *E. coli* (Tsai et al., 1988). A single UROSIII gene in humans has been mapped to chromosome region 10q25.3–10q26.3 (Astrin et al., 1991). Both human and mouse UROSIII have 5' and 3' untranslated region (UTR) and an open reading frame spanning 10 exons that encode 265 amino acids. The human and mouse share 80% nucleotide gene sequence, and 78% amino acid identity (Xu et al., 1995).

Modification of the peripheral side chains of the tetrapyrrole

Biosynthesis of Coproporphyrinogen III by Uroporphyrinogen Decarboxylase (EC4.1.1.37)

Reaction and Mechanism: Uroporphyrinogen decarboxylase (UROD) catalyses the stepwise decarboxylation of four acetate side chains in the 8-carboxylic (COOH) uroporphyrinogen III molecule through formation of 7-, 6-, and 5-COOH intermediates resulting in the formation of the 4-COOH coproporphyrinogen III (Figure 1.7). This reaction takes place in the cytoplasm. The decarboxylation of these porphyrins starts on ring D and proceeds through rings A, B, and C before the final formation of coproporphyrinogen III (Jackson et al., 1976). No cofactor is required. It has been postulated that this process could take place in 24 possible ways forming 14 possible isomeric intermediates (McDonagh and Bissel, 1998). The precise mechanism remains unclear. Each intermediate acts as a substrate for further decarboxylation until coproporphyrinogen III is formed. Both the series I and III isomers can act as substrates but the series III isomer is more rapidly decarboxylated (Smith and Francis, 1981).

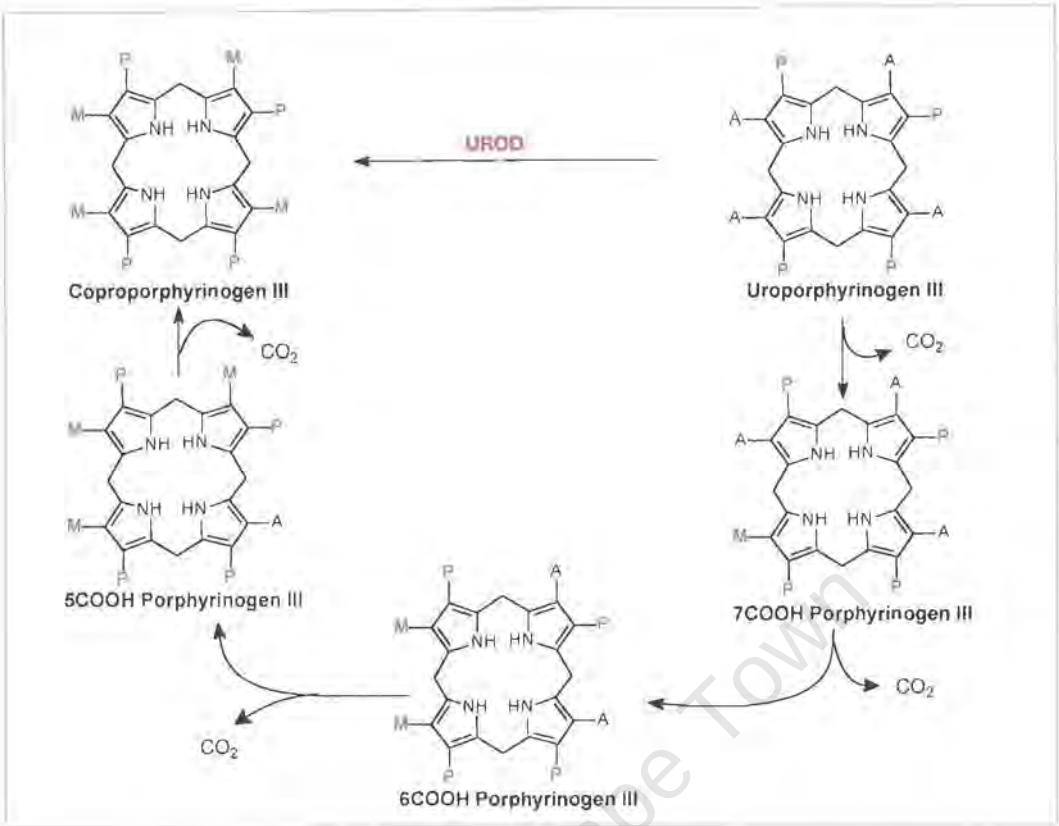

Figure 1.7: **Biosynthesis of coproporphyrinogen III from uroporphyrinogen III by UROD. A = acetate, P = propionate, M = methyl.**

Enzyme assay: UROD activity measurements are difficult to interpret because of the multiple substrates and products involved in the reaction. Activity can be monitored using uroporphyrinogen III as a substrate, and measuring product formed (hepta-, hexa-, pentacarboxyl porphyrin and coproporphyrinogen III) (Straka et al., 1982) by fluorimetric HPLC (or TLC). Uroporphyrinogen I can be used as a substrate since it is easier to prepare than uroporphyrinogen III. It is however preferable to use the penultimate component in the catalytic chain, 5-carboxyl porphyrinogen as substrate and to measure its conversion to coproporphyrinogen III, after oxidation which can be quantified to coproporphyrin (Straka et al., 1982; Elder and Wyvill, 1982; McManus et al., 1988).

Purification and molecular sizes: UROD has been purified from human erythrocytes (de Verneuil et al., 1983; Elder et al., 1983; Mukerji and Pimstone, 1992; Roberts and Elder, 1997), chicken erythrocytes (Kawanishi et al., 1983; Seki et al., 1986), bovine liver (Straka and Kushner, 1983), *E. gracilis* (Juknat et al., 1989), *S. cerevisiae* (Felix and Brouillet, 1990), and *R. sphaeroides* (Jones and Jordan, 1993). Most of these proteins are monomeric with molecular weight varying from 40000 Da (Elder et al., 1983) to 46000 Da

(de Verneuil et al., 1983). Chicken enzyme has been reported to exist as a dimer with molecular weight of 40000 for each monomer (Kawanishi et al., 1983).

Gene sequence: The UROD gene has been cloned and analysed from a number of species. Human and rat cDNA sequences show a homology of 85% and protein identity of 90% (Romeo et al., 1986; Romana et al., 1987a). Similarly UROD cDNA from mouse and human show a homology of 88% and 90% for protein identity (Wu et al., 1996). The cDNA sequence analysis of UROD between *S. cerevisiae* (Garey et al., 1992; Diflumeri et al., 1993), *Synechoccus* (Kiel et al., 1992) and human, showed a 50% homology and 32% protein identity. In addition, full-length UROD cDNA from *Nicotiana tabacum L.* (plant tobacco) and a partial UROD cDNA from *Hodeum vulgare L* (barley) have been cloned and sequenced (Mock et al., 1995). Their properties were similar to those of UROD obtained from other sources (mammals, plants, yeast and bacteria) (Elder and Roberts, 1995).

Human UROD (367 amino acid residues with molecular weight of (≈ 41000 dalton) is expressed by a single gene containing 10 exons within 3kb of DNA, which has been mapped to chromosome 1p34 (de Verneuil et al., 1984; Mclellan et al., 1985; Dubart et al., 1986; Romeo et al., 1986). Two transcriptional start sites separated by six nucleotides were identified by Romana et al. (1987b).

X-ray crystallographic studies on human UROD expressed with a histidine tag in *E. coli* were performed at 3.0 Å resolution (Phillips et al., 1997; Laterriere et al., 1997). Subsequently the UROD crystal structure has been determined at 1.6 Å resolution (Whitby et al., 1998). The structure showed a protein of 40 800 dalton composed of a single domain containing a (β/α) 8-barrel with a deep active site cleft formed by loops at the C-terminal ends of the barrel strands.

Enzyme inhibition: Experimental studies showed that iron and chlorinated hydrocarbons decrease enzyme activity. This effect is greatly enhanced when both are involved (Constantin et al., 1996). Inhibitor studies suggested that certain conserved histidines, lysines, and arginines are important residues for enzyme activity (Whitby et al., 1998). However, site-directed mutagenesis experiments indicate that no single cysteine is absolutely critical for the integrity of the catalytic site but one histidine residue (human H339) has been identified as important in imparting isomer specificity (Wyckoff et al., 1996).

Biosynthesis of Protoporphyrinogen IX by Coproporphyrinogen Oxidase (EC1.3.3.3.)

Reaction and Mechanism: CPOX is located within the mitochondrial intermembrane space (Sano and Granick, 1961; Batlle et al., 1965; Poulson and Polglase, 1974; Elder and Evans, 1978a; Grandchamp et al., 1978) and catalyses the decarboxylation and oxidation of the propionate side chains of the A and B pyrrole rings in coproporphyrinogen III to vinyl groups (Figure 1.8). The enzyme requires molecular oxygen for activity (Sano and Granick, 1961; Yoshinaga and Sano, 1980) and the end product of the reaction is protoporphyrinogen IX.

The enzymatic conversion of two propionate side chains proceeds via an intermediate tripropionate monovinyl porphyrinogen, harderoporphyrinogen (2-vinyl, 4-propionate porphyrinogen) in a clockwise fashion. The propionate side chain in position 2 is the first to decarboxylate and the reaction proceeds at a faster rate than the subsequent decarboxylation at position 4. Since protein tyrosine residues may be involved in β-hydroxypropionate formation (Sano and Granick, 1961; Yoshinaga and Sano, 1980; Dailey, 1990), free harderoporphyrinogen is not released from the enzyme and the oxygen-dependent reaction probably involves hydroxypropionate intermediates prior to decarboxylation. An alternative scheme suggested that a hydroxylation reaction does not occur, but that the reaction proceeds via a hydride removal during the decarboxylation (Seehra et al, 1982). It's possible that both schemes may occur in nature depending on the organism (Dailey, 1990).

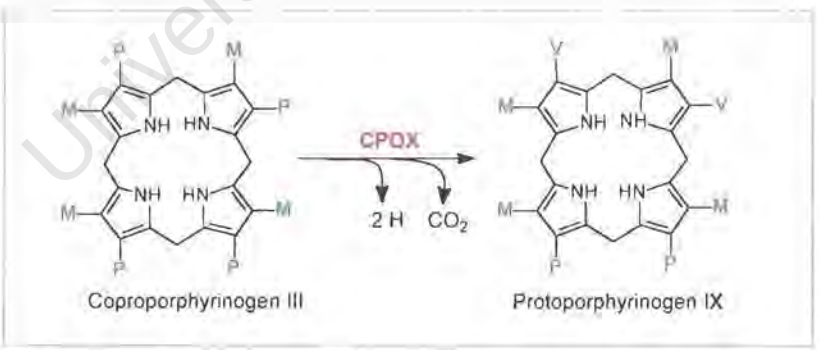

Figure 1.8: **Biosynthesis of protoporphyrinogen IX from coproporphyrinogen III by CPOX. P = propionate, M = methyl, V = vinyl.**

Enzyme assay: CPOX is assayed using either colourimetric or radiochemical methodology. The radiochemical method is more sensitive and measures the production of $^{14}CO_2$ from coproporphyrinogen III with ^{14}C-labelled carboxyl carbons in the 2 and 4 propionate groups (Elder and Evans, 1978b). An alternative method is to measure the

production of the ^{14}C-labelled protoporphyrin IX from labelled coproporphyrin III (Grandchamp and Nordmann, 1982).

Purification and molecular sizes: CPOX has been purified to homogeneity from different species such as rat (Batlle et al., 1965), bovine liver (Yoshinanga and Sano, 1980; Kohno et al., 1993), *S. cerevisiae* (Camadro et al., 1986), and mouse liver (Bogard et al., 1989). Human CPOX was expressed in *E. coli* and purified to homogeneity for characterisation. The protein is a nearly globular homodimer with subunits of molecular weight approximately 39000 Da (Medlock and Dailey, 1996; Martàsek et al., 1997). Spectroscopic analysis of purified protein did not show any detectable redox active metals. This is in contrast to other studies that indicate that the mouse enzyme was a metalloprotein associated with Cu^{2+} as essential cofactor (Kohno, et al., 1996).

The CPOX amino acid sequences derived from *S. cerevisiae* (Zagorec et al., 1988), mouse (Kohno et al., 1993), soyabeans (Madsen et al., 1993), *Salmonella typhimurium* (Xu and Elliot, 1993), and human (Martàsek et al., 1994a) were compared by progressive alignment and demonstrated a protein with 32% homology. Human and *S. cerevisiae* CPOX revealed 49% homology. The carboxyl-terminal parts of the two proteins are highly conserved when compared to the amino-terminal part. The amino-terminal domain of the mammalian CPOX is known to direct the protein into the intermembrane space of the mitochondria (Elder and Evans, 1978a; Grandchamp et al., 1978; Dailey, 1990) and is positively charged.

The cDNA sequence encoding human CPOX has been cloned, sequenced and characterised (Martàsek et al., 1994a; Delfau-Larue et al., 1994; Medlock and Dailey, 1996). The cloned gene and the N-terminal amino acid sequence of purified CPOX contains a 110-amino acid N-terminal signal peptide, and this signal peptide is removed on transportation into intermembrane space of mitochondria, where mature enzyme resides (Martàsek et al., 1994a; Delfau-Larue et al., 1994). The length of this leader sequence from mouse liver was initially proposed to be 31 amino acid residues (Kohno et al., 1993; Taketani et al., 1994).

Gene sequence: Cloning and characterisation of human CPOX cDNA (Delfau-Larue et al., 1994) revealed a single gene with multiple transcriptional initiation sites. The gene spans approximately 14 kb and consists of seven exons and six introns. The gene was mapped to chromosome 3q12 (Cacheux et al., 1994). Potential regulatory elements have been identified in the GC-rich region. These consist of six Sp1, four GATA, and one CACCC sites. It is postulated that a single promoter may be differentially regulated in erythroid and nonerythroid tissues (Taketani et al., 1994; Martasek et al., 1994), and

CPOX transcripts increase during eythroid cell differentiation (Conder et al., 1991; Taketani et al., 1995a). The CPOX gene also contains two polyadenylation signals that are separated by 126 base pairs (bps) (Martàsek et al., 1994a). These two signals, differently utilised may possibly play a role in tissue-specific expression of CPOX mRNA (Martàsek et al., 1997).

Enzyme inhibition: CPOX activity in human lymphocytes is inhibited by low concentrations of metals such as cadmium and mercury. Other organometal compounds (tetraethyl lead, tributyltin, and methylmercury) also inhibit CPOX activity. Haem breakdown products, haemin and bilirubin (BR) inhibit CPOX activity non-competitively at low concentration (Batlle et al., 1965; Woods and Southern, 1989; Rossi et al., 1992).

Oxidation of protoporphyrinogen IX and insertion of iron

Oxidation of Protoporphyrinogen IX to Protoporphyrin IX by Protoporphyrinogen Oxidase (EC1.3.3.4)

PPOX, the penultimate enzyme in the haem biosynthetic pathway, catalyses the oxidation of protoporphyrinogen IX to protoporphyrin IX (Porra and Falk, 1964; Poulson and Polglase, 1975; Dailey, 1990). The reaction involves the six-electron oxidation of the photodynamically inactive substrate, protoporphyrinogen IX, into a fluorescent product, protoporphyrin IX (Cox and Whitten, 1983; Girotti and Deziel, 1983). This enzyme forms the basis of this dissertation and is discussed in detail in Chapter 2.

Insertion of Iron by Ferrochelatase (EC4.99.1.1)

Reaction and Mechanism: The last step of the haem biosynthetic pathway is catalysed by FC. Ferrous iron (Fe^{2+}) is inserted into the protoporphyrin IX macrocycle to form haem (Figure 1.9) (Goldberg et al., 1956; Bugany et al., 1971; Bonkovsky et al., 1975; Dailey, 1990,1996). FC is located on the matrix side of the inner mitochondrial membrane and the mechanism of action appears relatively conserved among species. All have similar substrate specificity with their natural substrates being Fe^{2+} and protoporphyrin IX (Dailey, 1996). FC can in addition to Fe^{2+} incorporate other metal ions such as Co^{2+} and Zn^{2+} into protoporphyrin IX (Camadro et al., 1984) *in vitro*. Various bivalent metals (Mn^{2+}, Cd^{2+}, Hg^{2+}, and Pb^{2+}) are competitive inhibitors for all FCs examined to date (Dailey et al, 2000). Enzyme activity is stimulated by fatty acids (Labbe et al., 1968; Sawada et al., 1969).

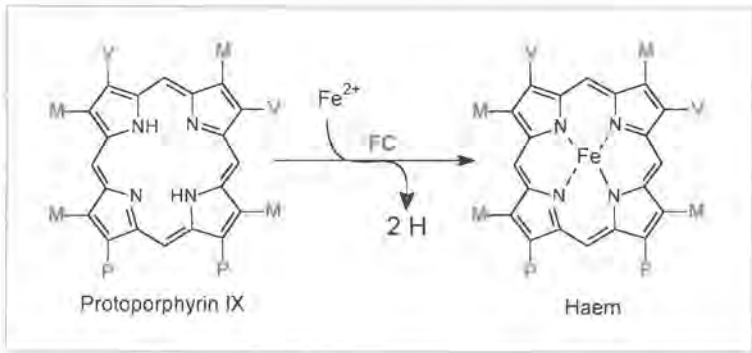

Figure 1.9: **Insertion of Iron into protoporphyrin IX molecule by FC. P = propionate, M = methyl, V = vinyl.**

FC is thought to follow an ordered "bi-bi" reaction mechanism in which Fe^{2+} binds the enzyme before porphyrin (Dailey and Fleming, 1983). Following metal binding to enzyme, the porphyrin undergoes distortion into a non-planar structure that facilitates porphyrin metal-chelation (Lavalle, 1988; Blackwood et al., 1997). Raman resonance spectroscopy of yeast FC demonstrated simultaneous tilting, or doming, of all four pyrrole rings on porphyrin distortion (Blackwood et al., 1997, 1998). Metal-chelation then occurs with the concomitant removal of the two pyrrolic protons.

Enzyme assay: Determination of FC activity is conducted under minimal light since the substrate is light sensitive. ^{59}Fe is used as a substrate, and radioactivity of the haem fraction after incubation with the enzyme is determined (Bloomer and Morton, 1982). An alternative method is to use mesoporphyrin as a substrate and measure the resultant mesohaem spectrophotometrically (Porra, 1976a).

Enzyme structure: Mature FC for both human and mouse have been cloned, expressed, purified and characterised by site-directed mutagenesis and spectroscopy (Dailey et al., 1994a, 1994b; Sellers et al., 1996; Brian et al., 1996). Unlike yeast or prokaryotic FC, human and mouse FC display iron sulphur clusters ([2Fe-2S] clusters capable of cycling between the +2 and +1 core oxidation levels) at the carboxyl end of the purified FC. FC activity may be regulated by lability of this cluster (Sellers et al., 1996). The cluster is destroyed by nitric oxide resulting in loss of activity (Burden et al., 1999). Brian et al. (1996) investigated the amino acid residues in the mammalian (bovine, mouse and human) FC that are involved in ligation of [2Fe-2S] cluster. Mammalian FC had nine conserved cysteine residues that were not present in yeast and bacterial FC which do not contain [2Fe-2S] cluster. Furthermore, mammalian FC contains a 30-residue C-terminal extension that is not in yeast and bacterial FC (Dailey et al., 1994b). Site-directed

mutagenesis and spectroscopic characterisation indicated that of nine conserved cysteine residues, those at positions 403, 406, and 411 serve as ligands for the [2Fe-2S] cluster (Crouse et al., 1996) whereas those at positions 360 and 395 are not involved. The remaining conserved cysteines at positions 31, 196, 236, and 323 were identified as the fourth ligands of the [2Fe-2S] cluster of human FC (Sellers et al., 1998).

The crystal structure of *Bacillus. subtilis* (*B. subtilis*) FC, which lacks the [2Fe-2S] cluster, has been solved to 1.9 Å resolution (Al-Karadaghi et al., 1997). More recently, x-ray structure of recombinant human FC has also been solved at 2.0 Å (Dailey et al., 2000). The enzyme is an 86000 dalton homodimer containing one [2Fe-2S] cluster per subunit. Each monomer contains 48% α-helix and 14% β-sheet structure and is folded into two similar domains. Two differences exist between the two domains: Firstly, an additional 50 residues at the amino-terminal end that constitute a portion of the active site, and secondly, a 30-residue addition at the carboxyl-terminus that participate in ligation of the [2Fe-2S] cluster and dimer stabilisation. Each monomer contains an active site pocket with two hydrophobic lips at its entrance. In the homodimer, both active sites are at the same molecular face, and this is the largest hydrophobic region of the protein. This region has been proposed to serve as the site of membrane attachment. The result of such organisation is that both active sites are within the membrane proper and in position to accept the hydrophobic substrate protoporphyrin IX. The active site pocket contains highly conserved residues such as His 263, which has been proposed to be involved in Fe^{2+} donation (Kohno et al., 1994), but most likely participates along with the highly conserved group of carboxylates in proton abstraction and not in iron donation (Dailey et al., 2000). Fe^{2+} is thought to be inserted from the opposite side of the pocket from His 263. Residues involved in porphyrin macrocycle distortion have not been identified.

Subcellular location, translocation and molecular sizes: FC is a mitochondrial enzyme but is synthesised in the cytoplasm with molecular weight of approximately 47000 Da. It is translocated to the matrix side of the inner mitochondrial membrane and proteolytically processed to the mature form with molecular weight of approximately 42000 Da (McKay et al., 1969; Jones and Jones, 1969; Harbin and Dailey, 1985; Karr and Dailey, 1988; Camadro and Labbe, 1988).

Purification: FC has been cloned, expressed, and purified from various sources including rat liver (Mailer et al., 1980; Taketani and Tokunaga, 1981), *R. sphaeroides* (Dailey, 1982), yeast (Labbe-Bois, 1990), mouse (Taketani et al., 1990; Brenner and Fraiser, 1991), human (Nakahigashi et al., 1990), bovine liver mitochondria (Taketani and Tokunaga, 1982; Dailey and Fleming, 1983; Siepker et al., 1987; Shibuya et al., 1995); *E. coli* (Miyamoto et al., 1991), *B. japonicum* (Frustaci and O'Brian, 1992), *B. subtilis*

(Hannsson and Hederstedt, 1992), *Arabidopsis. thaliana* (*A. thaliana*) (Smith et al., 1994), and barley and cucumber (Miyamoto et al., 1994). FC from all these sources exhibits similar properties.

Gene sequence: The human FC gene was isolated from a placental cDNA library using a radiolabelled mouse cDNA fragment. The gene is encoded by a single gene consisting of 11 exons that spans approximately 45 kb (Brenner et al., 1992), and the chromosomal DNA is localised to chromosome 18q 21.3 (Taketani et al., 1992). A single FC gene is regulated so as to prove for both housekeeping and erythroid-specific functions (Brenner and Frasier, 1991; Brenner et al., 1992). The promoter region contains a CpG island and a Sp1-driven promoter appears to be sufficient for FC expression in non-erythroid cell lines. Erythroid specificity is mediated via GATA-1 and NF-E2 elements. Further studies also suggest a role for chromosomal/chromatin structure and *cis*-acting elements in the regulation of the FC mRNA production in erythroid tissue (Tugores et al, 1994; Magness et al, 1998).

Haem Regulation in Erythroid and Non-erythroid tissues

Haem synthesis in mammals is normally an extremely efficient, tightly controlled process in which the amount of haem produced closely matches the needs of the body (Bloomer and Straka, 1988). This implies that enzymes involved in haem synthesis are normally able to use all of the substrate presented to them, that they can handle an increased flux through the pathway and that the pathway may be subjected to some form of "feedback" control. Indeed, there is much evidence to suggest that, at least in the liver and all nonerythroid tissues, haem itself modulates its own rate of production, principally at the level of ALAS, which is considered the rate-determining enzyme of the pathway. This tight regulation of liver cell haem occurs by several mechanisms (May and Bawden, 1989; Andrew et al., 1990).

Non-erythroid tissues

Firstly, haem regulates its own synthesis by controlling the amount of ALA-S1 mRNA. This occurs primarily at the transcriptional level (Srivasata et al., 1988; Yamamoto et al., 1988). Studies in avian systems suggest that this effect may be mediated by decreasing the stability of ALA-S1 mRNA, and therefore its half-life, thus minimising protein synthesis (Drew and Ades, 1989; Hamilton et al., 1991). Indeed, in mammals, the half-life of ALA-S1 is less than an hour, and half-life for the protein in the mitochondria is even shorter.

Secondly, haem synthesis may be controlled at an ALAS posttranslational level in which haem blocks translocation of pro-ALAS from cytosol into mitochondrion (Yamauchi et al.,

1980; Ades and Harpe, 1981; Hayashi et al., 1983; Srivastava et al., 1983; Drew and Ades, 1989). This is mediated by two cysteine-containing haem regulatory motifs in the leader sequence (Lathrop and Timko, 1993).

Erythroid tissues

The control mechanism of ALA-S2 in erythroid tissues is different (Ponka, 1997). ALA-S2 is controlled primarily at the transcriptional level by erythroid-specific transcription factors interacting with non-coding regions of the gene (Cox et al., 1991; May et al., 1995). The same factors are involved in induction of globin synthesis following induction of haem synthesis indicating the importance of haem *per se* as a regulatory molecule (Sassa, 1998).

ALA-S2 may also be controlled at posttranscriptional level but differently from non-erythroid tissue. In the ALA-S2 gene there is a *cis*-acting regulatory iron element in the 5'-UTR (Cox et al., 1991) that is similar to the stem-loop structure occurring in the 5'-UTR of ferritin mRNAs (Klausner et al., 1993). In this control mechanism, a protein binds to the iron regulatory element and inhibits translation of mRNA. However, in the presence of iron, the protein dissociates and the mRNA binds to the ribosomes and is translated (Melefors et al., 1993). The translation of ALA-S2 mRNA is therefore coupled to the availability of iron. In the leader sequence of ALA-S2, there are identical cysteine-containing haem regulatory motifs to those found in the ALA-S1 gene, and it has been suggested that similar mechanisms of haem-mediated feedback inhibition may occur in erythroid haem synthesis (Lathrop and Timko, 1993). Thus translocation of ALAS to the mitochondrion may also be a controlled event in erythroid tissue.

The Porphyrias

The porphyrias are characterised by a reduction in the activity of one or other of the enzymes in the haem biosynthetic pathway (Table 1.1) (Waldenström, 1957; Brodie et al., 1977; Elder, 1982; Rimington, 1985; Grandchamp and Nordmann, 1988; Kappas et al., 1989). Most are Mendelian autosomal dominant disorders; some are recessive or acquired disorders. In the inherited porphyrias mutations have been identified in genes encoding specific haem pathway enzymes, with resultant defective protein structure or reduced enzyme synthesis (Moore et al., 1987). The enzyme deficiency potentially blocks production of the end product haem, which may activate the rate-controlling enzyme ALAS, consequently resulting in an increase in production (and excretion) of haem precursors. In some circumstances, more than one enzyme may be affected (Watson et

al., 1975; Day et al., 1982; Martàsek et al., 1983; McColl et al., 1985; Doss, 1989; Sturrock et al., 1989; Nordmann et al., 1990; Gregor et al., 1994).

A particular type of porphyria may be identified, demonstrating a characteristic excretion pattern of porphyrins and precursors in the urine and faeces (Moore et al., 1987). The more water-soluble porphyrin precursors ALA and PBG are excreted mainly in the urine. Other porphyrins that are not water-soluble are excreted mainly in the faeces by way of the bile.

Clinically the porphyrias may be characterised by a propensity to acute neurovisceral crises, photosensitive skin disease, or both. The signs of the acute porphyric attack invariably include severe abdominal pain and may include nausea, vomiting and paralysis. The pathogenetic mechanisms whereby the acute attack is established are poorly understood. The most likely hypotheses include ALA neurotoxicity and haem deficiency, acting either directly within the neuron or via a deficiency of one or more essential haemoproteins (Meyer et al, 1998).

The skin may present as a classic photodermatitis with increased fragility and lesions of the sun-exposed surfaces. Occasionaly, patients who suffer repeated trauma and constant exposure to the sun develop progressive pseudosclerodermatous changes on the hands and fingers. Facial features may include hypertrichosis, thickening, grooving, and premature ageing (Meissner et al., 2002). The photocutaneous lesions result from the accumulation, in tissues, of oxidised porphyrins that can absorb ultraviolet and visible light energy to produce free-radical species.

The porphyrias have a worldwide distribution with some countries having an exceptionally high frequency (eg. AIP in Northern Scandinavia and VP in South Africa). The high frequency of VP in South Africa has been attributed to a founder effect (Dean, 1971; Meissner et al., 1987, 1996). A detailed study of this disorder will follow in the next chapter.

Table 1.2: **Enzyme etiology, clinical involvement, pattern of inheritance and chromosomal location**

A ***Acute porphyria***

Acute Porphyric Disorder	Enzymes	Acute attack/ Photosensitivity	Inheritance	Chromosome location
ALADP	ALA Dehydratase (PBG Synthase)	AA	AR	9q34
AIP	PBG deaminase (Hydroxymethylbilane synthase)	AA	AD	11q24.1-q24.2
HCP	Coproporphyrinogen oxidase	AA + PS	AD	3q12
VP	Protoporphyrinogen oxidase	AA + PS	AD	1q21-q23

B ***Non-acute porphyria***

Non-acute Porphyric Disorder	Enzymes	Acute attack/ Photosensitivity	Inheritance	Chromosome location
CEP	Uroporphyrinogen III Synthase	PS	AR	10q25.2-q26.3
PCT	Uroporphyrinogen decarboxylase	PS	AD	1p34
EPP	Ferrochelatase	PS	AD	18q21.3

Abbreviations:

PBG = PBG
ALADP = ALA dehydratase porphyria
HCP = Hereditary coproporphyria
AA = Acute attack
AD = autosomal dominant
CEP = Congenital erythropoietic porphyria
PCT = Porphyria cutanea tarda
ALA = Aminolaevulinic acid
AIP = Acute intermittent porphyria
VP = Variegate porphyria
PS = Photosensitivity
AR = autosomal recessive
EPP = Erythropoietic protoporphyria

The specific syndromes of porphyria

ALA Dehydratase deficiency

ALA dehydratase porphyria (ALADP) also known as plumboporphyria or "Doss" porphyria is an extremely rare autosomal recessive disorder and has its initial presentation during infancy and in adolescence (Doss et al., 1979; Thunell et al., 1987; Fujita et al., 1987; Kappas et al., 1995). Reduced ALAD activity has been demonstrated in erythrocytes (Doss et al., 1982; Doss and Sassa, 1994) and lymphocytes (Sassa et al., 1991). Five cases have been reported since the first description in 1979. Three of the patients have been shown to be compound heterozygotes bearing a single base substitution, unique to each patient, on each allele (Sassa, 1998); the other two are true homozygotes (De Verneuil et al., 1985).

Molecular Biology: The disease was first described at a molecular level in a German patient shown to be a compound heterozygote for two separate point mutations (A274T and A240W) (Ishida et al., 1990). Expression of the two mutant cDNA genes in Chinese hampster ovary (CHO) cells, demonstrated that A274T had little activity compared to A240W that has partial activity. Pulse-labelling studies demonstrated that the A240W mutant resulted in enzyme with a shortened-half life and A274T resulted in limited synthesis of a protein with a normal half-life (Ishida et al., 1992). It was suggested that survival of the patient is due to the residual activity of A274T mutant enzyme since A240W mutant enzyme is non-functional. A Swedish child has also demonstrated compound heterozygosity (Plewinska et al., 1991). The two missense mutations, G133R and V275M, occur at a CpG dinucleotide, and may alter the structure of the functional regions of the enzyme unit. Patients with such mutations, alone, do not present any clinical consequences (Bird et al., 1979).

PBG Deaminase deficiency

AIP is the clinical syndrome associated with PBGD deficiency. This is the commonest of the acute porphyrias and is transmitted as an autosomal dominantly inherited disorder with incomplete penetrance. There is a 50% decrease in PBG deaminase activity in all tissues including erythrocytes in most patients (Strand et al., 1972; Doss and Sassa, 1994). Decreased PBG deaminase activity has been detected in tissues such as liver (Miyagi, 1970), fibroblasts or in transformed lymphoblast culture of the affected patients (Meyer, 1973; Sassa et al., 1978; Kappas et al., 1989). Some individuals who carry a gene mutation associated with AIP do not show any clinical symptoms and may remain biochemically silent (Lamon et al., 1979; Kappas et al., 1989; Anderson et al., 1990). Clinical symptoms include the acute attack only. High prevalence AIP has been reported

in Europe (1-2/10000) by Elder et al., 1997. In Finland the prevalence has been estimated at 2/1000 (Mustajoki et al., 1992).

Molecular biology: The PBG deaminase gene was the first to be sequenced in a human porphyria, and the molecular genetics of AIP were the first to be analysed in detail (Mustajoki and Desnick, 1985). Over 120 mutations causing AIP have been identified (Astrin and Desnick, 1994; Puy et al., 1997). Most of these mutations lie in the region of the gene that is common to both the erythroid and non-erythroid isoenzymes. Four of the mutations lie in and around exon 1, affecting the activity of the housekeeping isoenzyme, leaving erythroid PBGD isoenzyme active (Kauppinen et al., 1995). This accounts for the small population of families with AIP who have a normal erythrocyte PBGD activity. Three of these mutations disrupt splicing of exon 1 while the remaining one blocks initiation of translation (Kauppinen et al., 1995). The mutations are heterozygous. No large deletions have been shown. Twenty five % of mutations code for small insertions or deletions (1 – 30 nucleotides), resulting in translational shifts, leading to premature termination of protein synthesis. Another 15% of the mutations are located at exon-intron junctions prevented normal splicing of primary transcripts or base substitutions that create stop codons leading to incomplete translation of mRNA. About 45% of mutations have a single base substitution resulting in amino acid substitution. Protein encoded by a mutant allele may be absent (85% of cases) or stable with abnormal catalytic properties (15% of cases) (Grandchamp et al, 1989a,b; Chen et al., 1994).

There is high variability in the prevalence of AIP mutations. Mutations investigated from Finland and France (Kauppinen et al., 1995; Puy et al., 1997) revealed a similar pattern with 52 – 60% of mutations clustered in exons 10, 12, and 14. About half of the mutations (44 – 56%) produce amino acid substitutions affecting the coding region of the gene. Some mutations are prevalent in countries like Sweden (W198X) (Mgone et al., 1992), Holland (R116W) (de Rooij et al., 1995), and Argentina (G111R) are reported and ascribed to a founder effect (Lee and Anvret, 1991; De Sjervi et al., 1996). About 10% of unrelated families in United Kingdom share the R173W mutation in exon 10 (Whatley et al., 1995).

Uroporphyrinogen III Synthase deficiency

The clinical syndrome associated with a deficiency of UROSIII is the rare congenital erythropoietic porphyria (CEP), inherited as an autosomal recessive erthropoietic porphyria (Kappas et al., 1995; McGovern et al., 1996) and presents with porphyric skin disease alone. Onset of CEP disease is normally from birth with some reports of late-onset cases (Deybach et al., 1987; Xu et al., 1996). The disease primarily affects haem

synthesis in the erythroid compartment. Severe UROSIII deficiency results in failure of production of physiologically relevant series III porphyrin isomers, and series I isomers of uroporphyrin, and its decarboxylated derivatives accumulate as a result of spontaneous cyclisation and decarboxylation. Apart from photomutilation (usually severe), clinical features include haemolysis, mild splenomegaly and anaemia. Mutations have been identified in diverse racial and demographic groups such as Japanese, Indians, Northern Europeans, Hispanics, and African Americans.

Molecular Biology: Some patients are homoallelic for a specific mutation whereas others are heteroallelic. The most common mutations are C73R, L4F, T288M, and S212P. A wide variety of UROSIII mutations have been reported including 12 single base substitutions, one nonsense and 11 missense mutations, a large deletion with two insertions, and three splicing mutations (de Verneuil et al., 1989; Warner et al., 1990; Deybach et al., 1990; Boulechfar et al., 1992; Bensidhoum et al., 1995; Xu et al., 1995; Tanigawa et al., 1996). Four single base changes (T288M, G225S, A66V, and A104V) occur at a hypermutatable CpG dinucleotide (Barker et al., 1984; Cooper and Krawezak, 1990). There is evidence for some genotype-phenotype correlation in CEP. Thus the C73R mutation results in the detection of <1% of normal activity when expressed in *E. coli.* Human homozygotes for this mutation appear to demonstrate an extremely severe phenotype, which may include profound anaemia, hydrops fetalis and transfusion dependency at birth. Patients who carry both C73R and a second mutation, which appears to express somewhat more residual activity may demonstrate a moderately severe phenotype; whereas patients who are allelic for mutations with more residual activity have milder forms of CEP (Desnick et al., 1998).

Uroporphyrinogen Decarboxylase deficiency

UROD deficiency results in porphyria cutanea tarda (PCT), which is the most common form of porphyria encountered in most countries and may be inherited or acquired (sporadic). PCT can be divided into these two main types based on measurements of erythrocyte enzyme activity (De Verneuil et al., 1978). Both types (sporadic and familial forms) are clinically indistinguishable. In sporadic PCT, UROD deficiency occurs in the hepatic tissues with erythrocyte UROD remaining active (Garey et al., 1993). In familial PCT, UROD deficiency occurs in all tissues including hepatic and erythroid (Elder, 1988). Clinical manifestations of PCT consist of skin photosensitivity (Grossman et al., 1979; Mascaro et al., 1986) on light-exposed skin. Porphyrin profiles show increased uroporphyrin and heptacarboxylic porphyrins, pentacarboxylic porphyrin and a small amount of isocoproporphyrin in urine and plasma (Seubert et al., 1985). In faeces, porphyrin fractionation shows a large fraction of isocoproporphyrin, followed by

heptacarboxylic, hexacarboxylic, and pentacarboxylic porphyrin (Smith and Francis, 1983).

Molecular biology (Familial PCT): About 20% of patients with PCT represent familial PCT in which it is inherited as an autosomal dominant trait but with low clinical penetrance: Most clinically expressed cases of familial PCT will be found to have associated risk factors known to produce sporadic PCT, though the average age of onset may be earlier (De Verneuil et al., 1978; McManus et al., 1988; Elder et al., 1989; Held et al., 1989; Koszo et al., 1992). This suggests that in many cases, the presence of a mutant UROD is not of itself sufficient to result in clinical symptoms, but that when exposed to factors thought to inhibit UROD, the threshold for development of symptoms is lower.

At least 34 UROD gene mutations have been shown in familial PCT. Most are restricted to single families (Garey et al., 1989; McManus et al., 1996; Sorkin et al., 1996; Moran-Jimenez et al., 1996). Where patients are homoallelic for a UROD mutation, or are heteroallelic for two such mutations, a severe phenotype referred to as hepatoerythropoietic porphyria (HEP) may result (Roberts et al., 1995a; McManus et al., 1996; Moran-Jimenez et al., 1996). HEP is expressed clinically as severe photosensitivity with overproduction of porphyrin associated with onset during early childhood (Elder and Roberts, 1994; Moran-Jimenez et al., 1996).

Conditions associated with sporadic PCT: Sporadic PCT is clearly associated with a number of associated, and presumably causally related, factors. These include hepatic iron overload, alcohol consumption, oestrogen therapy, viral infection – particularly hepatitis C virus (HCV) and human immunodeficiency virus (HIV) – certain hydrocarbon based toxins such as hexachlorobenzene and rarely, some systemic disorders including systemic lupus erythematosus and lymphoma (Doss et al., 1972; Dehlin et al., 1973; Hift and Kirsch, 1995; Elder, 1998;). In nearly all cases of PCT, at least one of these disorders is present; frequently, several are present in combination. Patients with chronic renal failure and patients treated with chronic dialysis may develop PCT (Day and Eales, 1982, Moore et al., 1987).

Excess iron has been reported to inhibit UROD activity *in vitro* (Kushner et al., 1975). Increased liver iron stores have been shown in many cases with increased ferritin and transferrin concentration (Lundvall et al., 1970; Rocchi et al., 1986; Fargion et al., 1996). Patients from Northern Europe showed homozygosity for the C282Y *HFE* gene mutation that has been associated with genetic haemochromatosis (Kushner et al., 1985; Roberts et al., 1997; Bonkovsky et al., 1998; Stuart et al., 1998). This association is not seen in other populations: the H63D mutation may be associated in patients of southern European

origin and suggests that a high transferrin saturation level in a patient with PCT might imply homozygosity for the hemochromatosis gene in European populations (Roberts et al., 1997; Bonkovsky et al., 1998; Stuart et al., 1998).

The pathogenesis of deficiencies in UROD is further complicated by the observation that ALA or its derivatives may inactivate UROD (Sweeney, 1986). Long-term administration of ALA to SWR mice decreases UROD activity and produces uroporphyria (Constantin et al., 1996). Decreased UROD activity leads to accumulation of its substrates and their metabolites (Sweeney, 1986). There is an increased concentration of uroporphyrin I and III, heptacarboxylic porphyrin, and other acetic-acid substituted porphyrins in the urine. Urinary PBG excretion is always normal. Uroporphyrin is the main component in increased plasma porphyrin concentration (Seubert et al., 1985).

A high prevalence of HCV antibodies in patients with PCT has been demonstrated in several studies from Southern Europe with seroprevalences ranging from 62 to over 90% (Chuang et al, 1999). However, studies from northern Europe and South Africa suggest a much weaker association. An association with HIV viral infection has also been suggested, though it appears that most such patients have other risk factors for the PCT as well (Drobacheff et al., 1998).

Coproporphyrinogen Oxidase Deficiency

Hereditary coproporphyria (HCP) (Berger and Goldberg, 1955) results from a deficiency in CPOX activity (50% of normal activity in heterozygotes) (Elder et al., 1976; Kappas et al., 1995). It is inherited as an autosomal dominant trait. Homozygous cases with CPOX activity decreased to about 2% of the normal activity have been reported (Kappas et al., 1989). HCP occurs less frequent than AIP, and VP (Doss, 1979; Kostrzewska and Gregor, 1995). Decreased CPOX activity has been shown in lymphocytes (Elder et al., 1976; Grandchamp and Nordmann, 1977), cultured fibroblasts (Elder et al., 1976), leukocytes (Brodie et al., 1977), and liver (Hawk et al., 1978). As with AIP, HCP may remain clinically and biochemically silent with symptoms showing only after puberty. Clinical features of HCP include both acute attack and cutaneous photosensitivity (Brodie et al., 1977; Kappas et al., 1989, 1995).

Molecular Biology: At least 19 mutations in the CPOX gene have been reported, including two for the homozygous form of HCP, (Delfau-Larue et al., 1994; Martàsek et al., 1994b; Fujita et al., 1994; Grandchamp et al., 1995; Sassa et al., 1997; Rosipal et al., 1999), confirming the genetic heterogeneity of HCP. Five missense mutations are reported to reduce CPOX activity, whereas a 5-bp insertion disrupts the presequence and prevents translocation to mitochondria in another (Bissbort et al., 1988). One of the

mutations described (R311W) is suspected to create a new porphyrin-binding site (Martàsek et al., 1997). Other mutations in HCP (Martàsek, 1998) include the G189S mutation, which is thought to abolish the inherent flexibility of the enzyme-substrate interaction; E201K mutant involve replacement of glutamic acid in position 201 by lysine, and reverses the charge (from negative to positive). The local electrostatic environment of the enzyme is altered affecting enzyme functioning. P249S mutant is thought to disrupt the rigidity of the CPOX structure. Three polymorphisms have been described, two in exon 4 and one in exon 5 (Martàsek et al., 1994b). Another mutation (K304E) is responsible for the accumulation of harderoporphyrin that characterises harderoporphyria (Lamoril et al., 1995; Grandchamp et al., 1995).

Protoporphyrinogen Oxidase Deficiency

VP results from decreased activity in the penultimate enzyme of the haem biosynthetic pathway, PPOX. A detailed study on VP and its molecular genetics will follow in Chapter 2.

Ferrochelatase Deficiency

Erythropoietic porphyria (EPP) is associated with decreased activity of the mitochondrial enzyme FC (Magnus et al., 1961). Typically, elevated concentrations of protoporphyrin IX in the erythrocytes, plasma, liver, bile, and faeces are found (DeLeo et al., 1976; Kappas et al., 1989; Goerz et al., 1996). In contrast to the skin disease of CEP, PCT, HCP and VP, which is marked by a vesiculo-erosive pattern of skin injury, skin disease in EPP takes the form of an immediate hypersensitivity. Characteristically patients who exceed an individual threshold of sun exposure manifest problems of burning, stinging, erythema and oedema in exposed areas and learn to associate these unpleasant symptoms with sun exposure; they will voluntarily seek to avoid exposure. These features usually begin in childhood rather than post-pubertally as in the case with the vesiculo-erosive forms of porphyria. Approximately 10% of clinically expressed cases show evidence of severe protoporphyrin IX accumulation in the liver, leading to hepatic injury and ultimately to liver failure. Typically liver decompensation occurs late in the illness, but once initiated, progresses rapidly.

Enzymatic studies performed in some affected families showed EPP to have a complex inheritance (Bloomer et al., 1976; Norris et al., 1990), and the description as an autosomal dominant trait with incomplete penetrance is not entirely accurate (Kappas et al., 1995) as there is evidence to suggest that, in some families at least, particularly those in whom liver damage occurs, an autosomal recessive mechanism appears to fit the observed pattern of inheritance more accurately. Most patients with manifest disease have severely reduced

FC activity, suggesting a disorder carried on both alleles. This has led to the belief that co-inheritance of two defects; one, presumably more severe, from the biochemically abnormal parent and the second, less severe, from an apparently normal parent, is necessary before clinical EPP arises. Since only one parent can be shown biochemically to carry EPP, the disease appears to be dominant, yet its actual inheritance will be recessive (Sarkany et al., 1994).

Molecular Biology: Molecular analyses of the FC gene have revealed missense mutations (Lamoril et al., 1991; Brenner et al., 1992; Imoto et al., 1996), splicing abnormalities (Nakahashi et al., 1992; Wang et al., 1994; Sarkany et al., 1994), intragenic deletions (Todd et al., 1993; Schneider-Yin et al., 1995; Henriksson et al., 1996), and nonsense mutations (Schneider-Yin et al., 1994) associated with functional deficiency of FC. These mutations are distributed throughout the gene, and in most cases are limited to single families (Cox et al., 1998), though in Northern Ireland, one mutation may account for 50% of cases, and for a further 3 families from the United States (Todd et al., 1993; Wang et al., 1994).

Recently, Gouya et al. (2002) using haplotype segregation analysis on 25 families with EPP (with identified mutations), identified an additional intronic single nucleotide polymorphism (IVS3-48T/C), which modulates the use of a constitutive aberrant receptor splice site resulting in mRNA that is degraded by a nonsense-mediated decay mechanism. It is believed that this additional FC enzyme deficiency is necessary for EPP phenotypic expression.

ALA Synthase deficiency

Although not strictly a porphyria, it is worth considering that inherited defects in ALAS may also occur. Indeed, a defect in ALA-S2 activity is responsible for the X-linked sideroblastic anaemia syndrome, an erythropoietic disorder (Cotter et al., 1992; Cox et al., 1994; Bottomley, et al., 1995) that renders the enzyme resistant to PFP binding. Sideroblastic anaemia is a refractory anaemia with hypochrornic microcytic circulating erythrocytes and characteristic ring sideroblasts in the bone morrow that demonstrates a ring or collar of iron granules around the nucleus (Cotter et al., 1992).

CHAPTER 2

PROTOPORPHYRINOGEN OXIDASE AND VARIEGATE PORPHYRIA

LITERATURE REVIEW 2

Protoporphyrinogen Oxidase

In the presence of oxygen and light, protoporphyrinogen IX undergoes auto-oxidation (in a non-enzymatic reaction) to protoporphyrin IX. Indeed, *in vitro* oxidation of protoporphyrinogen IX occurs very rapidly at neutral and acidic pH. However, in the reducing environment in the cell (where this reaction occurs) catalysis by the enzyme PPOX is required (Porra and Falk, 1964; Poulson and Polglase 1975; Porra, 1976b; Dailey, 1990). Thus, PPOX catalyses the oxidation of protoporphyrinogen IX to the fully conjugated, planar molecule protoporphyrin IX in the penultimate step of haem biosynthesis (Figure 2.1). PPOX appears to be widely distributed among plants, animals and bacteria (Jacobs and Jacobs, 1981; Dailey and Dailey, 1996a,b; Camadro et al., 1999).

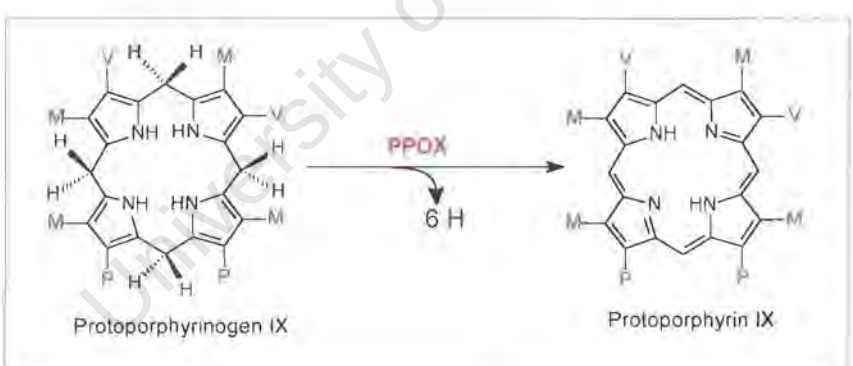

Figure 2.1: **Six electron oxidation of protoporphyrinogen IX to protoporphyrin IX by PPOX. M = methyl, P = propionate, V = vinyl.**

Enzymic oxidation of protoporphyrinogen IX to protoporphyrin IX

The reaction involves the six-electron oxidation of the photodynamically inactive substrate, protoporphyrinogen IX, into the fluorescent product, protoporphyrin IX (Cox and Whitten, 1983; Girotti and Deziel, 1983) and includes the oxidation of the methylene bridges (-CH_2-) into methene bridges (-CH=) and two of the pyrrolic nitrogens. There is little direct evidence to suggest a catalytic mechanism for PPOX,

but it is possible that different mechanisms may exist, especially in prokaryotes that can exist in both aerobic and anaerobic conditions (Camadro and Labbe, 1996; Klemm and Barton, 1987; de Marco et al., 2000). Three molecules of molecular oxygen serve as the final electron acceptor in the reaction, and are reduced to three molecules of hydrogen peroxide, rather than water, in the aerobic reaction, in both eukaryotic and prokaryotic PPOXs (Deybach et al., 1985; Dailey et al., 1994c; Hansson and Hederstedt, 1994; Dailey and Dailey, 1996a; Dailey and Dailey, 1996b). Alternative compounds such as fumarate, nitrate, NAD^+, $NADP^+$, nitrite and others are utilised during anaerobic oxidation (Jacobs and Jacobs, 1976; Klemm and Barton, 1985).

Dailey and Dailey (1997a) suggested two possible reaction mechanisms for PPOX. In the first, PPOX binds the protoporphyrinogen IX substrate and carries out the complete reaction without releasing the macrocycle, and in the second, PPOX catalyses three independent oxidation reactions with the release of tetrahydro and dihydro- intermediates. The latter is a model similar to that of the decarboxylation reactions catalysed by uroporphyrinogen decarboxylase. Subsequent studies by the same group, using stopped-flow fast kinetic analyses have shown that the reaction does indeed proceed via three, two electron oxidations rather than a single, six-electron oxidation (H. Dailey and L. Davids; personal communication, 2001).

Substrate specificity

PPOXs are specific for their natural substrate protoporphyrinogen IX, although oxidation of the non-physiological dicarboxylic mesoporphyrinogen IX has been reported for barley and spinach (Jacobs and Jacobs, 1984), *B. subtilis* (Dailey et al., 1994c; Corrigall et al., 1998a), rat (Poulson, 1975), mouse (Dailey and Karr, 1987) and human (Camadro et al., 1985). Both these porphyrinogen structures are similar, explaining their recognition as substrates by the same enzyme. The rate of oxidation of mesoporphyrin IX is usually slower than that of protoporphyrinogen IX.

B. subtilis PPOX is unique amongst PPOXs in that it catalyses the oxidation of the four carboxylic coproporphyrinogen III molecule in addition to protoporphyrinogen IX and mesoporphyrinogen IX (Hansson and Hederstedt, 1994; Dailey et al., 1994c; Corrigall et al., 1998a). However, *B. Subtilis* PPOX is not a general porphyrinogen oxidase as it is unable to oxidise uroporphyrinogen III (Hansson and Hederstedt, 1994). Although *B. subtilis* PPOX can oxidise coproporphyrinogen III, the organism definitely possesses a specific oxygen-dependent coproporphyrinogen III decarboxylating protein. This is supported by the report of cloning of the *hemN* gene from *B. subtilis,* which encodes a protein performing such a reaction (Hippler et al., 1997). However, the generalisation

of broad substrate specificity for all prokaryotic PPOXs cannot be made, since *Myxococcus xanthus* (*M. xanthus*) has high substrate specificity for protoporphyrinogen IX (Dailey and Dailey, 1996b).

pH optima

PPOXs from different species exhibit different pH optima. In the case of *S. cerevisae* (Poulson and Polglase, 1975), barley (Jacobs and Jacobs, 1984), *R. spheroides* (Klemm and Barton, 1987), potato, maize (Camadro et al., 1991) and *E. coli* (Sasarman et al., 1993), a pH optima in a range of 7.0 – 7.5 was observed. A broad pH optimum (7.0 – 11) for the oxygen-independent enzyme *D. gigas* has been reported. Its large multi-subunit protein complex may contribute to this tolerance over a wide pH range. The pH optima for mammalian PPOXs such as rat, 8.1 – 8.8 (Poulson, 1975); bovine, 8.7 (Siepker et al., 1987); human, 7.2 (Camadro et al., 1985); mouse, 7.1 (Dailey and Karr, 1987) and *B. subtilis*, 8.7 (Corrigall et al., 1998a) have been reported. In contrast, PPOX from Triton X-100 extracts of the mitochondrial and etioplast fractions of etiolated barley displayed maximal activity over a low pH range (5 – 6) (Jacobs and Jacobs, 1987).

Sub-cellular localisation

PPOX distribution in the cell

In mammals and yeast, PPOX activity has been detected in the mitochondrial inner membrane (Dailey, 1990) whereas in plant PPOX activity was found in both plastids and mitochondria (Jacobs and Jacobs, 1987, 1993; Matringe et al., 1992a). In plants, besides the mitochondria and chloroplast, PPOX activity has been found in other subcellular locations such as the plasma membrane (Jacobs et al., 1991; Lee et al., 1993), and the endoplasmic reticulum (Retzlaff and Boger, 1996). Interestingly, the plasma membrane associated with PPOX activity has been found to possess properties, which are different from those of the mitochondrial and chloroplast enzymes, such as its resistance to inhibition by the diphenyl ether herbicides (DPE) which are strong inhibitors of many known and characterised PPOX activities (Jacobs et al., 1991) (see later section on Inhibition).

Several approaches were used in establishing the localisation of PPOX within the cell of various species, and include: separation of subcellular fractions by differential centrifugation methods and assay of PPOX activity (Jacobs et al., 1982; Deybach et al., 1985), and identification of PPOX in isolated subcellular fractions using specific labelled PPOX ligands (Nishimura et al, 1995a).

Subfractionation studies

Deybach et al. (1985) used a digitonin method to fractionate rat liver mitochondria, and showed that PPOX is closely associated with the mitochondrial inner membrane fraction. By chemical treatment they suggested that PPOX was anchored within the lipid bilayer of the inner membrane, and that protoporphyrinogen IX had an equal access to the active site of the enzyme from both sides of the inner membrane.

A membrane impermeable water soluble inhibitor of PPOX (the ditaurine conjugate of BR and reported inhibitor of rat liver PPOX activity in both intact and sonicated mitochondria and mitoplasts) showed that the PPOX catalytic site was on the cytosolic side of the inner membrane since the membrane was impermeable to this inhibitor (Ferreira et al., 1988).

Matringe et al. (1992a) demonstrated that sub-fractionated chloroplast PPOX activity is found in thylakoids and the total envelope membranes, but not in stroma. Subfractionation of yeast mitochondria also showed PPOX activity in the inner membrane (Camadro et al., 1994).

PPOX labelling studies

In PPOX labelling studies, Nishimura et al., (1995a) performed an *in vitro* transcription and translation of the human PPOX to demonstrate the insertion of protein into mitochondria. The [^{35}S]methionine labelled mRNA is translated in the rabbit reticulocyte lysate system to produce labelled protein product. The labelled protein product is imported into isolated intact mouse mitochondria, and extracted from mitochondria. The protein displayed a molecular weight similar to that predicted from the human PPOX gene. This suggested that PPOX does not undergo modification on insertion into the mitochondrial membrane. Proteolytic digestion of the PPOX containing mitochondrial membrane demonstrated that PPOX is protected in the mitochondria. Furthermore, digestion of the PPOX protein on addition of 0.3% Triton X-100 demonstrates the intrinsic association of PPOX with the membrane lipid bilayer.

PPOX localisation in the light of its protein and gene sequence

Analysis of the PPOX gene and protein sequences has shown a lack of membrane targeting leader sequences or obvious internal targeting signals (Dailey and Dailey, 1994; Nishimura et al., 1995a; Dailey and Dailey, 1996a,b). Although human PPOX has an amino terminal portion with characteristic features of a presequence with three basic residues without any acidic residues (Nishimura et al., 1995a), these residues are not clustered on the opposite side of positively charged amino acids, and the hydroxylated amino acids are scattered.

Initial reports on yeast PPOX indicated that the protein was synthesised as a high molecular weight precursor, which is then converted into mature mitochondrial membrane-bound form (Camadro et al., 1994). In a later publication Camadro and Labbe (1996) suggested that the hydropathy profile of yeast PPOX demonstrated a moderately high hydrophobic protein with a single potential membrane-spanning segment for residues 13 – 33. However, analysis revealed that this was not a transmembrane domain.

Later work, on the other hand, demonstrated that palmitoleic acid is a major component involved in the post-translational modification of yeast PPOX (Arnould et al., 1999) and could account for a resultant shift in the electrophoretic mobility, which was at first attributed to a putative presequence form of the protein.

Translocation studies and immunological analysis demonstrated that plastid and mitochondrial isoforms of tobacco plant PPOX are imported into intact pea plant chloroplasts and mitochondria (Lermontova et al., 1997). The plastid PPOX isoform of the tobacco plant is synthesised as a 59000 Da precursor protein, which is processed into a 53000 Da mature PPOX. In contrast, the mitochondrial form did not demonstrate a precursor protein, yet it was targeted. PPOX from *A. thaliana* also indicates the synthesis of a precursor PPOX protein with a putative amino-terminal membrane targeting leader sequence (Narita et al., 1996).

Other PPOXs, which demonstrate a lack of such leader sequences, may possess internal membrane targeting signals, which have not yet been identified. Such unique internal targeting mechanisms have been proposed for other proteins destined for mitochondrial membranes (Lill et al., 1996; Stuart and Neupert, 1996). Examples of such proteins include: BCS1 protein ("branched chain sensitivity"), which is involved in the assembly of complex III. Complex III includes ubiquinol-cytochrome c reductase which is part of the of the mitochondrial respiratory chain which spans the inner mitochondrial membrane. Such proteins contain a stretch of positively charged amino acids (amphiphilic segment) after a transmembrane domain sequence, which are shown to function as the internal targeting signal through the formation of the amphipathic helix (Folsch et al., 1996). It was suggested that the amphipathic helix could react on its apolar side with the transmembrane domain and form a hairpin loop. This loop penetrates the translocation channel of the inner membrane and facilitates translocation.

Enzyme purification

PPOX is a hydrophobic membrane bound protein. Thus, early workers in the field experienced difficulties in attempting to purify it using a variety of standard chromatographic techniques. Solubilisation of PPOX may be achieved by using an appropriate detergent to keep the protein in solution in a stable form. Different detergents have been used in the purification of PPOX from different species and some have proved more suitable than others. For human and *M. xanthus* PPOX, *n*-octyl-β-D-glucopyranoside has been shown to be a suitable detergent (Dailey and Dailey, 1996a,b; 1997a,b). Using this detergent the human enzyme could be stored for days at 4°C, and even overnight storage at room temperature the enzyme retained significant activity (Dailey and Dailey, 1997b). In our laboratory both *M. xanthus* and *B. subtilis* have been purified successfully in the presence of 0.2% Tween 20 (Corrigall et al., 1998a). However, *M. xanthus* PPOX tends to precipitate out when stored at 4°C. Stability is significantly improved by the addition of FAD cofactor (A. Corrigall, personal communication). Prolonged storage of yeast mitochondrial membranes resulted in degradation of PPOX by proteolysis (Camadro et al., 1994). This proteolysis degradation appeared significantly less for PPOX stored at -80°C than at -20°C.

Purification of PPOX was often partial, and occasionally homogeneous. Purifications and subsequent characterisations of PPOX have been reported for rat (Poulson, 1976), *R. sphaeroides* (Jacobs and Jacobs, 1981), *D. gigas* (Klemm and Barton, 1987), mouse (Dailey and Karr, 1987, Ferreira and Dailey, 1988, Proulx and Dailey 1992), yeast (Camadro, et al, 1994), bovine (Siepker et al, 1987), barley (Jacobs and Jacobs, 1987; Jacobs et al., 1989), maize (de Marco et al 2000), spinach (Matringe et al., 1992a, Watanabe et al. 2000) and potato plant (Johnston et al., 1998). In addition to purification from liver mitochondria, human PPOX has been cloned, expressed and purified (Dailey and Dailey 1996a, Nishimura et al, 1995a).

Molecular size and subunit composition

PPOXs from various species such as human (Nishimura et al., 1995a; Dailey and Dailey, 1996a), mouse (Taketani et al., 1995a; Dailey et al., 1995), *B. subtilis* (Hansson and Hederstedt, 1992, Dailey et al., 1994c), *S. cerevisiae* (Camadro et al., 1994), *M. xanthus* (Dailey and Dailey, 1996b), *A. thaliana* (Narita et al., 1996), bovine (Siepker et al., 1987), tobacco plant (Lermontova et al., 1997), spinach (Matringe et al., 1992a), and potato plant (Johnston et al., 1998) exist as homodimers or monomers

with molecular weights ranging from 51000 to 57000 Da. The rat enzyme is the smallest of all mammalian PPOX reported with molecular weight of 33000 Da on SDS-PAGE (Poulson, 1976). Similar results were obtained for the purified barley PPOX (Jacobs and Jacobs, 1987) with molecular weight of 36000 Da. *E. coli* PPOX (Sasarman et al., 1993) and the *D. gigas* multisubunit enzyme (Klemm and Barton, 1987) represent anaerobic enzymatic oxidation and are distinct from the oxygen-utilising forms of the enzyme. Their molecular weights are 21200 and 148000 Da, respectively. The active form of *D. gigas* is a hexamer and is composed of two of each of three different subunits (12000, 18500, and 57000 Da), which are held together by disulfide bonds (Klemm and Barton, 1987).

Cofactor composition in PPOX

It is clear that FAD cofactor is essential in the six-electron oxidation of the PPOX catalysed reaction. Indeed, the human enzyme is a homodimer and contains one non-covalently bound FAD per dimer/0.5 FAD per monomer (Dailey and Dailey, 1996a, 1997b).

The indication of the presence of a prosthetic group, was first suggested by Poulson and Polglase (1975) when they partially purified yeast PPOX and observed an absorption peak at 410nm, although, no flavin was directly observed in their preparations. In studies of PPOX in the anaerobic bacterium *D. gigas*, several electron acceptors (NAD^+, $NADP^+$, FMN, and FAD) that stimulate the reaction were demonstrated (Klemm and Barton, 1985) suggesting the role of these compounds in enzyme activity. Spectral analysis of a purified bovine PPOX showed a typical flavoprotein spectrum. Subsequent characterisation of the extracted flavin cofactor indicated that it was FAD, and that the FAD was covalently bound to the protein (Siepker et al., 1987).

In contrast, Dailey and Karr (1987) performed studies on the purified mouse PPOX by UV/VIS spectral analysis to demonstrate the presence of flavin. The study did not show any flavin bound to PPOX. Several electron acceptors were tested on this enzyme with no significant stimulation of activity (Dailey and Karr, 1987; Ferreira and Dailey, 1988). In a subsequent re-investigation of flavoprotein nature of mouse PPOX by the same group, a flavin moiety was identified in the purified protein from UV/VIS spectral analysis (Proulx and Dailey, 1992). They used a shorter and more rapid scheme for the purification of the mouse PPOX, which gave a higher protein yield.

Purification and characterisation of the *B. subtilis hemY* cDNA sequence by Dailey et al. (1994c) allowed identification of dinucleotide binding domain in this *PPOX* gene, suggesting association of this enzyme with flavins. Subsequent spectral analysis of the purified *B. subtilis* PPOX revealed a typical flavoprotein spectrum (Hansson et al., 1997). The flavoprotein nature of *B. subtilis* PPOX was further confirmed by Hansson et al. (1997). They demonstrated the inhibition of the PPOX activity by a known inhibitor of FAD-containing enzymes, Quinacrine. The enzyme activity was simulated 2 – 3 fold in the presence of FAD, suggesting the role of the FAD cofactor in enzyme activity. Another aerobic bacterium *M. xanthus*, was also reported to be a flavoprotein that is non-covalently associated with FAD (Dailey and Dailey, 1996b). *PPOX* cDNA sequence showed the presence of the dinucleotide binding motif. The cofactor was reported to be present at a ratio of one FAD per homodimer of a protein. Flavin cofactor was also shown in purified yeast PPOX through its pH-dependent spectral shift (Camadro et al., 1994). Sequence analysis of the cloned yeast *hem*14 gene coding for PPOX, revealed a putative βαβ motif (Camadro and Labbe, 1996). In the *hemG* cDNA sequence of *E. coli*, Nishimura et al. (1995b) identified the flavodoxin motif suggesting a flavoprotein.

Jacobs and Jacobs (1987) demonstrated the absence of chromophoric compounds on a crude plant PPOX (barley) preparation by fluorometric analysis. Subsequent analysis of the purified barley PPOX, using extraction procedures for either covalent or non-covalently bound cofactors showed no evidence of a flavin cofactor association with this protein (Jacobs et al., 1989), suggesting that the plant PPOX is not a flavoprotein. However, cDNA analysis of *A. thaliana* PPOX revealed the presence of the typical dinucleotide binding motif (Narita et al., 1996). Other plant PPOX studies has shown the presence of this dinucleotiode binding domain in the cloned and characterised plastidal and mitochondrial PPOX isoforms of tobacco plant (Lermontova et al., 1997) and potato (Johnston et al., 1998). There is no physical analysis for the flavin association with these proteins, except for the available sequence information that indicates flavoprotein nature of plant PPOXs.

There are now many *PPOX* sequences available in databases such as Genbank. Gene/protein sequence analysis suggests that PPOXs are members of a protein superfamily that includes human (Nishimura et al., 1995b), mouse (Taketani et al., 1995a), plant (Narita et al., 1996), yeast (Camadro and Labbe, 1996), some bacteria (Dailey and Dailey, 1996b), animal phytoene desaturases and animal monamine oxidases (Dailey and Dailey, 1998). These proteins share significant sequence homology in a 60 amino acid residue stretch that includes the βαβ-dinucleotide

cofactor binding motif (GXGXXG) near the N-terminal sequence (Dailey et al., 1994c; Camadro and Labbe, 1996; Hansson et al., 1997).

Flavoproteins and flavins in nature

As part of this dissertation examines the FAD cofactor in PPOX, flavins and their measurement are reviewed in some detail here. Flavoproteins need to associate with a flavin cofactor for their biological activity. The most commonly occurring flavins are riboflavin (Rb), flavin mononucleotide (FMN) and flavin adenine dinucleotide (FAD). These flavins exist in tissues either as free compounds or in flavoproteins (Koziol, 1971). FMN and FAD are the most widely distributed prosthetic groups in flavoproteins, and sometimes are found together in the same purified protein (Trudgill et al., 1966; Miller and Stadtman, 1972).

Spectrophotometric analysis of flavins

Spectrophotometric measurements are used to determine total flavin content. Since the absorption spectra of Rb, FMN and FAD are similar to one another, this method cannot be used to determine individual flavin content, unless they have been previously separated using other methods (Kaziol, 1971). The flavins and their flavoproteins are yellow in colour when they are in their oxidised form, and have an absorption spectrum that is characterised by two well defined peaks at 375 and 450nm in the UV/VIS range (Müller et al., 1973; Ghisla, 1980). The spectra are markedly affected by pH, solvent polarity, and organic/inorganic compounds complexed to flavins or present in solution (Massey and Ganther, 1965; Roth and McCormick, 1967).

Fluorometric analysis

Rb, FMN and FAD have an identical excitation wavelength (450nm). The oxidised state state of free flavin in solution exhibit a strong fluorescence in the maximal region of 520nm. In the reduced state, these compounds do not fluoresce and have variable absorption above 300nm (Ghisla, 1974). In aqueous solutions, the fluorescent emission spectra of oxidised flavins are characterised by a broad band at maximum wavelength of about 520nm (Bessey et al., 1949; Cerletti and Siliprandi, 1958). The fluorescence spectrum is influenced by number of factors such as temperature, solvent polarity, pH, and other absorbing species in solution (Koziol, 1971).

Determination of noncovalently bound flavins

Noncovalently bound flavins may be removed from the protein by heating or treatment with acid in the cold. These methods may affect the protein tertiary structure. However, flavin content of biological tissues may be determined by comparing the fluorescence at neutral (7.5) and acidic (3.5) pH in aqueous solution (Faeder and Siegel, 1973). The principle of the method is based on the existence of FAD as a non-fluorescent internal complex at neutral pH, which dissociates into a fluorescent compound as pH is decreased to less than 3.0. The other flavins (Rb and FMN) have an unaltered fluorescence intensity in this pH range (3.5 – 7.5) (Bessey, 1949; Cerletti and Siliprandi, 1958).

PPOX Inhibition

PPOX is inhibited by many herbicidal compounds and results in accumulation of protoporphyrin IX (Matringe and Scalla, 1988a,b; Lydon and Duke, 1988; Witkowski and Halling, 1988; Sandmann and Böger, 1988; Becerril and Duke, 1989; Duke and Lydon, 1989). The inhibitory effect in cells is rapid and takes only a few minutes for a detectable increase in protoporphyrin IX when exposed to inhibitor (Bicerril and Duke, 1989; Matsumoto and Duke, 1990).

Inhibitors

Many PPOX inhibiting herbicides have been commercialised for over thirty years but their molecular site of action eluded scientists up until 1989 (Dayan and Duke, 1997a,b,c). Commercial PPOX inhibitors can be categorised in three broad chemical groups (Table 2.1): the DPEs, the phenyl heterocycles and the heterocyclic phenylimides (Anderson et al., 1994; Duke and Rebeiz, 1994; Reddy et al., 1997). Another group of herbicides reported include carboxylate and haloalkyl-substituted asoxazoles (Hamper et al., 1995). To date, only one phytotoxin of natural origin is known to inhibit PPOX i.e., the DPE, cyperin, which has been isolated from several weed fungal pathogens (Weber and Gloer, 1988, Striele et al., 1991; Venkatasubbaiah et al., 1992). However, it is a poor inhibitor with a high IC_{50} value of 60μM (Harrington et al, 1995).

Table 2.1: **Commercial PPOX inhibitors: Major chemical groups, which are typical phenyl heterocycles.**

	PPOX Inhibitors	
DPE	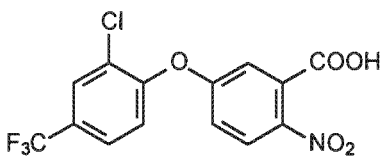 **Acifluorfen**	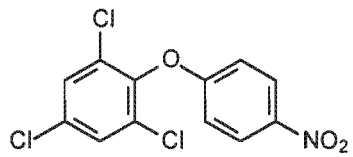 **Chloronitrofen**
Phenyl Heterocycles	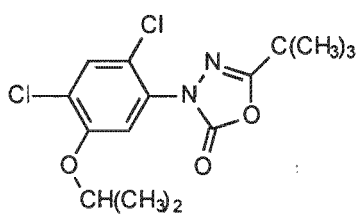 **Oxadiazon**	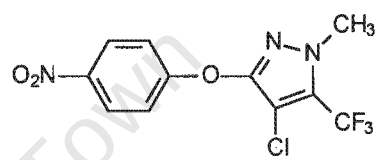 **AH 2.430**
Triazolinones	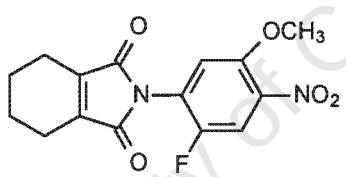 **Flumiclorac**	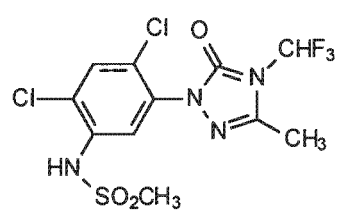 **Sulfentrazone**

Mode of inhibition

An important feature of these inhibitors is that they mimic portions of the substrate molecule, protoporphyrinogen IX (Figure 2.2) thereby effectively competing at the active site. The best PPOX inhibitors are those that most closely approximate the geometric shape and electronic characteristics of one-half of the protoporphyrinogen IX molecule (Dayan and Duke, 1997a). A study by Nandihalli et al. (1992a) showed that the inhibitory activity of the PPOX inhibitors was also positively related to their lipophilic nature. Indeed, quantitative structure-activity relationships (QSAR) analyses have been successful in the prediction of the herbicidal activities of certain compounds (Nandihalli et al, 1992a, Reddy et al, 1995). A major limitation in QSAR work is that the 3-D structure of PPOX remains unknown. Thus the topography of the binding pocket and conformational changes occurring during the binding and at each step of the oxidation as well as during the binding of the herbicide remains unknown.

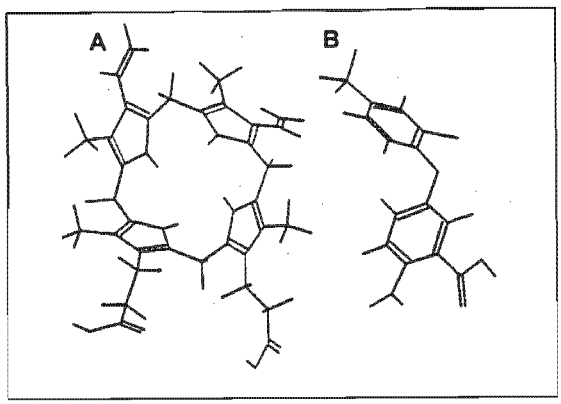

Figure 2.2: **Three dimensional optimised structures (A: Protoporphyrinogen, B: Acifluorfen)** (From Dyan and Duke, 1997a)

Inhibition by diphenyl ether herbicides

The DPEs have been shown to be potent inhibitors of PPOXs, and are competitive inhibitors with respect to the substrate protoporhyrinogen IX (Matringe et al., 1989a.b, 1992; Witkowski and Halling, 1989; Duke et al., 1990, 1991b; Scalla et al., 1990; Versano et al., 1990; Camadro et al., 1991; Nandihalli et al., 1992b; Nandihalli and Duke, 1993; Scalla and Mantringe, 1994; Lee et al., 1995) of plant, mouse and human PPOXs (Camadro et al., 1991; Corrigall et al., 1994). However, this inhibition by DPEs is not seen in all PPOXs, e.g., *B. subtilis*, *E. Coli* and *B. japonicum* PPOXs (Jacobs et al., 1990; Dailey et al., 1994c; Corrigall et al., 1998a). DPEs have been used as tools to investigate the substrate binding site/catalysis of the PPOX (Matringe et al., 1992b).

Effect of DPE on plants

In plants, this inhibition induces light-dependent phytotoxic damage through induction and accumulation of protoporphyrin IX in the exposed plant (Matringe and Scalla, 1988a; Becerril and Duke, 1989; Matsumoto and Duke, 1990; Sherman et al., 1991; Kojima et al., 1991; Camadro et al., 1994). Inhibition of PPOX results in the accumulation of colourless tetrapyrrole substrate, protoporphyrinogen IX that leaks out of the plastids (Jacobs and Jacobs, 1993) into cytoplasm and is rapidly oxidised in the presence of light into protoporphyrin IX (Jacobs et al., 1991; Jacobs and Jacobs, 1993; Lee et al., 1993; Duke et al., 1994). In the presence of light, highly reactive singlet oxygen radicals are generated and induce rapid membrane peroxidation, resulting in cellular death (Duke et al., 1990, 1991a; Scalla et al., 1990; Devine et al., 1993; Dayan and Duke, 1997a,b,c).

Effect of DPE on animals

Several studies on DPE inhibition of PPOX were performed in animals and were found to cause protoporphyrin IX accumulation, in a similar manner to that in plants (Kawamura et al., 1996). In humans this protoporphyrin IX accumulation has been associated with VP (Deybach et al., 1981) and results in dermatological and/or neurological problems (Eales et al., 1980). Administration of PPOX inhibiting herbicide (oxadiazon or oxyfluorfen) to male mice resulted in experimental porphyria with some characteristic biochemical features of human VP (Krijt et al., 1997). Increased porphyrin content was noticed in the livers and kidneys of these mice. Accumulation of porphyrins was noted in the trigeminal nerve of animals treated with oxadiazon suggesting a contribution of porphyrin to the peripheral neurophathy observed during the acute attack of porphyria. In a study by Rio et al. (1997), the effect of oxyfluorfen herbicide on human Burst and Colony Forming Unit-Erythroid (BFU-E/CFU-E) development and haemoglobin synthesis, in the presence of erythropoietin was investigated. The oxyfluorfen herbicide displays a cytotoxic effect only at a high concentration (0.01M). At lower concentrations (0.0001M) only haem biosynthesis inhibition was noted. Investigation of PPOX inhibition by S-53482 (an N-phenylamide photobleaching herbicide) in rat and rabbit embryos showed an increased protoporphyrin IX concentration in rat embryos by an order of two magnitudes when compared to that of untreated embryos (Kawamura et al., 1996). In rabbit embryos, no protoporphyrin IX accumulation was noted even at higher dose level of herbicide, and this was postulated to be true for humans as well.

PPOX resistance to DPE

Several plant species have shown tolerance to some of the peroxidative herbicidal compounds (Matsumoto et al., 1994; Komives and Gullner, 1994; Dayan and Duke, 1997a,b; Duke et al., 1997). The basis of this tolerance has been shown to arise at a number of levels: Decreased uptake or translocation of the herbicide to the site of action (Matsumoto et al., 1994; Komives and Gullner, 1994; Duke et al., 1997); rapid metabolic destruction of herbicide (Frear et al., 1983); resistance of the cells towards peroxidation by oxygen radicals (Matsumoto et al., 1994); and, rapid metabolic destruction of protoporphyrinogen IX or protoporphyrin IX to non-toxic compounds (Jacobs et al., 1996).

It has been shown that the prokaryotic PPOX from *B. subtilis* (Dailey et al., 1994c), *E. coli* and *B. japonicum* (Jacobs et al., 1990) exhibited different inhibition characteristics from other PPOXs studied. It has been postulated that *B. subtilis* PPOX exhibits a conformational difference compared to other PPOXs, making a good fit into

the active site for the DPEs more difficult (Corrigall et al., 1998a). Natural resistance to DPE inhibition does not, however, appear to be a general feature of all prokaryotic PPOXs as *M. xanthus* PPOX (Dailey and Dailey, 1996b) is not resistant to DPE inhibition.

Choi et al. (1998) reported that the expression of *hemY* gene of *B. subtilis* PPOX that is resistant to herbicides, demonstrated some 50% resistance against oxyfluorfen in the cytoplasm of transgenic tobacco plants. Other studies including that of Lee et al. (2000), which showed similar results in a transgenic rice plant that expressed the *hemY* gene of *B. subtilis* PPOX.

Prasad and Dailey (1995) showed that murine erythroleukemia (MEL) cells could grow at a near normal rate in 100μM acifluorfen (AF) after rendering them insensitive to inhibition by AF by continuous exposure to AF through many passages of cell growth. On isolation of the AF resistant cell lines, they discovered that neither the amount nor biochemical character of PPOX were responsible for resistance. They suggested that this cellular resistance is mediated through induction of a cytochrome P450. This enzyme is capable of metabolising the AF making it unable to inhibit.

A mutant strain of the green algae *C. reinhardtii* (rs-3) that is resistant to herbicides such as S-23142, oxadiazon, methyl acifluorfen (MeAF), and oxyfluorfen has been isolated and characterised (Kataoka et al., 1990; Oshio et al., 1993). A subclone of the mutant insert yielded a high frequency of herbicide-resistant transformant (Rondolph-Anderson et al., 1998). Characterisation of wild type *C. reinhardtii* revealed a protein identity of 51% to *A. thaliana* and 53% of *N. tabacum*. The mutant form of the algae, rs-3, revealed a G→A point mutation resulting in a valine to methionine substitution at a conserved position equivalent to Val-389 of wild type *C. reinhardtii* cDNA. This suggests that the Val-389 is critical for maintaining a PPOX conformation that is sensitive to inhibition by DPEs.

Lermontova and Grimm (2000) demonstrated the tolerance of transgenic *N. tabacum* plants that overexpresses *A. thaliana* plastid PPOX, against the action of AF herbicide. The overproduction of PPOX in the plastid cells neutralises the herbicidal action by increasing PPOX activity to five times that in the control wild type cells. There is therefore no accumulation of the substrate protoporphyrinogen IX.

Watanabe et al. (1998) performed electron microscopy on photomixotrophic cultured tobacco plant cells (YZI-1S). Cells grown in the presence of N-(4-chloro-2-fluoro-5-propagyloxy)-phenyl-3,4,5,6-tetrahydrophthalimide exhibited no grana stacking, which

was an indicative of resistance of these cells, due to overproduction of mitochondrial PPOX.

In addition, rice, tobacco and soyabean cells are also resistant to certain herbicides (Pornprom et al., 1994). Rice was shown to be resistant against PPOX inhibitors by being naturally resistant to the phytotoxic oxygen forms generated by protoporphyrin IX (Duke and Rebeiz, 1994).

Inhibition by haem and its metabolic products

Haem and its metabolic breakdown products, BR and biliverdin (BV), are also effective inhibitors of PPOX (Figure 2.3) (Poulson and Polglase 1975, Ferreira and Dailey, 1988, Corrigall et al, 1998a). The methylpropionyl and vinyl side chains of haem remain intact during the reductive metabolic breakdown into the BV and BR molecules. The inhibitory effect of these compounds is based on their structural resemblance to the substrate molecule (protoporphyrinogen IX). Ferreira and Dailey (1988) demonstrated competitive inhibition of the purified mouse PPOX by BR (Ki = 25μM), with respect to the substrate protoporphyrinogen IX.

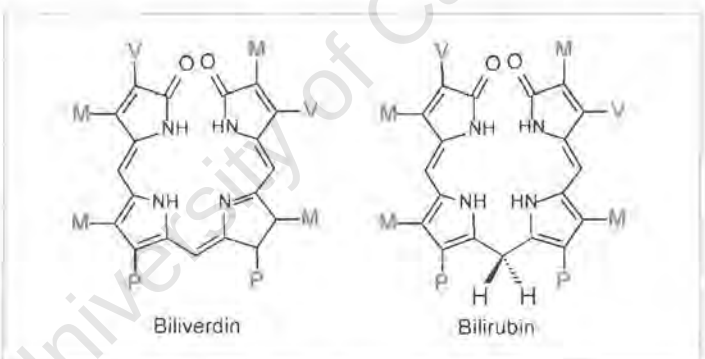

Figure 2.3: Chemical structures of BV and BR

Gilbert's syndrome is characterised by an unconjugated hyperbilirubinaemia, and affected patients have reduced PPOX activity accompanied by a compensatory increase in ALAS activity in leukocytes (McColl et al., 1987). This is a similar enzymic profile to that observed in VP patients, yet in Gilbert's patients the excretion of porphyrins and their precursors was normal. On the other hand, there is a single report of increased excretion of porphyrins in a patient with hyperbilirubinaemia (Evans et al., 1981).

Inhibition by diphenyleneiodonium

Diphenyleneiodonium (DPI^+) cations (Figure 2.4) and related species also inhibit several flavoproteins (Gatley and Sherratt, 1976; Ragan and Bloxham, 1977; Doussiere and Vignais, 1992; O'Donnell et al., 1994). These compounds act on the reduced flavin cofactors associated with flavoproteins, by removing electrons thereby causing formation of phenyl radicals and covalent modification of the flavin (O'Donnell et al., 1994). The mechanism of this inhibition by these compounds in PPOX has been studied and was, indeed, a different mechanism to that of inhibition by DPEs. Arnould et al. (1997) showed that a membrane bound yeast PPOX is inhibited by the DPI cation with irreversible slow binding kinetics, with maximum inhibition at pH 8.0. More potent slow-binding inhibitors are produced by substitution of one phenyl ring with methyl or nitro groups.

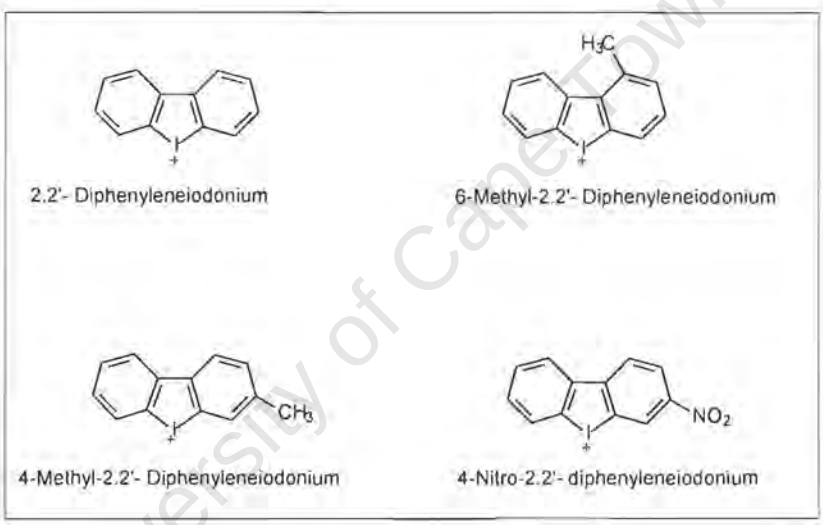

Figure 2.4: Chemical structures of DPIs.

In another study on the relation between the herbicide binding site and the flavin cofactor, Birchfield et al. (1998), postulated that DPI inhibits human PPOX by interaction with the FAD cofactor, reducing enzyme activity by 48% at 100μM. This inhibition does not affect binding of the photoaffinity radioligand, N-(5-azido-4-chloro-2-fluorophenyl)-3-4-5-6-[^{3}H] tetrahydrophthalimide ([^{3}H] AzTHP) in the presence or absence of 5μM substrate. Competitive PPOX inhibitors (AF and THP) were shown to compete for binding of [^{3}H]AzTHP (Birchfield et al., 1998). [^{3}H]AzTHP binds with high affinity to a single saturable site in the PPOX from solubulised mouse liver mitochondria and is displaced by the oxyfluorfen (DPE) *in vivo* (Birchfield and Casida, 1996). These findings demonstrate that the DPI was not sharing the same binding site occupied by [^{3}H]AzTHP, AF and THP on the enzyme molecule. This suggested that the FAD binding site is distant from the substrate/herbicide binding site of PPOX.

PPOX gene

Identification of the gene

Initial studies on the *PPOX* gene sequence, was performed by Hansson and Hederstedt (1992). They reported an open reading frame in the aerobic bacterium, *B. subtilis* (*hemY*), which they predicted to be PPOX. Two years later Dailey et al. (1994c) cloned and expressed the *B. subtilis hemY* gene in *E. coli* and showed that it encodes a 53000 Da protein that had oxygen-dependent PPOX activity. The cloning, sequencing and expression of prokaryotic PPOXs from *B. subtilis* (Hansson and Hederstedt, 1994; Dailey et al., 1994c; Hansson and Hederstedt, 1994) and *E. coli* (Sasarman et al., 1993) facilitated the discovery and identification of mammalian genes encoding mouse (Dailey et al., 1995; Taketani et al., 1995a), human (Taketani et al., 1995b; Nishimura et al., 1995a; Roberts et al., 1995b; Dailey and Dailey, 1996a; Dailey and Dailey, 1997a), yeast (Camadro, et al, 1994), *M. xanthus* (Dailey and Dailey, 1996b), *A. thaliana* (Narita et al., 1996), maize (de Marco et al., 2000), spinach (Matringe et al., 1992a, Watanabe et al. 2000) and potato plant PPOX (Johnston et al., 1998).

Gene sequence

The genomic DNA sequence for human PPOX has been reported (Roberts et al., 1995b). The gene encodes a 51000 Da protein (477 amino acid residues) that exists as a 100 000 Da homodimer (Dailey and Dailey, 1996a). The coding sequence of human *PPOX* is 1431 nucleotide base pairs long with 13 exons spanning approximately 5kb (Roberts et al., 1995b). All exon/intron boundaries have been characterised (Taketani et al., 1995b; Roberts et al., 1995b). A single mRNA transcript for human PPOX (~1.8kB in length) was reported from northern blot analysis of various tissues (Dailey and Dailey, 1995; Nishimura et al., 1995a; Taketani et al., 1995b). In these transcripts a short 3'-UTR and a 5'-UTR approximately 300 base pairs long were found. There is one predicted 5'-UTR stem-loop structure with possible regulatory functions, such as an iron-responsive element (Dailey et al., 1995). Start and termination codons as well as a consensus polyadenylation signal and polyadenylation site just downstream from the termination site, have been identified (Taketani et al., 1995b; Dailey and Dailey, 1996a; Puy et al, 1996).

Assignment of the gene to chromosome 1q22–23

The human *PPOX* gene was mapped by fluorescent *in situ* hybridisation to chromosome 1q22–23 of human genome (Roberts et al., 1995b; Taketani et al., 1995b). The gene was originally assigned to chromosome 14q32 (Bissbort et al.,

1988) due to the report of close linkage between the gene locus for VP and the α1-antitrypsin gene, which was known to reside on chromosome 14. Warnich et al. (1996b) were unable to confirm linkage between VP and 5 microsatellite markers on chromosome 14q, which was closely related to the α1-antitrypsin locus. The incorrect assignment of the gene was further confirmed by Roberts et al (1995b), who showed a significant linkage between the VP phenotype in a sample of British VP patients and microsatellite markers on chromosome 1 and used fluorescent *in situ* hybridisation to map the human *PPOX* gene to chromosome 1q22–23 (Roberts et al, 1995b; Taketani et al, 1995b).

Variegate Porphyria

As previously alluded to, VP is a low-penetrance, autosomal dominant disorder of haem synthesis due to reduced activity of PPOX. VP patients demonstrate PPOX activity of approximately 50% of normal (Brenner and Bloomer, 1980; Deybach et al 1981, Meissner et al, 1986). South Africa has the highest prevalence of VP in the world, attributed to a founder effect (Dean, 1971), resulting from a mutation (R59W) in exon 3 of the *PPOX* gene (Meissner et al, 1996, Warnich et al, 1996a). World-wide heterogeneity for VP exists and over 100 mutations have been identified (Poh-Fitzpatrick, 1980; Mustajoki, 1980; Long et al., 1993; Deybach et al., 1996; Lam et al., 1996; de Rooij et al., 1997; Frank et al., 1997;1998a,b,c,d,e; Kauppinen et al., 1997).

Clinical symptoms of VP include, skin photosensitivity and/or acute neurovisceral crises (Bickers et al., 1996, Frank and Christiano, 1997).

Historical perspective

VP was probably first described in a Dutch patient by van den Bergh and Grotepass in 1937. However, in many early reports that followed, it must be considered that the features of VP (as we now know them to be) were confused with those of PCT, AIP and HCP (Poh-Fitzpatrick, 1980; Long et al., 1993). Furthermore, the disease was described using different terms such as mixed porphyria (Watson, 1960), protocoproporphyria (Waldenström, 1957), porphyria cutanea tarda (Calvert and Rimington, 1953; MacGregor et al., 1952; Wells and Rimington, 1953; Holti et al., 1958), and porphyria cutanea tarda hereditaria (Cormane et al., 1971; Levene, 1968; Magnus, 1968; Rimington et al., 1967; Tio, 1958).

The first description of acute porphyria in South Africa was written and published by two medical students (Lennox Eales and Jack Chiat) in October 1939, in the University of

Cape Town's medical student's journal, *I'nyanga* (Eales and Chiat, 1939). A series of cases of porphyrinuria were first described in South Africa, by HD Barnes of the South African Institute for Medical Research in Johannesburg in 1951. Barnes, together with Geoffrey Dean, a Port Elizabeth physician, who had recognised that the disease could manifest with skin lesions, acute attacks or both, coined the terms *porphyria variegata* and *South African genetic porphyria* (Dean, 1953; Dean and Barnes, 1955).

Dean's genealogical studies (Jenkins, 1997) demonstrated that South African VP is common amongst the population of Dutch descent, a disorder that was distinct from the genetic porphyria found in Sweden (Dean and Barnes, 1959). Of 118 South African families he investigated, he showed that approximately 50% of children of porphyric patients inherited VP, and that the sex distribution was equal. He described some members of the family as asymptomatic, meaning that, they demonstrated excretion of abnormal urine and stool porphyrins but did not experience any clinical symptoms. He never observed homozygote individuals. In his studies, Dean suggested that the disease was brought to South Africa in 1688, when Adriaantje Adriaanse, an orphan from Rotterdam, arrived on the Dutch East India Company ship *China* and was married to one of the free burghers, Gerrit Jansz van Deventer (Dean, 1971) within a month of her arrival. Four of their children inherited the gene defect and passed it on to approximately 50% of the offspring. However, it is uncertain whether VP was introduced into South Africa by Gerrit Jansz himself or by his wife, Adriaantjie.

Prevalence

The prevalence of VP in South Africa has never been accurately determined as the disease is frequently non-expressed both clinically and biochemically. Based on the probability that the gene had arrived at the Cape in 1688, and the fact that there was a rapidly expanding population during the 18th century from just over 1000 to 17000 in 85 years (Jenkins, 1997), Dean suggested an overall prevalence of 8000 ± 2000 for the country as a whole (Dean, 1971; Eales and Blekkenhorst, 1980; Day, 1986). However, taking into account the approximate 70% (or less) sensitivity of the screening methods employed at that time, it is possible to predict that as many as 30 000 South Africans may carry the gene.

VP has been reported worldwide (Mustajoki, 1978). In Europe (Hamnström et al., 1967; Cochrane and Goldberg, 1968; Freinkel and Ashman, 1974; Fromke et al., 1978; Muhlbauer et al., 1982; Kostrzewska and Gregor, 1982; te Velde et al., 1989; Aquaron et al., 1992; Elder et al., 1997), the prevalence of clinically-overt VP is generally thought to be about 1/3 of that of AIP (Elder, 1997) which approximates to 0.5/100 000. Further

reports of VP have emanated from Israel (Krakowski et al., 1979), India (Bhargova, 1970; Handa, 1975), Taiwan (Tu et al., 1971), Japan (Kodama et al., 1979) and Australia (Coakley et al., 1990). In Finland the prevelance has been estimated at 1.3/100 000 population (Mustajoki, 1980). A few cases of VP have been described in the black population including a Curacao Negroid woman (Van der Sar, 1976), an American black man (Hughes and Davis, 1983) and more recently, an indigenous black South African woman (Corrigall et al., 2001).

Clinical Features

The clinical features of VP may be divided into two main categories: photocutaneous sensitivity (skin disease) and/or acute neurovisceral crises (acute attack). In 1980, Eales reported absence of clinical symptoms (for acute and skin disease) in 10% of the patients. Seventeen years later, Hift et al. (1997) showed 38% of patients that were asymptomatic. Patients with PPOX defect do not usually present with clinical symptoms of VP until puberty (Dean, 1971; Kramer, 1980; Meissner and Hift, 1991).

Skin disease

Eales reported that more than 80% of patients with VP had skin disease (Eales, 1960, 1980). An accumulation of porphyrins in the upper layers of dermis has been documented (Runge and Watson, 1962; Day, 1986) and skin damage is probably a result of photoreactive porphyrins, which interact with light (Poh-Fitzpatrick, 1985). The characteristic feature of the skin disease in VP is excessive skin fragility on the sun-exposed surfaces particularly of face, dorsa of the hands and feet, nape of neck, erosions, milia, blisters, and abnormal pigmentation, eventually leading to thickening, grooving, hirsutes, and premature aging (Dean, 1971; Eales and Blekkenhorst, 1980; Poh-Fitzpatrick, 1985; Day, 1986; Elder et al., 1997; Kirsch et al., 1998). Generally, lesions heal slowly, especially in the presence of secondary infection. This often results in scars, which may be pigmented or depigmented. The combined effect of trauma and constant sun exposure may cause progressive pseudosclerodermatous changes in hands and fingers.

Acute photosensitivity, more typical of EPP, has been reported in a few patients with VP in conjunction with liver disease or biliary obstruction (Eales, 1963).

Acute attack

The VP acute attack is not distinguishable from that of AIP and HCP. Clinical manifestations of the acute attack are intermittent, and include severe pain, most often in the abdomen, but sometimes in the lower back, buttocks and thighs. In some cases the attack may be associated with an obvious precipitating event (such as administration of porphyrinogenic medication or menstruation). Abdominal pain may be accompanied by few clinical signs and by an absence of peritonism and features of autonomic neuropathy (Yeung-Laiwah et al., 1987; Blom and Atsmon, 1996), such as hypertension, tachycardia, vomiting, ileus, and constipation (Kirsch et al., 1998). The attack may proceed to a typical motor neuropathy resembling the Guillain-Barre syndrome (McEneany et al., 1993; Bont et al., 1996). In severe cases, this leads to a severe flaccid quadriparesis and respiratory failure requiring ventilation.

Pathologically, the neuronal injury is characterised by severe axonal necrosis, though at times there may be a lesser element of demyelination as well (Windebank and Bonkovsky, 1992; Cavanagh and Mellick, 1965, Hierons, 1957; Gibson and Goldberg, 1956; Mustajoki and Seppäläinen, 1975; Albers et al., 1978; Flügel and Druschky, 1977). The histological changes associated with acute neuropathy in VP appear to be no different from those with other forms of porphyria. The cardinal features are those of severe qualitative and quantitative changes in myelinated and unmyelinated fibres, suggesting an axonopathy, in keeping with the dying-back phenomenon.

Biochemical features and diagnosis

Characteristic biochemical features may identify VP patients. This remains the mainstay of diagnosis in most cases of VP, though its place has been modified by the identification of some of the molecular defects accounting for VP.

The biochemical diagnosis of VP may be based on quantitation and analysis of excreted porphyrins in stool and urine and/or analysis of circulating porphyrins in the plasma, and measurement of urinary porphyrin precursors (ALA and PBG) in the case of the suspected acute attack.

In essence, the porphyrin excretory profile observed in VP arises as a result of porphyrin(ogen) accumulation resulting from the primary enzymatic defect in PPOX. During the acute attack ALA and PBG concentrations are always raised. This is thought to arise from a secondary "deficiency" in PBG deaminase, which may arise in response to increasing intracellular concentrations of coproporphyrinogen III and protoporphyrinogen IX resulting from decreased PPOX activity. Indeed, allosteric

inhibition of PBG deaminase by copro- and protoporphyrinogen IX has been demonstrated *in vitro* (Meissner et al, 1993).

Stool

The classic biochemical indicator of VP is elevated stool protoporphyrin IX, and to a lesser extent coproporphyrin. The presence of either 5-COOH- or pseudo 5-COOH-porphyrin compounds (Moore et al., 1987; Hift et al., 1997) in stool of VP patients is a useful differential for diagnosis of VP. During the acute attack, all these porphyrin concentrations rise and the additional presence of URO-, 7-COOH and 6-COOH-porphyrins can be seen.

Urine

There are significant elevations in the concentrations of all urinary porphyrins during the acute attack of VP, and the porphyrin precursors, ALA and PBG. In contrast, urinary porphyrin excretion in VP patients not in an acute attack is highly variable, and may be completely normal. The most consistent changes are mild elevations in copro- and uroporphyrin but these are only significantly raised in about 30% of quiescent VP subjects (Eales et al., 1980; Day, 1986; Kappas et al., 1989; Nordmann and Deybach, 1990; Hift et al., 1997).

Plasma

Plasma and serum porphyrin levels are elevated when the VP disease is active. A plasma porphyrin complex gives a distinctive fluorescence emission spectrum (between 625 – 626nm) at excitation wavelength of 405nm that is diagnostic for VP (Poh-Fitzpatrick, 1980; Long et al., 1993; Gregor et al., 1994; Da Silva et al., 1995).

PPOX activity

PPOX is a mitochondrial enzyme and therefore found only in nucleated cells. This makes the determination of enzyme activity in erythrocytes a much less useful diagnostic modality in VP than it is in certain of the other porphyrias. Though it is possible to determine PPOX activity in the lymphocytes of the buffy layer, the low level of expressed activity, coupled with the difficulties of the assay renders the distinction of normal from reduced activity unreliable in a non-specialist laboratory, and the assay is therefore not suitable for routine diagnostic use. Measurement of PPOX activity on Epstein-Barr virus transformed lymphoblasts (Meissner et al., 1986) and fibroblasts (Brenner and Bloomer, 1980) showed 50% reduction in PPOX activity. However, in general, it takes 3 – 7 weeks in culture to prepare sufficient cells for reliable assay (Meissner et al., 1986; 1993).

Genetic diagnosis

Elucidation of the DNA sequence and characterisation of the gene encoding human PPOX has enabled the molecular approach to the diagnosis of VP (Deybach, 1996; Meissner et al., 1996; Roberts et al., 1996, 1998; Kauppinen et al., 1996; Warnich et al., 1996a; Lam et al., 1996, 1997; Puy et al., 1996; de Rooij et al., 1997; Corrigall et al., 1998b; Frank et al., 1998a,b,c,d,e; Whatley et al., 1999). However, this approach does have its limitations as it is now clear that numerous defects at the molecular level may underline human VP. The exception has been the South African experience where one defect (R59W) may account for as many as 95% of all VP in this country (Meissner et al, 1996), though even here, at least 9 other defects contribute to the total pool of disease (Corrigall et al, 2001). Given the frequency of this gene, screening for the R59W defect is highly sensitive and specific for the diagnosis of VP and will diagnose the condition before puberty unlike all other diagnostic methods.

Gene screening for VP normally takes the form of restriction enzyme analysis on PCR-amplified DNA. In cases where the family mutation is unknown or no suitable restriction enzyme exists, genomic DNA isolated from whole blood is amplified by PCR using appropriate primers. *PPOX* DNA fragments are produced by PCR and sequenced to demonstrate the presence of a possible mutation in patients.

PPOX gene mutations responsible for VP

PPOX gene mutations accounting for VP were first reported shortly after the molecular cloning and sequencing of cDNA encoding human PPOX (Deybach et al., 1996; Meissner et al., 1996; Roberts et al., 1996; Kauppinen et al., 1996; Warnich et al., 1996a). Specifically two *PPOX* gene mutations in three French families (Deybach et al., 1996) and the founder mutation (R59W) and a further missense mutation in South African VP patients (Meissner et al., 1996; Warnich et al, 1996a) were reported.

Over a hundred VP mutations have now been reported worldwide (Table 2.2). Additional intragenic polymorphic sites have also been identified. The mutations comprise of deletions, insertions, missense, nonsense, and splicing defects (Meissner et al., 1996; Warnich et al., 1996a; Deybach et al., 1996; Whatley et al., 1999;). In most countries there is considerably allelic heterogeneity except in South Africa due to high number of patients who carry the R59W mutation. In Finland, a single point mutation (R152C) accounts for 60% of all VP families (Kauppinen et al. (1997), and in Chile a frameshift mutation in exon 11 (1194–1198delTACAC) was found in four unrelated families.

The mutations reported to date are evenly distributed throughout the *PPOX* gene from exons 2 to 13. While an earlier report suggested a clustering of mutations in exon 6 (Frank et al., 1998a), the reported mutations show no exon having more than 14 (exon 10) or fewer than 3 (exon 9) mutations with the exception of exon 1, the UTR of the gene, where no mutations have yet been detected, despite the suggestion by Kotze et al. (1998) that exon 1 is particularly mutation-prone. No mutations have yet been reported in introns 1, 5, 8 and 13.

Mutations in South Africa

In addition to the predominant R59W mutation in South Africa, other mutations (R168C, H20P, 537delAT, Y348C, R138P, 769delG; 770T > A, L15F, Q375X and V290M) have been identified (Warnich et al., 1996a; Corrigall et al., 1998b, 2000) including the first report in a black South African family (V290M) (Corrigall et al., 2000). Three of these mutants (R168C, Y348C and R138P) have been shown in the compound heterozygous state heteroallelic to the R59W mutation (Meissner et al., 1996; Corrigall et al., 2001).

Correlation between mutation and clinical presentation

There is no significant correlation that has been established to date between the types of mutations (missense, nonsense, splice site or frame shift) and a specific clinical presentation (photosensitivity or the acute attack). In addition, the frequencies of each type of presentation have been noted in to be similar in France, UK and South Africa. This suggests that allelic heterogeneity does not substantially alter the pattern of clinical expression of the disease, and that VP in any other geographical region is clinically representative of the disease elsewhere. The PPOX genotype does not appear to be a significant determinant of clinical severity other than in the so-called "homozygous" state.

Homozygous variegate porphyria

Homozygous variegate porphyria (HVP) results from mutations in both alleles of the *PPOX* gene. This results in a severe decrease in PPOX activity (<20% of normal) (Hift et al., 1993; Roberts et al., 1998). There is also a highly exaggerated VP porphyrin excretory profile although, interestingly, a feature appears to be the absence of acute symptomology other than in one case (Corrigall et al, 2000). Most cases of HVP result from inheritance of a different mutation in each allele (compound heterozygosity) (Hift et al., 1993; Roberts et al., 1998) but in a few cases true homozygosity exists (Roberts et al., 1998). HVP was first

reported by Kordac et al. (1984), after which further reports followed (Murphy et al., 1986; Mustajoki et al., 1987; Coakley et al., 1990; Norris et al., 1990; Gandolfo et al., 1991; Hift et al., 1993; Meissner et al, 1996; Warnich et al, 1996a; Roberts et al., 1998; Corrigall et al., 2000).

Clinical features

The distinguishing feature of HVP is its clinical presentation. It is characterised by severe skin and neurological disease manifesting in an early infancy. However, a case of late presentation (19 years of age) was reported by Corrigall et al. (2000). Clinical symptoms include mental retardation, delayed neurological development, seizures, nystagmus, brachydactyly, and convulsions. Structural abnormalities of the hands were frequently reported, ranging from clinodactyly to severe deformity. Growth retardation also occurs.

Molecular biology

Table 2.2 indicates which mutations have been reported in the "homozygous" state. Molecular analysis of the mutations in HVP support the hypothesis that at least one mutant allele must code for PPOX with residual catalytic activity ("mild" mutation), whether a compound heterozygote or surviving homozygote. No cases of R59W homozygosity have been reported although its frequency is such that homozygosity would have been expected to occur (Jenkins, 1996). It would appear therefore that homozygosity for R59W mutation is lethal (Corrigall et al., 2000). The R59W mutation exhibits extremely low activity and as such can be considered a "severe" mutation. However, the R168C mutation appears to be associated with some residual activity (Meissner et al., 1996; Dailey and Dailey, 1997b). Further indirect support that one or both mutations in an HVP patient must be "mild", is the observation that most of the parents of the cases described thus far appear to have been latent carriers, and none are reported to have expressed VP clinically.

Table 2.2: ***PPOX* gene mutations** (From Meissner et al., 2002)

Exon/Intron and Mutations	Effect	Restriction enzyme	Country	No. of families	References and Comments
Exon 2					
1A>G	M1V	NlaIII	France	1	Maeda et al. (2000)
1A>C	M1L	NlaIII	France	1	Maeda et al. (2000)
1A>T	M1L	Hsp92II	Lebanon	1	Frank et al. (1999)
2T>C	M1T	Hsp92II	Ireland / Poland	1	Frank et al. (1999)
3G>C	M1I	NlaIII	France	1	Whatley et al. (1999)
31G>A	G11S		USA	1	Frank et al. (2001a)
35T>C	I12T	BanI	Finland	2	Kauppinen et al. (1997), Fraunberg et al. (2000) (reported as 35C>T); Kauppinen et al. (2001) Compound heterozygote with P256R.
45G>C	L15F	EaeI	UK	7	Whatley et al. (1999), Corrigall et al. (2001)
			SA	1	Corrigall et al. (2001)
59A>C	H20P		SA	1	Warnich et al. (1996b), Hift et al. (1997)
78insC	Frameshift, premature stop codon		Finland	1	Fraunberg et al. (2000), Fraunberg et al. (2001)
Intron 2					
IVS2-2A>C	Splicing defect, premature stop codon in exon 3	BstNI	Finland	1	Fraunberg et al. (2000), Fraunberg et al. (2001)
Exon 3					
113G>C	R38P	BslI	France	1	Whatley et al. (1999)
119G>A	G40E	MnI1	France	1	Whatley et al. (1999)
157-160delATCT	Frameshift, premature stop codon		UK	1	Whatley et al. (1999)
165insAG	Frameshift, premature stop codon		Germany	1	Lam et al. (1997)
175C>T	R59W	AvaI, StyI	SA	Common, founder mutation	Meissner et al. (1996), Warnich et al. (1996b)
			Holland	5	De Rooij et al. (1997)
199-200insT	Frameshift, premature stop codon	BglI	France	1	Whatley et al. (1999)
218T>C	L73P	BsaJ1	UK	1	Whatley et al. (1999)
Intron 3					
IVS3-1G>C	Splicing defect, deletion of exon 4	MaeIII	France	1	Whatley et al. (1999)

Exon 4	Effect	Restriction enzyme	Country	No. of families	References and Comments
251T>G	V84G	CviJI	UK	1	Whatley et al. (1999)
254T>C	L85P		France	2	Whatley et al. (1999)
317A>C	H106P		Argentina	1	De Siervi et al. (2000)
338G>C	Splicing defect, deletion of exon 4, premature stop codon in exon 5	Bsu36I	Finland	2	Fraunberg et al. (2001)
Intron 4					
IVS4+1G>A	Splicing defect		USA	1	Frank et al. (2001a), reported as 333+1G>A in table 1.
Exon 5					
363-364insC	Frameshift, premature stop codon		UK	2	Whatley et al. (1999)
376-377delCT	Frameshift, premature stop codon	MnlI	UK	1	Whatley et al. (1999)
396G>T	E133X (nonsense mutation)		Germany	1	Frank et al. (1998b)
413G>C	R138P		SA	1	Corrigall et al. (2000), compound heterozygote with R59W
428A>T	D143V		France	1	Whatley et al. (1999)
454C>T	R152C	HbaI	France	1	Whatley et al. (1999)
			Finland	2	Kauppinen et al. (1997); Fraunberg et al. (2000), Fraunberg et al. (2001)
460del23	Frameshift, premature stop codon		UK	1	Whatley et al. (1999)
461T>C	L154P	EcoRI	France	1	Whatley et al. (1999)
470A>C	Deletion of exon 5 and 20bp retention of intron 5	Bsu36I	Finland	1	Fraunberg et al. (2001)
Intron 5					
None reported to date					
Exon 6					
472G>A	V158M		France	1	Whatley et al. (1999)
502C>T	R168C	BsaJI	SA	1	Meissner et al. (1996);Warnich et al. (1996b), compound heterozygote with R59W
503G>A	R168H	NcoI	France/UK	2	Whatley et al. (1999)
			Holland	1	De Rooij et al. (1997)
			USA / Germany	No detail	Frank et al. (1997)

Exon 6 (continued)	Effect	Restriction enzyme	Country	No. of families	References and Comments
			Chili	3	Frank et al. (2001b)
G505G>A	G169E		UK	1	Roberts et al. (1998); Frank et al. (1998a), compound heterozygote with G358R
515C>T	A172V		France	1	Whatley et al. (1999)
528-529insT	Frameshift, premature stop codon		France	1	Whatley et al. (1999)
532C>G	L178V		Argentina	1	De Siervi et al. (2000)
538-539delAT	Frameshift, premature stop codon	MvaI	SA	1	Corrigall et al. (1998b), reported as 537delAT
			UK	2	Whatley et al. (1999)
542-556del15	Frameshift, premature stop codon		France	1	Whatley et al. (1999)
565delC	Frameshift, premature stop codon		UK	1	Whatley et al. (1999)
565C>T	Q189X (nonsense mutation)		UK	4	Whatley et al. (1999), reported as E189X
			US/Holland	1	Frank et al. (2001a)
571G>T	E191X (nonsense mutation)		US / Germany	1	Frank et al. (2001a)
593T>G	L198X (nonsense mutation)		France	1	Whatley et al. (1999)
Intron 6					
IVS6+1G>T	Deletion of exon 6		France	1	Whatley et al. (1999)
IVS6-1G>T	Deletion of exon 7	PstI	France	1	Whatley et al. (1999)
IVS6+7G>A	Not determined (but relatively close to intron/exon boundary)		Denmark	1	Christiansen et al. (2001)
Exon 7					
657ins12	A219KANA	BstXI	UK	1	Roberts et al. (1998), compound heterozygote with IVS11-11T>G
657-658ins12	A219KASA		UK	1	Palmer et al. (2001), Compound heterozygotes with IVS11-1G>A
672G>A	W224X (nonsense mutation)	NlaIV	France	2	Whatley et al. (1999)
694G>C	G232R	AcyI, MnlI	France	2	Deybach et al. (1996); Whatley et al. (1999)
695G>C	G232R	MnlI	France	1	Whatley et al. (1999)
745-746insC	Frameshift, premature stop codon	DdeI	France	1	Deybach et al. (1996), Whatley et al. (1999)
745-746insG	Frameshift, premature stop codon	TaqI	France	1	Deybach et al. (1996), Whatley et al. (1999)
745delG	Frameshift, premature stop codon		France and UK	2	Whatley et al. (1999)

Exon 7 (Continued)	Effect	Restriction enzyme	Country	No. of families	References and Comments
759-760delAG	Frameshift, premature stop codon	MnlI	Japan	1	Maeda et al. (2000), reported as 759delAG
769delG;770T>A	Frameshift, premature stop sodon	HpaII	SA	1	Corrigall et al. (2001)
803G>A	W268X (nonsense mutation)	MaeI	UK	2	Whatley et al. (1999)
Intron 7					
IVS7+2T>C	Deletion of exon 7		UK	1	Whatley et al. (1999)
IVS7+1del18	Splicing defect, exon 7 deleted		UK	1	Roberts et al. (1998), compound heterozygote with G358R
IVS7-9T>G	Creation of an additional splice acceptor site results in 8bp added to 5' end of exon 8	NlaIII	UK	1	Whatley et al. (1999)
Exon 8					
841-843delCAC	H281del		France	3	Whatley et al. (1999)
849insT	Frameshift, premature stop codon		Holland	1	De Rooij et al. (1997), reported as 1126+T
845T>A	V282D	MaeIII	UK	2	Whatley et al. (1999)
856delA	Frameshift, premature stop codon		France	1	Whatley et al. (1999)
868G>A	V290M	BsiYI	SA	1	Corrigall et al. (2001)
868G>C	V290L	MaeIII	UK	1	Whatley et al. (1999)
915-916delTG	Frameshift, premature stop codon		US/Italy	1	Frank et al. (2001a)
Intron 8					
None reported to date					
Exon 9					
872T>C	L291P		Holland	5	De Rooij et al. (1997)
884T>C	L295P		UK	6	Whatley et al. (1999)
Intron 9					
IVS9-1G>C	Deletion of exon 10	EcoRII	UK	1	Whatley et al. (1999)
Exon 10					
998A>T	H333L		Holland	1	De Rooij et al. (1997), reported as within exon 9
1004T>G	V335G		France	1	Whatley et al. (1999)
1043A>G	Y348C	MaeIII	SA	1	Corrigall et al. (2000), compound heterozygote with R59W
1046A>C	D349A		UK	1	Roberts et al. (1998), homozygote
1048T>C	S350P	HinfI	UK	1	Whatley et al. (1999)

Exon 10 (Continued)	Effect	Restriction enzyme	Country	No. of families	References and Comments
1072G>A	G358R		UK	2	Roberts et al. (1998), compound heterozygotes with G169E and IVS7+1del18, Frank et al. (1998d)
1043-1044insT	Frameshift, premature stop codon		Argentina	2	De Siervi et al. (2000), reported as 1320insT
1053-1054insT	Frameshift, premature stop codon		UK	1	Whatley et al. (1999)
1081-1082insG	Frameshift, premature stop codon	BglI	UK	1	Whatley et al. (1999)
1082-1083insC	Frameshift, premature stop codon	BglI	France	6	Whatley et al. (1999)
1083delT	Frameshift, premature stop codon	BglI	France	1	Whatley et al. (1999)
			USA	1	Frank et al. (2001a)
1083-1084insG	Frameshift, premature stop codon	BglI	France	1	Whatley et al. (1999)
1090-1091delAG	Frameshift, premature stop codon	AlwNI	UK	1	Whatley et al. (1999)
1091insA	Frameshift, premature stop codon		USA	1	Frank et al. (2001a)
1093G>A	V365M		No details	No details	Frank et al. (1997)
Intron 10					
IVS10-1G>T	Deletion of exon 11	DdeI	France	1	Whatley et al. (1999)
IVS10+1G>A	Aberrant splicing, premature stop codon		China	1	Lam et al. (2001)
Exon 11					
1106T>C	L369P, predicted to be disease related considering introduction of non-flexible proline		Denmark	1	Christiansen et al. (2001), reported as 1383T>C
1119G>A	W373X	ApyI	France	1	Whatley et al. (1999)
1123C>T	Q375X (nonsense mutation)	MaeIII	Canada	1	Corrigall et al. (2001)
1136C>Ains13	Frameshift, premature stop codon		Holland	1	De Rooij et al (1997), reported as 1413C>A+13bp
1144-1145delGT	Frameshift, premature stop codon		American / Indian	1	Frank et al. (2001a)
1147-1148delGT	Frameshift, premature stop codon		France	1	Whatley et al. (1999)
1194-1198delTACAC	Frameshift, premature stop codon		Chile	4	Frank et al. (2001b), reported as 1239delTACAC
1203A>C	L401F		Finland	1	Fraunberg et al. (2001)

Intron 11	Effect	Restriction enzyme	Country	No. of families	References and Comments
IVS11-1T>G	Normal mRNA <90%		UK	1	Roberts et al. (1998), compound heterozygote with A219KANA
IVS11-1G>A	Probable deletion of exon 11 and frameshift		UK	1	Palmer et al. (2001), compound heterozygote with A219KASA
Exon 12					
1274-1275delGT	Frameshift, premature stop codon	MaeIII	UK	1	Whatley et al. (1999)
1281G>A	W427X (nonsense mutation)	BstI	UK	1	Whatley et al. (1999)
1287delA	Frameshift, premature stop codon		France	2	Whatley et al. (1999)
1289insT	Frameshift, premature stop codon		Holland	1	De Rooij et al. 1997, reported as 1566+T
Intron 12					
IVS12+1delG	Deletion of exon 12	SpeI	France	2	Whatley et al. (1999)
IVS12+1G>C	Splicing defect		USA	1	Frank et al. (2001a), reported as 1290+1G>C
IVS12-2A>G	Deletion of exon 13	MspI	UK	1	Whatley et al. (1999)
			Turkey	1	Frank et al. (2001a), reported as 1291-2A>G.

CHAPTER 3

STUDIES ON HUMAN PROTOPORPHYRINOGEN OXIDASE

DEVELOPMENT OF THIS THESIS

Introduction

As detailed in the previous chapters, defects in PPOX (the penultimate enzyme in the haem biosynthetic pathway) result in reduced enzyme activity and is responsible for VP. The high incidence of VP in South Africa, due to a founder effect (R59W), has resulted in this disease being the focus of studies performed in the Lennox Eales Porphyria Laboratories since their inception.

Human PPOX, an inner mitochondrial membrane protein, is a homodimer and each monomer contains a FAD binding site close to the NH_2 terminus and a separate substrate binding site. PPOX requires molecular oxygen and a flavin cofactor for the conversion of protoporphyrinogen IX to protoporphyrin IX. No trans-membrane spanning region or typical leader sequence has been identified. To date, no PPOX crystal structure from any species has been published. Indeed, characterisation of human PPOX is limited, and little is known of the specific residues involved in the 6-electron oxidation catalysed by this enzyme.

Previous studies on human mutant PPOX

When this study commenced (1996), little work had been published on expressed mutant PPOXs. Subsequently, the direct effect of some mutations on PPOX activity has been investigated (Meissner et al., 1996; Dailey and Dailey, 1997b; Roberts et al., 1998; Fraunberg et al., 2001; Kauppinen et al., 2001; Morgan et al., 2002). In some of these studies, activity of expressed mutant PPOX has been determined by direct fluorescence assay (Meissner et al., 1996, Dailey and Dailey 1997b, Fraunberg et al., 2001). In others, PPOX activity was screened for by complementation of the *E. coli* strain SAS38X, which lacks PPOX activity (Roberts et al., 1998; Morgan et al., 2002).

This study

In this study the significance and effects of various "clinical" PPOX mutations responsible for VP in South Africa were examined. We also attempted to gain insight into the role of the R59 residue, and the glycines in the highly conserved GXGXXG FAD binding site of PPOX in catalysis and/or cofactor binding.

Chapter 4 describes the expression of human wild type recombinant PPOX. Thereafter, the generation, by site-directed mutagenesis, of a selection of both naturally occurring ("clinical") mutants relevant to South Africa (H20P, R59W, R168C and Y348C), and self-designed mutants (the non-"clinical" mutants) is documented. To examine the relevance of the positively charged R59 residue, a conservative R59K (positive to positive), and two non-conservatives, R59S (polar) and R59I (aliphatic or neutral) replacements were introduced.

The role of the glycine residues in the "GXGXXG" FAD binding motif was investigated by replacing the glycine residues at positions 9, 11, and 14 by alanine to produce the G9A, G11A and G14A mutations, respectively.

Finally, the expression and purification of the wild type and mutant PPOXs to apparent homogeneity by metal chelate affinity chromatography is described.

Chapter 5 describes a partial characterisation of these enzymes by investigating their pH optima, cofactor composition and kinetic behaviour.

Chapter 6 documents the inhibitor profiles of wild type and mutant PPOX with respect to both DPE inhibitors (AF and MeAF) and the haem breakdown products (BV and BR).

Chapter 7 focuses on the physicochemical characteristics of these proteins utilising CD spectroscopy and UV melting.

Finally, Chapter 8 provides a summary overview and directions for future research.

CHAPTER 4

PRODUCTION OF HUMAN WILD TYPE AND MUTANT PROTOPORPHYRINOGEN OXIDASES, THEIR EXPRESSION AND PURIFICATION

Introduction

The identification of the *B. subtilis hemY (hemG) gene* sequence (Hansson and Hederstedt, 1992), followed by the development of a viable expression system of the soluble form of the *B. subtilis* PPOX from the pBTac1 expression vector in *E. coli* (Dailey et al., 1994c), provided a breakthrough for workers in that field. This enabled the production of milligram quantities of the protein, greatly facilitating its purification. Dailey and Dailey (1996a) published the purification and characterisation of human recombinant PPOX using a nickel-based affinity method. A second publication, describing the purification and characterisation of 3 human PPOX mutants using Talon resin (cobalt based), followed (Dailey and Dailey, 1997b). This has, both directly and indirectly, impacted on this study.

This chapter describes the transformation and expression of recombinant wild type human PPOX with a 6X histidine (His) tag at its N-terminus using the isopropyl-1-thio-β-D-galactoside (IPTG) inducible pTrcHis vector. Thereafter, the creation of a number of PPOX mutants using the GeneEditor site-directed mutagenesis kit is reported. Competent *E coli* JM109 cells were transformed with the human wild type (HPPO-X) and mutant plasmids and their expression optimised. The single step purification of both wild type and mutant PPOX is documented.

Objectives

- To express wild type PPOX in *E.coli* JM109 cells.
- To generate mutant PPOXs by site-directed mutagenesis.
- To optimise expression of these mutant proteins in *E. coli* cells.
- To purify these proteins to apparent homogeneity.

Methods

Transformation of wild type PPOX

A wild type HPPO-X/pTrcHis vector was kindly donated by Professor HA Dailey, University of Georgia, Athens, Georgia, USA. Human *PPOX* cDNA was modified in his laboratory in order that the 6X His tag could be placed upstream to the ATG start site. A nine amino acid spacer was added to the front of the protein facilitating good binding to the metal affinity column (insertion of the tag immediately adjacent to the ATG start site resulted in poor binding). The engineered cDNA was inserted into the unique *Nhe*I site of pTrcHis B vector (pHPPO-X).

The PPOX-containing plasmid was transformed in our laboratory into competent JM109 *E.coli* cells as detailed in Appendix 1. Briefly, 1ml of an overnight *E. coli* cell culture was added to 100ml sterile Luria-Bertani (LB) medium and incubated at 37°C with shaking until mid log phase (an OD_{600} of 0.5 – 0.7). The culture was decanted into pre-chilled tubes, chilled on ice for 10min, and the cells pelleted at 4°C. The pellet was resuspended in ice-cold $CaCl_2$ pH 8.0 to a volume equal to half the original volume. After placing on ice for 15min, centrifugation followed. The cells were then resuspended in $CaCl_2$ to $1/15^{th}$ the original culture volume, aliquoted into chilled sterile tubes, and stored at 4°C for 12 – 24h to increase competency.

Wild type human recombinant DNA (40ng in maximum 100µl TE buffer) was added to 200µl of the cells suspension and placed on ice for 30min and thereafter heated at 42°C for 2min. One ml sterile LB medium was added and the cells incubated for 1h without shaking. Aliquots of the transformed cells were then spread over LB plates with ampicillin (100µg/ml) and incubated at 37°C overnight. Apparent single colonies were replated to ensure single colonies. Single colonies were then inoculated into LB medium containing 100µg/ml ampicillin and the culture grown overnight at 37°C. Glycerol stocks were then prepared.

PPOX activity was assayed (see Appendix 13.4) in cultures made from 6 individual colonies, and the colony that expressed the highest PPOX activity/mg protein was utilised for further studies.

Site-directed mutagenesis

The R168C mutant plasmid was kindly donated by Professor H.A. Dailey, University of Georgia, Athens, Georgia, USA. All other mutants were produced as described below.

Principle

The Promega GeneEditor Site-directed mutagenesis system uses antibiotic selection to obtain a high frequency of mutants. The selection oligonucleotides provided encode mutations that alter the ampicillin resistance gene, thus creating a new, additional resistance to the GeneEditor antibiotic selection mix. The selection oligonucleotide is annealed to the double-stranded DNA template at the same time as the mutagenic oligonucleotide. Synthesis and ligation of the mutant strand links the two oligonucleotides. The resistance to the antibiotic selection mix encoded by this mutant DNA strand facilitates selection of the desired mutation. The efficiency of mutagenesis is improved by an initial transformation into competent *mut*S cells. This repair minus strain of *E. coli* is used to avoid selection against the desired mutation. A second transformation is performed into JM109 to ensure segregation of mutant and wild type plasmids and results in a high proportion of mutants.

Procedure

Mutants were engineered from the wild type HPPO-X/pTrcHis vector using the GeneEditor kit as follows: A 10ml overnight culture of HPPOX was prepared and 6ml of the PPOX expressing cells harvested by centrifugation, and plasmid miniprep performed (see Appendix 3 for details). The extracted DNA was quantified on a GeneQuant spectrophotometer.

Four sets of oligonucleotides were designed to cover the entire *PPOX* cDNA sequence enabling polymerase chain reaction (PCR) to be performed on the cDNA, generating 4 fragments (see Appendix 6.1). In addition, mutagenic oligonucleotides were designed for creation of the desired mutants. All mutagenic oligonucleotides were 5'-phosphorylated as this significantly increases the number of mutant clones (see Appendix 5). The mutagenic and the selection oligonucleotide used were complimentary to the same strand of DNA to achieve coupling of the antibiotic selection to the desired mutation. The appropriate hybridisation (annealing) temperature for each mutant oligonucleotide, was determined by performing gradient PCR on the relevant cDNA fragment, using either the fragment forward or reverse oligonucleotide, together with the appropriate mutagenic oligonucleotide (see Appendix 5.3) using extracted DNA from wild type PPOX as template. The hybridisation temperatures used are shown in table 4.1.

The annealing reactions were prepared by mixing appropriate amounts of DNA template (0.05pmol), phosphorylated selection oligonucleotide (0.25pmol), phosphorylated mutagenic oligonucleotide (1.25pmol), annealing buffer (2μl) and deionised water (to final volume 20μl). After heating at the appropriate annealing temperature for 5min the reaction

was cooled slowly to 37°C. Mutant strand synthesis and ligation was performed by incubating the reaction at 37°C for 90min with 1µl T4 DNA polymerase and 1µl T4 DNA ligase in 3µl of 10 x synthesis buffer in a final volume of 30µl.

Table 4.1: Optimum hybridisation temperatures as determined by gradient PCR

Mutants	Hybridisation temperatures (°C)
Y348C	50
H20P	53
R59W	57
R59K	51
R59S	51
R59I	51
G9A	57
G11A	57
G14A	59

Transformation of BMH 71-18 mutS competent cells

After thawing, 100µl *mut*S competent cells were placed in chilled culture tubes and 1.5µl of mutagenesis reaction added. After standing on ice for 10min, cells were heat-shocked for 50s at exactly 42°C without shaking, then placed on ice for 2min. Nine hundred µl of LB medium at room temperature (without antibiotic) was added to the reaction. Incubation for 1h at 37°C with shaking followed, to allow expression of the resistance gene. A 5ml LB culture containing GeneEditor Antibiotic Selection Mix was then prepared from the above, and incubated overnight at 37°C with shaking (for details see Appendix 5.5).

Plasmid DNA Purification

The plasmid DNA was purified from the above overnight culture using the Wizard Plus SV miniprep DNA purification procedure (see Appendix 3) and the DNA quantified on a GeneQuant spectrophotometer.

Transformation into JM109

This transformation is detailed in Appendix 5.6. LB agar plates containing ampicillin and antibiotic selection mix were prepared. Thawed, JM109 cells (100µl) were transferred into pre-chilled tubes on ice. Two transformations were performed (approximately 2.5ng and 5ng of plasmid DNA used) and tubes kept on ice for 30min. Cells were heat-shocked for 50s in a water bath at exactly 42°C without shaking. SOC medium (900µl) at room

temperature was added to each transformation reaction, and incubated for 1h at 37°C with shaking. Cells were plated and incubated at 37°C for 12 – 14h. A selection of single colonies were inoculated into 10ml LB medium containing 100μg/ml ampicillin in each case, and grown overnight, with shaking at 37°C. Glycerol stocks were prepared for each culture growth and stored at -70°C. Plasmid minipreps were performed on the remains of the culture growth and the DNAs quantified on a GeneQuant spectrophotometer.

Mutational analysis

The appropriate cDNA fragment (which included the mutation) was amplified by PCR utilising DNA (approximately 250ng) extracted from each of the cultures (see Appendix 6.1 for details). The PCR products were analysed on a 6% polyacrylamide gel to check for successful amplification of pure product. Where possible, restriction analysis was utilised to screen colonies as outlined in Appendix 7.1. If not, colonies were sequenced directly. Mutations were confirmed by automated direct sequencing of the relevant cDNA fragment, which included the mutation of interest. Furthermore, once a mutation had been confirmed, the entire cDNA sequence was sequenced to ensure the absence of any erroneous mutations.

Expression of protoporphyrinogen oxidase

Prior to purification of the PPOX proteins, their expression was optimised.

Effect of culture time and temperature on expression

Transformed *E. coli* JM109 cells (500μl) containing wild type (or mutant) plasmid were inoculated into 1L of LB medium with100μg/ml of ampicillin and mixed thoroughly. Under sterile conditions, seven 100ml aliquots of the culture were placed in sterile 500ml flasks and grown with shaking at 37°C. Single flasks were removed from the incubator at time intervals of 12, 14, 16, 18, 20, 22, and 24h. Cells were harvested with centrifugation at 3000g at 4°C for 30min. Cells were resuspended in 5ml assay buffer, sonicated, centrifuged, and the supernatant retained for analysis of enzyme activity. The procedure was repeated at 25°C and 30°C.

Effect of IPTG induction on PPOX expression

Transformed *E. coli* JM109 cells (100μl) containing wild type (or mutant) plasmid were inoculated into 10ml of LB medium containing 100μg/ml of ampicillin and grown overnight with shaking at 37°C. The overnight culture (100μl) was inoculated into 2 x 1L of LB medium containing 100μg/ml ampicillin and the cells grown with shaking at 37°C to mid-log phase. IPTG was added to one of the flasks to a final concentration of 1mM and the

culture thoroughly mixed. From each L of culture, six 100ml aliquots were removed into 500ml sterile flasks. For both IPTG-induced and non-induced, one of the flasks was kept for processing (time zero) and the remaining five were grown further with shaking. Flasks were removed at time intervals of 1, 2, 3, 4, and 5h and cells processed as above.

Purification of wild type and mutant PPOX

Principle

The 6X His tag renders the PPOX susceptible to immobilised metal affinity chromatography. Talon resin was utilised in this study. This uses a dentate metal chelator for purifying recombinant poly-His tagged proteins, thus overcoming the problem of metal leakage encountered with other resins. This chelator holds the electropositive metal in an electronegative pocket tightly. The binding pocket is an octahedral structure in which four of the six metal coordination sites are occupied by the Talon ligand, thus enhancing the Talon's protein binding capacity. Nickel based immobilised metal affinity chromatography (IMAC) resins often bind unwanted host proteins whereas Talon has a significantly reduced affinity for host proteins, thus avoiding extensive washing. Another advantage is that His tagged proteins elute under slightly less stringent conditions than with nickel based IMAC resins.

Procedure

pHPPO-X was initially transfected into and maintained in JM109 *E. coli* cells, as were the various mutants. JM109 cells (0.5ml of a 30% glycerol stock) containing wild type or mutant recombinants were inoculated into 1L LB medium containing 100μg/ml ampicillin and incubated for 18h at 30°C on a rotary shaker. Cells were harvested by centrifugation for 30min at 4°C. The pellet was resuspended in 30ml sonication buffer (0.02M Tris/HCl, 0.3M NaCl, 0.01M imidazole, 1% (w/v) *n*-octyl-β-D-glucopyranoside, pH 8.0), and the cells sonicated. The lysate was then centrifuged at 105000g for 30min at 4°C and the supernatant retained.

The entire purification was performed at 4°C for both wild type and mutant PPOX. One ml of Talon resin was pre-equilibrated with 10ml sonication buffer and the supernatant loaded. The column was washed with 10 ml of sonication buffer followed by 10ml 0.02M Tris/HCl, 0.3M NaCl, 0.02M imidazole, 0.2% (w/v) n-octyl-β-D-glucopyranoside, pH 8.0, prior to elution in elution buffer (0.02M Tris/HCl, 0.3M NaCl, 0.2M imidazole, 0.2% (w/v) *n*-octyl-β-D-glucopyranoside, pH 8.0). Phenylmethylsulfonylfluoride (PMSF) was added to all buffers to a final concentration of 1μg/ml, throughout the purification procedure. The

purification is detailed in Appendix 11. Enzyme purity was confirmed by SDS-PAGE (Laemmli, 1970) (Appendix 12).

PPOX activity was assayed using the procedure by Meissner et al. (1986). This assay is described in detail in the next chapter and Appendix 13.4.

Protein concentration of the purified PPOXs were determined by the Bio-Rad Protein assay (Bradford, 1976) with BSA as protein standard (see Appendix 14).

Results

Engineering of mutants

Nine mutants were engineered: G9A, G11A, G14A, H20P, R59W, R59K, R59S, R59I and Y348C.

Figure 4.1a–g shows restriction analyses on 6% acrylamide gels used for screening mutant colonies. Full details on fragment sizes, pre- and post digestion, for both wild type and mutants are given in Appendix 7.1.

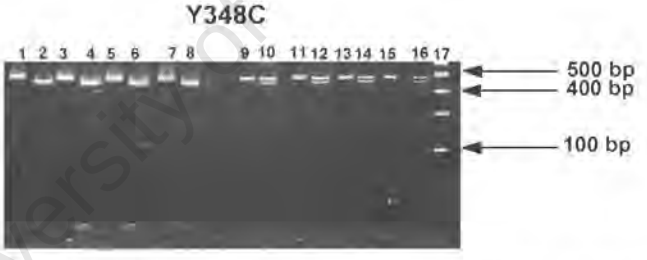

Figure 4.1a: ***Mae III*** **restriction analysis of the PCR product of fragment 3 to identify the Y348C mutant. Lanes 1, 3, 5, 7, 9, 11, 13, 15 are pre-digests, lanes 2, 4, 6, 8, positive clones (post-digestion), lanes 10, 12, 14, 16, mixed clones (post-digestion) and lane 17 is the bp marker.**

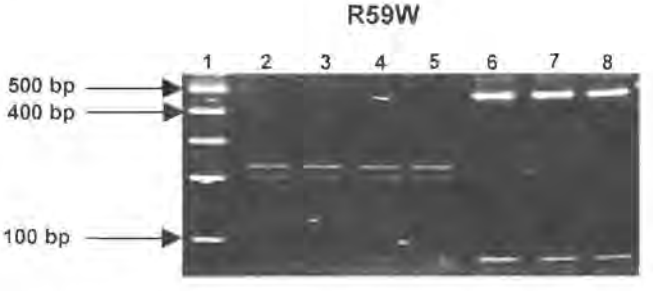

Figure 4.1b: ***Ava I*** **restriction analysis of the PCR product of fragment 1 to identify the R59W mutant. Lane 1, bp markers, lane 2-5, wild type (post digestion), and lanes 6-8 are positive clones (post digestion).**

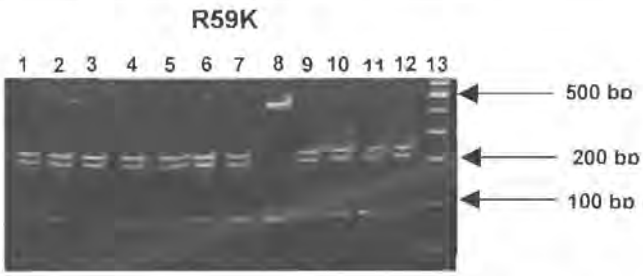

Figure 4.1c: *Ava I* restriction analysis of the PCR product of fragment 1 to identify the R59K mutant. Lanes 1-7 and 9-12, wild type post-digestion, lane 8 is a positive clone (post-digestion) and lane 13, the bp markers.

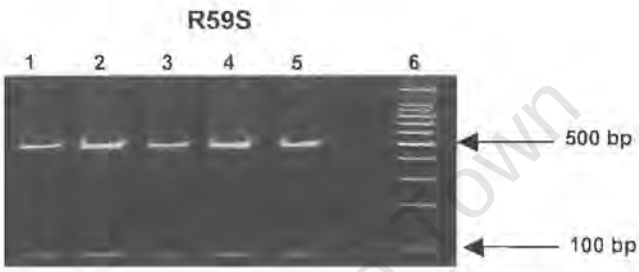

Figure 4.1d: *Ava I* restriction analysis of the PCR product of fragment 1 to identify the R59S mutant. Lanes 1-5 are positive clones (post-digestion), and lane 6 is bp markers.

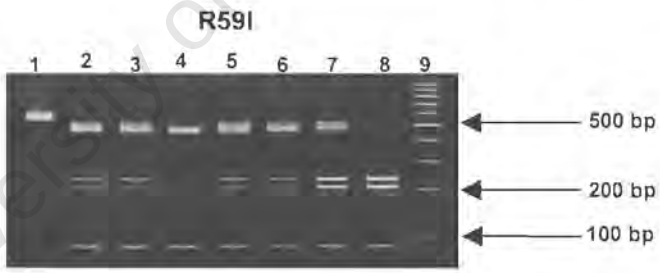

Figure 4.1e: *Ava I* restriction ana ysis of the PCR product of fragment 1 to identify the R59I mutant. Lane 1 is pre-digestion, lanes 2-3 and 5-7 are mixed clones (post digestion), lane 4 is a positive clone (post-digestion), lane 8, wild type (post-digestion) and lane 9 is bp markers.

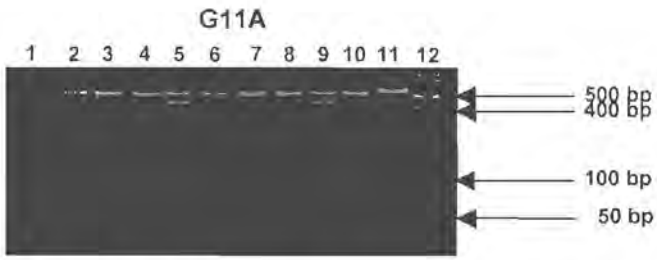

Figure 4.1f: *Xcm I* restriction analysis of the PCR product of fragment 1 to identify the G11A mutant. Lane 1, a positive clone (post-digestion), lanes 2, 5, 9, are mixed clones (post-digestion), lanes 3, 4. 6, 7, 8, 10, 11, are wild type clones, and lane 12 bp markers

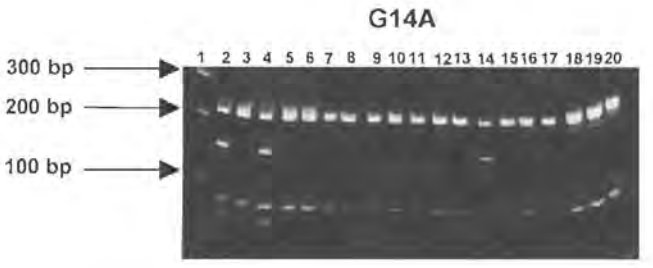

Figure 4.1g: *Msp AI* restriction analysis of the PCR product o fragment 1 to identify the G14A mutant. Lane 1, bp markers, lanes 2, 4, 14 are wild type clones (post-digestion) and lanes 3, 5-13 and 15-20 positive clones.

Figure 4.2 shows partial sequences of the engineered mutants performed in order to confirm the presence of the required mutation. Full length cDNA sequences were analysed to verify that no further mutations had been inadvertently created (data not shown).

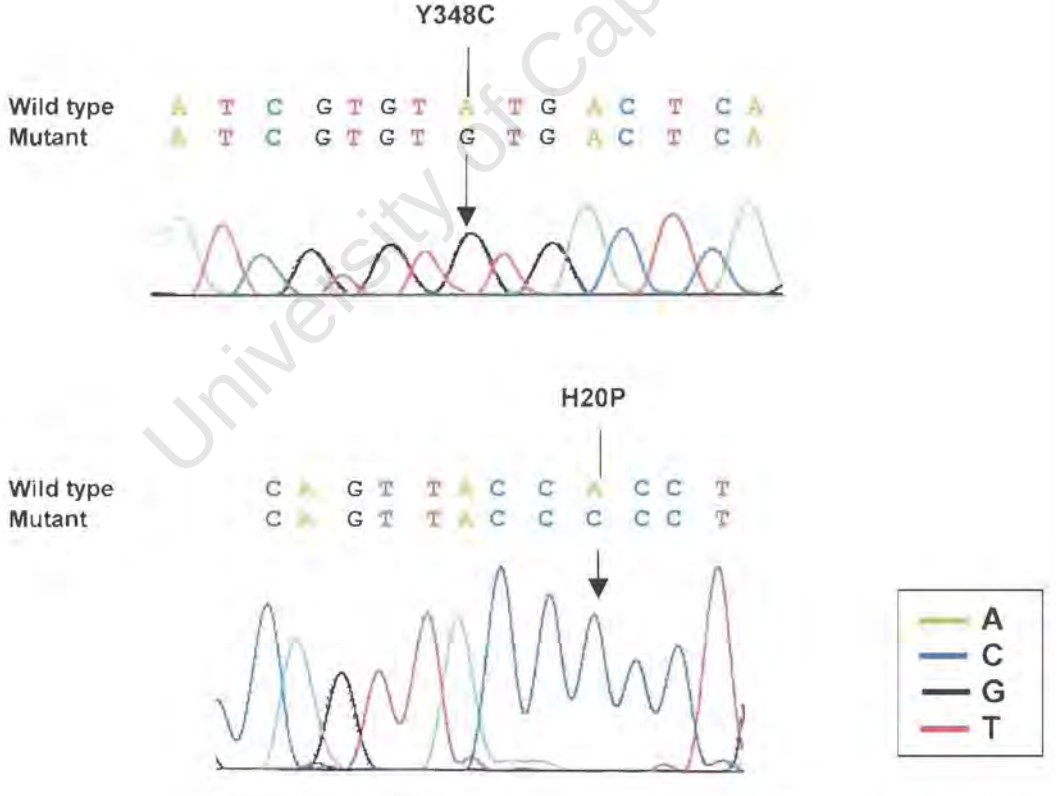

Figure 4.2: Partial sequences of the created mutants. Primer PF1 was used in all cases, except for the Y348C mutant, where primer PF3 was utilised. The arrows indicate the mutated bp (s). For comparative purposes the wild type sequences are shown above the mutant sequence.

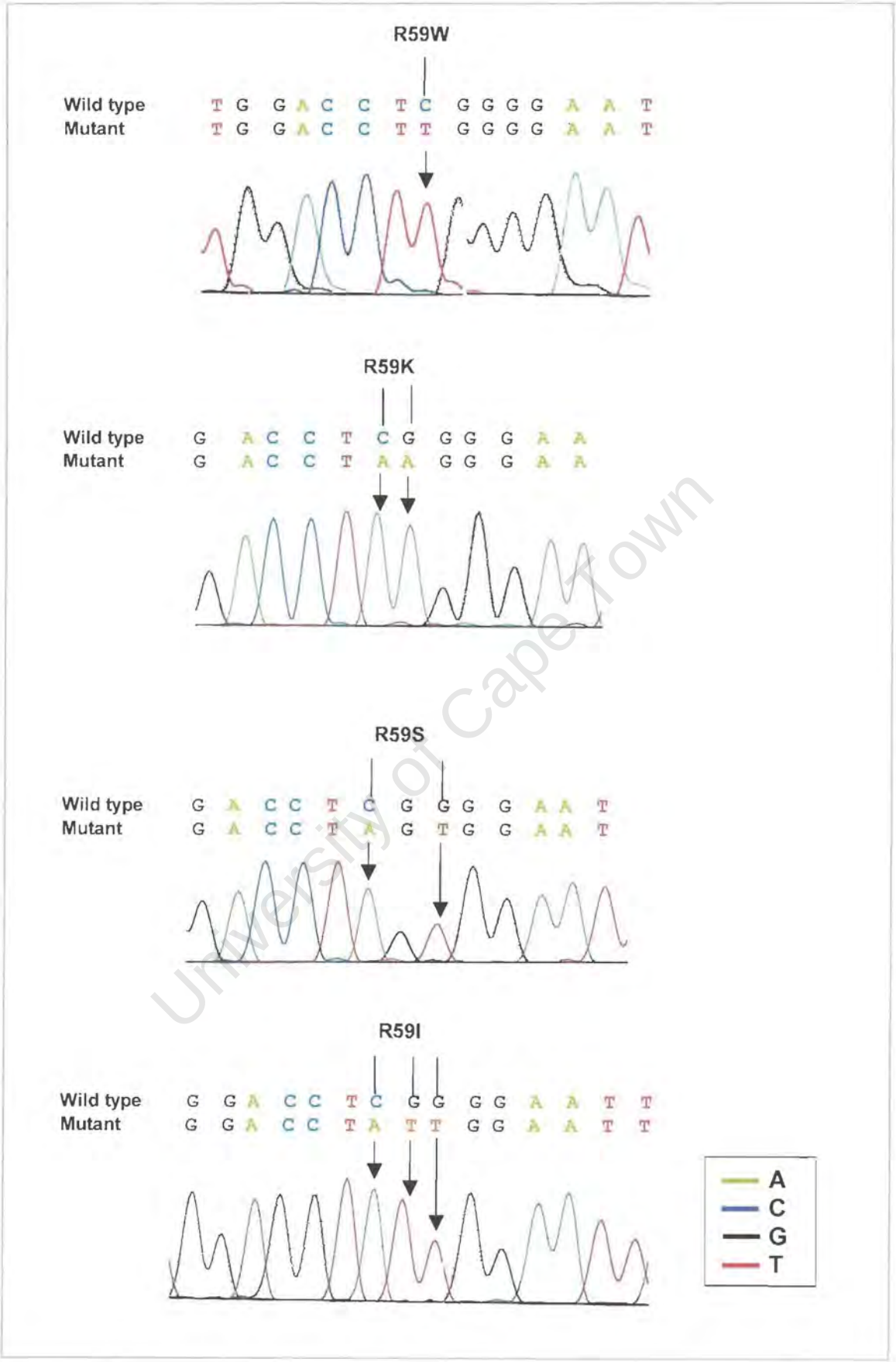

Figure 4.2: Continued

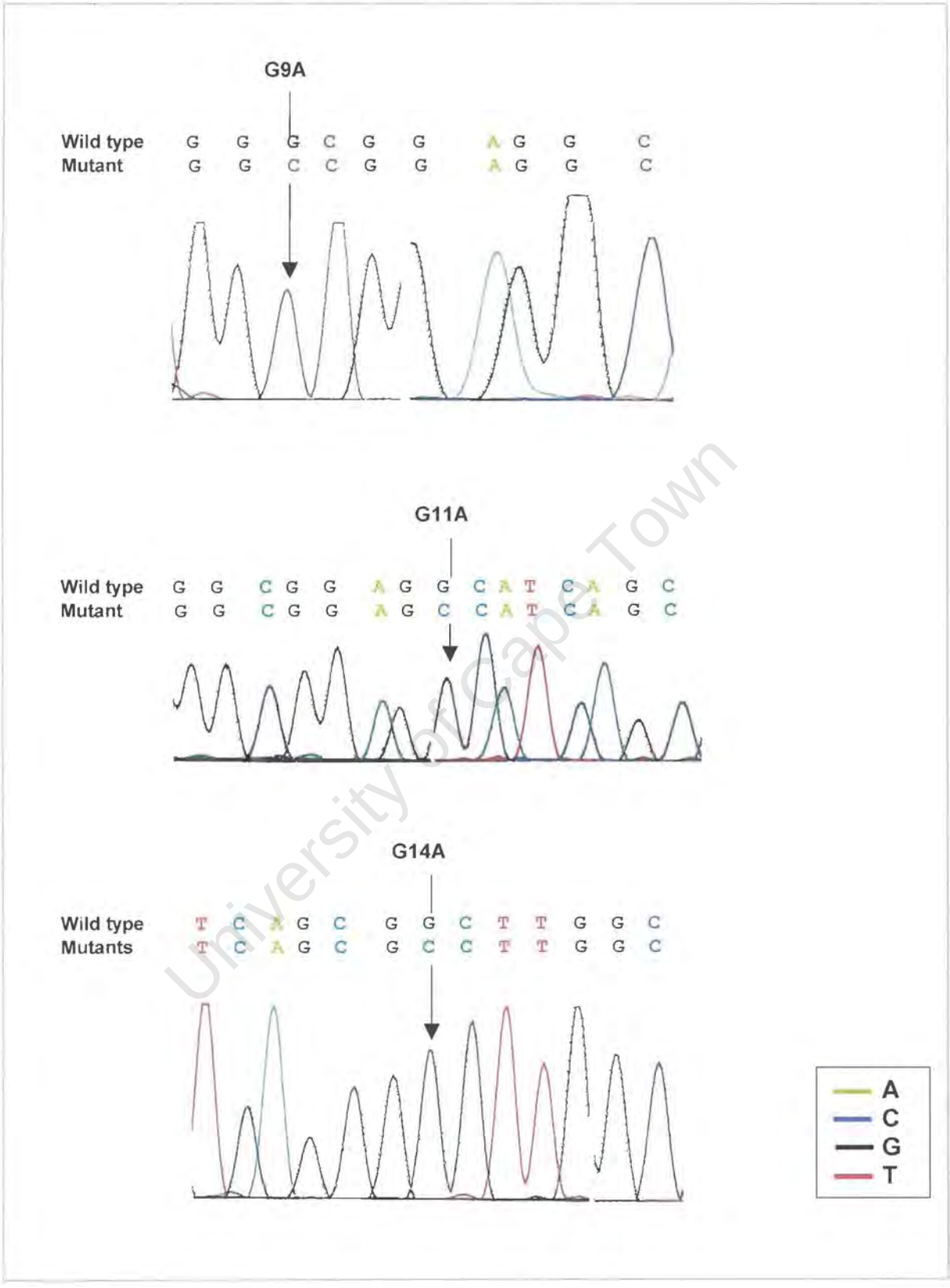

Figure 4.2: Continued

Expression of Protoporphyrinogen oxidase

Measurement of PPOX activity in the sonicates from expressed wild type PPOX at the various time intervals (25, 30 and 37°C) revealed maximum PPOX activity with incubation at 30°C for 18 – 20h (data not shown). Furthermore, no IPTG induction was necessary as growth into stationary phase was sufficient for good expression of PPOX.

As with wild type, incubation of all the PPOX mutants at 30°C for 18h resulted in maximum expression. Figure 4.3A shows an analysis of PPOX activity for the R168C mutant at the 3 temperatures over the period 12 – 24h, and is a typical example. Also illustrated is the fact that IPTG induction did not improve expression to any significant extent at 5h Figure 4.3B).

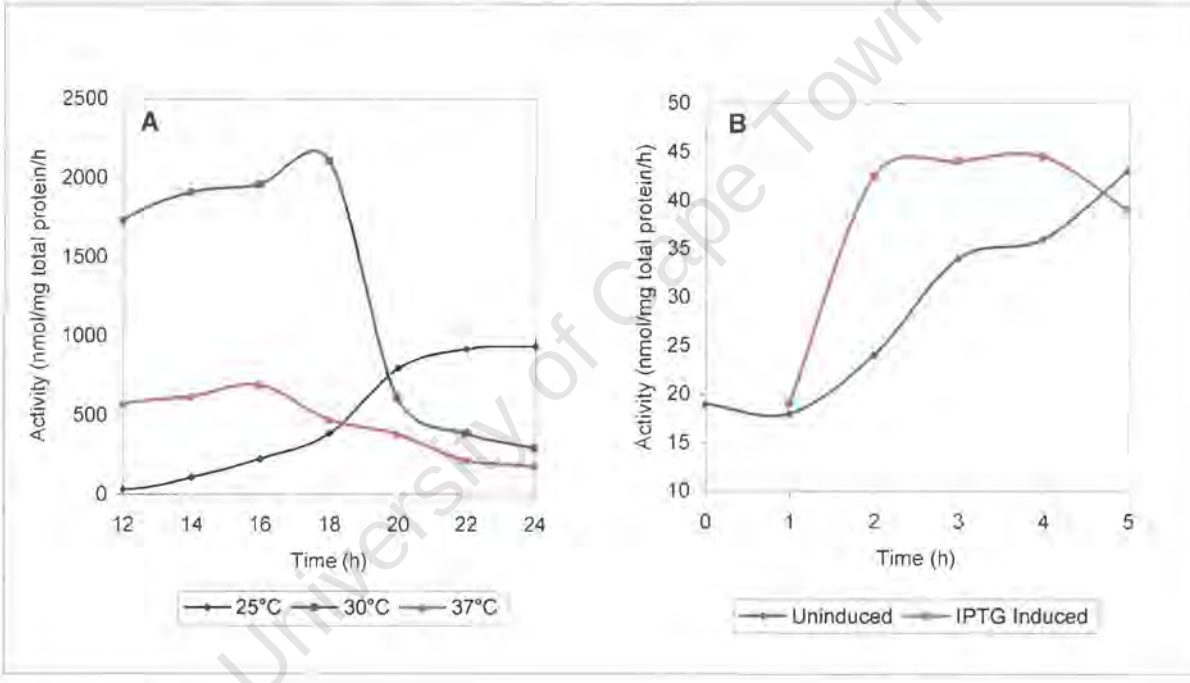

Figure 4.3: **A: Time-course analysis of the expression of R168C mutant protein**
B: Effect of IPTG induction on the expression of R168C mutant

Purification

Talon metal affinity chromatography of the supernatant from 30ml of sonicate of expressed wild type or mutant PPOX yielded pure enzyme, M_r ± 51000 Da, as judged against molecular weight markers on SDS–PAGE (figure 4.4).

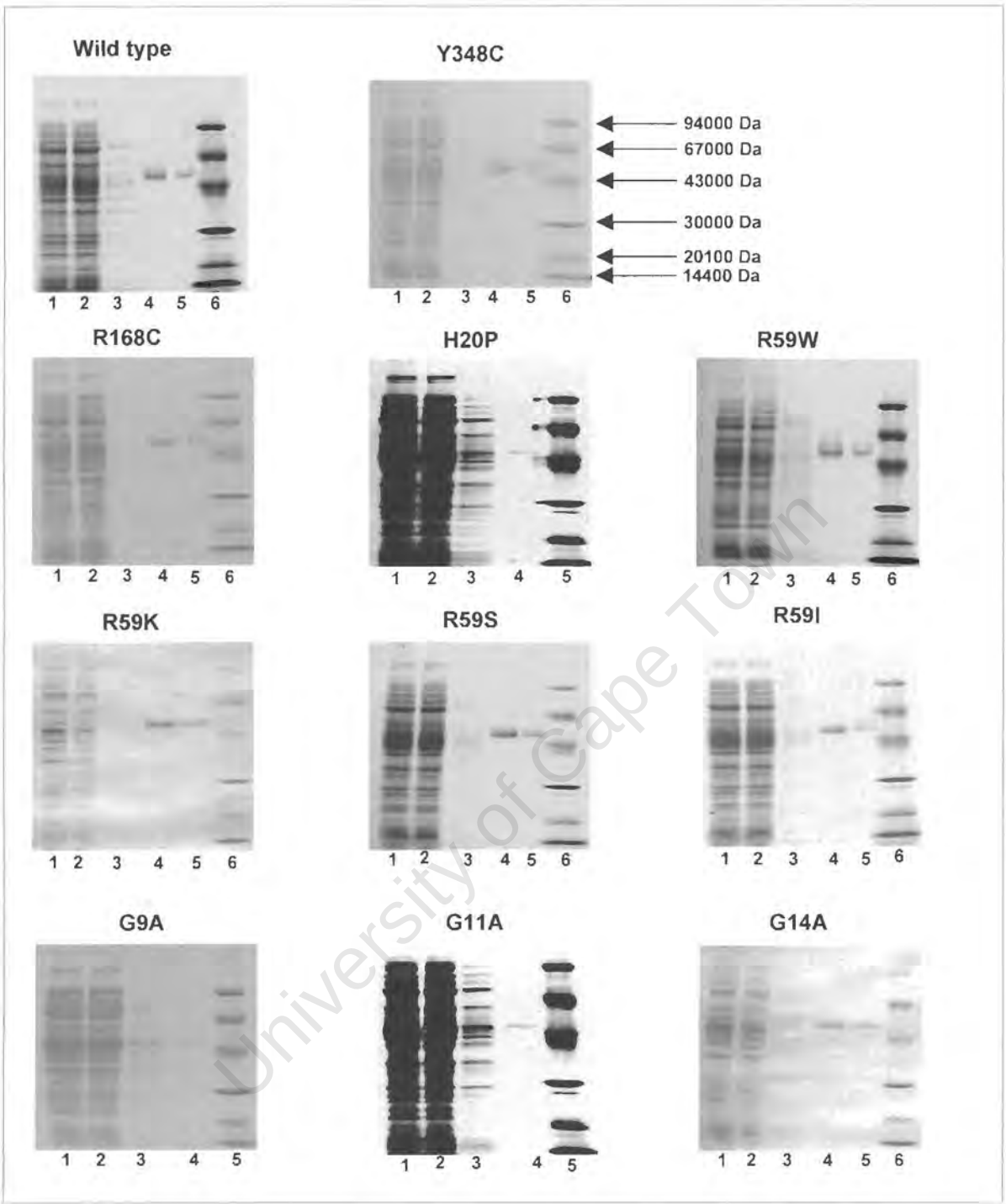

Figure 4.4: SDS-PAGE of wild type and mutant PPOXs as shown above each gel. Lane 1 is the load/supernatant from sonicate *E. coli* cells expressing PPOX, lane 2 is the void, lane 3 is the wash, lane 4 and 5 are the purified PPOX proteins, and lane 6 the molecular weight markers. For H20P, G9A, and G11A only one lane of purified PPOX is shown (lane 4). Lane 5 is the molecular weight markers (molecular sizes of wild type and other mutants are as those shown for Y348C). 5µl of load and void were loaded in all cases. For washes 100µl and eluates, 5µl (lane 4) and 2.5µl (lane 5) of wild type and 100µl (lane 4) and 50µl (lane 5) of all mutants loaded, except for H20P, G9A, and G11A where only 100µl (lane 4) of the eluate was loaded.

Purification data for wild type and mutants are shown in table 4.2. Total amounts of mutant protein obtained from 1L of culture varied considerably and were lower than wild type except for R59S in which the yield was similar. Binding to the column appeared weak for the H20P, G9A and G11A since most of their activity was present in the void and/or wash fractions. Thus, very low yields were obtained for these three mutant enzymes making it impossible to determine a full set of kinetic parameters (see Chapters 5 and 6) other than specific activity.

Table 4.2: Purification yield, activity and percentage recovery of wild and mutant PPOXs.

Fractions	Volume (ml)	Protein Concentration (mg/ml)	Total Protein (mg/L culture)	Total Activity (nmol/h)	Activity (nmol/mg/h)	Percentage Recovery
LOAD						
Wild type	25	4.70	118	2452125	20781	100
Y348C	30	5.30	159	189360	1190	100
R168C	28	6.20	174	335048	1930	100
H20P	19	5.37	102	800	8	100
R59W	25	6.10	152	2750	19	100
R59K	29	5.30	154	717460	4659	100
R59S	25	3.79	95	25350	268	100
R59I	27	4.44	120	11097	92	100
G9A	30	7.20	216	2529	12	100
G11A	19	4.19	80	86	1	100
G14A	30	9.20	276	352800	1278	100
VOID						
Wild type	25	4.40	110	427050	3882	17
Y348C	30	4.50	135	48690	361	26
R168C	28	5.40	151	20286	134	6
H20P	19	4.30	82	522	6.36	65
R59W	25	5.50	138	332	2	12
R59K	29	4.90	142	23635	166	3
R59S	25	3.59	90	1800	20	7
R59I	27	4.35	117	1242	11	11
G9A	30	7.20	216	1341	6	53
G11A	19	3.70	70	10	0.14	11
G14A	30	8.50	255	22950	90	6

Table 4.2: continued

Fractions	Volume (ml)	Protein Concentration (mg/ml)	Total Protein (mg)	Total Activity (nmol/h)	Activity (nmol/mg/h)	Percentage Recovery
WASH						
Wild type	15	0.17	2.6	12210	4696	1
Y348C	14	0.35	4.9	7590	1581	4
R168C	14	0.54	7.6	4529	608	1
H20P	13	0.36	4.7	231	49	29
R59W	15	0.66	9.9	0	0	0
R59K	14	0.19	2.66	2744	1032	0.4
R59S	17	0	0	0	0	0
R59I	15	0.38	5.70	129	23	1
G9A	12	0.62	7.75	325	42	13
G11A	16	0.26	4.16	30	7	35
G14A	15	0.43	6.45	5475	849	2
ELUATE						
Wild type	4	0.47	1.90	872928	436464	36
Y348C	4	0.15	0.60	27660	46100	15
R168C	1	0.40	0.40	34694	78850	10
H20P	1	0.03	0.03	22	688	3
R59W	2	0.39	0.78	1000	1282	36
R59K	2.8	0.54	1.51	233612	155741	33
R59S	4.7	0.47	2.21	21808	9868	86
R59I	2.7	0.61	1.65	9315	5646	84
G9A	1.0	0.12	0.12	239	1988	9
G11A	0.9	0.03	0.03	3	106	4
G14A	1.5	0.46	0.69	122400	177391	35

Discussion

The GeneEditor mutagenesis kit was successfully utilised to generate 9 PPOX mutants. In the transformation of *mutS* competent cells the volume of the antibiotic selection mix added to the overnight culture was reduced by 50% as repeated attempts utilising the concentration recommended in the manufacturer's protocol proved unsuccessful. In some cases, in the transformation into JM109 cells, co-transfection of cells with both wild type and mutant plasmids occurred and was clearly seen on restriction analysis. Reduction of the amount of DNA used in the transformation reaction reduced this problem considerably.

As this study included the purification and kinetic characterisation of human wild type and mutant PPOXs, it was important that soluble, functionally active protein be expressed. It is known that growth temperatures often directly affect both expression levels and protein solubility (The QIAexpressionist, 2001), and lower temperatures can reduce expression levels leading to a higher amount of soluble protein. Overly high levels of expression may produce insoluble inclusion bodies (Kane and Hartley, 1988). It is, however, difficult to generalise as the formation of inclusion bodies is influenced by several factors including: the nature of the protein (such as hydrophobicity), the level of expression (high levels result in aggregation), the host cell (Coligan et al., 1995), and finally the choice of vector. Therefore, it was important to determine the activity of expressed protein at various time intervals and different temperatures, with or without IPTG induction.

In our laboratory, 30°C without IPTG induction was found to be the best condition for growth of wild type and mutant PPOXs. This yielded acceptable amounts of soluble protein in most cases, which could be purified to homogeneity and characterised.

The soluble protein so produced allowed the purification of PPOX under native conditions using metal affinity chromatography. This avoided the need to solubilise with detergents such as 8M urea or 6M guanidinium hydrochloride prior to purification, and having to attempt to renature after the purification (Wingfield et al., 1995).

We chose to use Talon resin in preference to Ni-NTA agarose. In preliminary experiments we found that non-specific binding to Ni-NTA agarose was problematic, resulting in impure protein being eluted. Indeed, even in the case of wild type PPOX, where excellent yields were obtained with Ni-NTA agarose, slight contaminants were still apparent on SDS-PAGE. Furthermore, wild type PPOX bound extremely tightly to the Ni-NTA agarose, requiring very high NaCl and imidazole concentrations in the elution buffer.

We included a low concentration of imidazole in the sonication and wash buffers to prevent non-specific, low affinity binding of background proteins. In addition, 0.3M NaCl was present throughout the procedure. Finally, we minimised the amount of resin utilised in an attempt to competitively elute off non-specifically bound proteins. 6X His-tagged proteins have a higher affinity for the resin than background proteins. Thus, very few non-tagged proteins should be retained on the resin, if nearly all the binding sites are occupied by the tagged proteins. All purifications were performed at 4°C, as binding to Talon resin appeared to be stronger for many of the mutants at this temperature.

An imidazole-based purification was used. Imidazole eluted the PPOX, as it binds competitively to the histidine side chain. The low concentration of imidazole present during loading did not prevent the bulk of PPOX from binding to the resin.

The protein yields varied considerably (Table 4.2). This variation may be explained by observed differences in binding affinities for the resin and/or the fact that mutant proteins could be more poorly expressed and unstable and undergo proteolytic cleavage in the cell (Dailey and Dailey, 1997a).

Conclusions

- The pTrcHis expression system for cloned human PPOX was viable in our laboratory.
- The GeneEditor kit was suitable for the generation of PPOX mutants. Nine mutant PPOXs were generated.
- Both wild type and mutant PPOXs could be expressed and purified to apparent homogeneity by a single step purification procedure based on metal affinity chromatography under native conditions. However, it is important that the purification procedure is optimized.
- Acceptable yields of pure protein could be obtained for wild type, and most mutants, allowing their characterisation, which forms the basis of the remainder of this dissertation.

CHAPTER 5

PARTIAL CHARACTERISATION AND KINETICS OF WILD TYPE AND MUTANT PROTOPORPHYRINOGEN OXIDASE

Introduction

As stated in Chapter 3 missense mutations in the translated region of PPOX may directly affect substrate specificity, binding, stability or catalysis, the ability to bind and utilise FAD, or the ability to translocate to the mitochondria. Studies of specific mutant functionality may allow us to draw conclusions with regard to the functioning of PPOX generally. Indeed, there have been some kinetic characterisations of wild type and three mutant PPOXs (R59W, R168C, and A433P) reported (Dailey and Dailey, 1997b). However, most studies are limited to the effects of the mutations on PPOX activity alone (Roberts et al., 1998; Fraunberg et al, 2001; Morgan et al., 2002). This chapter reports a detailed characterisation with respect to enzyme activities, kinetics and FAD cofactor binding of wild type and a selection of mutant PPOXs, the expression and purification of which has been described in Chapter 4.

Objectives

- To study the kinetic behaviour (k_{cat}, K_m and catalytic efficiency) of human wild type and mutant PPOXs.
- To study the effects of mutations on the flavin cofactor (FAD) binding.

Methods

Protoporphyrinogen oxidase activity assay

Our method for the measurement of PPOX activity (Meissner, 1986) is based on the quantitation of fluorescent product (protoporphyrin IX), which results from the oxidation of the non-fluorescent substrate protoporphyrinogen IX. The constant velocity formation of product from substrate is measured under saturating conditions. In essence, the reaction mixture comprised assay buffer, substrate, and enzyme preparation. A corresponding blank (with heated enzyme) was prepared for each reaction tube. All enzyme assays were performed no less than three times on different days using different enzyme preparations.

Data presented in this entire thesis as mean (+/-) were calculated for standard deviation. The method is detailed in Appendix 13.4.

pH optima

The effect of pH on PPOX activity was determined over the range 5.8 – 9.8 using the following buffer systems: Na phosphate (pH range 5.8 – 7.8), Tris/HCl (pH range 7.4 – 9.0), and Na carbonate (pH range 9.4 – 9.8).

Derivation of kinetic constants

The Michaelis constant K_m and the maximal velocity V_{max} was determined by measuring the constant velocity formation of protoporphyrin IX from protoporphyrinogen IX in the substrate range 0.5 – 25 μM over an incubation time of maximum 1h. Substrate velocity plots were created from sufficient representative points to allow accurate determination of the constants.

Calculated values were determined by the computerised Gauss-Newton iterative, non-linear curve fitting procedure. The catalytic constant k_{cat} was calculated from the V_{max}.

Fluorimetric analysis of cofactor from purified PPOX

Purified wild type and mutant PPOXs were subjected to trichloroacetic acid (TCA) precipitation to extract the flavin cofactor as detailed in Appendix 15. Briefly, after centrifugation to remove the TCA precipitate, the supernatant was retained, divided into 2 aliquots, and the pH adjusted to 3.5 and 7.4 respectively. The fluorescence spectra were then recorded between wavelengths of 480 and 600nm at an excitation wavelength of 450nm. This allows identification of the cofactor as either FAD or FMN as these two flavins display characteristic spectra at these two pHs.

Spectrophotometric analysis of purified PPOX and FAD binding

To analyse potential effects of the mutations on FAD binding to the protein, PPOX UV/VIS spectra were recorded from 250 – 550nm for both wild type and mutants under identical conditions (in elution buffer) at room temperature. The UV/VIS spectrum of a FAD standard (10μM) was also recorded for comparative purposes (Appendix 15).

To assess the FAD content, absorption at the maximum wavelength of 450nm was measured and expressed as absorption/mg protein/ml.

Results

pH Optima

Generally, there was rapid auto-oxidation at acidic pHs, which was difficult to control for. However, all pH optima were in the basic range. The pH optimum for the oxidation of protoporphyrinogen IX for wild type and all mutants was 8.2, with the exception of Y348C where the optimum was 7.8 (Figure 5.1). The pH optima could not be determined for mutants H20P, G9A and G11A due to low yield. Seeing that all other forms of PPOX had similar basic pH optima, we opted to assay these 3 at a pH of 8.2.

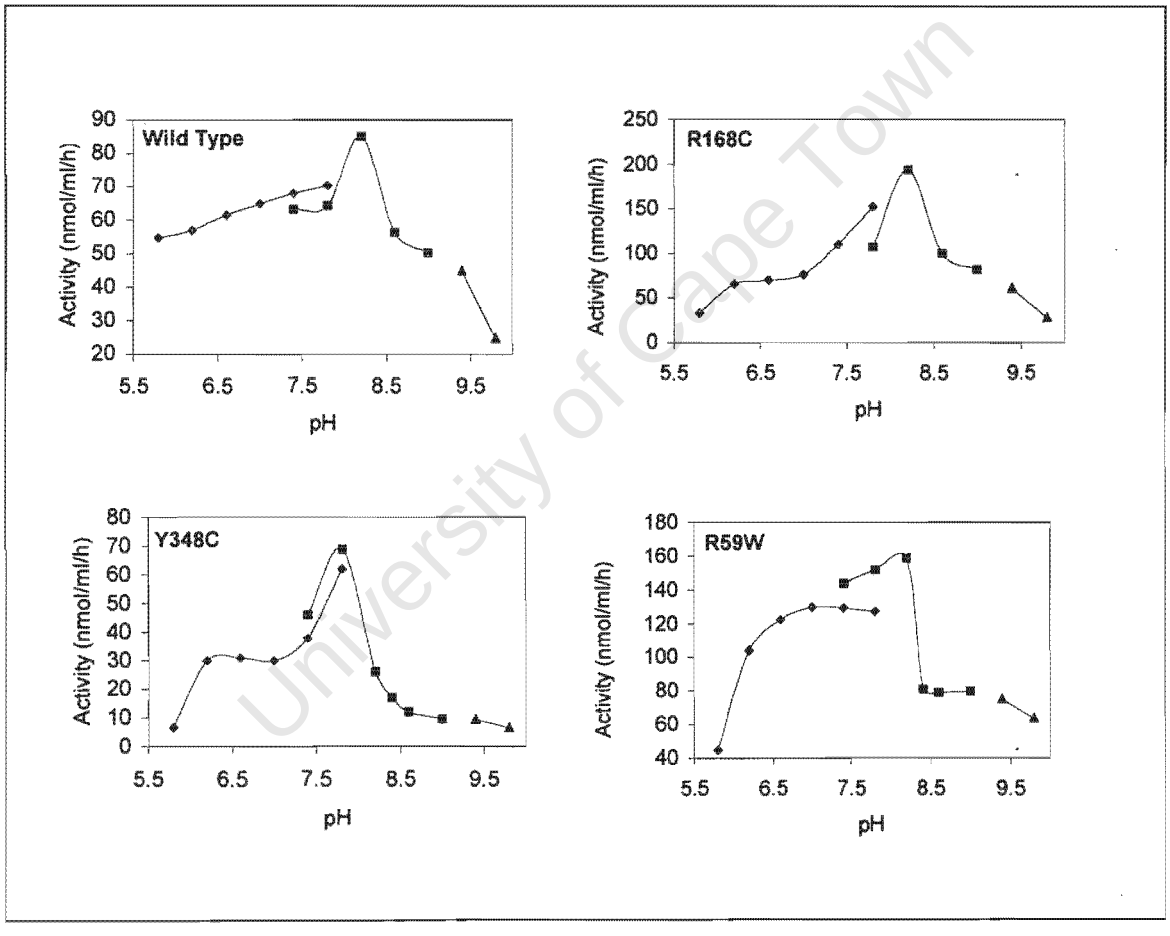

Figure 5.1: pH optima of wild type and mutant PPOXs measured in Na Phosphate (•), Tris/HCl (■) and Na Carbonate(▲).

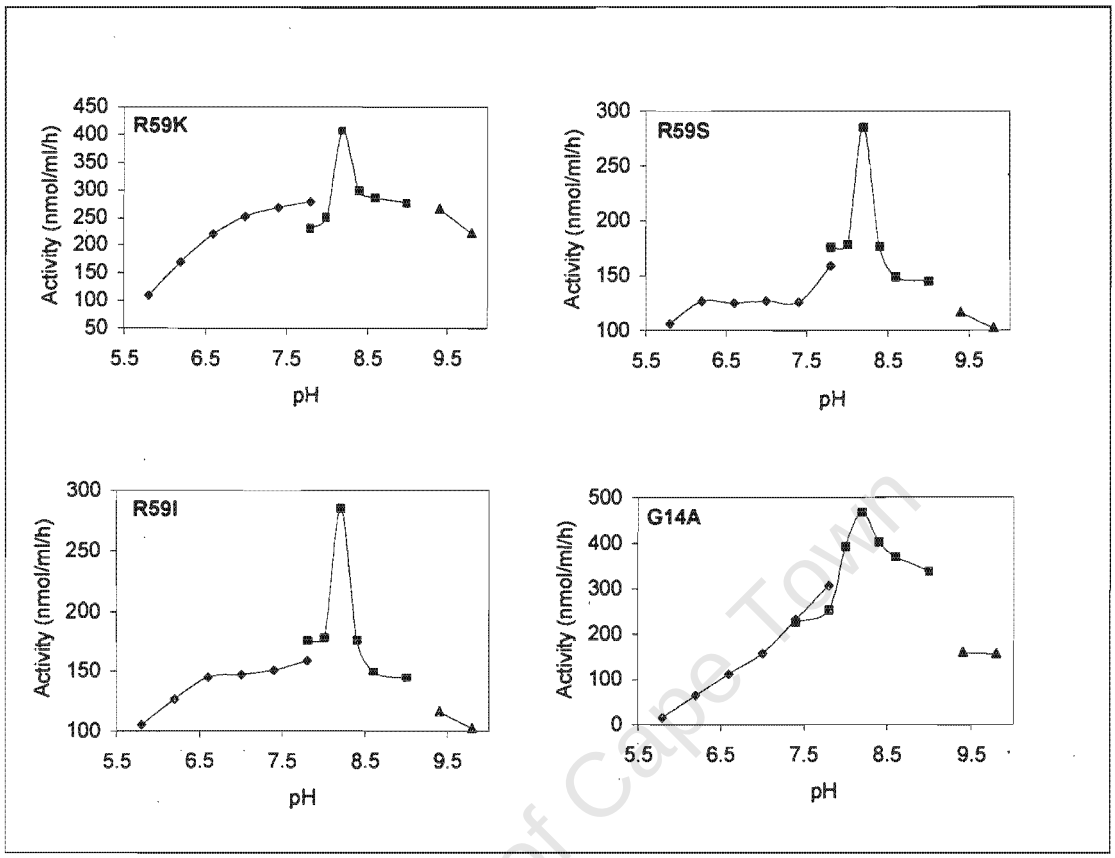

Figure 5.1: Continued

PPOX activity assay and kinetics

Figure 5.2A shows a typical wild type substrate velocity plot used in the determination of K_m and V_{max}. For human PPOX the oxidation of protoporphyrinogen IX to protoporphyrin IX obeyed Michaelis-Menten kinetics as seen by the typical saturation of enzyme by high concentrations of substrate and yielded a straight line when the double-reciprocal was plotted (Lineweaver-Burke plot) (Figure 5.2B). A complete set of kinetic data could not be determined for mutants H20P, G9A and G11A due to low yield. PPOX activity assays were performed at substrate concentration of 15μM under saturation conditions.

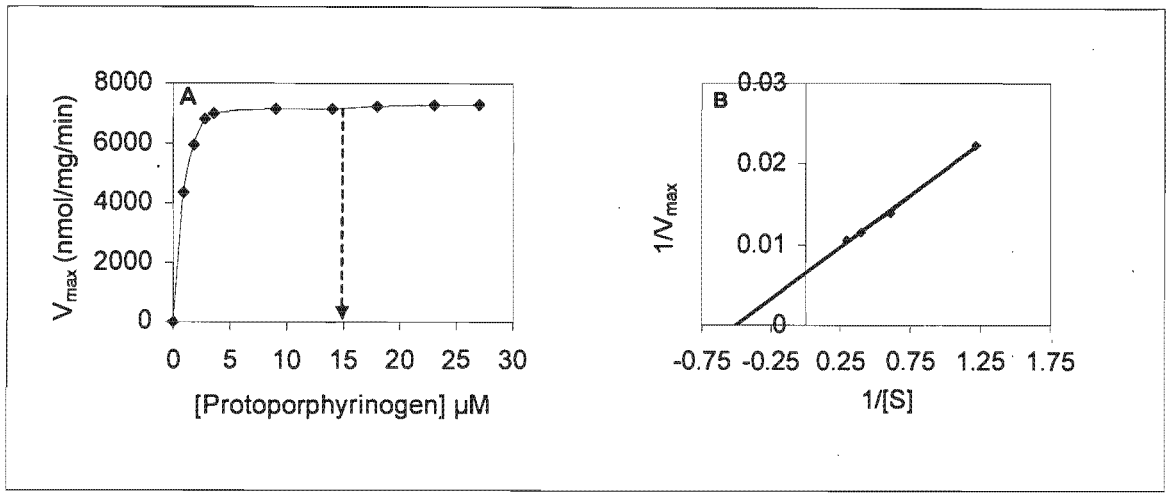

Figure 5.2: **A: Typical substrate-velocity plot for enzymatic oxidation of protoporphyrinogen IX to protoporphyrin IX by human wild type PPOX. The curve followed typical Michaelis-Menten kinetics.**
B: Lineweaver-Burke plot showing 1/V vs 1/S.

Figure 5.3 shows the kinetics of enzymic and non-enzymic (heat denatured enzyme) formation of protoporphyrin IX for a highly active enzyme (wild type) and less active enzyme (R59W). For both wild type and R59W the enzyme catalysed reaction was higher than the auto-oxidation reaction. Similar were observed for all other mutants.

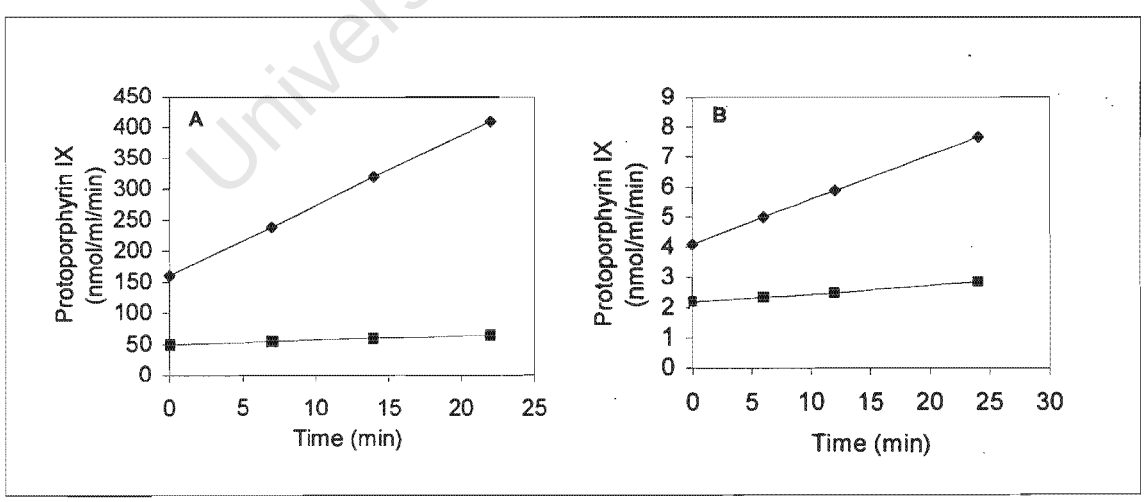

Figure 5.3: **Kinetics of the enzymic (▲) and non-enzymic (■) formation of protoporphyrin IX.**
A: Wild type
B: R59W

Table 5.1 lists the specific activity (nmol/mg/min) for wild type and mutant PPOXs and expresses them as a percentage of wild type activity (See Appendix 21 for actual data). Y348C and R168C mutants showed some residual activity of 8 and 17% of wild type PPOX activity, respectively, whereas for R59W and the H20P the activity was negligible. R59K resulted in considerably less disruption (37% of wild type activity) than when the positive charge was removed (<3% of wild type activity, for R59S and R59I). The substitution of glycine by alanine in codon position 14 resulted in less disruption (G14A activity, 42.6% of the wild type activity) than in codons 9 and 11 (G9A and G11A activity, <1%).

Table 5.1: Specific activities of wild type and mutants, and percentage activity of wild type PPOX

PPOX	Specific activity (nmol//mg/min)	Percentage of wild type activity
Wild type	7150.00 ± 192 (n = 4)	100
Y348C	617.00 ± 8.97 (n = 4)	8.6
R168C	1257.00 ± 41.4 (n = 3)	17.5
H20P	11.32 ± 0.75 (n = 3)	0.2
R59W	19.75 ± 1.05 (n = 4)	0.3
R59K	2690.00 ± 66.7 (n = 3)	37.6
R59S	183.10 ± 11.0 (n = 4)	2.6
R59I	106.00 ± 7.27 (n = 4)	1.5
G9A	36.85 ± 2.90 (n = 3)	0.5
G11A	1.57 ± 0.14 (n = 3)	0.02
G14A	3044.00 ± 67.2 (n = 3)	42.6

Table 5.2 gives the K_m, K_{cat} and catalytic efficiency (k_{cat}/K_m) (See Appendix 21 for actual data). There was a relative invariance in K_m for all enzymes except for R59S and R59I, which had an approximately two-fold lower affinity for the substrate. As in the case of their specific activities, the catalytic efficiencies of Y348C and R168C were lower than wild type (7 and 14% respectively) but higher than R59W. The study of the catalytic efficiency on R59 mutants showed 44% of wild type for R59K, 1.4% of wild type for R59S, and 1% of wild type for R59I. R59W had lowest catalytic efficiency (0.42% of wild type). Repeated attempts to determine K_m, FAD binding and T_m (see chapter 7) for the H20P, G11A and G9A mutants proved unsuccessful due to the low protein yield and very low apparent activity, making it impossible to obtain accurate kinetic data.

Table 5.2: Substrate binding affinity and catalytic efficiency of wild type and mutant PPOXs

PPOX	K_m (μM)	k_{cat} (s^{-1})	k_{cat}/K_m ($s^{-1}.\mu M^{-1}$)
Wild type	0.85 ± 0.09 (n = 6)	5.95 ± 0.44 (n = 6)	7.00
Y348C	1.07 ± 0.09 (n = 6)	0.53 ± 0.07 (n = 6)	0.50
R168C	1.00 ± 0.06 (n = 4)	1.02 ± 0.03 (n = 4)	1.02
H20P	ND	ND	ND
R59W	1.26 ± 0.10 (n = 5)	0.04 ± 0.01 (n = 5)	0.03
R59K	0.83 ± 0.09 (n = 3)	2.57 ± 0.12 (n = 3)	3.10
R59S	1.70 ± 0.24 (n = 4)	0.17 ± 0.01 (n = 4)	0.10
R59I	2.09 ± 0.06 (n = 3)	0.15 ± 0.01 (n = 3)	0.07
G9A	ND	ND	ND
G11A	ND	ND	ND
G14A	0.85 ± 0.03 (n = 3)	3.90 ± 0.15 (n = 3)	4.59

ND = not determined

Fluorometric identification of the cofactor

The fluorescence spectra of extracted cofactor from purified wild type PPOX when measured at acidic and neutral pH showed the characteristic FAD pH–dependent shift (Figure 5.4). FAD was readily extracted from the protein by TCA precipitation.

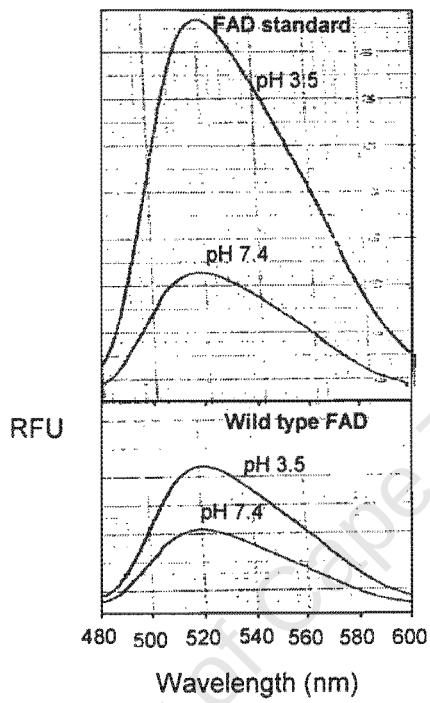

Figure 5.4: **Fluorescence emission spectrum of wild type and standard FAD. The spectrum was recorded at an excitation wavelength of 450nm and had a maximum emission wavelength at 520nm.**

UV/VIS spectra of FAD cofactor

UV/VIS spectra were recorded for FAD standard, purified wild type, and mutant PPOXs. The spectra for wild type and mutants R168C, Y348C, R59K, R59S, R59I, G14A were similar. Figure 5.5 shows the spectra for FAD standard, purified wild type, R59K and R59W PPOX. All PPOXs except for R59W showed FAD-type spectra with absorption maxima at 375 and 450nm.

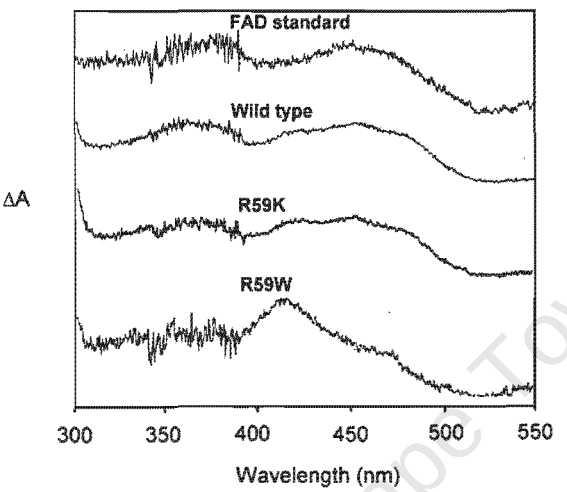

Figure 5.5: UV/VIS spectra of FAD standard, purified wild type, R59K and R59W PPOXs. Absorption maxima at 375 and 450nm are apparent for FAD standard, wild type and R59K mutant PPOX. A spectral change can be seen for R59W.

Figure 5.6 (See Appendix 21 for actual data) shows the absorption maxima at 450nm expressed per mg protein giving an indication of the amount of FAD bound/not bound.

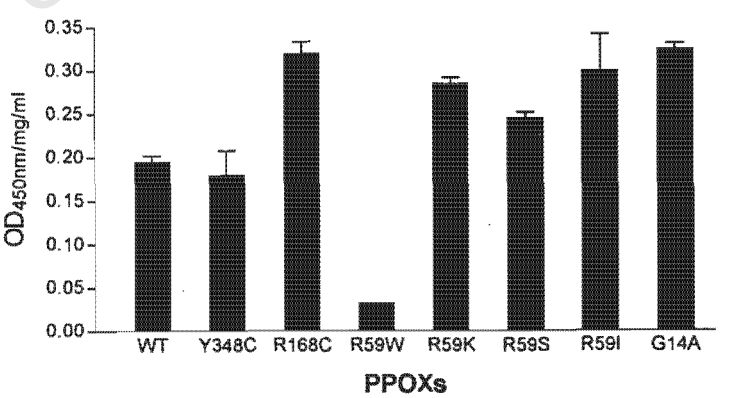

Figure 5.6: FAD absorption at 450nm for wild type and mutant PPOXs. FAD content was expressed as OD/mg/ml of protein. Data are means ± S.D. for n = 3.

Effect of FAD on catalytic activity

Addition of exogeneous FAD (10μM-100μM) to the PPOX assay did not increase activity for both wild type and mutants.

Discussion

PPOX kinetics

The results obtained from PPOX assays were reliable even though no error bars were shown. Assays were performed for more than once to ensure reproducibility of data.

PPOX activity was reduced in all mutants, to some extent. The presence of some residual activity is apparent in both Y348C and R168C, in contrast to R59W and H20P, where the activity was negligible. Both the Y348C and R168C mutations were identified in compound heterozygous individuals, i.e. they have one of these mutations in addition to the common South African R59W mutation (Meissner et al., 1996, Corrigall et al., 2000). Although these patients are clinically severely affected, the fact that they survive suggests that at least this level of residual PPOX activity, together with the negligible R59W activity, is compatible with life, as has been suggested previously (Roberts et al., 1998; Whatley et al., 1999; Corrigall et al., 2000; and Morgan et al., 2002). Interestingly, our activity results demonstrate that both R168C and Y348C have catalytic activity an order of magnitude greater than that of R59W. This, in spite of the possibility, that R168C lies within a membrane-anchoring domain (Arnould et al., 1999), which may alter enzyme stability and the possibility that additional cysteine residues in both cases may cross-react to form alternative disulfide linkages and could thus be predicted as relatively severe replacements. On the other hand, a recent report (Morgan et al., 2002) demonstrated that R168H had negligible activity in spite of a relatively conservative replacement. This underlines the necessity to exercise caution in predicting the effects of specific mutations in PPOX.

Of note, is that in the case of Y348C, all other family members who tested positive for this single mutation had normal porphyrin biochemistry (Corrigall et al., 1998b). The patient's father did, however, demonstrate a small peak at 626nm on plasma fluoroscanning, indicative of VP. These findings are supportive of a "lesser" mutation. Similarly no other relatives of the R168C/R59W homozygote, who were heterozygous for this mutation, showed any clinical or biochemical symptoms of VP (Meissner et al, 1996).

The activity in H20P is severely diminished, probably because it involves substitution of a positively charged amino acid, histidine, by a hydrophobic amino acid, proline. Proline

residues have the propensity to form reverse turn structures in which its ring structure fits well and decreases protein flexibility by disruption of α-helices (Tian et al, 1998). In addition, the H20P falls in the putative dinucleotide binding site (Wierenga et al., 1986, Dailey and Dailey 1997) and occurs immediately adjacent to a conserved leucine (L21). Our findings of severely reduced K_{cat}s and relatively invariant K_ms for R168C and R59W are in agreement with the findings of Dailey and Dailey (1997b). There was a relative invariance in K_m for all enzymes except for R59S and R59I, which had an approximate two-fold lower affinity for the substrate and R59W where a slight decrease in binding affinity is apparent. This suggests, at least in part, a substrate binding problem in R59 mutants rather than a mechanistic problems.

In the study of the relevance of the R59, the introduction of both a conservative R59K and two non-conservative replacements R59S and R59I showed almost complete loss of PPOX activity for non-conservative substitutions underlining the requirement of a positive charge in codon 59.

FAD cofactor

This study identifies FAD as the flavin cofactor present in human PPOX. The relative ease of extraction of the FAD cofactor from the PPOX, suggests that it is non-covalently associated with the protein. This data is in keeping with earlier reports (Dailey and Dailey, 1996a; Dailey and Dailey, 1997b).

The common South African founder mutation, R59W (Meissner et al., 1996), falls within the 60 bp flanking region of the putative FAD dinucleotide binding motif of PPOX (Nishimura et al., 1995a, Dailey and Dailey, 1998). This makes it attractive to speculate that this may account for the severe loss of enzyme activity of the R59W. The UV/VIS spectrum of R59W PPOX is different to that of wild type and all other mutants indicating that FAD interaction with the protein is compromised (Figure 5.5). The low OD_{450}/mg/ml (figure 5.6) confirms this.

However, both conservative and non-conservative replacements in R59 appeared to bind FAD, although in R59W binding was reduced (Figure 5.6). The activity data and the fact that FAD binding is reduced in the R59W mutant suggests that R59 is required for catalytic activity (either directly or via impaired substrate binding) and the lack of FAD binding is due to the bulky nature of the aromatic tryptophan, rather than the loss of the positive charge. Reduced FAD binding confirms earlier studies of Dailey and Dailey (1997b). Hydrophobicity at this position would appear to be unimportant for FAD binding

as both R59I and R59W are hydrophobic replacements, yet differed in their ability to bind FAD.

Considering the FAD and activity data together: The R59W mutant has both severely compromised activity and FAD binding, while the R59S and R59I mutants (uncharged replacements) had reduced activity yet maintained FAD binding, and the R59K (positive charge replacement) had activity and bound FAD, strongly suggests that the positive charge at position 59 is required for catalytic activity and not FAD binding. Furthermore, the fact that additional FAD was ineffective in overcoming any potential impairment of FAD binding supports this.

The FAD binding motif

PPOX exhibits a highly conserved GXGXXG (where X denotes any residue) motif at the N-terminus, which is recognised as a signature sequence in a large number of dinucleotide-containing proteins. Crystallographic studies performed on other flavoproteins confirm that the involvement of these residues in FAD binding (Vrielink et al., 1991, Roberts et al., 1996). Careful analysis of the known three-dimensional structures (using amino acids that are available in the Protein Sequence Database of Protein Identification Resource) of ADP-binding βαβ-folds revealed the importance of the GXGXXG motif in this region (Wierenga et al., 1986). Our results for substitution of glycine by alanine in the mutations G9A, G11A and G14A were in agreement to those of Nishiya and Imanaka (1996). G9A and G11A demonstrated <1% of wild type activity; G14A 42%. They investigated the importance of the glycine in the 1st, 3rd and 6th positions of the GXGXXG motif in *Athrobacter* sarcosine oxidase. They showed that substitution at positions 1 and 3 of the motif sequence was highly significant, and at the 6th position less so. Clearly these glycines are critical for structural maintenance of the dinucleotide binding site and consequent activity of the protein. The "X"-residues are much less important. Furthermore, our results indicate that FAD binds to the G14A mutant although no comparison with G9A and G11A was possible, due to low yields of a low activity enzyme.

Nishiya and Iminaka (1996) examined the frequencies of amino acids appearing in the GXGXXG motif. Apart from the 3 highly conserved glycines, only the first X showed any clear tendency, in that glycine and alanine appeared in approximately 42% of the 133 sequences of the FAD or NAD-dependent proteins studied. It was noted that overall, large amino acids were infrequent and the frequencies of basic, acidic and aromatic amino acids were especially low.

Nishiya and Imanaka were able to reverse the deleterious effects of certain mutations on the FAD spectra of *Arthrobacter* sarcosine oxidase (also a flavoprotein) by addition of

chloride ions, thereby reactivating the protein (Nishiya and Imanaka, 1996). In our study there was no need for addition of chloride ions for reactivation since a relatively high concentration of NaCl was present in the elution buffer.

Conclusions

- All the mutations under investigation in this study resulted in reduced PPOX activity to varying degrees.
- R59W, H20P, G9A, G11A had negligible PPOX activity and represent "severe" mutations, but Y348C and R168C can be considered "lesser" mutations.
- This work suggests that the positive charge at R59 is directly involved in catalysis and not for FAD binding.
- A "bulky" residue (such as tryptophan) at position 59 impairs FAD binding, yet hydrophobicity appears unimportant.
- The substitution of glycine by alanine in codon 14 is less disruptive than in codons 9 and 11 in the conserved GXGXXG motif.

CHAPTER 6

INHIBITION STUDIES ON HUMAN WILD TYPE AND MUTANT PROTOPORPHYRINOGEN OXIDASE

Introduction

The study of the structure and function of PPOX was stimulated by the fact that DPEs are potent inhibitors of PPOX and provide a useful tool to investigate the substrate binding site/catalysis of the enzyme. (Matringe et al., 1989a; Witkowski and Halling, 1989; Duke et al., 1990, 1991b; Camadro et al., 1991; Nandihalli and Duke, 1993; Scalla and Matringe, 1994; Reddy et al., 1995). The details of this inhibition have been reviewed in Chapter 2. Generally they are competitive inhibitors (with respect to the tetrapyrrole substrate protoporphyrinogen IX), however, this inhibition by DPEs is not seen in all PPOXs, eg *B. subtilis*, *E. Coli* and *B. japonicum* PPOXs (Jacobs et al., 1990; Dailey et al., 1994).

An important feature of these inhibitors is that their structure mimics half of that of the protoporphyrinogen IX enabling geometric fit into the active site (Nandihalli and Duke 1993). It could also be expected that certain other tetrapyrrolic compounds may also inhibit PPOX. Indeed, haem and its metabolic products BR and BV are also effective inhibitors of PPOX (Poulson and Polglase, 1975; Camadro, 1985; Ferreira and Dailey, 1988; Corrigall et al., 1998a).

In this chapter, the effect of two DPEs, AF and MeAF, and the haem breakdown products, BV and BR on activity of wild type and some mutant PPOXs, is examined. This investigation was undertaken in an attempt to gain further insight into the nature of the active site of PPOX.

Objective

To investigate the inhibitory effect of AF, MeAF, BV and BR on the oxidation of protoporphyrinogen IX to protoporphyrin IX by human wild type and a selection of mutant PPOXs by determining the kinetic parameters, IC_{50}, K_i, K_s, α, and mode of inhibition.

Methods

Inhibition studies and determination of kinetic data

These studies were performed as described by Corrigall, et al. (1994) using AF, MeAF, BV and BR. A complete set of data representing all kinetic inhibition parameters in every mutant, using all inhibitors was not performed due to the difficulties and tedium associated with PPOX assay. However, enough data was collected to allow certain conclusions to be drawn.

PPOX activity was assayed in the presence of the inhibitor by measuring constant velocity formation of protoporphyrin IX from protoporphyrinogen IX (see Chapter 5 and Appendix 13.4). The reaction mixture comprised assay buffer (0.1M Tris/HCl, 0.001M EDTA, 0.003M DTT, 0.1% Tween 20, pH 8.2), substrate, inhibitor and enzyme preparation. A corresponding blank (with heated enzyme) was prepared for each reaction tube. Protoporphyrin fluorescence was directly proportional to the time over interval 10 – 40 min. The slope of the line was used to calculate reaction rate (expressed in nmol protoporphyrin IX produced/ml/h).

The inhibitors were dissolved in DMSO to a final solvent concentration of 2.5%.

IC_{50} was determined by measuring PPOX activity at a range of inhibitor concentrations (0 – 100μM), at a single substrate concentration of 15μM. A double exponential curve of inhibitor concentrations vs PPOX activity was fitted using the computerised software package (Enzfitter).

IC_{50} is that inhibitor concentration which at any fixed saturating substrate concentration (S^0) reduces the V_i (uninhibited) to $V_i/2$.

Kinetic constants, K_i, K_s and α and model discriminations were determined from secondary replots of K_m/V_{max} vs [I] and $1/V_{max}$ vs [I] where [I] represents the inhibitor concentration. The derivation and form of these equations is detailed in Appendix 16.

The substrate was added at 8 different concentrations over a range of 0.5 – 25μM. Four different inhibitor concentrations were added for each substrate concentrations within the range of 0 – 10μM (final concentration). Both substrate and inhibitor concentrations were selected from pilot experiments to provide sufficient representative points on substrate-velocity plots to enable the accurate determination of the Michaelis-Menten constant (K_m) and the maximal velocity (V_{max}) using the computerised Gauss-Newton iterative non-linear curve fitting procedure as described in the previous chapter. Data represent the mean of at least three independent sets of data performed on different enzyme preparations.

Results

IC_{50}s

Figure 6.1 is representative of a typical IC_{50} plot, showing inhibition of wild type PPOX by AF and MeAF. Both are good inhibitors of PPOX with an IC_{50} of 4.20 $\pm$ 0.39 and 0.18 $\pm$ 0.01μM respectively. Further data is presented in tabular form.

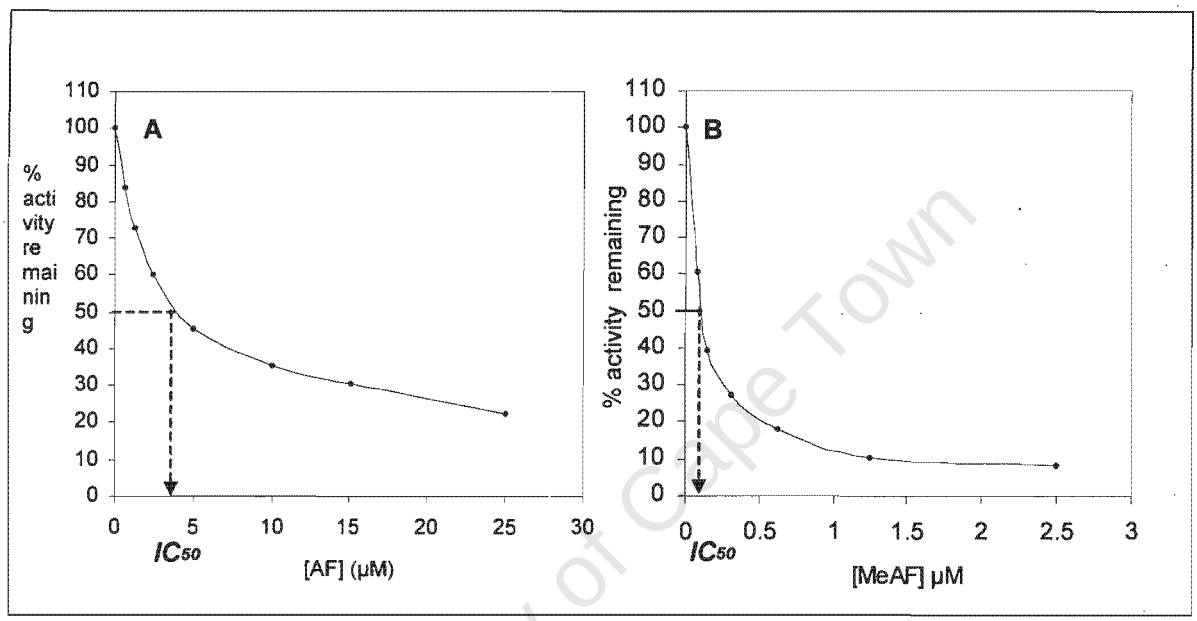

Figure 6.1: Determination of IC_{50} values from curves of the percentage activity remaining of wild type PPO vs [I] (A: AF, B: MeAF).

Table 6.1 summarises the IC_{50}s for the inhibitors AF, MeAF, BR and BV (See Appendix 21 for actual data). It is apparent that the AF and MeAF are good inhibitors of wild type and R59W mutant PPOX. However, Y348C and R168C mutants were less sensitive to inhibition by both AF and MeAF compared to wild type and R59W.

Of the self-designed mutants, R59K and R59S were less sensitive to inhibition by AF when compared to their counterpart R59I.

Inhibition by BV was in contrast to the effects of AF and MeAF in that wild type PPOX was relatively insensitive to inhibition by BV compared to R59W which was more sensitive by approximately 50%, and Y348C and R168C even more so.

BR did not inhibit wild type PPOX or any clinical mutants except Y348C where the inhibition was weak.

Table 6.1: IC_{50} of the wild type and mutant PPOXs.

PPOX	IC_{50} (μM)			
	AF	MEAF	BV	BR
Wild type	4.20 ± 0.39 (n = 5)	0.18 ± 0.01 (n = 4)	41.00 ± 1.80 (n = 4)	No inhibition
Y348C	70.00 ± 4.30 (n = 6)	55.60 ± 2.60 (n = 3)	3.10 ± 0.35 (n = 4)	34.20 ± 3.80 (n = 4)
R168C	46.00 ± 4.40 (n = 4)	1.10 ± 0.08 (n = 4)	0.40 ± 0.02 (n = 3)	No inhibition
R59W	4.20 ± 0.33 (n = 4)	0.20 ± 0.03 (n = 4)	21.00 ± 0.96 (n = 4)	No inhibition
R59K	3.33 ± 0.24 (n = 3)	ND	ND	ND
R59S	2.67 ± 0.19 (n = 3)	ND	ND	ND
R59I	0.90 ± 0.01 (n = 3)	ND	ND	ND
G14A	5.70 ± 0.22 (n = 3)	ND	ND	ND

ND = not determined

Kinetic parameters (K_i, K_s, and α) and mode of inhibition

Table 6.2 is an example of one of the independently determined sets of inhibition data for wild type human PPOX in the presence of increasing concentration of inhibitor (AF). Note the increasing K_m and invariant V_{max} in the presence of increasing inhibitor concentration, indicative of competitive inhibition. An α value of infinity (∞) calculated from secondary replots confirmed this mode of inhibition (Figure 6.2, inset).

Table 6.2: The effect of AF on human wild type PPOX activity. The increasing K_m, and invariant V_{max} are indicative of competitive inhibition.

[AF] (μM)	K_m (μM)	V_{max} (nmol/ml/h)	K_m/V_{max}	I/V_{max}
0.00	0.62 ± 0.066	486 ± 4.27	0.0013	0.0021
0.25	1.02 ± 0.41	472 ± 2.25	0.0022	0.0021
0.50	1.58 ± 0.14	478 ± 7.26	0.0022	0.0021
0.75	2.04 ± 0.47	459 ± 2.11	0.0044	0.0022
1.00	2.72 ± 0.38	467 ± 13.6	0.0058	0.0021

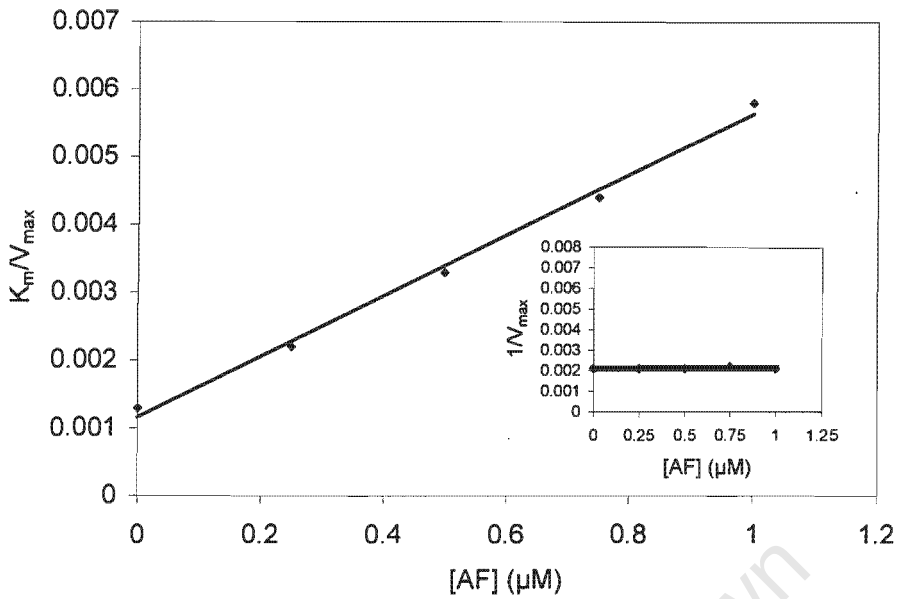

Figure 6.2: Secondary replot of K_m/V_{max} vs AF (Inset is $1/V_{max}$ vs [AF]).

The determined kinetic constants are shown in Table 6.3 (See Appendix 21 for actual data). The K_i values determined from the secondary replots correlated well to those calculated from the experimental IC_{50} data, confirming the internal consistency of the model.

Table 6.3: Kinetic parameters (K_i, K_s and α) of wild type and mutant PPOXs for inhibitor AF.

PPOX	Calculated K_i (μM)	Observed K_i (μM)	Observed K_s (μM)	α	Mode of inhibition
Wild type	0.23 ± 0.019 (n = 4)	0.20 ± 0.005 (n = 3)	0.51 ± 0.012 (n = 3)	∞	Competitive
Y348C	4.72 ± 0.280 (n = 6)	ND	ND	ND	ND
R168C	3.00 ± 0.260 (n = 4)	3.13 ± 0.530 (n = 3)	0.38 ± 0.037 (n = 3)	∞	Competitive
R59W	0.33 ± 0.025 (n = 4)	ND	ND	ND	ND
R50K	0.18 ± 0.013 (n = 3)	ND	ND	ND	ND
R59S	0.27 ± 0.019 (n = 3)	ND	ND	ND	ND
R59I	0.11 ± 0.002 (n = 3)	ND	ND	ND	ND
G14A	0.31 ± 0.012 (n = 3)	ND	ND	ND	ND

ND = not determined

Discussion

This study illustrates that the DPEs are generally good inhibitors of human PPOX. This is in keeping with earlier studies performed on human PPOX lymphoblast sonicates (Corrigall et al., 1994). However, Y348C and R168C mutants were less sensitive to inhibition by AF and MeAF compared to both wild type and R59W, which were equally sensitive to inhibition by these DPEs. Yet, R59W clearly exhibited the greatest loss of activity. If the inhibitors were binding at the active site it would be expected that R59W would be the least sensitive to inhibition. The fact that the behaviour in the presence of these inhibitors does not parallel the observed differences in activity parameters may indicate that the inhibitor is binding near the active site rather than at the active site.

Interestingly, inhibition by BV was in contrast to the effects of AF and MeAF in that wild type and R59W were poorly inhibited and Y348C and R168C were strongly inhibited. The other haem degradation product, BR did not inhibit wild type PPOX or any other mutants except Y348C where the inhibition was weak. Interestingly, the Y348C mutant was the only one that was unable to be stabilised by inhibitor in thermal induced unfolding studies (see Chapter 7). Differences in sensitivity to BV and BR have been ascribed to differences in rigidity between the two structures, BR being more convoluted and rigid than BV. Although BV has a double bond at the C(9)–C(10) methene bridge, rotation can still occur at C(10)–C(11) which may present the dipyrrole moiety to the active site more favourably. (Corrigall et al., 1998a).

Conclusion

- The DPEs are good inhibitors of wild type and R59W mutant PPOX.
- The behaviour in the presence of DPE inhibitors does not parallel the observed differences in activity parameters, which suggests that the inhibitor is binding near the active site rather than at the active site.
- A detailed kinetic analysis of wild type and R168C confirms that the mode of inhibition by AF is competitive.
- BV is a strong inhibitor of Y348C and R168C but not wild type and R59W. In contrast, BR inhibits only the Y348C mutant.

CHAPTER 7

PHYSICOCHEMICAL CHARACTERISATION OF HUMAN WILD TYPE AND MUTANT PROTOPORPHYRINOGEN OXIDASE

Introduction

As this chapter involves the study of PPOX unfolding, and is focussed on the thermodynamics of folding, we include an appropriately detailed review of protein folding.

Protein folding

For a native biologically active protein, the polypeptide chain will fold upon itself to the same unique three-dimensional (3D) structure consistently, *in vitro* and *in vivo* (Anfensen, 1973). Protein folding normally does not involve a single folding pathway, and usually there is more than one. Although there are potentially multiple folding routes to achieve the correct conformation, certain routes are more feasible than others due to a bias in the energy landscape towards particular structures (Dinner et al., 2000; Onuchic et al., 2000). These routes are more populated than others and they are the ones observed. The description of folding mechanisms of specific proteins and the interpretation of experimental data are based on folding pathways using symbols to represent microscopic states such as the unfolded state, intermediate state, and native state (Dinner et al., 2000; Bilsel and Matthew, 2000).

The folding process for a globular protein can best be pictured as a "funnel" referred to as an energy landscape (Figure 7.1). Many possible equivalent unfolded states are represented at the rim on top of the funnel. With the interaction between residues increasing, polypeptides "fall down" the wall of the funnel through different folding possibilities, leading to any one of a family of semi-compact structures. From this stage there is a rapid progression to the native (folded) tertiary structure represented at the bottom of the funnel.

When polypeptide chains fold, they minimise their hydrophobic surface area exposed to the aqueous environment resulting in a folded structure with a hydrophobic core of tightly packed amino acid side chains (Honig, 1999). The tight packing of side chains enhances attractive interaction energy but minimises chain conformational entropy. The uniqueness of the folded structure for a given sequence is a consequence of a balance between the interaction energy and chain entropy, i.e., only one fold with its tightly packed hydrophobic

and cooperative core will have low enough energy for a given sequence (Dinner et al., 2000, Rumbly et al., 2001).

Figure 7.1: **A model for the steps involved in the folding of globular proteins** (From Gareth and Grisham, 2002)

Thermodynamics of protein folding

Folding is under thermodynamic control in that it occurs only if the 3D structure is sufficiently stable relative to the ensemble of unfolded states (Bilsel and Matthew, 2000). However, the energy difference between the folded structure and its unfolded state is very small, and consequently, the folded states exist on the edge of stability/instability. This accounts for the conformational flexibility of proteins and explains why they are so easily denatured. This conformational flexibility of folds enables them to accommodate significant changes in amino acid sequence such as may occur in mutant proteins. This results in a different structural conformation and may have serious implications to the normal functioning of the protein (Govindarajan and Goldstein, 1996; Honig, 1999).

A protein adopts a folded native conformation when the energy of inter-strand interaction is greater than the conformational entropy of a full length sequence. For protein stability, the equilibrium between folded and unfolded protein is shifted towards the native state. The free energy change (ΔG) for the folding must be negative. A negative ΔG of folding is achieved by balancing several thermodynamic factors that include, conformational entropy ($-T\Delta S$), enthalpy (ΔH) and hydrophobic effects ($-T\Delta S$) (Figure 7.2). This may be expressed by the following equation:

$$\Delta G = \Delta H - T\Delta S$$

The free energy difference of the two states is determined by summing up all the physical interactions that take place within the protein molecule, and between the solvent and protein (ΔH), plus all entropic interactions ($-T\Delta S$). From the equation shown above it is noted that the conformational entropy is a thermodynamic quantity that prevents folding. A large negative ΔH, resulting from energetically favourable interactions between groups within folded molecule, including noncovalent interactions, is required to overcompensate the effect of the conformational entropy.

A relatively small ΔG for folding reactions corresponds to the difference between large ΔH and $T\Delta S$ terms that has to be balanced to allow for cooperative folding of a protein. Non-covalent interactions form and break in cooperative manner. As a result of this, thermal denaturation usually occurs over a narrow temperature range. Entropy and enthalpy almost compensate each other, as ΔH and ΔS make adjustments to keep ΔG fairly constant.

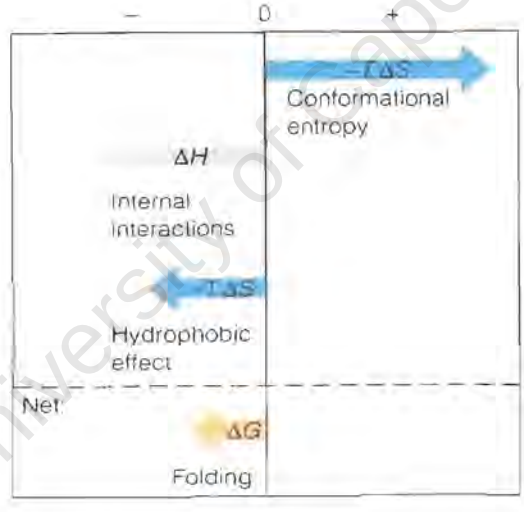

Figure 7.2: Contribution to the free energy of folding of globular proteins (From Mathew and Van Holde, 2000)

Thermal denaturation

Ideally, proteins are purified in their folded conformation, from natural biological sources. However, changes may occur in the properties of proteins upon heating, acidification or treating with chemical reagents, resulting in their denaturation. These changes may, under certain conditions, be reversed with complete recovery of biological function. This is referred to as renaturation. The simple folding reaction.

$$\text{Unfolded} \underset{\text{Denaturation/Unfolding}}{\overset{\text{Renaturation/Folding}}{\rightleftharpoons}} \text{Native}$$

is described by a two state process, i.e., the reaction proceeds to the right or left without any intermediate states (Privalov, 1979; Privalov and Gill, 1988; Jackson, 1998). The ratio of the rate constants represents the equilibrium constant for the reaction. There is no other visible component in the reaction. Partial unfolding in the course of denaturation may yield information on the unfolding process i.e, on the independence or coupling of the unfolding of folding units (domains).

Protein stability is measured by monitoring unfolding under denaturing conditions using different techniques (either thermal denaturation or chemical denaturation with urea or guanidinium chloride). In this study, UV spectroscopy was used at different temperatures to determine the stability of PPOX. When a folded protein structure is heat denatured (Figure 7.3), the UV absorbance increases due to the exposing of aromatic amino acids, resulting in a change in the extinction coefficient (hyperchromic effect) at a certain wavelength (270nm for PPOX). This hyperchromic absorbance change occurs over a narrow temperature range. The melting temperature (T_m) is defined as the temperature at which 50% of the protein is denatured. Thus, T_m is generally dependent on the nature of the protein and the UV thermal (melting) curve is useful in determination of the thermodynamic parameters of the protein.

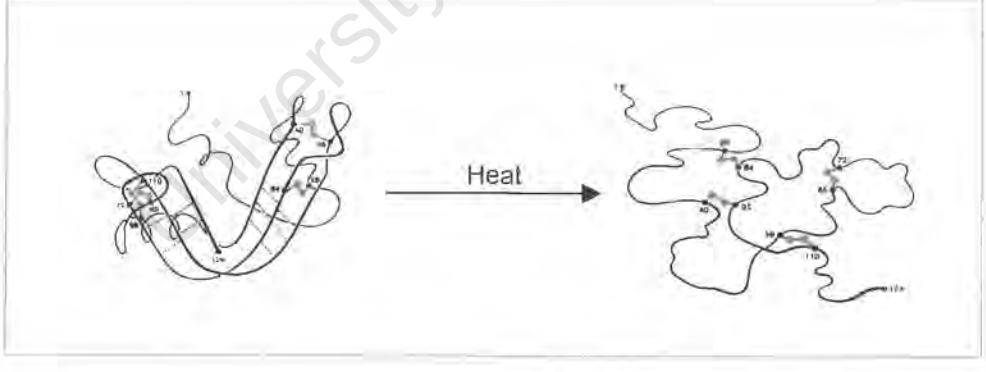

Figure 7.3: **Thermal denaturation of protein** (From Mathew and Van Holde, 2000)

Protein Circular Dichroism spectrum

Circular dichroism (CD) spectroscopy is used to measure the optical activity of asymmetric molecules in solution. CD is sensitive to conformational change (Hennessey and Johnson, 1981), and may be used to measure conformational change of proteins (or mutant proteins) under different circumstances, such as a variety of denaturing conditions

or in the absence/presence of ligand or inhibitor. The CD spectrum can also be used to determine the relative contribution of secondary structural components (e.g. α-helix and β-sheet) of proteins in solution. Figure 7.4 shows CD spectra of the three basic structures (α-helix, β-sheet and random coil conformations) of polypeptide chains. The CD spectrum for each secondary structure was calculated from a set of CD spectra of a whole protein. The percentages of each secondary structural component were determined from analysis of the corresponding crystal structure (Feldman, 1976). Thus, standard CD curves of a given secondary structure are produced and the percentage of each secondary structure in a protein derived from its CD spectrum (Hennessey and Johnson, 1981).

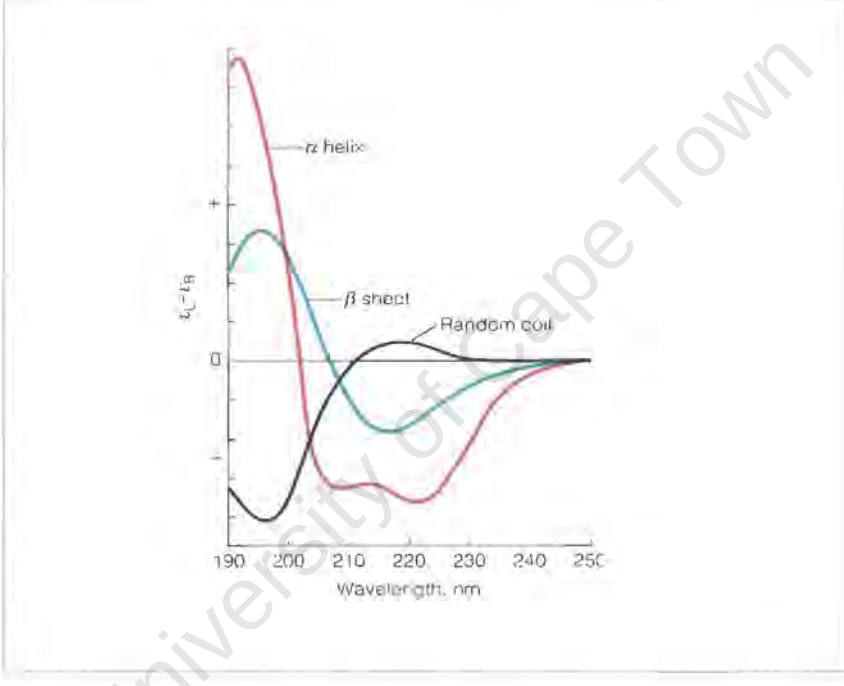

Figure 7.4: Circular dichroism spectra of polypeptide in various conformations (From Mathew and Van Holde, 2000)

Thus, useful information about the relative effects of different amino acid substitutions can be obtained by using the techniques described above. It is reasonable to study mutant proteins by such techniques as many mutants have some biological activity (as in the case of PPOX, see Chapter 5) suggesting that these amino acid substitutions do not destabilise the protein to such an extent that they are unable to fold to a structure roughly similar to wild type, native protein.

In this chapter, semi-quantitative and quantitative information about the effect of specific amino acid substitutions on the stability and the folding mechanism of PPOX are obtained

by comparing the folding thermodynamics and secondary structure of the mutant protein with those of the wild-type protein.

Objectives

- To determine the effect of temperature on wild type and mutant PPOX activity by measuring $T_{1/2}$.
- To determine and compare the thermodynamic parameters (ΔH, ΔS, ΔG, and T_m) of wild type and mutant PPOX from UV melting curves.
- To determine secondary structure of wild type and mutant PPOX from their CD spectra.

Methods

Protein preparation

In order to assess the thermodynamic properties and secondary structures of the PPOXs the proteins had to be in an appropriate buffer (NaCl free). Hence the purified PPOX preparations were subjected to PD10 chromatography in order to effect a buffer exchange into 0.01M Tris-acetate, 0.2% (w/v) *n*-octyl-β-D-glucopyranoside, pH 7.2 (Tris-acetate buffer). This was performed at 4°C and is detailed in Appendix 17. Protein concentration was determined (Appendix 14) and PPOX diluted to 0.15mg/ml for UV melting or CD measurements.

Effect of temperature on PPOX activity

Homogeneous wild type and mutant PPOXs were divided into aliquots and each aliquot denatured in a Hybaid Omnigene thermal cycler at a specific temperature for 3 min and kept on ice (see Appendix 17 for details). The temperatures ranged from 30 to 65°C in 5°C steps. One aliquot was not heat denatured and was used as a reference. PPOX activity was assayed (Appendix 13) and the temperature that reduces enzyme activity to half its maximal velocity ($T_{1/2}$) determined from the plot of residual activity vs temperature.

Temperature induced denaturation

The unfolding transition of the wild type and mutant PPOXs were obtained by UV spectroscopy and thermodynamic data including the melting temperature (T_m), enthalpy (ΔH), entropy (ΔS), and Gibbs free energy (ΔG) determined (Appendix 17). We have used the terms ΔH, ΔS, ΔG to refer to the cooperative unit (number of amino acid residues that change conformation simultaneously) rather than stipulating them to be van't Hoff

thermodynamic state functions in each case (ΔH_{vH}, ΔS_{vH}, ΔG_{vH}). Thermal denaturation experiments were performed on a Pye-Unicam SP1800 spectrophotometer with a custom-made heating block interfaced to an IBM PC through an Oasis digital converter. 0.15mg/ml of PPOX in Tris-acetate buffer was used in the experiments. Temperature was increased from 15°C to 75°C at a rate of 1°C/min. First derivative curves were generated for each scan.

To assess the reversibility of folding, PPOX was heated to 75°C (past the unfolding temperature) and cooled to an initial temperature of 15°C before re-heating back to 75°C.

To determine the stability of folding domains, PPOX was heated to a temperature just below the T_m value and cooled to 15°C, before re-heating back to 75°C.

To investigate the effects of either AF or FAD on T_m, melting curves were generated at an enzyme:AF or FAD molar ratio of 1:1, 1:5 1:10 and 1:20.

Melting curves were analysed by the method of Marky and Breslauer (1987).

CD spectrum

CD spectra of wild type and mutants (0.15mg/ml, in Tris-acetate buffer) were measured on a Jasco J-810 spectropolarimeter using a 0.1 cm path length quartz cuvette. The temperature(s) at which the spectra were collected were determined from melting curves for wild type and mutants. The temperatures were extracted from four regions (native, marginally native, T_m, and unfolded region) and used to generate four CD spectra (see Appendix 20). All spectra were analysed by a 10 spectra accumulation and the secondary structure estimated using computer software by Deléage and Roux (1987).

Results

Effects of temperature on PPOX activity

To examine the effect of temperature on wild type and mutant PPOX activity, $T_{1/2}$ was measured. Figure 7.5 shows typical activity curves obtained during denaturation of wild type and mutants. Generally there was a decrease in enzyme activities at temperatures over 45°C except for R168C which was affected from 40°C.

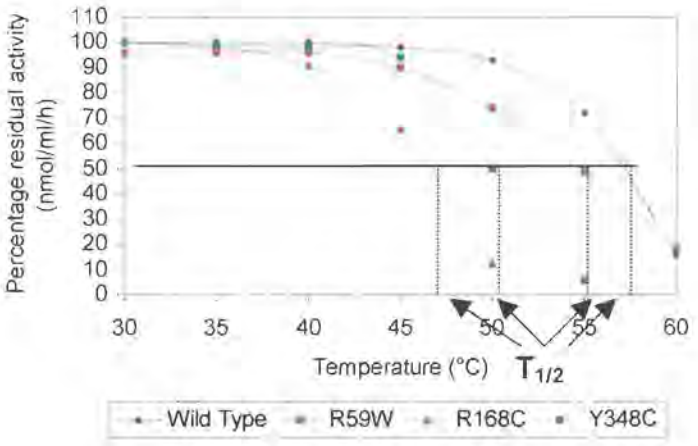

Figure 7.5: Temperature induced reduction in activity of wild type and mutant PPOXs showing the effects of temperature on their activity. Curves for R59K, R59S, R59I and G14A are not shown, and they all fall between wild type and R59W.

$T_{1/2}$s are shown in Table 7.1 (see Appendix 21 for actual data). For convenience, we have separated the values into three groups representing those higher, lower or approximately equal to wild type. Although the data is not sufficient to determine a statistical significance we feel they may represent trends. The $T_{1/2}$ values of G14A and R59K are similar to that of wild type (shown in black bold). R59I, R59W, Y348C and R168C have reduced $T_{1/2}$ values (shown in blue) and $T_{1/2}$ for R59S is increased (shown in red).

Table 7.1: $T_{1/2}$s of wild type and mutant PPOXs

PPOX	$T_{1/2}$ (°C)
R59S	60.3 ± 0.33 (n = 3)
Wild type	**56.8 ± 0.47 (n = 4)**
G14A	**56.3 ± 0.62 (n = 3)**
R59K	**56.3 ± 0.47 (n = 3)**
R59I	54.2 ± 0.25 (n = 3)
R59W	53.0 ± 0.71 (n = 4)
Y348C	50.2 ± 0.43 (n = 4)
R168C	47.6 ± 0.51 (n = 4)

Thermal unfolding of PPOX

The thermal equilibrium transition curves, as determined by measuring absorbance at 270nm, were similar in all PPOXs studied, except for R168C and Y348C (Figure 7.6). The first derivative curves are shown as insets. The melting curves generated for all PPOXs

(except R168C and Y348C) were monophasic and showed co-operative unfolding. However, R168C and Y348C melting curves were different. In both these cases, the onset of melting reflects the beginning of the unfolding process, but once past the T_m, irreversible aggregation occurs leading to a continuous increase in absorbance.

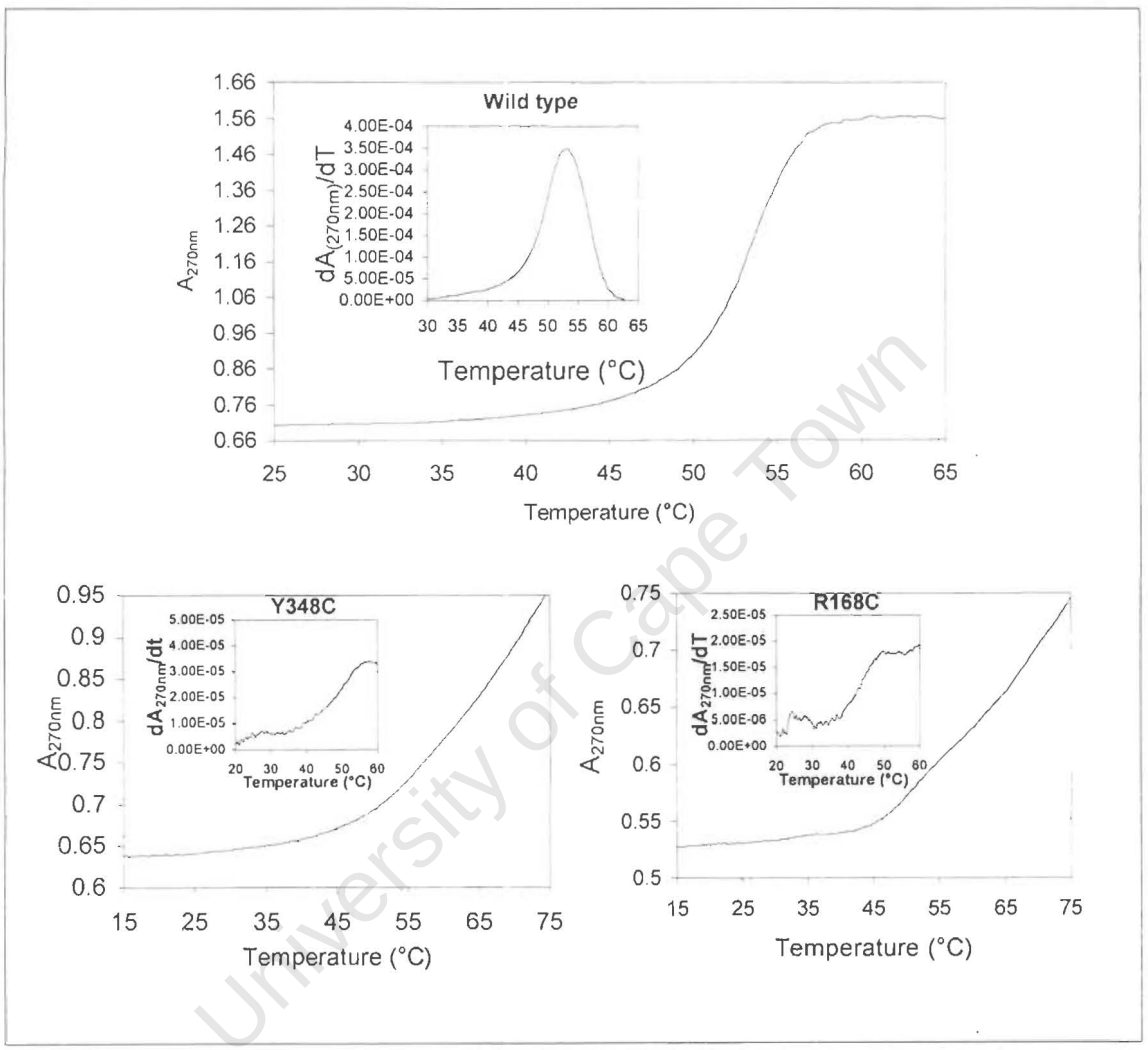

Figure 7.6: **Equilibrium transition curves for thermal unfolding of wild type, Y348C and R168C PPOX. The net stability of PPOX was determined from melting temperature (T_m) in the middle of the transition region. Insets show the first derivative curves. All mutants other than the two shown here, behaved similarly to the wild type.**

The thermodynamic parameters (T_m, ΔH, ΔS, and ΔG) were calculated from these melting curves and yielded values shown in Table 7.2 (see later).

When PPOX (for both wild type and mutants) was denatured and re-heated after cooling, there was no melting curve observed for the second heating process. Instead, aggregation of PPOX was apparent (data not shown).

When PPOX was heated to a temperature just below the T_m region, and slowly cooled back to a partially folded state (as seen by a higher absorbance), re-heating to a fully unfolded state (denatured) showed a melting curve with co-operative unfolding. The T_m value of the partially folded PPOX was the same as for the fully folded structure (Figure 7.7). The inset in figure 7.7 shows that unfolding started at a slightly higher temperature in the case of the partially folded structure. This effect was demonstrated for both wild type and mutant PPOXs and shown to be the same.

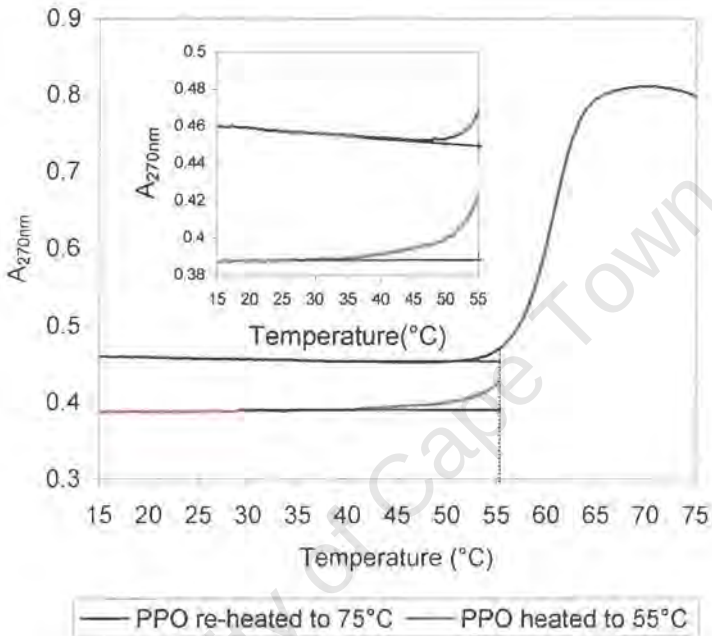

Figure 7.7: Typical equilibrium transition curve for thermal unfolding of reheated PPOX (in this case wild type). The curves demonstrate partially folded PPOX that with co-operative unfolding. An inset shows a region where heating was stopped before re-heating. The partially folded structure maintains its stability and starts unfolding at a slightly higher temperature.

Thermal equilibrium studies

Mutating wild type PPOX to Y348C, R168C, and R59W had a small effect on the T_ms (≈ 50°C) at pH 7.2. T_ms in the case of R59K, R59S, and R59I were higher (≈ 60°C). Negative ΔH and reduced ΔS resulting in negative ΔG was observed for wild type and all mutants, with R59K, R59S, and R59I having the largest negative ΔGs (Table 7.2). Changes in ΔH and ΔS are so small as compared to the data obtained from the wild type that no case can be made for an influence by any mutations.

Table 7.2: **Thermodynamic parameters from an analysis of thermal unfolding curve for wild type and mutant PPOXs at pH 7.2.**

PPOX	T_m (°C) [a]	ΔH (kcal.mol^{-1}) [b]	ΔS (kcal.mol^{-1}.K^{-1}) [c]	$\Delta G^*_{25°C}$(kcal.mol^{-1}) [d]
Wild type	52.10 ± 1.90	-121	0.377	-9.1
Y348C	53.70 ± 0.30	-123	0.375	-11
R168C	47.90 ± 0.10	-118	0.368	-8.4
R59W	52.00 ± 0.25	-123	0.377	-11.1
R59K	59.40 ± 0.40	-130	0.390	-13.7
R59S	60.60 ± 0.60	-132	0.394	-14
R59I	59.25 ± 0.75	-127	0.384	-12.8

*Free energy of folding

See Appendix 17 for equations

[a] Midpoint of the transition area of the melting curve

[b] From equation 2

[c] From equation 3

[d] From equation 5

Figure 7.8 shows the effect of temperature on ΔG when PPOX is denatured thermally. At 25°C, ΔG is negative (also refer to Table 7.2) for wild type and mutants. As the temperature is increased ΔG also increases and by definition, reaches 0 at the T_m and thereafter becomes positive.

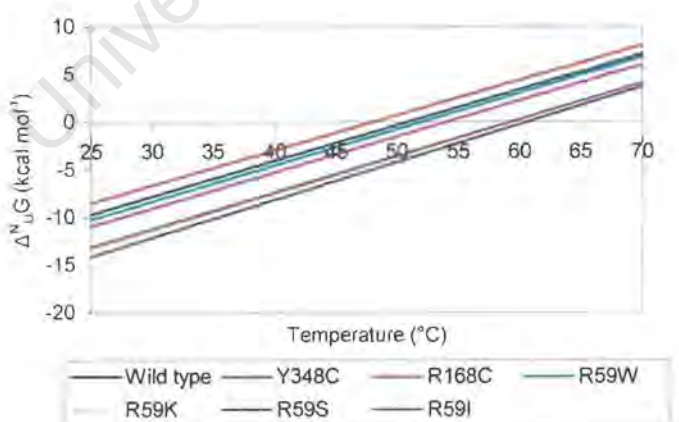

Figure 7.8: **Gibbs free energy of unfolding plotted as a function of temperature for wild type and mutant PPOXs. Data was obtained from melting curves and expressed in terms of T_m (in K) and ΔH at $T_m = \Delta H_{vH}$.**

The calculated ΔT and $\Delta\Delta G_{25°C}$ values give an indication of relative stability/instability (Table 7.3). All mutants, except for R168C, were thermodynamically more stable than wild type PPOX as positive ΔT and $\Delta\Delta G_{25°C}$ values were observed for all mutants, except R168C. Mutants, R59K, R59S, and R59I appeared to be the most stabilised.

Table 7.3 Thermodynamic parameters measuring change in melting temperature ($_{\Delta}T_m$) and instability $_{\Delta}(_{\Delta}G°_{25°C})$ of wild type caused by missense mutations

PPOX	$_{\Delta}T_m$ (°C) [e]	$_{\Delta}(_{\Delta}G°_{25°C})$ (kcal.mol^{-1}) [f]
Wild type	-	-
Y348C	2.6	1.9
R168C	-3.2	-0.7
R59W	0.9	2
R59K	8.3	4.6
R59S	9.5	4.9
R59I	8.1	3.7

*Free energy of folding

See Appendix 17 for equations

[e] Difference between the T_m values, equation 6

[f] Difference between the $_{\Delta}G°_{25°C}$ values, equation 7

Effect of AF and FAD on T_m of PPOX

Figure 7.9 illustrates that T_m of PPOX increases in the presence of increasing concentration of the inhibitor AF. When the protein:AF ratio is increased from 1:1 to 1:5, there is a significant increase in T_m value on all PPOXs except Y348C.

The effect of FAD on the enzyme stability was investigated. There was no significant increase in T_m in the presence of FAD for both wild type and mutants tested (data not shown).

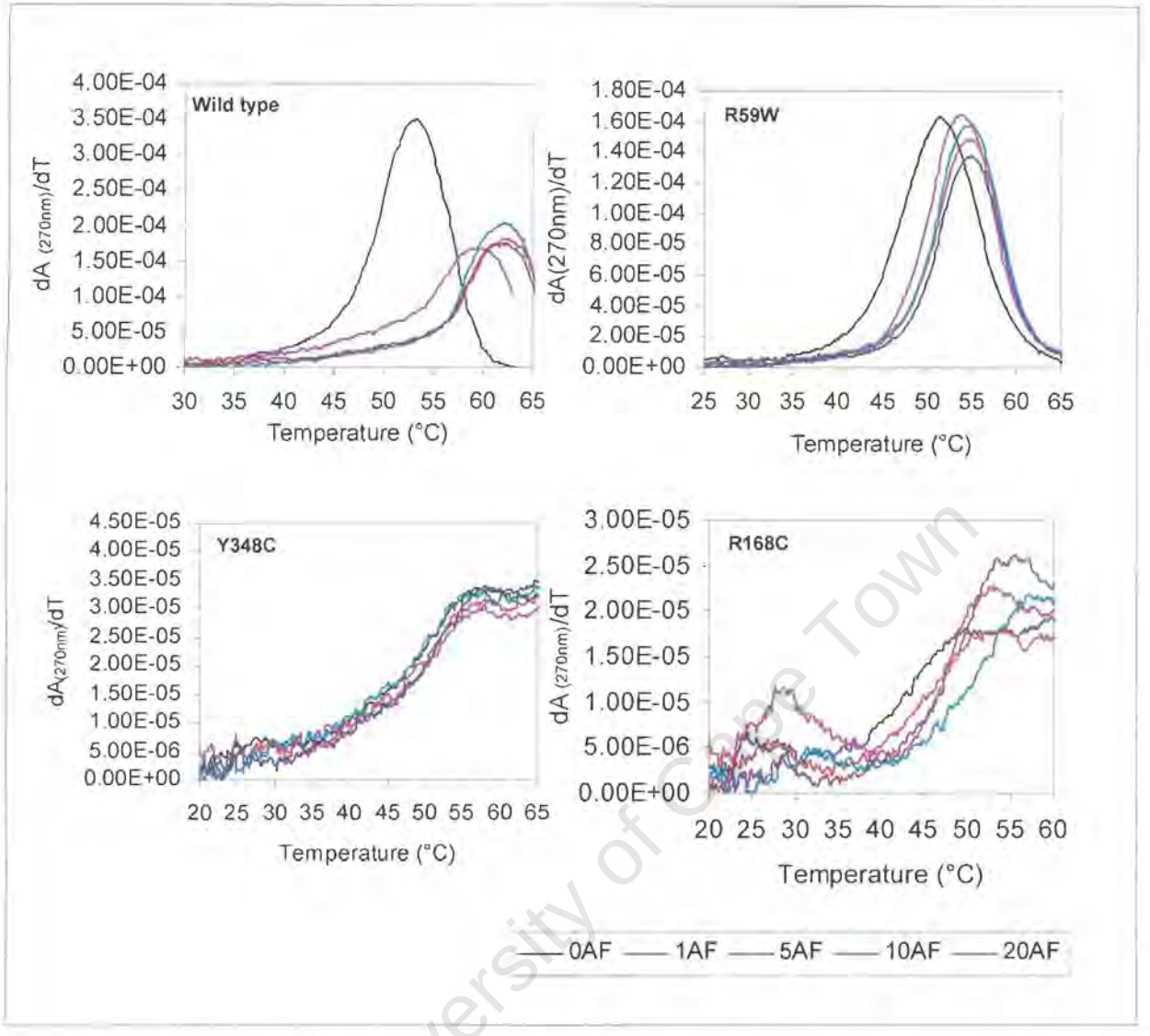

Figure 7.9: Typical first derivative of PPOX showing how T_m increases with increased AF concentration. All PPOXs except for Y348C were stabilised (increase in T_m) by AF up to a protein: AF ratio of 1: 5, after which there was no further stabilisation.

Figure 7.10 shows the comparative T_m values at a protein:AF ratio of 1:5. At protein:AF ratios above 1:5, there is no further increase in T_m. The increase in T_m in the presence of AF was observed for the wild type and other mutants, except for R168C that had a small increase, and Y348C that had no increase. The R59I mutant had the highest increase in T_m.

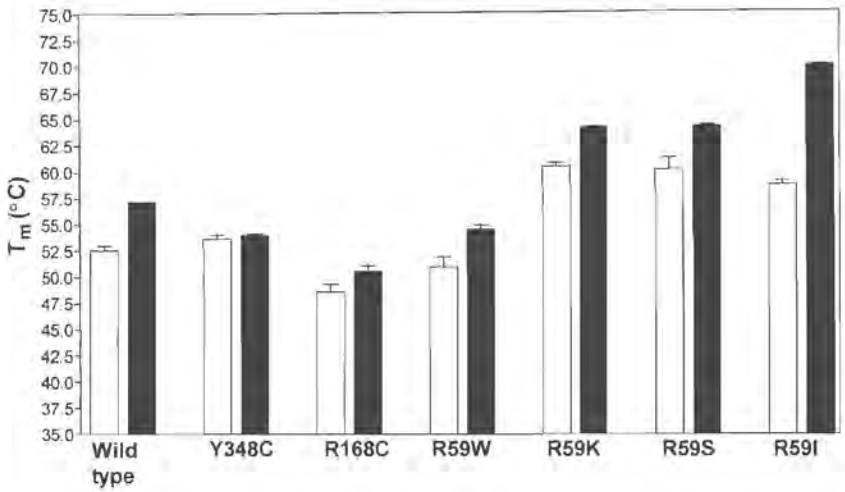

Figure 7.10: Melting temperatures for wild type and mutant PPOXs in the absence (white bars) and presence (black bars) of AF (protein: AF ratio: 1: 5). Thermal denaturation of wild type and mutant PPOXs was performed by slowly heating samples from 15°C to 75°C.

Secondary structure

CD spectra of the wild type and mutant PPOX were recorded and analysed between wavelengths of 200 and 260nm (Hennessey and Johnson, 1981). Changes in secondary structure of wild type and mutant PPOX on unfolding was monitored at increasing temperatures. Figure 7.11A shows such spectra with increasing ellipticity when the temperature is increased, for wild type PPOX. Figure 7.11B is derived from these spectra and shows how the percentage of α-helix decreases with increasing β-sheet and random coil. Mutants display similar spectra and are shown in Appendix 20.

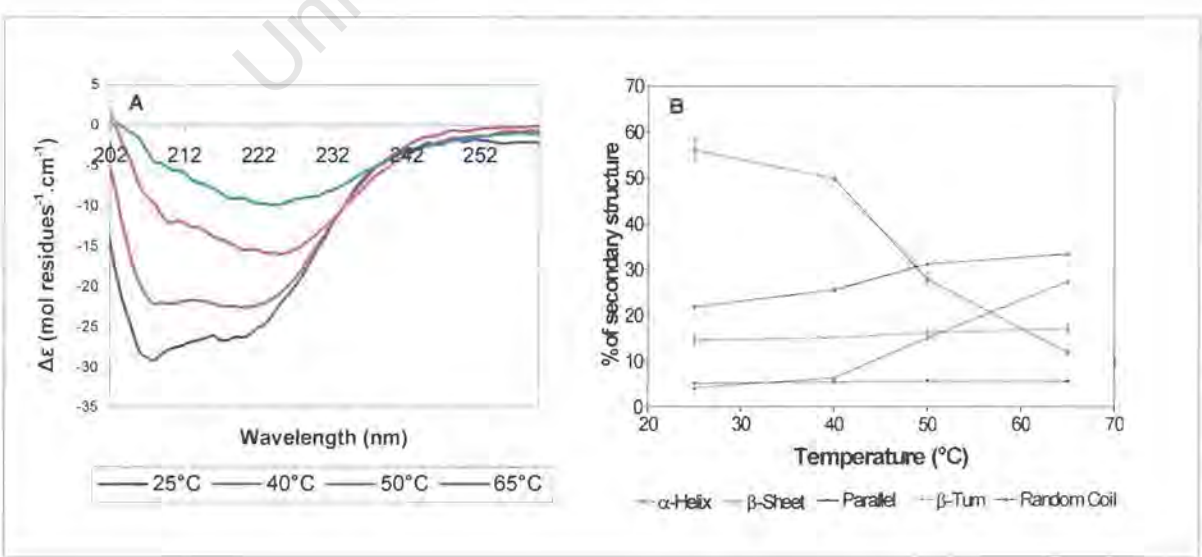

Figure 7.11: A: CD spectra of wild type PPOX at different temperatures (25, 40, 50, and 65°C). B: Percentage of secondary structures for wild type CD spectra, shown in A.

The CD spectra generated at 25°C for wild type PPOX showed a secondary structure with a dominating α-helix structure. The α-helix structure of the wild type PPOX decreased to varying degrees for Y348C, R168C, and R59W (Figure 7.12) with increasing β-sheet and random coil structures. In contrast, R59K, R59S and R59I have severely decreased α-helical content with R59I having the most dramatic reduction. Generally, in all the mutants, β-sheet and random coil structures increased as α-helix decreased.

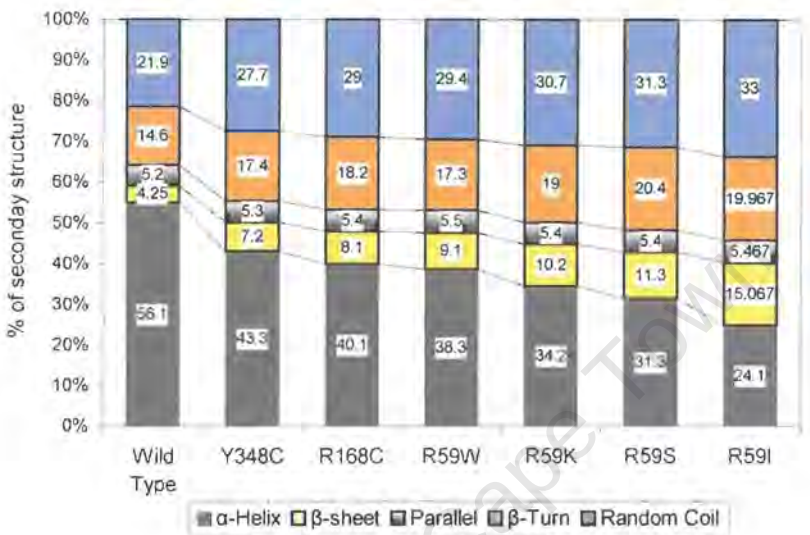

Figure 7.12: Deconvolution into secondary structures of wild type and mutant PPOXs obtained from CD spectra according to Deléage and Roux (1987)

Discussion

We effected a buffer exchange into Tris-acetate buffer. Other recommended buffers such as Na phosphate, Na sulphate, Na cacodylate proved unsuccessful for PPOX resuspension due to precipitation of the protein at the required high concentrations. Tris-acetate buffer could be used for PPOX at a concentration high enough (0.15mg/ml) to be used for CD spectrum recording and UV melting experiments. PPOX (0.15mg/ml or less) remained in Tris-acetate buffer solution at 4°C for two to three days.

UV melting and CD spectra of PPOX were performed on the same sample immediately after preparation, so as to prevent possible premature unfolding. Pilot studies showed that CD spectra of wild type and mutants changed dramatically on the third day after preparation, indicating a mixture of folded and unfolded PPOX structures. However, results obtained on the first and second day after preparation were consistent. All experiments were performed at least in duplicate, on different preparations. Following our

sample preparation protocol we considered that the PPOX that was melted and used for CD spectra was in its native conformation.

Effect of temperature on PPOX activity ($T^1/_2$)

The effects of increasing temperature on the enzymatic activity of PPOX varied (Table 7.1). Y348C, R168C, R59W and R59I had reduced $T_{1/2}$ values and R59S had an increased $T_{1/2}$ suggesting that these mutations have an influence on the structure of the active site. R59K was unaffected.

Effect of temperature on PPOX unfolding (T_m)

The UV melting curve of all PPOXs studied (except for R168C and Y348C) was sigmoidal in shape, indicating cooperative denaturation. Generally, the kinetics of unfolding was a single first-order reaction. The melting curve is characteristic for a two-state transition indicative of the equilibrium that holds between the native and unfolded PPOX protein. Because PPOX is a large molecule, it is reasonable to assume that it forms a multi-domain structure, and these domains could unfold via a two state process, independently. R168C and Y348C mutants have the potential to form additional or non-native disulfide bonds that influence unfolding equilibrium. With these mutants, multi-equilibrium with other cysteine residues may exist on unfolding, favouring aggregation, which may explain the high-temperature section of the curves in Figure 7.6.

In the re-heating experiments (Figure 7.7), it was demonstrated that, when the temperature is increased to approach the T_m region, a first domain unfolds leaving another domain(s) folded. This partially unfolded structure is indicated by high absorbance, even after cooling to lower temperatures (15°C), meaning that the protein does not become completely refolded. However the remaining ordered structure maintains its stability and on re-heating unfolds via a two state mechanism. These domains remain undefined, as there is no PPOX crystal structure available yet.

The experiments in which PPOX was denatured and re-heated after cooling showed no melting curve for the second heating process. Instead, aggregation of PPOX was apparent. This higher order reaction involves slow aggregation of PPOX on denaturing, making the overall unfolding irreversible.

The observed data did not show any significant correlation between T_m and $T_{1/2}$ values. T_m involves the overall structural stability while $T_{1/2}$ reflect changes in the environment of the active site. The fact that there was no correlation in thermostability of these mutant

PPOXs to their catalytic efficiency suggests that enzyme stability is not correlated to its activity in a simple way.

Thermal equilibrium studies

A mutation in a protein may stabilise or destabilise it. Either scenario may affect enzyme function in that native proteins have relatively small and fast structural fluctuations. Such fluctuations may play an essential role in protein function. These small rapid fluctuations may act as "lubricants" to make possible large-scale motions important for substrate binding and catalysis and/or allow ligand binding (Brooks et al., 1988; Bruccoleri et al., 1986). For example, rapid fluctuations in haemoglobin facilitate the quaternary structural transitions allowing effective oxygen binding, in this protein (Gelin et al., 1983; Perutz, 1989). In another example, in studies performed on myoglobin the oxygen was unable to access its ligand-binding pocket when the protein was rendered rigid by mutations in the oxygen channel (Case and Karplus, 1979; Elber and Karplus, 1990).

We determined the relative thermal (in)stability of PPOX mutants and compared them to the stability of the wild type protein using equilibrium unfolding parameters. This was reflected in T_m and ΔG values. Negative ΔHs and positive conformational entropies (ΔS) for wild type and mutants resulted in negative ΔGs. A comparison of mutant ΔGs to that in the wild type showed an increased net stability of the native (folded) protein of all mutants apart from R168C. The enthalpy of interaction (ΔH) and hydrophobic effect ($-T\Delta S$) of wild type was not affected on mutation indicating that the forces that fold wild type are similar to those that fold the mutants. The reduced entropy values are indicative of hydrophobic interactions as the dominating forces in PPOX folding. From ΔT_m and $\Delta\Delta G$ data, one can conclude that the mutations stabilise the protein (except for R168C). At present there is no detailed PPOX molecular structure that will help to explain the observed differences.

Effect of FAD/AF ligand binding on PPOX stability

AF is a strong inhibitor of PPOX (see Chapter 2 and 6), and may protect it from thermal denaturation. AF was shown to increase the thermostability of yeast PPOX (increased T_m) (Arnould et al., 1998). The same effect was observed on all PPOXs (except Y348C) in this study, using AF.

When comparing the protein stabilisation between wild type and mutants in the presence of AF, two transitions for R168C were observed. There appeared to be a first transition at a lower temperature between 20 and 36°C, followed by the transition between 50 and 60°C. The increased stability in the presence of AF is reflected in the high temperature peak. However, the low temperature transition was most pronounced at a protein:AF ratio

of 1:1. This observation suggests that a certain protein domain is preferentially destabilised on interaction with AF.

The insensitivity of Y348C to all concentrations of AF tested suggests that alternative disulfide bridges which may be formed by this mutant, makes the canonical AF binding site inaccessible. This is in agreement with our earlier findings (Chapter 6, table 6.1).

As PPOX contains FAD as a cofactor the proper folding of the native enzyme probably involves the correct assembly of the apoprotein with FAD. Previous work has shown that additional FAD (10 – 50 μM) increased the thermostability of PPOX marginally (Arnould et al., 1998). In this study the effect of FAD on the enzyme's stability was investigated. No significant increase in the melting temperature of wild type and mutants was noted when incubated in the presence of increasing amounts of FAD.

Secondary structure analysis of PPOX

High concentrations of PPOX restricted CD recordings in the region below 200nm due to FAD absorbance. Thus for accurate recordings it was necessary to use a PPOX concentration of 0.15mg/ml.

Our results indicated the predominance of α-helix in PPOX secondary structure. Previous studies on yeast PPOX by Arnould et al, (1998), also showed an α-helix as the dominating structure. In contrast, CD studies performed on murine PPOX by Proulx and Dailey, (1992) showed the β-sheet as a dominating structure. These secondary structural differences are suggestive of the possibility of polymorphic structured PPOX.

AF is a strong inhibitor of human PPOX and has a stabilising influence on thermal denaturation except for Y348C. An attempt to study the effects of AF on the secondary structure of the protein was unsuccessful even at low AF concentration (protein:AF ratio of 1:0.5). This was probably due to the high intense positive ellipticity of the inhibitor and the fact that AF is unable to be maintained in buffer solution in the absence of DMSO.

Physicochemical analysis of R59 residue

One of the foci of this work is the role of the R59 residue on PPOX structure/activity. R59W had a reduced $T_{1/2}$. A conservative replacement (R59K) resulted in a similar $T_{1/2}$ to that of the wild type whereas an aliphatic (R59I) substitution had a similar $T_{1/2}$ to that of R59W.

A polar substitution (R59S) increased $T_{1/2}$ considerably indicating that alteration in polarity at R59 is an important factor in the active site environment. This supports our previous

conclusion, based on kinetic data (Chapter 5), that R59 is directly involved in catalysis and not simply important for FAD binding.

Thermal equilibrium studies showed an increased T_m when mutating the R59. This increased thermostability suggests that the overall structure of the protein is affected when replacing this arginine. Seeing that R59 appears important at the active site as well, it is therefore possible to speculate that flexibility and/or charge distribution at the active site could be important for catalysis.

Secondary structure analysis of the R59 mutants reveals that the degree of α-helix present does not correlate linearly with the $T_{1/2}$ nor the T_m values again supporting the assumption that R59 is important for catalysis at the active site. If the effects were purely structural it could be expected that the structure/function relationship would correlate consistently.

AF stabilised all the R59 mutants. R59I appeared to be the most stabilised (Figure 7.10). This suggests that the inhibitor is "most comfortable" in the vicinity of a non-polar side chain, as compared to the native arginine.

Conclusions

- Comparison of the $T_{1/2}$ values obtained for the R59 mutants show that a positive charge at codon 59 is required for the integrity of the active site structure.
- Y348C and R168C mutants had the lowest $T_{1/2}$ values suggesting that alternative choices for non-native disulfide bridges exist.
- The UV melting curve of all PPOXs studied (except for R168C and Y348C) showed cooperative denaturation.
- The melting curves showed a two-state transition making it reasonable to assume that PPOX forms a multi-domain structure, and these domains unfold via a two state process, independently.
- There was no correlation between T_m and $T_{1/2}$ values suggesting that enzyme stability is not correlated to its activity in a simple way.
- Except for R168C, all mutants studied were more stable to thermal denaturation compared to wild type.
- AF increased the thermostability of all PPOXs (except Y348C). This suggests that alternative disulfide bridges, which may be formed by the Y348C mutant, make the AF binding site inaccessible.
- The two melting transitions for R168C observed, in the presence of AF, suggests that a certain protein domain is preferentially destabilised in this mutant.

- The secondary structure of PPOX showed a dominant α-helix. In the mutants there was a decreased α-helical content, compensated for by increased β-sheet and random coil.
- AF had a stabilising influence on thermal denaturation (except for Y348C).
- A comparison of the physicochemical parameters measured in the R59 mutants support the conclusion that R59 is directly involved in catalysis and not simply important for FAD binding. Flexibility and/or charge distribution at the active site could be important for catalysis.

CHAPTER 8

OVERVIEW, IMPLICATIONS AND FUTURE DIRECTIONS

Overview and Implications

In this study, both naturally occurring ("clinical") PPOX mutants relevant to South Africa, and self-designed mutants (non-"clinical" mutants) were engineered, expressed and purified. Their characterisation involved comparisons of their kinetic behaviour, including inhibition and cofactor profiles, and physicochemical properties.

We successfully expressed and purified all PPOXs to homogeneity by a single step purification procedure based on metal affinity chromatography. Clearly, this method should now be considered as the method of choice when detailed kinetic or physical studies of native enzyme are required. Compared to some previously described methods, which involve multiple chromatography steps, the purification is rapid, yields generally good and can be performed under native conditions.

All the mutations under investigation in this study resulted in reduced PPOX activity to varying degrees. However, the activity data did not correlate with the ability/inability of various mutants to bind FAD. Indeed, R59W had negligible activity, extremely poor FAD binding, R59K (positive charge replacement) had activity and bound FAD, whereas R59S and R59I both had dramatically reduced activity, yet could bind FAD. These comparisons strongly suggest that the positive charge at R59 is directly involved in catalysis and not for FAD binding. The fact that R59W does not bind FAD is more likely a result of its aromatic bulky nature. A consideration of the K_ms for the R59 mutants allow us to further speculate that the involvement by the R59 in catalysis is more likely a substrate binding problem than a mechanistic one.

The $T_{1/2}$ studies in the R59 mutants lend weight to the argument that R59 is directly involved in catalysis, required for the integrity of the active site structure, and not simply important for FAD binding. As $T_{1/2}$ reflects changes in the environment of the active site, we observed significant differences in the $T_{1/2}$ values amongst the R59 mutants. If R59 was only involved in FAD binding then it could be expected that all their $T_{1/2}$s would be similarly affected.

The secondary structure of PPOX showed a dominant α-helix. In the mutants there was a decreased α-helical content, compensated for by increased β-sheet and random coil. Yet the degree of α-helix present does not correlate linearly with the $T_{1/2}$ or the T_m values,

again supporting the assumption that R59 is important for catalysis at the active site. If the effects were purely structural it could be expected that the structure/function relationship would correlate consistently.

An examination of the relative importance of the glycine in positions 9, 11 and 14 of the conserved dinucleotide binding motif showed that substitution by alanine in codon 14 is far less disruptive than substitutions in codons 9 and 11. It would therefore be anticipated that mutations occurring in PPOX positions 9 and 11 in nature could be classified as "severe" and almost certainly lead to disease. Indeed, a VP family with a G11S PPOX mutation has been reported (Frank et al., 2001a).

Both R168C and Y348C exhibited residual activity an order of magnitude greater than other mutations, which is in keeping with the concept of "lesser" and "severe" PPOX mutations. Both these two mutations are only associated with clinical VP in a compound heterozygous state.

The cysteine mutants had the lowest $T_{1/2}$ values suggesting that alternative choices for non-native disulfide bridges exist in these cases. Furthermore, the fact that Y348C did not show increased thermostability in the presence of AF, suggests that these alternative disulfide bridges which may be formed, make the AF binding site inaccessible in this mutant.

UV melting curves generally showed a two-state transition making it reasonable to assume that PPOX forms a multi-domain structure, and these domains unfold via a two state process, independently. Generally all mutants studied were more stable to thermal denaturation compared to wild type, except for R168C. In this mutant, two melting transitions were observed in the presence of AF, suggesting that a certain protein domain is preferentially destabilised in this mutant.

One of the well-known features of PPOX is its inhibition by DPEs. In these comparative studies, using AF as a representative DPE inhibitor, it appeared that the PPOX-inhibitor parameters measured did not parallel the observed kinetic activity parameters. This adds to our knowledge of PPOX inhibition by the DPEs as it suggests that the inhibitor is binding near, rather than at, the active site.

Future work

While this study does not identify the PPOX active site, it does illustrate the use of studying expressed, purified mutant PPOXs in attempting to elucidate the importance of specific amino acid residues in relation to factors effecting PPOX structure-function *per se*, and/or in the study of VP. Clearly there are many more designed mutants that could

yield further insight. For example, if an R59Y mutant also demonstrated compromised FAD binding, this could be taken as confirmation that bulky aromatic residues impair FAD binding at this site. An R59H mutant may be highly informative as its ability to switch from being an acid to a base at different pHs could yield information on the influence of a positive charge on catalysis. Other conserved amino acids such as L15, E34, G41, G57 would be good candidates for mutational characterisation studies as their conservation could be signifying residues important for substrate binding or conversion, crucial structural components, or cofactor interaction. Once the crystal structure for PPOX becomes available it should be possible to predict active site and cofactor binding domains and facilitate design of highly appropriate mutants for investigating detailed enzyme mechanism, channelling and steric properties. Therefore, it would be extremely worthwhile to crystallise and resolve a PPOX structure to an appropriate resolution.

Translocation of PPOX to the mitochondria remains somewhat enigmatic. Thus, studies aimed at identifying and characterising a definitive/putative targeting sequence are important as defects in the targeting sequence may have different disease consequences to those seen in structural/activity defects. These studies could take the form of fluorescent labelling studies based on green fluorescent protein (GFP)-PPOX, or GFP-mutant PPOX constructs.

As in all partially penetrant genetic diseases, questions arise concerning the phenotype-genotype relationship and specifically, what factors may be involved. Thus, the continued clinical and biochemical profiling of porphyric patients, in association with careful PPOX mutant protein characterisation could be meaningful in identifying potential susceptibility factors. In addition, the phenotypic effects of specific mutations could be tested in knock-in mouse models, which may yield further information in this regard. Such mouse models are perfectly feasible and recently one such model (R59W) has been engineered (Medlock et al., 2002) and is currently under investigation in our laboratories.

Bibliography

Abdulla, M. and Haeger-Aronsen, B. (1971). ALA dehydratase activation by zinc. *Enzyme* **12:** 708 – 710.

Ades, I.Z. and Harpe, K.G. (1981). Biogenesis of mitochondrial proteins. Identification of the mature and precursor forms of the subunit of delta-aminolevulinate synthase from embryonic chick liver. *J. Biol. Chem.* **256:** 9329 – 9333.

Adler, A.D. (ed), (1973). The chemical and physical behaviour of porphyrin compounds and related structures, *Ann. NY Acad. Sci.* **206:** 1 – 761.

Agorec, M., Buhler, J.M., Treich, I., et al. (1988). Isolation, sequence and regulation by oxygen of the yeast *HEM13* gene coding for coproporphyrinogen oxidase. *J. Biol. Chem.* **263:** 9718 – 9724.

Akagi, R., Prchal, J.T., Eberhart, C.E. et al. (1992). An acquired acute hepatic porphyria: a novel type of delta-aminolevulinate dehydratase inhibition. *Clin. Chim. Acta.* **212:** 79 – 84.

Albers, J.W., Robertson, W.C. and Daube, J.R. (1978). Electrodiagnostic findings in acute porphyric neuropathy. *Muscle Nerve* **1:** 292 – 296.

Al-Karadaghi, S., Hansson, M., Nikonov, S., et al. (1997). Crystal structure of ferrochelatase the terminal enzyme in heme bosynthesis. *Structure* **5:** 1501 – 1510.

Alwan, A.F. and Jordan, P.M. (1988). Isolation of uroporphyrinogen III synthase from *Escherichia coli*. *Biochem. Soc. Trans.* **16:** 965 – 966.

Alwan, A.F., Mgbeje, B.I. and Jordan, P.M. (1989). Purification and properties of uroporphyrinogen III synthase (co-synthase) from an overproducing recombinant strain of Escherichia coli K-12. *Biochem. J.* **264:** 397 – 402.

Amillet, J.M. and Labbe-Bois, R. (1995). Isolation of the gene *HEM4* encoding uroporphyrinogen III synthase in *Saccharomyces cerevisiae*. *Yeast* **11:** 419 – 424.

Anderson, P.M. and Desnick, R.J. (1979). Purification and properties of δ-amiolevulinic acid dehydratase from human erythrocytes. *J. Biol. Chem.* **254:** 6924 – 6930.

Anderson, P.M. and Desnick, R.J. (1980). Purification and properties of uroporphyrinogen I synthase from human erythrocytes. *J. Biol. Chem.* **255:** 1993 – 1999.

Anderson, P.M. and Desnick, R.J. (1982). Porphobilinogen deaminase: Methods and principles of the enzymatic assay. *Enzyme* **28:** 146 – 157.

Anderson, D.E., Becktel, W.J. and Dahlquist, F.W. (1990). pH induced denaturation of proteins: a single salt bridge contributes 3 – 5 kcal/mol to the free energy of folding T4 lysozyme. *Biochem.* **29:** 2403 – 2408.

Anderson, R.J., Norris, A.E. and Hess, F.D. (1994). Synthetic organic chemicals that act through the porphyrin pathway. *Am. Chem. Soc. Symp. Ser.* **559:** 18 – 33.

Andrew, T.L., Riley, P.G. and Dailey, H.A. (1990). Regulation of heme biosynthesis in higher animals. In: Biosynthesis of heme and chlorophyll. (H.A. Dailey, ed), New York, McGraw-Hill, pp. 163 – 200.

Aquaron, R.; Lacombe, D.; Topi, G.C.; Lamoril. J. (1992). Neurological, dermatological and biological manifestations of porphyria variegate. A study of 3 families of Italian origin in Marseilles area. *Rev. Neurol.* **148:** 532 – 540.

Arnould, S., and Camadro, J.-M. (1998). The domain structure of protoporphyrinogen oxidase, the molecular target of diphenyl ether-type herbicides. *Proc. Natl. Acad. Sci. U.S.A.* **95:** 10553 – 10555.

Arnould, S., Takahashi, M. and Camadro, J.-M. (1998). Stability of recombinant yeast protoporphyrinogen oxidase: Effect of diphenyl ether-type herbicides and diphenyleneiodonium. *Biochem.* **37:** 12818 – 12828.

Arnould, S., Takahashi, M. and Camadro, J-M. (1999). Acylation stabilizes a protease-resistant conformation of protoporphyrinogen oxidase, the molecular target of diphenyl ether-type herbicides. *Proc. Natl. Acad. Sci. USA* **96:** 14825 – 14830.

Astrin, K.H. and Desnick, R.J. (1994). Molecular basis of acute intermittent porphyria: mutations and polymorphisms in the human hydroxymethylbilane synthase gene. *Hum. Mutat.* 4: 243 – 252.

Astrin, K.H., Warner, C.H., Yoo, H.W., et al. (1991). Regional assignment of the human uroporphyrinogen III synthase (UROS) gene to chromosome 10q25.2---q26.3. *Hum. Genet.* **87:** 18 – 22.

Awan, S.J., Siligardi, G., Shoolingin-Jordan, P.M. et al. (1997). Reconstitution of the holoenzyme form of *Escherichia coli* porphobilinogen deaminase from apoenzyme with porphobilinogen and preuroporphyrinogen: a study using circular dichroism spectroscopy. *Biochem.* **36:** 9273 – 9282.

Barbara, L., Randolph-Anderson, R.S., Anita, M., et al. (1998). Isolation and characterisation of a mutant protoporphyrinogen oxidase gene from *Chlamydomonas reinhardtii* conferring resistance to porphyric herbicides. *Plant Miol. Biol.* **38:** 839 – 859.

Barker, D.F., Shafer, M. and White, R. (1984). Restriction sites containing CpG show a higher frequency of polymorphism in human DNA. *Cell* **36:** 131 – 138.

Barnes, H. D. (1951). Further South African cases of porphyrinuria. *S. Afr. J. Clin. Sci.* **2:** 117 – 169.

Batlle, A.M. del C., Benson, A. and Rimington, C. (1965). Purification and properties of coproporphyrinogenase. *Biochem. J.* **97:** 731 – 740.

Becerril, J.M. and Duke, S.O. (1989). Protoporphyrin IX content correlates with activity of photobleaching herbicides. *Plant. Physiol.* **90:** 1175 – 1181.

Bensidhoum, M., Ged, C., Hombrados, I., et al. (1995). Identification of two new mutations in congenital erythropoietic porphyria. *Eur. J. Hum. Genet.* **3:** 102 – 107.

Berger, H. and Goldberg, A. (1955). Hereditary coproporphyria. *Br. Med. J.* **2:** 85 – 88.

Berzelius, J.J. (1840). *Lehrbuch der chemie*, volume 9, Arnoldische Buchhandlung, Dresden, Leipzig, pp. 67 – 69.

Bevan, D.R., Bodlaender, P. and Shemin, D. (1980). Mechanism of porphobilinogen synthase. Requirement of Zn^{2+} for enzyme activity. *J. Biol. Chem.* **255:** 2030 – 2035.

Bhargova, R.K. and Gupta, H.K. (1970). Porphyria in Bikaner Distric of Rajasthan. *J. Assoc. Phys. India* **18:** 677.

Bilsel, O. and Matthews, C.R. (2000). Barriers in protein folding reactions. *Adv. Protein. Chem.* **53:** 153 – 207.

Birchfield, N.B. and Casida, J.E. (1996). Protoporphyrinogen oxidase: High affinity tetrahydrophthalimide radioligand for the inhibitor/herbicide-binding site in mouse liver mitochondria. *Chem. Res. Toxicol.* **9:** 1135 – 1139.

Birchfield, N.B., Latli, B. and Casida, J.E. (1998). Human protoporphyrinogen oxidase: Relation between the herbicide binding site and the flavin cofactor. *Biochem.* **37:** 6905 – 6910.

Bird, T.D., Hamernyik, P., Nutter, J.Y. (1979). Inherited deficiency of δ-aminolevulinic acid dehydratase. *Am. J. Hum. Genet.* **31:** 662 – 668.

Bishop, D.F. (1990). Two different genes encode delta-aminolevulinate synthase in humans: nucleotide sequences of cDNAs for the housekeeping and erythroid genes. *Nucleic Acid Res.* **18:** 7187 – 7188.

Bishop, D.F., McBride, L. and Desnick, R.J. (1982). Fluorimetric coupled-enzyme assay for delta-aminolevulinic acid synthase. *Enzyme* **28:** 94 – 108.

Bishop, T.R., Miller, M.W., Beall, J., et al. (1996). Genetic regulation of δ-aminolevulinic dehydratase during erythropoiesis. *Nucleic Acid Res.* **24:** 2511 – 2518.

Bissbort, S., Hitzeroth, H.W., du Wentzel, D.P., et al. (1988). Linkage between the variegate porphyria (VP) and the alpha-1 antitrypsin (PI) genes on human chromosome 14. *Hum. Genet.* **79:** 289 – 290.

Bissell, D.M. and Schmid, R. (1987). Hepatic porphyrias. In: *Diseases of the liver*, (L. Schiff, and E.R. Schiff, J. B. Lippincott, eds) 6Th ed, Philadelphia, pp 1075 – 1092.

Blackwood, M.E. Jr., Rush, T.S. 3rd., Romesberg, F., et al. (1998). Alternative modes of substrate distortion in enzyme and antibody catalyzed ferrochelation reactions. *Biochem.* **37:** 779 – 782.

Blackwood, M.E., Rush, T.S., Medlock, A., et al. (1997). Resonance spectra of ferrochelatase reveal porphyrin distortion upon metal binding. *J Am Chem Soc* **119:** 12170 – 12174.

Bloomer, J.R. and Morton, K.O. (1982). A radiochemical method for heme synthase activity. *Enzyme* **28:** 220 – 232.

Bloomer, J.R. and Straka, J.G. (1988). Porphyrin Metabolism. In: The Liver: Biology and Pathobiology. (I.M. Arias, W.B. Jakoby H. Popper, D. Schachter and D.A. Shafritz, ed), 2nd edition, Raven Press, New York, pp. 451 – 466;

Bloomer, J.R., Bonkowsky, H.L., Ebert, P.S. et al. (1976). Inheritance in protoporphyria. Comparison of haem synthase activity in skin fibroblasts with clinical features. *Lancet* **II:** 226 – 228.

Blum, I. and Atsmon, A. (1976). Reduction of porphyrin excretion in porphyria variegata by propranolol: A case report. *S. Afr. Med. J.* **50:** 898 – 899.

Boese, Q.F., Spano, A.J., Li, J.M. et al. (1991). Aminolevulinic acid dehydratase in pea (*Pisum sativum L.*). Identification of an unusual metal-binding domain in the plant enzyme. *J. Biol. Chem.* **266:** 17060 – 17066.

Bogard, M., Camadro, J-M., Nordmann, Y. et al. (1989). Purification and properties of mouse liver coproporphyrinogen oxidase. *Eur. J. Biochem.* **181:** 412 – 421.

Bonkovsky, H.L., Bloomer, J.R., Ebert, P.S. et al. (1975). Heme synthetase deficiency in human protoporphyria. Demonstration of the defect in liver and cultured skin fibroblasts. *J Clin Invest.* **56:**1139 – 1148.

Bonkovsky, H.L., Poh-Fitzpatrick, M., Pimstone, N., et al. (1998). Porphyria cutanea tarda, hepatitis C, and HFE gene mutations in North America. *Hepatology* **27:** 1661 – 1669.

Bont, A., Steck, A.J. and Meyer, U.A. (1996). Die akuten hepatischen porphyrien und ihre neurologischen Sindrome. *Shweize Med. Wschrf* **126:** 3 – 14.

Borthwick, I.A., Srivastava, G., Booker, J.D., et al. (1983). Purification of 5-aminolaevulinate synthase from liver mitochondria of chick embryo. *Eur. J. Biochem.* **129:** 615 – 620.

Borthwick, I.A., Srivastava, G., Day, A.R., et al. (1985). Complete nucleotide sequence of 5-aminolaevulinate synthase precursor. *Eur. J. Biochem* **150:** 481 – 484.

Bottomley, S.S., May, B.K., Cox, T.C., et al. (1995). Molecular defects of erythroid 5-aminolevulinate synthase in X-linked sideroblastic anaemia. *J. Bioenerg. Biomembr.* **27:** 161 – 168.

Boulechfar, S., Da Silva, V., Deybach, J.C. et al. (1992). Heterogeneity of mutations in the uroporphyrinogen III synthase gene in congenital erythropoietic porphyria. *Hum. Genet.* **88:** 320 – 324.

Bradford, M. (1976). A rapid and sensitive method for quantitation of microgram quantities of protein utilising the principle of protein-dye binding. *Anal. Biochem.* **72:** 248 – 254.

Branden, C. and Tooze, J. (1991). In: Introduction to protein structure. (C. Branden and J. Tooze, eds), Garland, New York, pp. 141 – 159.

Brenner, D. A. and Frasier, F. (1991). Cloning of murine ferrochelatase. *Proc Natl. Acad. Sci. USA* **88:** 849 – 853.

Brenner, D.A. and Bloomer, J.R. (1980). The enzymatic defect in variegate porphyria. *N. Engl. J. Med.* **302:** 765 – 769.

Brenner, D.A., Didier, J.M., Frasier, F. et al. (1992). A molecular defect in human protoporphyria. *Am. J. Hum. Genet.* **50:** 1203 – 1210.

Brian, R.C., Sellers, V.M., Finnegan, M.G., et al. (1996). Site-directed mutagenesis and spectroscopic characterisation of human ferrochelatase: identification of residues coordinating the [2Fe-2S] cluster. *Biochem.* **35:** 16222 – 16229.

Brodie, M.J., Thompson, G. G., Moore, M.R., et al. (1977). Hereditary coproporphyria. *Quart. J. Med.* **46:** 229 – 241.

Brooker, J.D., Srivastava, B.K., May, B.K., et al. (1982). Radiochemical assay for delta-aminolevulinic acid synthase. *Enzyme* **28:** 109 – 119.

Brooks, C.L. III, Karplus, M. and Petitt, B.M. (1988). Proteins. In: A Theoretical Perspective of Dynamics, Structure and Thermodynamics, in *Adv. Chem. Phys. LXXI,* John Wiley & Sons, New York.

Bruccoleri, R.E., Karplus, M. and McCammon, J.A. (1986). The hinge-bending mode of a lysozyme-inhibitor complex. *Biopolymers.* **25:** 1767 – 1802

Bugany, H., Flohe, L. and Weser, U. (1971). Kinetics of metal chelatase from rat liver mitochondria. *FEBS Lett.* **13:** 92 – 94.

Burden, A.E., Wu, C.K., Dailey, T.A. et al. (1999). Human ferrochelatase: crystallization, characterization of the [2Fe-2S] cluster and determination that the enzyme is a homodimer. *Biochem Biophys Acta* **1435** : 191 – 197.

Cacheux, V., Martasek, P., Fougerousse, F., et al. (1994). Localization of the human coproporphyrinogen oxidase gene to chromosome band 3q12. *Hum. Genet.* **94:** 557 – 559.

Calvert, R.J. and Rimington, C. (1953). Porphyria cutanea tarda: a case report. *Br. Med. J.* **2:** 1131 – 1134.

Camadro, J-M. and Labbe, P. (1988). Purification of ferrochelatase from the yeast Saccharomyces cerevisiae. Evidence for a precursor form of the protein. *J. Biol. Chem.* **263:** 11675 – 11682.

Camadro, J-M. and Labbe, P. (1996). Cloning and characterisation of the yeast Heme 14 gene coding for protoporphyrinogen oxidase, the molecular target of diphenyl ether type herbicides. *J. Biol. Chem.* **271:** 9120 – 9128.

Camadro, J.M., Ibraham, N.G. and Levere, R.D. (1984). Kinetic studies of human liver ferrochelatase. Role of endogenous metals. *J. Biol. Chem.* **259:** 5678 – 5682.

Camadro, J-M., Abraham, N.G. and Levere, R.D. (1985). Kinetic properties of the membrane-bound human liver mitochondrial protoporphyrinogen oxidase. *Arch. Biochem. Biophys.* **242:** 206 – 212.

Camadro, J-M., Chambon, H., Jolles, J. et al. (1986). Purification and properties of coproporphyrinogen oxidase from the yeast *Saccharomyces cerevisiae*. *Eur. J. Biochem.* **156:** 579 – 587.

Camadro, J.–M., Matringe, M., Scalla, R., et al. (1991). Kinetic studies on protoporphyrinogen oxidase inhibition by diphenyl ether herbicides. *Biochem. J.* **277:** 17 – 21.

Camadro, J-M., Thome, F., Brouillet, N., et al. (1994). Purifiaction and properties of protoporphyrinogen oxidase from the yeast *Saccaromyces cerevisiae*. The mitochondrial location and evidence for a precursor form of the protein. *J. Biol. Chem.* **269:** 32085 – 32091.

Camadro, J.M., Arnould, S., Le Guen, L., et al. (1999). Characteristics of protoporphyrinogen oxidase. In: Peroxidizing Herbicides. (P. Böger, K. Wakabayashi, eds), Springer, Berlin, pp. 245 – 277.

Case, D.A. and Karplus, M. (1979). Dynamics of ligand binding to heme proteins. *J. Mol. Biol.* **132:** 343 – 368.

Cavanagh, J.B. and Mellick, R.S. (1965). On the nature of peripheral nerve lesions associated with acute intermittent porphyria. *J. Neurol. Neurosurg.* **28:** 320 – 327.

Cerletti, P. and Siliprandi, N. (1958). *Arch. Biochem. Biophys.* **76:** 214.

Chadwick, D.J. and Ackrill, K. (eds) (1994). In: The Biosynthesis of Tetrapyrrole Pigments, Ciba Foundation Symposium 180, Wiley, Chichester.

Chauhan, S. and O`Brian, M.R. (1993). *Bradyrhizobium japonicum* delta-aminolevulinic acid dehydratase is essential for symbiosis with soybean and contains a metal-binding domain. *J. Bacteriol.* **175:** 7222 – 7227.

Chen, C.H., Astrin, K.H. and Lee, G., (1994). Acute intermittent porphyria: identification and expression of exonic mutations in the hydroxymethylbilane synthase gene. An initiation codon missense mutation in the housekeeping transcript causes "variant acute intermittent porphyria" with normal expression of the erythroid-specific enzyme. *J. Clin. Invest.* **94:** 1927 – 1937.

Cheung, K.-M., Spencer, P., Timko, M.P. et al. (1997). Characterization of a recombinant pea 5-aminolevulinic acid dehydratase and comparative in inhibition studies with the *Escherichia coli* dehydratase. *Biochem.* **5:** 1148 – 1156.

Choi, K.W., Han, O.H., Lee, H.J., et al. (1998). Generation of resistance to the diphenyl-ether herbicide, oxyfluorfen, via expression of the *Bacillus subtilis* protoporphyrinogen oxidase gene in transgenic tobacco plants. *Biosci. Biotechnol. Biochem.* **62:** 558 – 560.

Chretien, S., Dubart, A., Beaupain, D., et al. (1988). Alternative transcription and splicing of the human porphobilinogen deaminase gene results in tissue-specific or in housekeeping expression. *Proc. Natl. Acad. Sci. USA* **85:** 6 – 10.

Chuang, T.Y., Brashear, R. and Lewis, C. (1999). Porphyria cutanea tarda and hepatitis C virus: a case-control study and meta-analysis of the literature. *J. Am. Acad. Dermatol.* **41:** 31 – 36.

Coakley, J., Hawkins, R., Crinis, N., et al. (1990). An unusual case of variegate porphyria with possible homozygous inheritance. *Aust. N. Z. J. Med.* **20:** 587 – 589.

Cochrane, A.L. and Goldberg, A. (1968). A study of faecal porphyrin levels in a large family. *Ann. Hum. Genet.* **32:** 195 – 208.

Coligan, J.E., Dunn, B.M., Ploegh, H.L., et al. (1995). Current protocols in protein science, vol 1, John Wiley and sons, New York.

Conboy, J.G., Cox, T.C., Bottomley, S.S., et al. (1992). Human erythroid 5-aminolevulinate synthase. Gene structure and species-specific differences in alternative RNA splicing. *J. Biol. Chem.* **267:** 18753 – 18758

Conder, L.H., Woodard, S.I., and Dailey, H.A. (1991). Multiple mechanisms for the regulation of haem synthesis during erythroid cell differentiation. Possible role for coproporphyrinogen oxidase. *Biochem. J.* **275:** 321 – 326.

Constantin, D.,Francis, J.E., Akhtar, A. et al. (1996). Uroporphyria induced by 5-aminolevulinic acid in *Ahrd* SWR mice. *Biochem. Pharmacol.* **52:** 1407 – 1413.

Cookson, G.H. and Rimington, C (1954). Porphobilinogen. *Biochem. J.* **57:** 476 – 484.

Cooper D.N. and Krawezak, M. (1990). The mutational spectrum of single base-pair substitutions causing human genetic disease: Patterns and predictions. *Hum Genet* **85:** 55 – 74.

Cormane, R.H., Szabo, E. and Tio, T.H. (1971). Histopathology of the skin in acquired and hereditary porphyria cutanea tarda *Br. J. Dermatol.* **85:** 531 – 539.

Corrigall, A.V., Meissner, P.N. and Kirsch, R.E. (1991). Purification of human erythrocyte porphobilinogen deaminase. *S. Afr. Med. J.* **80:** 294 – 296.

Corrigall, A.V., Hift, R.J., Adams, P.A., et al. (1994). Inhibition of mammalian protoporphyrinogen oxidase by acifluorfen. *Biochem. Mol. Biol. Internat.* **34:** 1283 – 1289.

Corrigall, A.V., Siziba, K.B., Maneli, M.H., et al. (1998a). Purification of and kinetic studies on a cloned protoporphyrinogen oxidase from aerobic bacterium *Bacillus subtilis. Arch. Biochem. Biophys.* **358:** 251 – 256.

Corrigall, A.V., Hift, R.J., Hancock, V., et al. (1998b). Identification and characterisation of a deletion (537delAT) in the protoporphyrinogen oxidase gene in a South African variegate porphyria family. *Hum. Mutat.* **12:** 403 – 407.

Corrigall, A.V., Hift, R. J., Davids, L.M., et al. (2001). Identification of the first variegate porphyria mutation in an indigenous black South African and further evidence for heterogeneity in variegate porphyria. *Mol. Genet. Metab.* **73:** 91 – 96.

Cotter, P.D., Willard, H.F., Gorski, J.L. et al. (1992). Assignment of human erythroid delta-aminolevulinate synthase (ALAS2) to a distal subregion of band Xp11.21 by PCR analysis of somatic cell hybrids containing X; autosome translocations. *Genomics* **13:** 211 – 212.

Cox, G.S. and Whitten, D.G. (1983). Excited state interactions of protoporphyrin IX and related porphyrins with molecular oxygen in solutions and organized assemblies. In: Porphyrin Photosensitization. (D. Kessel and T.J. Dougherty, eds), Plenum Press, New York.

Cox, T.C., Bawden, M.J., Abraham, N.G., et al. (1990). Erythroid 5-aminolevulinate synthase is located on the X chromosome. *Am J Hum Genet* **46:** 107 – 111.

Cox, T.C., Bawden, M.J., Martin, A. et al. (1991). Human erythroid 5-aminolevulinate synthase: promoter analysis and identification of an iron-responsive element in the mRNA. *EMBO J*, **10:** 1891 – 1902.

Cox, T.C., Bottomley, S.S., Wiley, J.S., et al. (1994). X-linked pyridoxine-responsive sideroblastic anemia due to a Thr388-to-Ser substitution in erythroid 5-aminolevulinate synthase. *N. Engl. J. Med.* **330:** 675 – 679.

Cox, T.M., Graeme, M.D., Alexander, J.M., et al. (1998). Protoporphyria. *Semin. Liv. Dis.* **18:** 85 – 93.

Crouse, B.R., Sellers, V.M., Finnegan, M.G., et al. (1996). Site-directed mutagenesis and spectroscopic characterization of human ferrochelatase: identification of residues co-ordinating the [2Fe-2S] cluster. *Biochem.* **35:** 16222 – 16229.

Da Silva, V., Simonin, S., Deybach, J.C., et al. (1995). Variegate porphyria: diagnostic value of fluorometric scanning of plasma porphyrins. *Clin. Chim. Acta.* **238:** 163 – 168.

Dailey, H.A. (1982). Purification and characterization of membrane-bound ferrochelatase from *Rhodopseudomonas sphaeroides. J. Biol. Chem.* **257:** 14714 – 14718.

Dailey, H.A. (1990). Conversion of coproporphyrin to protoheme in higher eukaryotes: Terminal three enzymes. In: Biosynthesis of haem and chlorophylls (H.A. Dailey, ed) McGraw-Hill, New York, pp. 123 – 161.

Dailey, H. (1996) Ferrochelatase. In: Mechanism of metallocenter assembly (G.L. Eichorn, L.G. Marzilli, R.P. Hausinger, eds). New York: VCH Publishers, pp 77 – 89.

Dailey, H.A. and Fleming, J.E. (1983). Bovine ferrochelatase. Kinetic analysis of inhibition by N-methylprotoporphyrin, manganese, and heme. *J. Biol. Chem.* **258:** 11453 – 11459.

Dailey, H.A. and Karr, S.W. (1987). Purification and characterisation of murine protoporphyrinogen oxidase. *Biochem.* **26:** 2697 – 2701.

Dailey, T.A. and Dailey, H.A. (1996a). Human protoporphyrinogen oxidase: Expression, purification and characterization of the cloned enzyme. *Prot. Sci.*, **5:** 98 – 105.

Dailey, T.A., and Dailey, H.A. (1996b). Protoporphyrinogen oxidase of *Myxococcus xanthus.* Expression, purification, and characterisation of the cloned enzyme. *J. Biol. Chem.* **271:** 8714 – 8718.

Dailey, T.A. and Dailey, H.A. (1997a). Expression, purification and characterization of mammalian protoporphyrinogen oxidase. *Methods Enzymol.* **281:** 340 – 349.

Dailey, H.A., and Dailey, T.A. (1997b). Characteristics of human protoporphyrinogen oxidase in controls and variegate porphyria. *Cell. Mol. Biol.* **43:** 67 – 73.

Dailey, T.A., and Dailey, H.A. (1998). Identification of an FAD superfamily containing protoporphyrinogen oxidases, monoamine oxidases, and phytoene desaturase. *J. Biol. Chem.* **273:** 13658 – 13662.

Dailey, H.A., Sellers, V.M. and Dailey, T.A. (1994a). Mammalian ferrochelatase. Expression and characterization of normal and two human porphyric ferrochelatases. *J. Biol. Chem.* **269:** 390 – 395.

Dailey, H.A., Finnegan, M.G. and Johnson, M.K. (1994b). Human ferrochelatase is an iron-sulfur protein. *Biochem.* **33:** 403 – 407.

Dailey, T.A., Meissner, P.N., and Dailey, H.A. (1994c). Expression of a cloned protoporphyrinogen oxidase. *J. Biol. Chem.* **269:** 813 – 815.

Dailey, T.A., Dailey, H.A., Meissner, P., et al. (1995). Cloning, sequencing, and expression of mouse protoporphyrinogen oxidase. *Arch. Biochem. Biophys.* **324:** 379 – 384.

Dailey, H.A., Dailey, T.A., Wu, C.K., et al. (2000). Ferrochelatase at the millennium: structures, mechanisms and [2Fe-2S] clusters. *Cell. Mol. Life Sci.* **57:** 1909 – 1926.

Davies, R.C. and Neuberger, A. (1973). Polypyrroles formed from porphobilinogen and amines by uroporphyrinogen synthetase of *Rhodopseudomonas spheroides*. *Biochem. J.* **133:** 471 – 492.

Day, R.S. (1986). Variegate porphyria. *Semin. Dermatol.* **5:** 138 – 154.

Day, R.S. and Eales, L. (1982). Porphyrins in renal transplantation. *Nephron* **30:** 22 – 27.

Day, R.S., Eales, L., and Meissner, D. (1982). Coexistent variegate porphyria and porphyria cutanea tarda. *N. Engl. J. Med.* **307:** 36 – 41.

Dayan, F.E and Duke, S.O. (1997a). Overview of protoporphyrinogen oxidase-inhibiting herbicides. In: The 1997 Brighton Crop Protection Conference-Weeds, pp. 83 – 92.

Dayan, F.E. and Duke, S.O. (1997b). Phytotoxicity of protoporphyrinogen oxidase inhibitors: Phenomenology, mode of action and mechanism of resistance. In: Herbicide activity: Toxicology, biochemistry and molecular biology (R.M. Roe, J.D. Burton, and R. J. Kuhr, eds), I.O.S. Press Inc., Amsterdam, pp. 11 – 35.

Dayan, F.E. and Duke, S.O. (1997c). Porphyrin-generating Herbicides. In: Herbicides. United States Department of Agriculture- Agricultural Research Services, USA.

De Barreiro, O.L. (1967). 5-aminolaevulinate hydrolyase from yeast. Isolation and purification. *Biochim. Biophys. Acta* **139:** 479 – 486.

De Marco, A., Volrath, S., Bruyere, T., et al. (2000). Recombinant maize protoporphyrinogen IX oxidase expressed in *Escherichia coli* forms complexes with GroEL and DnaK chaperones. *Protein expr. Purif.* **20:** 81 – 86.

De Rooij, F.W.M., Voortman, G., De Baar, E., et al. (1995). Frequency and distribution of mutations in the gene of porphobilinogen deaminase in Dutch acute intermittent porphyria patients. *Scand. J. Clin. Lab. Med.* **55:** 24A.

De Rooij, F.W.M., Minderman, G., De Baar E., et al. (1997). Six new protoporphyrinogen oxidase mutations in Dutch variegate porphyria patients and the R59W mutation in historical perspective. *Acta. Haematol.* **98:** Suppl 1:103.

De Sjervi, A., Glass, J.A., Rossetti, M.V., et al. (1996). Identification of nine new mutations and a common mutation in the hydroxymethylbilane synthase gene in patients with acute intermittent porphyria. *Am. J. Hum. Genet.* **59:** A256.

De Verneuil, H., Aitken, G. and Nordmann. Y. (1978). Familial and sporadic porphyria cutanea: two different diseases. *Hum. Genet.* **44:** 145 – 151.

De Verneuil, H., Sassa, S. and Kappas, A. (1983). Purification and properties of uroporphyrinogen decarboxylase from human erythrocytes – a single enzyme catalysing the four sequential decarboxylations of uroporphyrinogens I and III. *J. Biol. Chem.* **258:** 2454 – 2460.

De Verneuil, H., Grandchamp, B., Foubert, C., et al (1984). Assignment of the gene for uroporphyrinogen decarboxylase to human chromosome 1 by somatic cell hybridization and specific enzyme immunoassay. *Hum. Genet.* **66:** 202 – 205.

De Verneuil, H., Doss, M., Brusco, N., et al. (1985). Hereditary hepatic porphyria with δ-aminolevulinate dehydratase deficiency: immunologic characterization of the non-catalytic enzyme. *Hum. Genet.* **69:** 174 – 177.

De Verneuil, H., Deybach, J.C., Grandchamp, B. et al. (1989). Coexistence of two point mutations in the uroporphyrinogen III synthase gene in one case of congenital erythropoietic porphyria. *Blood* **74:** 105A.

De Verneuil, H., Labbe, P. and Grandchamp, B. (1994). Molecular cloning, sequencing and functional expression of a cDNA encoding human coproporphyrinogen oxidase. *Proc. Natl. Acad. Sci. USA* **91:** 3024 – 3028.

Dean, G. (1953). Porphyria. *Br. Med. J.* **2:** 1291 – 1294.

Dean, G. (1971). The Porphyrias: A Story of Inheritance and Environment, 2d ed., Pitman Medical, London.

Dean, G. and Barnes, H.D. (1955). The inheritance of porphyria. *Br. Med. J.* **2:** 89.

Dean, G. and Barnes, H.D. (1959). Porphyria in Sweden and South Africa. *S. Afr. Med. J.* **33:** 246 – 253.

Dehlin, O., Enerback, L. and Lundvall, O. (1973). Porphyria cutanea tarda-a genetic disease? A biochemical and fluorescence microscopical study in four families. *Acta. Med. Scand.* **194:** 265 – 270.

Deléage, G. and Roux, B. (1987). An algorithm for protein secondary structure prediction based on class prediction. *Protein Eng.* **1:** 289 – 294.

Deleo, V.A., Poh-Fitzpatrick, M.B., Matthews-Roth, M. et al. (1976). Erythropoietic protoporphyria. 10 years experience. *Am. J. Med.* **60:** 8 – 22.

Delfau-Larue, M.H., Martàsek, P. and Grandchamp, B. (1994). Coproporphyrinogen oxidase: gene organisation and description of a mutation leading to exon 6 skipping. Hum. *Mol. Genet.* **3:** 1325 – 1330.

Desnick, R.J., Glass, I.A., Xu, W., et al. (1998). Molecular genetics of congenital erythropoietic porphyria. *Sem. Liv. Dis.* **18:** 77 – 84.

Devine, M.D., Duke, S.O. and Fedke, C. (1993). Oxygen toxicity and herbicidal action. In: Physiology of herbicidal action, Prentice Hall, Englewood Cliffs, New Jersey, pp. 177 – 189.

Deybach, J.Ch., de Verneuil, H., and Nordmann, Y. (1981). The inherited defect in porphyria variegata. *Hum. Genet.* **58:** 425 – 428.

Deybach, J., Da Silva, V., Grandchamp, B. et al. (1985). The mitochondrial location of protoporphyrinogen oxidase. *Eur. J. Biochem.* **149:** 431 – 435.

Deybach, J.C., Da Silva, V., Phung, L.N., et al. (1987). Drug risk of hepatic porphyria. Development of an animal experiment model. *Presse. Med.* **16:** 68 – 71.

Deybach, J.C., de Verneuil, H., Boulechfar, S., et al. (1990). Point mutations in the uroporphyrinogen III synthase gene in congenital erythropoietic porphyria (Gunther's disease). *Blood.* **75:** 1763 – 1765.

Deybach, J., Puy, H., Robréau, A., et al. (1996). Mutations in the protoporphyrinogen oxidase gene in patients with variegate porphyria. *Hum. Mol. Genet.* **5:** 407 – 410.

Diflumeri, C., Larocque, R. and Keng, T. (1993). Molecular analysis of *HEM6* (*HEM12*) in *Saccharomyces cerevisiae*, the gene for uroporphyrinogen decarboxylase. *Yeast* **9:** 613 – 623.

Dinner, A.R., Sali, A., Smith, L.J., et al. (2000). Understanding protein folding via free-energy surfaces from theory and experiment. *Trends Biochem. Sci.* **25:** 331 – 339.

Dolphin, D. (1979). *The Porphyrins,* 7 volumes; Academic Press, New York.

Doss, M. (1979). Diagnose and differentialdiagnose der akuten hepatischen Porphyrien. *Müch. Med. Wschr.* **121:** 1531 – 1535.

Doss, M.O. (1989). New form of dual porphyria: coexistent acute intermittent porphyria and porphyria cutanea tarda. *Eur. J. Clin. Invest.* **19:** 20 – 25.

Doss, M.O. and Sassa, S. (1994). The porphyrias. In: Laboratory medicine. (D.A. Noe, R.C. Rock, eds), Williams and Wilkins, Baltimore, pp. 535 – 553.

Doss, M., Look, D., Henning, H., et al. (1972). Hepatic porphyrins and urinary porphyrins and porphyrin precursors in liver cirrhosis. *Klin. Wochenschr.* **50:** 1025 – 1032.

Doss. M., von Tiepermann, R., Schneider, J., et al. (1979). New type of hepatic porphyria with porphobilinogen synthase defect and intermittent acute clinical manifestations. *Klin. Wschrf.* **57:** 1123 – 1127.

Doss, M., Schneider, J., von Tiepermann, R. et al. (1982). A new type of acute porphyria with porphobilinogen synthase defect in the homozygous state. *Clin. Biochem.* **15:** 52 – 55.

Doussiere, J. and Vignais, P. V. (1992). Diphenylene iodonium as an inhibitor of the NADPH oxidase complex of bovine neutrophils. Factors controlling the inhibitory potency of diphenylene iodonium in a cell-free system of oxidase activation. *Eur. J. Biochem.* **208:** 61 – 71.

Drew, P.D.and Ades, I.Z. (1989). Regulation of the stability of chicken embryo liver delta-aminolevulinate synthase mRNA by hemin. *Biochem. Biophys. Res. Commun.* **162:** 102 – 107.

Drobacheff, C., Derancourt, C., Van Landuyt, H., et al. (1998). Porphyria cutanea tarda associated with human immunodeficiency virus infection. *Eur. J. Dermatol.* **8:** 492 – 496.

Dubart, A., Mattei, M.G., Raich, N., et al. (1986). Assignment of human uroporphyrinogen decarboxylase (URO-D) to the p34 band of chromosome1. *Hum. Genet.* **73:** 277 – 279.

Duke, S.O. and Rebeiz, C.A. (1994). Porphyrin biosynthesis as a tool in pest management. In: Porphyric Pesticides: Chemistry, Toxicology, and Pharmaceutical Applications. (S.O. Duke, and C.A. Rebeiz, eds), American Chemical Society, pp. 1 – 16.

Duke, S.O., Lydon, J. and Paul, R.N. (1989). Oxadiazon activity is similar to that of *p*-nitro-diphenyl ether herbicides. *Weed Science* **37:** 152 – 160.

Duke, S.O., Becerril, J.M., Sherman T.D., et al. (1990). The role of protoporphyrin IX in the mechanism of action of diphenyl ether herbicides. *Pestic. Sci.* **30:** 367 – 378.

Duke, S.O., Becerril, J.M., Matsumoto, H. et al. (1991a). Photosensitizing porphyrins as herbicides. *Am. Chem. Soc. Symp. Ser.* **449:** 371 – 386.

Duke, S.O., Lydon, J., Becerril, J.M., et Al. (1991b). Protoporphyrinogen oxidase-inhibiting herbicides. *Weed Science* **39:** 465 – 473.

Duke, S.O., Lee, H.J., Nandihalii, U.B. et al. (1994). Protoporphyrinogen oxidase as optimal herbicide target in the porphyric pathway. *Am. Chem Soc. Symp. Ser.* **559:** 191 – 204.

Duke, S.O., Lee, H.J., Duke, M.V., et al. (1997). Mechanisms of resistance to protoporphyrinogen oxidase-inhibiting herbicides. In Weed and Crop Resistance to Herbicides (R. De prado, J. Joriin, and L. Garcia-Torres, eds) Kluwer Academic Publishers, Amsterdam.

Duydu, Y., Suzen, H.S., Aydin, A., et al. (2001). Correlation between lead exposure indicators and sister chromatid exchange (SCE) frequencies in lymphocytes from inorganic lead exposed workers. *Environ. Contam. Toxicol.* **41:** 241 – 246.

Dzelzkalns, V., Foley, T., Beale, I. (1982). Delta-aminolevulinic acid synthase of *Euglena gracilis*: physical and kinetic properties. *Arch. Biochem. Biophys.* **216:** 196 – 203.

Eales, L. (1960). Cutaneous porphyria. Observations on 111 cases in 3 racial groups. *S. Afr. J. Lab. Clin. Med.* **6:** 63 – 86.

Eales, L. (1963). Porphyria as seen in Cape Town. A survey of 250 patients and some recent studies. *S. Afr. J. Lab. Clin. Med.* **9:** 151 – 162.

Eales, L., Day, R.S. and Blekkenhorst, G.H. (1980). The clinical and biochemical features of variegate porphyria: an analysis of 300 patients studied at Groote Schuur Hospital, Cape Town. *Int. J. Biochem.* **12:** 837 – 853.

Echelard, Y., Demetryszyn, J., Drolet, M. et al. (1988). Nucleotide sequence of the *hemB* gene of *Escherichia coli* K12. *Mol. Gen. Genet.* **214:** 503 – 508.

Elber, R. and Karplus, M. (1990). *J. Am. Chem. Soc.* **112:** 9161 – 9175.

Elder, G.H. (1982). Enzymatic defects in porphyria: An overview. *Semin. Liv. Dis.* **2:** 87 – 99.

Elder, G.H. (1997). Hepatic porphyria in children. *J. Inher. Metab. Dis.* **20:** 237 – 246.

Elder, G.H. (1998). Porphyria cutanea tarda. *Semin. Liv. Dis.* **18:** 67 – 75.

Elder, G.H. and Evans, J.O. (1978a). Evidence that the coproporphyrinogen oxidase activity of rat liver is situated in the intermembrane space of mitochondria. *Biochem. J.* **172:** 345 – 347.

Elder, G.H. and Evans, J.O. (1978b). A radiochemical method for the measurement of coproporphyrinogen oxidase and the utilization of substrate other than coproporphyrinogen III by the enzyme from rat liver. *Biochem. J.* **169:** 205 – 214.

Elder, G.H. and Wyvill, P.C. (1982). Measurement of uroporphyrinogen decarboxylase using porphyrinogens prepared by chemical reduction. *Enzyme* **28:** 186 – 195.

Elder, G.H. and Roberts, A.G. (1994). Uroporphyrinogen decarboxylase. *J. Bioenerg. Biomembr.* **27:** 207 – 214.

Elder, G.H., Evans, J.O. and Thomas, N. (1976). The primary enzyme defect in hereditary coproporphyria. *Lancet* **2:** 1217 – 1219.

Elder, G.H., Tovey, J.A. and Sheppard, D.M. (1983). Purification of uroporphyrinogen decarboxylase from human erythrocytes. *Biochem. J.* **215:** 45 – 55.

Elder, G.H., Hift, R.J. and Meissner, P.N. (1997). The acute porphyrias. *The Lancet* **349:** 1613 – 1617.

Elder, G.H., Roberts, A.G. and De Salamanca, R.E. (1989). Genetics and pathogenesis of human uroporphyrinogen decarboxylase defects. *Clin. Biochem.* **22:** 163 – 168.

Erskine, P.T., Senior, N., Awan, S., et al. (1997a). X-ray structure of 5-aminolaevulinate dehydratase, a hybrid aldolase. *Nat Struct Biol* **12:** 1025 – 1031.

Erskine, P. T., Senior, N., Maignan, S., et al. (1997b). Crystallization of 5-aminolaevulinic acid dehydratase from *Escherichia coli* and *Saccharomyces cerevisiae*. *Protein. Sci.* **6:** 1774 – 1776.

Erskine, P.T., Newbold, R., Brindley, A.A., et al. (2001). The x-ray structure of yeast 5-aminolaevulinic acid dehydratase substrate and three inhibitors. *J. Mol. Biol.* **7:** 133 – 141.

Evans, J., Lefkowitch, J., Lim, C.K. et al. (1981). Faecal porphyrin abnormalities in a patient with features of Rotor's syndrome. *Gastroenterol.* **81:** 1125 – 1130.

Faeder, E.J. and Siegel, L.M. (1973). A rapid micromethod for determination of FMN and FAD in mixtures. *Anal. Biochem.* **53:** 332 – 336.

Falk, J.E. (1964). *Porphyrins and metalloporphyrins*, Elsevier, New York.

Falk, J.E., Dresel, E.I.B. and Rimington, C. (1953). Porphobilinogen as a porphyrin precursor, and interconversion of porphyrins in a tissue system. *Nature* **172:** 292.

Falk, J.E., Lemberg, R., and Morton, R.K. (1961). *Haematin Enzymes*, 2 volumes, Pergamon Press, Oxford, London, New York.

Fargion, S., Fracanzani, A.L., Romano, R., et al. (1996). Genetic hemochromatosis in Italian patients with porphyria cutanea tarda: possible explanation for iron overload. *J. Hepatol.* **24:** 564 – 569.

Feldman, R.J. (1976). *Atlas of Macromolecular Structure on Macrofiche*, Tracor Jitco, Inc., Rockville, MD.

Felix, F. and Brouillet, N. (1990). Purification and properties of uroporphyrinogen decarboxylase from *Saccharomyces cerevisiae*. Yeast uroporphyrinogen decarboxylase. *Eur. J. Biochem.* **188:** 393 – 403.

Ferreira, G.C. and Dailey, H.A. (1988). Mouse protoporphyrinogen oxidase. Kinetic parameters and demonstration of inhibition by bilirubin. *Biochem. J.* **250:** 597 – 603.

Ferreira, G.C. and Dailey, H.A. (1993). Expression of mammalian 5-aminolevulinate synthase in Escherichia coli. Overproduction, purification, and characterization. *J. Biol. Chem.* **268:** 584 – 590.

Ferreira, G.C. and Gong, J. (1995). 5-Aminolevulinate synthase and the first step of heme biosynthesis. *J. Bioenerg. Biomembr.* **27:**151 – 159.

Ferreira, G.C., Naeme, P.J. and Dailey, H.A. (1993). Heme biosynthesis in mammalian systems: evidence of a Schiff base linkage between the pyridoxal 5'-phosphate cofactor and a Lysine residue in 5-aminolevulinate synthase. *Protein. Sci.* **2:** 1959 – 1965.

Ferreira, G.C., Andrew, T.L., Karr, S.W. et al. (1988). Organisation of the terminal two enzymes of the heme biosynthetic pathway. Orientation of protoporphyrinogen oxidase and evidence for a membrane complex. *J. Biol. Chem.* **263:** 3835 – 3839.

Ferreira, G.C., Vajapey, U., Hafez, O., et al. (1995). Aminolevulinate synthase: lysine 313 is not essential for binding the pyridoxal phosphate cofactor but is essential for catalysis. *Protein Sci.* **4:** 1001 – 1006.

Fischer, H. (1915). Uber das Urinporphyrin. I. Mitteilung. *Hoppe-Syler's Z. physiol. Chem.* **95:** 34 – 60.

Fischer, H. (1916). Beobachtungen am frischen Harn und Kot von Porphyrinpatienten. *Hoppe-Seyler's Z. Physiol. Chem.* **97:** 148 – 170.

Fischer, H. and Zerweck, W. (1924). Uber den Harnfarbstoff bei normalen und pathologischen Verhaltnissen und seine lichtschutzende Wirkung. Zugleich einige Beitrage zur Kenntnis der Porphyrinurie. *Hoppe-Syler's Z. physiol. Chem.* **137:** 176 – 241.

Flügel, K.A. and Druschky, K.F. (1977). Electromyogram and nerve condition in patients with acute intermittent porphyria. *J. Neurol.* **214:** 267 – 279.

Folsch, H., Guiard, B., Neupert, W. et al. (1996). Internal targeting signal of the BCS1 protein: a novel mechanism of import into mitochondria. *EMBO. J.* **15:** 479 – 487.

Ford, R.E., Ou, C.N. and Ellefson, R.D. (1980). Assay for erythrocyte uroporphyrinogen I synthase activity with porphobilinogen as substrate. *Clin. Chem.* **26:** 1182 – 1185.

Frank, J. and Christiano, A.M. (1997). Genetic research strategies: a review of the acute porphyrias. *Retinoids* **13:** 88 – 92.

Frank, J.; Zaider, E.; Jugert, F.K.; et al. (1997). Variegate porphyria: identification of three novel missense mutations in the protoporphyrinogen oxidase gene. *Acta Haematol.* **98:** (suppl 1), 96.

Frank, J., Jugert, F.K., Breitkopf, C., et al. (1998a). Recurrent missense mutation in the protoporphyrinogen oxidase gene underlies variegate porphyria. *Am. J. Med. Genet.* **79:** 22 – 26.

Frank, J., Jugert, F.K., Kalka, K., et al. (1998b). Variegate porphyria: Identification of a nonsense mutation in the protoporphyrinogen oxidase gene. *J. Invest. Dermatol.* **110:** 449 – 451.

Frank, J., Lam, H., Zaider, E., et al. (1998c). Molecular basis of variegate porphyria: a missense mutation in the protoporphyrinogen oxidase gene. *J. Med. Genet.* **35:** 244 – 247.

Frank, J., McGrath, J., Lam, H., et al. (1998d). Homozygous variegate porphyria: Identification of mutations on both alleles of protoporphyrinogen oxidase gene in a severely affected proband. *J. Invest. Dermatol.* **110:** 452 – 455.

Frank, J., Poh-Fitzpatrick, M.B., King, L.E. et al. (1998e). The genetic basis of "Scarsdale Gourmet Diet" variegate porphyria: a missense mutation in the protoporphyrinogen oxidase gene. *Arch. Dermatol. Res.* **290:** 441 – 445.

Frank, J., McGrath, J.A., Poh-Fitzpatrick, M.B., et al. (1999). Mutation in the translation initiation codon of the protoporphyrinogen oxidase gene underlie variegate porphyria. *Clin. exp. Dermatol.* **24:** 296 – 301.

Frank, J., Jugert, F.K., Merk, H.K., et al. (2001a). A spectrum of novel mutations in the protoporphyrinogen oxidase gene in 13 families with variegate porphyria. *J. Invest. Dermatol.* **116:** 821 – 823.

Frank, J., Aita, V.M., Ahmad, W., et al. (2001b). Identification of a founder mutation in the protoporphyrinogen oxidase gene in variegate porphyria patients from Chile. *Hum. Hered.* **151:** 160 – 168.

Frankenberg, N., Erskine, P.T., Cooper, et al. (1999). High resolution crystal structure of a Mg^{2+}-dependent porphobilinogen synthase. *J. Mol. Biol.* **289:** 591 – 602.

Frankenberg, N., Kittel, T., Hungerer, C., et al. (1998). Cloning, mapping and functional characterization of the *hemB* gene of *Pseudomonas aeruginosa*, which encodes a magnesium-dependent 5-aminolevulinic acid dehydratase. *Mol. Gen. Genet.* **257:** 485 – 489.

Fraunberg, M., Tenhunen, R., and Kauppinen, R. (2001). Expression and characterization of six mutations in the protoporphyrinogen oxidase gene among Finnish variegate porphyria patients. *Mol. Med.* **7:** 320 – 328.

Frear, D.S, Swanson, H.R. and Mansager, E.R. (1983). Acifluorfen metabolism in soybean: diphenyl ether bond cleavage and the formation of homoglutathione, cysteine and glucose conjugates. *Pestic. Biochem Physiol.* **20:** 299 – 310.

Freinkel, R.K. and Ashman, M. (1974). Variegate porphyria. *Arch. Dermatol.* **110:** 653.

Fromke, V.L., Bossenmaier, I., Cardinal, R. et al. (1978). Porphyria variegata. A study of a large kindred in the United States of America. *Am. J. Med. Sci.* **65:** 80 – 88.

Frustaci, J.M. and O'Brian, M (1992). Characterization of a *Bradyrhizobium japonicum* ferrochelatase mutant and isolation of the *hemH* gene. *J. Bacteriol.* **174:** 4223 – 4229.

Frydman, R.B. and Fenstein, G. (1974). Studies on porphobilinogen deaminase and urporphyrinogen III cosynthase from human erythrocytes. *Biochim. Biophys. Acta.* **350:** 358 – 373.

Fujita, H., Sassa, S., Lundgren, J., et al. (1987). Enzymatic defect in a child with hereditary hepatic porphyria due to homozygous delta-aminolevulinic acid dehydratase deficiency: immunochemical studies. *Pediatrics.* **80:** 880 – 885.

Fujita, H., Yamamoto, M., Yamagami, T., et al. (1991) Erythroleukemia differentiation. Distinctive responses of the erythroid-specific and the nonspecific delta-aminolevulinate synthase mRNA. *J Biol Chem* **266:** 17494 – 17502.

Fujita, H., Kondo, M., Taketani, S., et al. (1994). Characterization and expression of cDNA encoding coproporphyrinogen oxidase from a patient with hereditary coproporphyria. *Hum. Mol. Genet.* **3:** 1807 – 1810.

Gandolfo, L.D., Macri, A., Biolcati, G., et al. (1991). Homozygous variegate porphyria: revision of a diagnostic error. *Br. J. Med (Lett.)* **124:** 211.

Garey, J.R., Hansen, J.L., Harrison, L.M., et al. (1989). A point mutation in the coding region of uroporphyrinogen decarboxylase associated with familial porphyria cutanea tarda. *Blood* **73:** 892 – 895.

Garey, J.R., Labbe-Bois, R., Chelstowska, A., et al. (1992). Uroporphyrinogen decarboxylase from *Saccharomyces cerevisiae*. *HEM12* gene sequence and evidence for two conserved glycines essential for enzymatic activity. *Eur. J. Biochem.* **205:** 1011 – 1016.

Garey, J.R., Franklin, K.F., Brown, D.A., et al. (1993). Analysis of uroporphyrinogen decarboxylase complementary DNAs in sporadic porphyria cutanea tarda. *Gastroenterology* **105:** 165 – 169.

Garrett, R.H. and Grishman, C.M. (2002). In:Principles of Biochemistry. Harcourt College Publishers, New York, pp 113 – 152.

Gatley, S.J. and Sherratt, S.A. (1976). The effects of diphenyleneiodonium and 2,4-dichlorodiphenyleneiodonium on mitochondrial reaction. Relationship of binding of diphenylene [^{125}I]iodonium to mitochondria to the extent of inhibition of oxygen uptake. *Biochem. J.* **158:** 307 – 315.

Gelin, B.R., Lee, A.W. and Karplus, M. (1983). Hemoglobin tertiary structural change on ligand binding. Its role in the co-operative mechanism. *J. Mol. Biol.* **171:** 489 – 559.

Ghisla, S. (1980). Fluorescence and optical characteristics of reduced flavins and flavoproteins. *Methods Enzymol.* **66:** 360 – 373.

Gibbs, P.N.B. and Jordan, P.M. (1986). Identification of lysine at the active site of human 5-aminolevulinate dehydratase. *Biochem. J.* **236:** 447 – 451.

Gibbs, P.N.B., Chaudhry, A.G. and Jordan, P.M. (1985). Purification and properties of 5-aminolaevulinate dehydratase from human erythrocytes. *Biochem. J.* **230:** 25 – 34.

Gibson, J.B. and Goldberg, A. (1956). The neuropathology of acute porphyria. *J. Pathol. Bact.* **LXXI:** 495 – 510.

Gibson, K.D., Laver, W.G. and Neuberger, A. (1958). Initial stages in the biosynthesis of porphyrins. II. The formation of 5-ALA from glycine and succinyl CoA by particles from chicken erythrocytes. *Biochem. J.* **70:** 71 – 76.

Girotti, A.W. and Deziel, M.R. (1983). Photodynamic action of protoporphyrin resealed erythrocyte membranes: *Porphyrin Photosensitization.* (D. Kessel and T.J. Dougherty, eds), Plenum Press, New York, pp. 213 – 225.

Goerz, G., Bunselmeyer, S., Bolsen, K., et al. (1996). Ferrochelatase activities in patients with erythropoietic protoporphyria. *Br. J. Dermatol.* **134:** 880 – 885.

Goldberg, A., Ashenbrucker, M., Cartwright, G.E. et al. (1956). Studies on the biosynthesis of haem *in vitro* by avian erythrocytes. *Blood* **11:** 821 – 833.

Gong, J., Hunter, G.A. and Ferreira, G.C. (1998). Aspartate-279 in aminolevulinate synthase affects enzyme catalysis through enhancing the function of the pyridoxal 5'-phosphate cofactor. *Biochem.* **37:** 3509 – 3517.

Gouya, L., Puy, H., Robreau, A-M., et al. (2002). The penetrance of dominant erythropoietic protoporphyria is modulated by expression of wildtype *FECH*. *Nat. Genet.* **30:** 27 – 28.

Govindarajan, S. and Goldstein, R.A. (1996). Why are some proteins structures so common? *Proc. Natl. Acad. Sci. U S A.* **93:** 3341 – 3345.

Grandchamp, B. and Nordmann, Y. (1977). Decreased lymphocyte coproporphyrinogen III oxidase activity in hereditary coproporphyria. *Biochem. Biophys. Res. Commun.* **74:** 1089 – 1095.

Grandchamp, B. and Nordmann, Y. (1982). Coproporphyrinogen III oxidase assay. *Enzyme* **28:** 196 – 205.

Grandchamp, B. and Nordmann, Y. (1988). Enzymes of the heme biosynthesis pathway: recent advances in molecular genetics. *Semin. Hematol.* **25:** 303 – 311.

Grandchamp, B., Phung, N. and Nordmann, Y. (1978). The mitochondrial localization of coproporphyrinogen III oxidase. *Biochem. J.* **176:** 97 – 102.

Grandchamp, B. Limoril, J. and Puy, H. (1995). Molecular abnormalities of coproporphyrinogen oxidase in patients with hereditary coproporphyria. *J. Bioenerg. Biomem.* **27:** 215 – 219.

Grandchamp, B., de Verneuil, H., Beaumont, C., et al. (1987). Tissue-specific expression of porphobilinogen deaminase. Two isoenzymes from a single gene. *Eur. J. Biochem.* **162:** 105 – 110.

Grandchamp, B., Picat, C., Mignotte, V., et al. (1989a). Two tissue-specific splicing mutation in acute intermittent porphyria. *Proc. Natl. Acad. Sci. USA* **86:** 661 – 664.

Grandchamp, B., Picat, C., Kauppinen, R., et al. (1989b). Molecular analysis of acute intermittent porphyria in a Finnish family with normal erythrocyte porphobilinogen deaminase. *Eur. J. Clin. Invest.* **19:** 415 – 418.

Granick, S. (1958). Porphyrin synthesis in erythrocytes. Formation of 5-aminolaevulinic acid in erythrocyte. *J. Biol. Chem.* **232:** 1101 – 1117.

Granick, S. (1966). The induction *in vitro* of the synthesis of delta-aminolaevulinic acid synthase in chemical porphyria: A response to certain drugs, sex hormones and foreign chemicals. *J. Biol. Chem.* **241:** 1359 – 1375.

Granick, S. and Sassa, S. (1971). Delta-aminolaevulinic acid synthase and the control of haem and chlorophyll synthesis. In Metabolic regulation (H.J. Vogel, Ed.). Academic Press, New York, London, pp. 77 – 141.

Gray, C.H. (1952). Isotope studies in porphyria. *Br. Med. Bull.* **8:** 229.

Greenfield, N. and Fasman, G.D. (1969). The use of computed optical rotatory dispersion curves for the evaluation of protein conformation. *Biochem.* **8:** 4108 – 4116.

Gregor, A., Kostrewska, E., Tarczynska-Nosal, S. et al.. (1994). *Polski Tygodnik Lekarski* **49:** 12 – 13.

Grinstein, M., Aldrich, R.A., Hawkinson, V. et al. (1949). An isotopic study of porphyrin and haemoglobin metabolism in a case porphyria. *J. Biol. Chem.* **179:** 983 – 989.

Grossman, M.E., Bickers, D.R., Poh-Fitzpatrick M.B. (1979). Porphyria cutanea tarda. Clinical features and laboratory findings in 40 patients. *Am. J. Med.* **67:** 277.

Günther, H. (1911). Die haematoporphyrie. *Deutshe Arch. Klin. Med.* **105:** 89 – 146.

Günther, H. (1912). Die Bedeutung der haematoporphyrinurie in der Physiologie und Pathologie. *Ergeb. Allgemein. Pathol. Pathologisch. Anat.* **20:** 608 – 764.

Hamilton, J.W., Bement, W.J., Sinclair, P.R., et al. (1991). Heme regulates hepatic 5-aminolevulinate synthase mRNA expression by decreasing mRNA half-life and not by altering its rate of transcription. *Arch. Biochem. Biophys.* **289:** 387 – 392.

Hamnström, B., Haeger-Aronson, B., Waldenström, J., et al. (1967). Three Swedish families with porphyria variegata. *Br. Med. J.* **4:** 449 – 453.

Hamper, B.C., Leschinsky, K.L., Massey, S.S., et al. (1995). Synthesis and herbicidal activity of 3-aryl-5-(holoalkyl)-4-isoxazolecarboxamides and their derivatives. *J. Agric. Food Chem.* **43:** 219 – 228.

Handa, F.; Kumar, K.; Kumar, R. (1975). A case of variegate porphyria in an Indian. *Br. J. Dermatol.* **92:** 347.

Hansson, M. and Hederstedt, L. (1992). Cloning and characterization of the *Bacillus subtilis hemEHY* gene cluster, which encodes protoheme IX biosynthetic enzymes. *J. Bacteriol.* **174:** 8081 – 8093.

Hansson, M. and Hederstedt, L. (1994). *Bacillus subtilis hemY* is a peripheral membrane protein essential for protoheme IX synthesis which can oxidize coproporphyrinogen III and protoporphyrinogen IX. *J. Bacteriol.* **176:** 5962 – 5970.

Hansson, M., Gustafsson, M.C.U., Kannangara, C.G. et al. (1997). Isolated *Bacillus subtilis hemY* has coproporphyrinogen III to coproporphyrin III oxidase activity. *Biochim. et Biophys. Acta.* **1340:** 97 – 104.

Harbin, B.M. and Dailey, H.A. (1985). Orientation of ferrochelatase in bovine liver mitochondria. *Biochem.* **24:** 366 – 370.

Harley, V. (1890). Two fatal cases of an unusual form of nerve disturbance associated with red urine, probably due to defective tissue oxidation. *Br. Med. J.* **2:** 1169 – 1170.

Harrington, P.M., Singh, B.K., Szamosi, I.T. et al. (1995). Synthesis and herbicidal activity of cyperin. *J.Agric. Food Chem.* **43:** 804 – 808.

Hart, G. J. and Battersby, A.R. (1985). Purification and properties of uroporphyrinogen III synthase from *Euglena gracilis. Biochem. J.* **232:** 151 – 160.

Hawk, J.L., Magnus, I.A., Parkes, A., et al. (1978). Deficiency of hepatic coproporphyrinogen oxidase in hereditary coproporphyria. *J. Roy. Soc. Med.* **71:** 775 – 777.

Hayashi, N., Yoda, B. and Kikuchi, G. (1969). Mechanism of allylisopropyl acetamide induced increase of δ-aminolevulinate synthetase in liver mitochondria. IV. Accumulation of the enzyme in the soluble fraction of rat liver. *Arch. Biochem. Biophys.* **131:** 83 – 91.

Hayashi, N., Yoda, B. and Kikuchi, G. (1970). Differences in molecular sizes of δ-aminolevulinate synthetases in the soluble and mitochondrial fractions of rat liver. *J. Biochem.* (Tokyo) **67:** 859 – 861.

Hayashi, N., Yoda, B. and Kikuchi, G. (1976). Difference in molecular sizes of ALA synthetases from the soluble and mitochondrial fractions of rat liver. *Cell Tissue Res.* **232:** 257 – 264.

Hayashi, N., Watanabe, N. and Kikuchi, G. (1983). Inhibition by hemin of *in vivo* translocation of chicken liver 5-aminolaevulinate synthase into mitochondria. *Biochem. Biophys. Res. Commun.* **115:** 700 – 706.

Held, J.L., Sassa, S., Kappas, L., et al. (1989). Erythrocyte uroporphyrinogen decarboxylase activity in porphyria cutanea tarda: a study of 40 consecutive patients. *J. Invest. Dermatol.* **93:** 332 – 334.

Hennessey, J.P., Jr., and Johnson, W.C., Jr. (1981). Information content in the circular dichroism of proteins. *Biochem.* **20:** 1085 – 1094.

Henriksson, M., Timonen, K., Mustajoki, P., et al. (1996). Four novel mutation in the ferrochelatase gene among erythropoietic protoporphyria patients. *J. Invest. Dermatol.* **106:** 346 – 350.

Hierons, R. (1957). Acute intermittent porphyria. *Postgrad. Med. J.* **43:** 605.

Hift, R.J. and Kirsch, R.E. (1995). Porphyria cutanea tarda as a manifestation of alcohol-induced liver disease. In: Alcoholic Liver Disease, 2nd ed. (P. Hall, ed), London: Edward Arnold, pp. 219 – 231.

Hift, R.J., Meissner, P.N., Todd, G., et al. (1993). Homozygous variegate porphyria: an evolving clinical syndrome. *Postgrad. Med. J.* **69:** 781 – 786.

Hift, R.J., Meissner, P.N., Corrigall, A.V., et al. (1997). Variegate porphyria in South Africa, 1688 – 1996 - new developments in an old disease. *S. Afr. J. Med.* **87:** 718 – 727.

Higuchi, M. and Bogorad, L. (1975). The purification and properties of uroporphyrinogen I synthetase and uroporphyrinogen III cosynthetase. Interaction between the enzymes. *Ann. N Y. Acad. Sci.* **244:** 401 – 408.

Hippler, B., Homuth, G., Hoffmann, T., et al. (1997). Characterization of *Bacillus subtilis hemN*. *J. Bacteriol.* **179:** 7181 – 7185.

Holti, G., Rimington, C., Tate, B.C. et al. (1958). An investigation of porphyria cutanea tarda. *Q.J. Med.* **27:** 1 – 17.

Honig, B. (1999). Protein folding: from the levinthal paradox to structure prediction. *J. Mol. Biol.* **293:** 283 – 293.

Hoppe-Syler, F. (1871). Das Hamatin, *Tubinger Med.-Chem. Untersuchungen* **4:** 523 – 533.

Hughes, G.S. and Davis, L. (1983). Variegate porphyria and heavy metal poisoning from ingestion of "moon shine". *Southern Med. J.* **76:** 1027 – 1029.

Hyde, C.C., Ahmed, S.A., Padlan, E.A., et al. (1988). Three-dimensional structure of the tryptophan synthase alpha 2 beta 2 multienzyme complex from *Salmonella typhimurium*. *J. Biol. Chem.* **263:** 17857 – 17871.

Imoto, S., Tanizawa, Y., Sato, Y., et al. (1996). A novel mutation in the ferrochelatase gene associated with erythropoietic protoporphyria. *Br. J. Haematol.* **94:** 191 – 197.

Ishida, N., Fujita, H., Fukuda, Y., et al. (1992). Cloning and expression of the defective genes from a patient with delta-aminolevulinate dehydratase porphyria. *J. Clin. Invest.* **89:** 1431 – 147.

Ishida, N., Fujita, N., Noguchi, T., et al. (1990). Message amplification phenotyping of an inherited δ-aminolevulinate dehydratase deficiency in a family with acute hepatic porphyria. *Biochem. Biophys. Res. Commun.* **172:** 237 – 242.

Jackson, A.H., Games, D.E., Couch, P., et al. (1974). Conversion of coproporphyrinogen III to protoporphyrin IX. *Enzyme* **17:** 81 – 87.

Jackson, A.H., Sancovich, H.A., Ferramola, A.M., et al. (1976). Macrocytic intermediates in the biosynthesis of porphyrins. *Philos. Trans. R. Soc. Lond. B. Biol. Sci.* **273:** 191 – 206.

Jackson, SE. (1998). How do small single-domain proteins fold? *Fold. Des.* **3:** R81 – 91.

Jacobs, N.J. and Jacobs, J.M. (1976). Nitrate, fumarate and oxygen as electron acceptors for a late step in microbial heme synthesis. *Biochim. Biophys. Acta* **449:** 1 – 9.

Jacobs, N.J. and Jacobs, J.M. (1981). Protoporphyrinogen oxidation in *Rhodopseudomonas spheroides*, a step in heme and bacteriochlorophyll synthesis. *Arch. Biochem. Biophys.* **211:** 305 – 311.

Jacobs, J.M., and Jacobs, N.J. (1984). Protoporphyrinogen oxidation, an enzymatic step in heme and chlorophyll synthesis: Partial characterization of the reaction in plant organelles and comparison with mammalian and bacterial systems. *Arch. Biochem. Biophys.* **229:** 312 – 319.

Jacobs, J.M. and Jacobs, J.N. (1987). Oxidation of protoporphyrinogen to protoporphyrin, a step in chlorophyll and haem biosynthesis: Purification and partial characterization of the enzyme from barley organelles. *Biochem. J.* **244:** 219 – 224.

Jacobs, J.N. and Jacobs, N.J. (1993). Porphyrin accumulation and export by isolated barley (*Hordeum vulgare*) plastids. *Plant Physiol.* **101:** 1181 – 1187.

Jacobs, N.J., Borotz, S.E. and Jacobs, J.M. (1989). Characteristics of purified protoporphyrinogen oxidase from barley. *Biochem. Biophys. Res. Commun.* **161:** 790 – 796.

Jacobs, N.J., Jacobs, J.M. and De Maggio, A. (1982). Protoporphyrinogen oxidation in chloroplasts and plant mitochondria, a step in heme and chlorophyll synthesis. *Arch. Biochem. Biophys.* **218:** 233 – 239.

Jacobs, J.M., Jacobs, N.J. and Duke, S.O. (1996). Protoporphyrinogen destruction by plant extracts and correlation with tolerance to protoporphyrinogen oxidase inhibiting herbicides. *Pestic. Biochem. Physiol.* **55:** 77 – 83.

Jacobs, J.M., Jacobs, N.J., Borotz, S.E., et al. (1990). Effects of photobleaching herbicide, acifluorfen methyl, on protoporphyrinogen oxidation in barley organelles, soyabean root mitochondria, soya bean root nodules, and bacteria. *Arch. Biochem. Biophys.* **280:** 369 – 375.

Jacobs, J.M., Jacobs, N.J., Sherman, T.D. et al. (1991). Effect of diphenyl ether herbicides on oxidation of protoporphyrinogen to protoporphyrin in organellar and plasma membrane enriched fractions of barley. *Plant. Physiol.* **97:** 197 – 203.

Jenkins, T. (1996). The South African malady. *Nat. Genet.* **13:** 7 – 9.

Jenkins, T. (1997). The molecular basis of South African genetic porphyria established at last. *S. Afr. Med. J.* **87:** 733 – 735.

Johnston, D.J., Droz, E., Rochaix, J-D, et al. (1998). Cloning and characterisation of potato cDNAs involved in tetrapyrrole biosynthesis (accession nos. ferrochelatase AJ005802, chloroplastic protoporphyrinogen IX oxidase AJ225107, mitochondrial protoporphyrinogen IX oxidase AJ225108) (PG 98-156). *Plant. Physiol.* **118:** 330.

Jones, M.S. and Jones, O.T.G. (1969). The structural organisation of heme synthesis in the rat liver mitochondria. *Biochem. J.* **113:** 507.

Jones, R.M. and Jordan, P.M. (1993). Purification and properties of the uroporphyrinogen decarboxylase from *Rhodobacter sphaeroides*. *Biochem. J.* **293:** 703 – 712.

Jordan, P.M. (1982). Uroporphyrinogen III cosynthase: A direct assay method. *Enzyme* **28:** 158 – 169.

Jordan, P.M. (1990). The Biosynthesis of 5-aminolaevulinic acid and its transformation into coproporphyrinogen in animals and bacteria. In: Biosynthesis of Heme and Chlorophylls. (H.A. Dailey, ed), McGraw Hill publishing Co. New York, pp. 55 – 122.

Jordan, P.M. (1991). In: Biosynthesis of tetrapyrroles. (P.M. Jordan, ed), Elsevier, Amsterdam, pp. 1 – 66.

Jordan, P.M. and Seehra, J.S. (1980). Mechanism of action of δ-aminolevulinic acid dehydratase. Stepwise order of addition of the two molecules of δ-aminolevulinic acid in the enzyme synthesis of porphobilinogen. *J. Chem. Soc. Chem. Commun.* **240:** 242.

Jordan, P.M. and Seehra, J.S. (1986). Purification of porphobilinogen synthase from bovine liver. *Methods Enzymol.* **123:** 427 – 434.

Jordan, P.M. and Warren, M.J. (1987). Evidence for a dipyrromethane cofactor at the catalytic site of *E. coli* porphobilinogen deaminase. *FEBS Lett* **225:** 87 – 92.

Jordan, P.M., Thomas, S.D. and Warren, M.J. (1988). Purification, crystallization and properties of porphobilinogen deaminase from a recombinant strain of *Escherichia coli* K12. *Biochem. J.* **254:** 427 – 435.

Jordan, P.M. and Woodcock, S.C. (1991). Mutagenesis of arginine residues in the catalytic cleft of *Escherichia coli* porphobilinogen deaminase that affects dipyrromethane cofactor assembly and tetrapyrrole chain initiation and elongation. *Biochem. J.* **280:** 445 – 449.

Jordan, P.M., Warren, M.J., Mgbeje, N.I., et al. (1992). Crystallization and preliminary X-ray investigation of *Escherichia coli* porphobilinogen deaminase. *J. Mol. Biol.* **224:** 269 – 271.

Juknat, A.A., Seubert, A., Seubert, S. et al. (1989). Studies on uroporphyrinogen decarboxylase of etiolated *Euglena gracilis Z. Eur. J. Biochem.* **179:** 423 – 428.

Kaczor, C.M., Smith, M.W., Sangwan, I. et al. (1994). Plant delta-aminolevulinic acid dehydratase. Expression in soybean root nodules and evidence for a bacterial lineage of the ALAD gene. *Plant Physiol.* **104:** 1411 – 1417.

Kane, J.F., and Hartley. D.L. (1988). Formation of recombinant protein inclusion bodies in *Escherichia coli*. *TIBTECH.* **6:** 95 – 101.

Kappas, A., Sassa, S., Galbraith, R.A., et al. (1989). In: The porphyrias. (C.R. Wyngaarden, D.S. Frederickson, eds). *The metabolic basis of inherited disease*, 6th ed. McGraw-Hill, New York: p. 1305.

Kappas, A., Sassa, S., Galbraith, R.A., et al. (1995). The porphyrias. In: The metabolic basis of inherited diseases. (C.R. Scriver, A.L. Beaudet, W.S. Sly, D. Valle, eds), 7th ed, volume. 2. McGraw Hill, New York, pp. 2103 – 2159.

Karr, S.R. and Dailey, H.A. (1988). The synthesis of murine ferrochelatase *in vitro* and *in vivo*. *Biochem. J.* **254:** 799 – 803.

Kast, A. (1888). Über die art der Darreichung und Verordnung des Sulfonals. *Ther. Mh.* **11:** 316 – 319.

Kataoka, M., Sato, R., and Oshio, H. (1990). Isolation and partial characterization of mutant *Chlamydomonas rheinhardtii* resistant to herbicide S-23142. *J. Pestic. Sci.* **15:** 449 – 451.

Kauppinen, R., Mustajoki, P., Pihlaja, H., et al. (1995). Acute intermittent porphyria in Finland: 19 mutations in the porphobilinogen deaminase gene. *Hum. Mol. Genet.* **4235:** 215 – 222.

Kauppinen, R., Timonen, K., Taketani, S. et al. (1996). Homozygous variegate porphyria: ten years follow-up and characterisation of a molecular defect. *Hepatol.* **23:** 1 – 90.

Kauppinen, R., Timonen, K., Laitinen, E., et al. (1997). Molecular genetics and clinical characteristics of variegate porphyria. *Acta. Haematol.* **98 (Suppl 1):** 96.

Kauppinen, R., Timonen, K., von und zu Fraundberg, K., et al. (2001). Homozygous variegate porphyria: 20y follow-up and characterization of molecular defect. *Soc. Invest. Dermatol.* **16:** 610 – 613.

Kawamura, S., Kato, T., Matsuo, M., et al. (1996). Species difference in protoporphyrin IX accumulation produced by an *N*-phenylimide herbicide in embryos between rats and Rabbits. *Toxicol. Appl. Pharmacol.* **141:** 520 – 525.

Kawanishi, S., Seki, Y. and Sano, S. (1983). Uroporphyrinogen decarboxylase - purification, properties and inhibition by polychlorinated biphenyl isomers. *J. Biol. Chem.* **258:** 4285 – 4292.

Kaya, A.H., Plewinska, M., Wong, D.M., et al. (1994). Human δ-aminolevulinate dehydratase (ALAD) gene: structure and alternative splicing of the erythroid and housekeeping mRNAs. *Genomics* **19:** 242 – 248.

Kiel. J.A., Ten Berge, A.M. and Venema, G. (1992). Nucleotide sequence of the *Synechococcus sp.* PCC7942 *hemE* gene encoding the homologue of mammalian uroporphyrinogen decarboxylase. *DNA Sequence* **2:** 415 – 418.

Kikuchi, G., Kumar, A., Talmage, P. et al. (1958a). The enzymatic synthesis of 5-ALA. *J. Biol. Chem.* **233:** 1214 – 1219.

Kikuchi, G., Shemin, D. and Bachmann, B.J. (1958b). The enzymatic synthesis of 5-aminolevulinic acid. *Biochim. Biophys. Acta.* **28:** 219 – 220.

Kirsch, R.E., Meissner P.N. and Hift, R.J. (1998). Variegate porphyria. *Semin. Liv. Dis.* **18:** 33 – 41.

Klausner, R.D., Rounault, T.A., Harford et al. (1993). Regulating the fate of mRNA: The control of cellular iron metabolism. *Cell* **72:** 19 – 28.

Klemm, D.J. and Barton, L.L. (1985). Oxidation of protoporphyrinogen in the obligate anaerobe *Desulfovibrio gigas*. *J. Bacteriol.* **164:** 316 – 320.

Klemm, D.J. and Barton, L.L. (1987). Purification and properties of protoporphyrinogen oxidase from an anaerobic bacterium, *Disulfovibrio gigas*. *FEMS Microbiol. Lett.* **61:** 61 – 64.

Kodama, T.; Takagi, M.; Kobayashi, T., et al. (1979). A case of variegate porphyria and her hepatic delta-aminolevulinic synthetic activity. *Nippon Naika Gakkai Zasshi* **68:** 1293 – 1300.

Kohashi, M., Clement, R.P., Tse, J. et al. (1984). Rat hepatic uroporphyrinogen III cosynthase. Purification and evidence for a bound folate coenzyme participating in the biosynthesis of uroporphyrinogen III. *Biochem. J.* **220:** 755 – 765.

Kohno, H., Furukawa, T., Yoshinaga, T., et al. (1993). Coproporphyrinogen oxidase. Purification, molecular cloning, and induction of mRNA during erythroid differentiation. *J. Biol. Chem.* **268:** 21359 – 21363.

Kohno, H., Okuda, M., Furukawa, T., et al. (1994). Site-directed mutagenesis of human ferrochelatase: Identification of histidine-263 as a binding site for metal ions. *Biochim. Biophys. Acta.* **1209:** 95 – 100.

Kohno, H., Furukawa, T., Tokunaga, R., et al. (1996). Mouse coproporphyrinogen oxidase is a copper-containing enzyme: expression in *Escherichia coli* and site-directed mutagenesis. *Biochim. Biophys. Acta* **1292:** 156 – 162.

Kojima, S., Matsumoto, H. and Ishizuka, K. (1991). Protoporphyrin accumulation in *Lemna paucicostata* Hegelm caused by diphenyl ether herbicides and their herbicidal activity. *Weed Res.* **36:** 318 – 323.

Komives, T. and Gullner, G. (1994). Mechanisms of plant tolerance to photodynamic herbicides. *Am. Chem. Soc. Symp. Ser.* **559:** 177 – 190.

Kordac, V., Deybach, J.C., Martasèk, P., et al. (1984). Homozygous variegate porphyria. *Lancet* **1:** 851.

Kostrzewska, E. and Gregor, A. (1982). Acute hepatic porphyria in Poland. *Lancet* **1:** 1354 – 1355.

Kostrzewska, E. and Gregor, A. (1995). Thirty years with porphyria. International symposium on porphyria and heme related disorders, Helsinki, Finland, June 28-July 2, Abstracts, p. 16.

Koszo, F., Morvay, M., Dobozy, A. et al. (1992). Erythrocyte uroporphyrinogen decarboxylase activity in 80 unrelated patients with porphyria cutanea tarda. *Br. J. Dermatol.* **126:** 446 – 449.

Kotze, M.J., De Villiers, J.N., Groenewald, J.Z., et al. (1998). Molecular analysis reveals a high mutation frequency in the first untranslated exon of the PPOX gene and largely excludes variegate porphyria in a subset of clinically affected Afrikaner families. *Mol. Cell Probes* **12:** 293 – 300.

Koziol, J. (1971). Fluorometric analysis of riboflavin and its coenzymes. *Methods Enzymol.* **18B:** 253 – 285.

Krakowski, A., Brenner, S., Tur, E., et al. (1979). Variegate porphyria. *Hertuah* **96:** 528 – 532.

Kramer, S. (1980). Porphyria Variegata. *Clin. Haematol.* **9:** 303 – 322.

Krijt, J., Stranska, P., Maruna, P., et al. (1997). Herbicide-induced experimental variegate porphyria in mice: tissue porphyrinogen accumulation and response to porphyrinogenic drugs. *Can. J. Physiol. Pharmacol.* **75:** 1181 – 1187.

Kushner, J.P., Steinmuller, D.P. and Lee, G.R. (1975). The role of iron in the pathogenesis of porphyria cutanea tarda. II. Inhibition of uroporphyrinogen decarboxylase. *J. Clin. Invest.* **56:** 661 – 667.

Kushner, J.P., Edwards, C.Q., Dadone, M.M. et al. (1985). Heterozygosity for HLA-linked hemochromatosis as a likely cause of hepatic siderosis associated with sporadic porphyria cutanea tarda. *Gastroenterology* **88:** 1232 – 1238.

Küster, W. (1912). Beiträge zur Kenntnis des Bilirubins and Hämins. *Hoppe-Syler's Z. physiol. Chem.* **82:** 463 – 483.

Labbe, P., Volland, C. and Chaix, P. (1968). Study of the ferrochelatase activity of yeast mitochondria. *Biochim. Biophys. Acta.* **159:** 527 – 539.

Labbe-Bois, R. (1990). The ferrochelatase from *Saccharomyces cerevisiae*. Sequence disruption, and expression of its structural gene HEM15. *J. Biol. Chem.* **265:** 7278 – 7283.

Laemmli, U.K. (1970). Cleavage of structural proteins during the assembly of head of bacteriophage T4. *Nature (London)* **277:** 680 – 685.

Laidlaw, P.P. (1904). Some observation on blood pigments. *J. Physiol.* **31:** 464 – 472.

Lam, H.M., Dragan, L., Tsou, H.C., et al. (1996). Molecular basis of variegate porphyria: a de novo insertion mutation in the protoporphyrinogen oxidase gene. *Hum. Genet.* **99:** 126 – 129.

Lam, C-W., Hui, K-N., Poon, P.M-K., et al. (2001). Novel splicing mutation of the *PPOX* gene (IVS10 + 1G→A) detected by denaturing high-performance liquid chromatography. *Clini. Chim. Acta.* **305:** 197 – 200.

Lamon, J.M., Frykholm, B.G., and Tschudy, D.P. (1979). Family evaluation in acute intermittent porphyria using red cell uroporphyrinogen I synthase. *J. Med. Genet.* **16:** 134 – 139.

Lamoril, J., Boulechfar, S., De Verneuil, H. et al. (1991). Human erythropoietic protoporphyria: Two point mutations in the ferrochelatase gene. *Biochem. Biophys. Res. Commun.* **181:** 594 – 599.

Lamoril, J. Martàsek, P. Deybach, J.C., et al. (1995). A molecular defect in coproporphyrinogen oxidase gene causing harderoporphyria, a variant form of hereditary coproporphyria. *Hum. Mol. Genet.* **4:** 275 – 278.

Lander, M., Pitt, A.R., Alefounder, P.R., et al. (1991). Studies on the mechanism of hydroxymethylbilane synthase concerning the role of arginine residues in substrate binding. *Biochem. J.* **275:** 447 – 452.

Lannfelt, L., Wetterberg, L., Lilius, L., et al., (1989). Porphobilinogen deaminase in human erythrocytes: purification of two forms with apparent molecular weights of 40 kDa and 42 kDa. *Scand. J. Clin. Lab. Invest.* **49:** 677 – 684.

Laterriere, M., d'Estaintot, B.L., Dautant, A., et al. (1997). Expression, purification, crystallization and preliminary X-ray diffraction analysis of human uroporphyrinogen decarboxylase. *Acta Crystallogr. D. Biol. Crystallogr.* **54:** 476 – 478.

Lathrop, J.T. and Timko, M.P. (1993). Regulation by heme of mitochondrial protein transport through a conserved amino acid motif. *Science* **259:** 522 – 525.

Lavalle, D.K. (1988). Porphyrin metalation reactions in biochemistry. In: Mechanistic Principles of Enzyme Activity. (J.F. Liebman, A. Greenberg, eds), VCH Publishers, New York, pp. 279 – 311.

Lecanu, L.R. (1837). Études chimiques sur le sang humain, cited by Berzelius, 1840.

Lee, J.S. and Anvret, M. (1991). Identification of the most common mutation within the porphobilinogen deaminase gene in Swedish patients with acute intermittent porphyria. *Proc. Natl. Acad. Sci. USA* **88:** 10912 – 10915.

Lee, H.J. and Duke, S.O. (1994). Protoporphyrinogen IX-oxidizing activities involved in the mode of action of peroxidizing herbicides.

Lee, H.J., Duke, M.V. and Duke, S.O. (1993). Cellular localization of protoporphyrinogen oxidizing activities of etiolated barley (*Hordeum vulgare L.*) leaves. *Plant Physiol.* **102:** 881 – 889.

Lee, H.J., Duke, M.V., Birk, J.H., et al. (1995). Biochemical and physiological effects of heterocycles and related compounds. *J. Agric. Food Chem.* **43:** 2722 – 2727.

Lee, H.J., Lee, S.B., Chung, J.S., et al. (2000). Transgenic rice plants expressing a *Bacillus subtilis* protoporphyrinogen oxidase gene are resistant to diphenyl ether herbicide oxyfluorfen. *Plant Physiol.* **41:** 743 – 749.

Leeper, F.J. (1994). The evidence of a spirocyclic intermediate in the formation of uroporphyrinogen III by cosynthase. *Ciba Found. Symp.* **180:** 111 – 123.

Lemberg, R. and Legge, J.W. (1949). Haematin Compounds and Bile Pigments, Interscience, New York.

Lermontova, I., Kruse, E., Mock, H-P. et al. (1997). Cloning and characterisation of a plastidal and a mitochondrial isoforms of tobacco protoporphyrinogen IX oxidase. *Proc. Natl. Acad. Sci. USA* **94:** 8895 – 8900.

Lermontova, I., and Grimm, B. (2000). Overexpression of plastidic protoporphyrinogen IX oxidase leads to resistance to diphenyl-ether herbicide acifluorfen. *Plant Physiol.* **122:** 75-83.

Levene, G.M. (1968). Porphyria cutanea tarda hereditaria. *Proc. R. Soc. Med.* **61:** 591 – 592.

Liedgens, W., Lutz, C. and Schneider, H.A.W. (1983). Molecular properties of 5-aminolevulinic acid dehydratase from *Spinacia oleracea*. *Eur. J. Biochem.* **135:** 75 – 79.

Li-Fen, L. and Beattie, D.S. (1982). Comparisons and modifications of the colorimetric assay for delta-aminolevulinic acid synthase. *Enzyme* **28:** 120 – 132.

Lill, R., Nargang, L.E. and Neupert, W. (1996). Biogenesis of mitochondrial proteins. *Curr. Opinion Cell Biol.* **8:** 505 – 512.

Lindblad, B., Lindstedt, S. and Steen, G. (1977). On the genetic defects in hereditary tyrosinemia. *Proc. Natl. Acad. Sci. USA* **74:** 4641 – 4645.

Llambias, E.B.G. and Batlle, A.M. del C. (1970). Porphyrin biosynthesis in soybean callus. IX. The porphobilinogen deaminase-uroporphyrinogen III cosynthetase kinetic studies. *Biochim. Biophys. Acta* **220:** 552 – 559.

Long, C., Smyth, S.J., Woolf, J., et al. (1993). Detection of latent porphyria by fluorescence emission spectroscopy of plasma. *Br. J. Dermatol.* **129:** 9 – 13.

Louie, G.V., Brownlie, P.D., Lambert, R., et al. (1996). The three-dimensional structure of Escherichia coli porphyrinogen deaminase at 1.76-Å resolution. *Prot.* **25:** 48 –78.

Lu, Z., Nagata, S., McPhie, P. and Miles, E.W. (1993). Lysine 87 in the beta subunit of tryptophan synthase that forms an internal aldimine with pyridoxal phosphate serves critical roles in transimination, and product release. *J. Biol. Chem.* **268:** 8727 – 8734.

Lundvall, O., Weinfeld. A. and Lundin, P. (1970). Iron storage in porphyria cutanea tarda. *Acta. Med. Scand.* **1-2:** 37 – 53.

Lydon, J. and Duke, S.O. (1988). Porphyrin synthesis is required for photobleaching activity of the p-Nitrosubstituted diphenyl ether herbicides. *Pestic. Biochem. Physiol.* **31:** 74 – 83.

MacGregor, A.G., Nicholls, R.E.H. and Rimington, C. (1952). Porphyria cutanea tarda. Investigation of a case including isolation of some hitherto-undescribed porphyrins. *Arch. Int. Med.* **19:** 483 – 504.

Madsen, O, Sandal, L., Sandal, N. N. et al. (1993). A soybean coproporphyrinogen oxidase gene is highly expressed in root nodules. *Plant Mol. Biol.* **23:** 35 – 43.

Maeda, N., Horie, Y., Sasaki, Y., et al. (2000). Three novel mutations in the protoporphyrinogen oxidase gene in Japanese patients with variegate porphyria. *Clin. Biochem.* **33:** 495 – 500.

Magness, S.T., Tugores, A., Diala, E.S. et al. (1998). Analysis of the human ferrochelatase promoter in transgenic mice. *Blood* **92:** 320 – 328.

Magnus, I.A., Jarrett, A., Prankerd, T.A.J. et al. (1961). Erythropoietic protoporphyria: a new porphyria

syndrome with solar urticaria due to protoporphyrinaemia. *Lancet* **2:** 448 – 451.

Mailer, K., Poulson, R., Dolphin, D. et al. (1980). Ferrochelatase: isolation and purification via affinity chromatography. *Biochem. Biophys. Res. Commun.* **96:** 777 – 784.

Marceau, M., Lewis, S.D. and Shafer, J.A. (1988). The glycine-rich region of Escherichia coli D-serine dehydratase. Altered interactions with pyridoxal 5'-phosphate produced by substitution of aspartic acid for glycine. *J. Biol. Chem.* **263:**16934 – 16941.

Marks, G.S. (1969). *Heme and Chlorophyll: Chemical, Biochemical, and Medical aspects*, Van Nos Rheinhold, Princeton, NJ.

Marky, L.A., and Breslauer, K.J. (1987). Calculating thermodynamic data for transitions of any molecularity from equilibrium melting curves. *Biopolymers* **26:** 1601 – 1620.

Martásek, P. (1998). Hereditary coproporphyria. *Semin. Liv. Dis.* **18:** 25 – 41.

Martàsek, P, Kordac, V. and Jirsa, M. (1983). Variegate porphyria and porphyria cutanea tarda. *Arch. Dermatol.* **119:** 537 – 538.

Martàsek, P., Camadro, J-M., Delfrau-Larue, M.H., et al. (1994a). Molecular cloning, sequencing and functional expression of a cDNA encoding human coproporphyrinogen oxidase. *Proc. Natl. Acad. Sci. USA* **91:** 3024 – 3028.

Martàsek, P., Nordmann, Y. and Grandchamp, B. (1994b). Homozygous hereditary coproporphyria caused by an arginine to tryptophan substitution in coproporphyrinogen oxidase and common intragenic polymorphisms. *Hum. Mol. Genet.* **3:** 477 – 480.

Martàsek, P., Camadro, J-M., Raman, C.S., et al. (1997). Human coproporphyrinogen oxidase. Biochemical characterization of recombinant normal and R231W mutated enzymes expressed in *E. coli* as soluble, catalytically active homodimers. *Cell Mol. Biol.* **43:** 47 – 58.

Massey, V. and Ganther, H. (1965). On the interpretation of the absorption spectra of flavoproteins with special reference to D-amino acid oxidase. *Biochem.* **4:** 1161 – 1173.

Mathews, C.K. and Van Holde, K.E. (2000). In: Biochemistry 3rd ed. Addison Wesley Longman Inc. New York, pp 161 – 211.

Matringe, M., and Scalla, R. (1988a). Effects of acifluorfen-methyl on cucumber cotyledons: porphyrin accumulation. *Pectic Biochem. Physiol.* **32:** 164 – 172.

Matringe, M., and Scalla, R. (1988b). Studies on the mode of action of acifluorfen-methyl in the non-chlorophyllous soyabean cells: accumulation of soyabean cells. *Plant. Physiol.* **86:** 619 – 622.

Matringe, M., Camadro, J.M., Labbe, P., et al. (1989a). Protoporphyrinogen oxidase as a molecular target for diphenyl ether like herbicides. *Biochem. J.* **260:** 231 – 235.

Matringe, M., Camadro, J-M., Labbe, P. et al. (1989b). Protoporphyrinogen oxidase inhibition by three peroxidizing herbicides: oxadiazon, LS 82-556 and M & B 39279. *FEBS Lett.* **245:** 35 – 38.

Matringe, M., Camadro, J-M., Block, M.A., et al. (1992a). Localization within chloroplasts of protoporphyrinogen oxidase, the target enzyme for diphenylether-like herbicides. *J. Biol. Chem.* **267:** 4646 – 4651.

Matringe, M., Mornet, R. and Scalla, R. (1992b). Characterization of [^{3}H]acifluorfen binding to purified pea etioplasts, and evidence that protoporphyrinogen oxidase specifically binds acifluorfen. *Eur. J. Biochem.* **209:** 861 – 868.

Matsumoto, H. and Duke, S.O. (1990). Acifluorfen-methyl effects on porphyrin synthesis in *Lemna pausicostata* Hegelm. 6746 *J. Agric. Food Chem.* **38:** 2066 – 2071.

Matsumoto, H., Lee, J. J. and Ishizuka, K. (1994). Variation in crop response to protoporphyrinogen oxidase inhibitors. *Am. Chem. Soc. Symp. Ser.* **559:** 120 – 132.

Matters, G.L. and Beale, S.I. (1995). Structure and expression of the *Chlamydomonas reinhardtii* ALAD gene encoding the chlorophyll biosynthetic enzyme, delta-aminolevulinic acid dehydratase (porphobilinogen synthase). *Plant Mol. Biol.* **27:** 607 – 617.

May, B.K. and Bawden, M.J. (1989). Control of heme biosynthesis in animals. *Semin Hematol.* **26:** 150 – 156.

May, B.K., Dogra, S.C., Sadlon, T.J., et al. (1995). Molecular regulation of heme biosynthesis in higher vertebrates. *Prog. Nucl. Acid Res. Mol. Biol.* **51:** 1 – 51.

McCall-Anderson, T. (1898). Hydroa aestivale in two brothers, complicated with the presence of haematoporphyrin in the urine. *Br. J. Dermatol.* **10:** 1 – 4

McColl, K.E., Thompson, G.G., Omar, E., et al. (1987). Porphyrin metabolism and haem biosynthesis in Gilbert`s syndrome. *Gut.* **28:** 125 – 130.

McColl, K.E., Thompson, G.G., Moore, M.R., et al. (1985). Chester porphyria: biochemical studies of a new form of acute porphyria. *Lancet.* **2:** 796 – 799.

McDonagh, A.F. and Bissell, D.M. (1998). Porphyria and Porphyrinology – the past fifteen years. *Semin. Liv. Dis.* **1:** 3 – 15.

McEneany, D., Hawkins, S., Trimble, E., et al. (1993). Porphyric neurophathy – a rare and often neglected differential diagnosis of a new form acute porphyria. *Lancet* **2:** 796 – 799.

McGovern, M.M., Anderson, K.E., Astrin, K.H. et al. (1996). Inherited porphyrias. In: Emery and Rimoin's principles and practice of medical genetics. (D.L. Rimoin, J.M. Connor and R.E. Pyeritz, eds), Vol. 2. 3rd ed, Churchill-Livingstone, New York, pp. 2009 – 2037.

McKay, R., Druyan, R., Getz, G.S et al. (1969). Intramitochondrial localization of δ-aminolevulinate synthetase and ferrochelatase in rat liver. *Biochem. J.* **114:** 455 – 461.

McLellan, T., Pryor, M.A., Kushner, J.P., et al. (1985). Assignment of uroporphyrinogen decarboxylase (UROD) to the pter----p21region of human chromosome1. *Cytogenet. Cell Genet.* **39:** 224 – 227.

McManus, J., Blake, D. and Ratnaike, S. (1988). An assay of uroporphyrinogen decarboxylase in erythrocytes. *Clin. Chem.* **34:** 2355 – 2357.

McManus, J.F., Begley, C.G., Sassa, S. et al. (1996). Five new mutations in the uroporphyrinogen decarboxylase gene identified in families with cutaneous porphyria. *Blood* **88:** 3586 – 3600.

McNeill, L.A. and Shoolingin-Jordan, P.M. (1998). Dipyrromethane cofactor assembly in porphobilinogen deaminase. *Biochem. Soc. Trans.* **26:** S286.

Medlock, A.E. and Dailey, H.A.. (1996). Human coproporphyrinogen oxidase is not a metalloprotein. *J. Biol. Chem.* **271**: 32507 – 32510.

Medlock, A.E., Meissner, P.N., Davidson, B.P., et al. (2002). A mouse model for South African (R59W) variegate porphyria: construction and initial characterisation. *Cell. Mol. Biol.* **48:** 71 – 78.

Meissner, P. and Hift, R. (1991). Porphyria. In: Liver Update – a practical guide to the diagnosis and management of liver disease. (R. Kirsch, S. Robson, and P. Meissner, eds), University of Cape Town Printing Department, pp. 199 – 228.

Meissner, P.N. (1990). Enzyme Studies in Variegate Porphyria. PhD Thesis, University of Cape Town.

Meissner, P.N., Adams, P. and Kirsch, R.E. (1993). Allosteric inhibition of human lymphoblast and purified porphobilinogen deaminase by protoporphyrinogen and coproporphyrinogen. A possible mechanism for the acute attack of variegate porphyria. *J. Clin. Invest.* **91:** 1436 – 1444.

Meissner, P.N., Hift, R.J. and Corrigall, A.V. (2002). Variegate porphyria. In Porphyrin Handbook, Vol 18, (K. Smith, K. Kadish and R. Guillard, eds.) *in press.*

Meissner, P.N., Day, R.S., Moore, M.R., et al. (1986). Protoporphyrinogen oxidase and porphobilinogen deaminase in variegate porphyria. *Eur. J. Clin. Invest.* **16:** 257 – 261.

Meissner, P.N., Meissner, D.M., Sturrock, E.D., et al. (1987). Porphyria - The UCT experience. *S. Afr. Med. J.* **72:** 755 – 761.

Meissner, P.N., Dailey, T.A., Hift, R.J., et al. (1996). A R59W in human protoporphyrinogen oxidase results in decreased enzyme activity and is prevalent in South Africans with variegate porphyria. *Nat. Genet.* **13:** 95 – 97.

Melefors, O., Goossen, B., Johansson, R.S., et al. (1993). Translational control of 5-aminolevulinate synthase mRNA by iron-responsive elements in erythroid cells. *J. Biol. Chem.* **268:** 5974 – 5978.

Meredith, P.A. and Moore, M.R. (1978). The effects of zinc and lead on 5-aminolaevulinate dehydratase. *Biochem. Soc. Trans.* **6:** 760 – 762.

Meyer, U.A. (1973). Intermittent acute porphyria: Clinical and biochemical studies of disordered heme biosynthesis. *Enzyme* **16:** 334 – 342.

Meyer, U.A., Macé, M., Schuurmans, M.M. et al. (1998). Acute porphyrias: pathogenesis of neurological manifestations. *Semin. Liver Dis.* **18:** 43 – 52.

Meyer-Betz, F. (1913). Untersuchungen über die biologische (photodynamische) wirkung des hamatoporphyrins und anderen derivate des blut und gallenfarbstoffs. *Dtsch. Arch. Klin. Med.* **112:** 476 – 503.

Mgone, C.S., Lanyon, W.G., Moore, M.R. et al. (1992). Detection of seven point mutations in the porphobilinogen deaminase gene in patients with acute intermittent porphyria, by direct sequencing of in vitro amplified cDNA. *Hum. Genet.* **90:** 12 – 16.

Miller, R.E. and Stadtman, E.R. (1972). Glutamate synthase from *Escherichia coli*. An iron-sulfide flavoprotein. *J. Biol. Chem.* 247: 7407 – 7419.

Miller, A.D., Hart, G.J., Packman, L.C., et al. (1988). Evidence that the pyrromethane cofactor of hydroxymethylbilane synthase (porphobilinogen deaminase) is bound to the protein through the sulphur atom of cysteine-242. *Biochem J* **254:** 915 – 918.

Miyagi, K. (1970). Deficiency of hepatic porphobilinogen deaminase in acute intermittent porphyria. *J. Kyushu Haematol. Soc.* **20:** 190 – 203.

Miyamoto, K., Nakahigashi, Y., Nishimura, K. et al. (1991). Isolation and characterization of visible light-sensitive mutants of *Escherichia coli* K12. *J. Mol. Biol.* **219:** 393 – 398.

Miyamoto, K., Tanaka, R., Teramoto, H., et al. (1994). Nucleotide sequence of cDNA clones encoding ferrochelatase from barley and cucumber. *Plant Physiol.* **105:** 769 – 770.

Mock, H.P., Trainotti, L., Kruse, E. et al. (1995). Isolation, sequencing and expression of cDNA sequences encoding uroporphyrinogen decarboxylase from tobacco and barley. *Plant Mol. Biol.* **28:** 245 – 256.

Moore, M.R. and Goldberg, A. (1985). Health implications of the hematopoietic effects of lead. In: Dietary and Environmental Lead-Human Health Effects. (K.R. Mahaffey, ed), Elsevier, Amsterdam, pp. 261 – 299.

Moore, M.R., McColl, K.E. and Goldberg, A. (1984). The effects of alcohol on porphyrin biosynthesis and metabolism. *Clin. Biochem.* **1:** 161 – 187.

Moore, M.R., McColl, K.E.L., Rimington, C., et al. (1987). Porphyrins and Products of Haem Biosynthetic Pathway. In: Disorders of Porphyrin Metabolism. Plenum Publishing Corporation, New York, pp. 21 – 72.

Moran-Jimenez, J.M., Ged, C., Romana, M., (1996). Uroporphyrinogen decarboxylase: Complete gene sequence and molecular study of three families with hepatoerythropoietic porphyria. *Am. J. Hum. Genet.* **58:** 712 – 721.

Morgan, R.R., Da Silva, V., Puy, H., et al. (2002). Functional studies of mutations in the human protoporphyrinogen oxidase gene in variegate porphyria. *Cell. Mol. Biol.* **48:** 79 – 82.

Muhlbauer, J.E., Pathak, M.A., Tishler, P.V. et al. (1982). Variegate porphyria in New England. *JAMA* **247:** 3095 – 3102.

Muir, H.M. and Neuberger, A. (1950). The biogenesis of porphyrins. 2. The origin of the methyne carbon atoms. *Biochem. J.* **47:** 97 – 104.

Mukerji, S.K. and Pimstone, N.R. (1992). Uroporphyrinogen decarboxylase from human erythrocytes: purification, complete separation and partial characterization of two isoenzymes. *Int. J. Biochem.* **24:** 105 – 119.

Mulder, G.H. (1844). Uber eisenfreis Hamatin. *J. Prakt. Chem.* **32:** 186 – 197.

Murphy, G.M., Hawk, J.L.M., Magnus, I.A., et al. (1986). Homozygous variegate porphyria: two similar cases in unrelated families. *J. Royal Soc. Med.* **79:** 361 – 363.

Mustajoki, P. (1978). Variegate porphyria. *Ann. Intern. Med.* **89:** 238 – 244.

Mustajoki, P. (1980). Variegate porphyria. 12 years experience in Finland. *Q. J. Med.* **49:** 191 – 203.

Mustajoki, P. and Seppäläinen, A.M. (1975). Neuropathy in latent hereditary hepatic porphyria. *Br. Med. J.* **2:** 310 – 312.

Mustajoki, P. and Desnick, R.J. (1985). Genetic heterogeneity in acute intermittent porphyria: characterisation and frequency of porphobilinogen deaminase mutations in Finland. *Br. Med. J. (Clin Res Ed).* **291:** 505 – 509.

Mustajoki, P., Tenhunen, R., Niemi, K.M., et al. (1987). Homozygous variegate porphyria. A severe skin disease of infancy. *Clin. Genet.* **32:** 300 – 305.

Mustajoki, P., Himberg, J.J., Tokola, O., et al.. (1992). Rapid normalization of antipyrine oxidation by heme in variegate porphyria. *Clin. Pharmacol. Therap.* **51:** 320 – 324.

Nakahigashi, Y., Taketani, S., Okuda, M., et al. (1990). Molecular cloning and sequence of cDNA encoding human ferrochelatase. *Biochem. Biophys. Res. Commun.* **173:** 748 – 755.

Nakahashi, Y., Fujita, H., Taketani, S., et al. (1992). The molecular defect of ferrochelatase in a patient with erythropoietic protoporphyria. *Proc. Natl. Acad. Sci. USA* **89:** 281 – 285.

Namba, H., Narahara, K., Tsuji, X., et al. (1991). Assignment of human PBGD to 11q24.1 →11q24.2 by in situ hybridisatin and gene dosage studies. *Cytogenet. Cell. Genet.* **57:** 105 – 108.

Nandi, D.L., Baker-Cohen, K.F. and Shemin, D. (1968). Delta-aminolevulinic acid dehydratase of *Rhodopseudomonas spheroides*: 3. Mechanism of porphobilinogen synthesis. *J. Biol. Chem.* **243:** 1224 – 1230.

Nandihalli, U.B. and Duke, S.O. (1993). The porphyrin pathway as a herbicide targeting site . *Am. Chem. Soc. Symp. Ser.* **524:** 62 – 78.

Nandihalli, U.B., Duke, M. V. and Duke, S.O. (1992a). Quantitative structure-activity relationships of protoporphyrinogen oxidase-inhibiting diphenyl ether herbicides. *Pestic. Biochem. Physiol.* **43:** 193 – 211.

Nandihalli, U.B., Sherman, T.D., Duke, M.V., et al. (1992b). Correlation of protoporphyrinogen oxidase inhibition by O-phenyl pyrrolidino- and piperidino-carbamates with their herbicidal effects. *Pestic. Sci.* **35:** 227 – 235.

Narita, S., Tanaka, R., Ito, T., et al. (1996). Molecular cloning and characterization of a cDNA that encodes protoporphyrinogen oxidase of *Arabidopsis thaliana*. *Gene* **182:** 169 – 175.

Neier, R. (1996). *Adv. Nitrogen Heterocycles* **2:** 35 – 146.

Nencki, M. and Sieber, N. (1888). Über das Hamatoporphyrin. *Arch. Exp. Pathol. Pharmacol.* **24:** 430 – 446.

Neuberger, A. and Scott, J.J. (1953). Aminolaevulinic acid and porphyrin synthesis. *Nature* **172:** 1093 – 1094.

Nishimura, K., Nakayashiki, T. and Inokuchi, H. (1995a). Cloning and identification of the *hemG* gene encoding protoporphyrinogen oxidase (PPO) of *Escherichia coli* K-12. *DNA Res.* **2:** 1 – 8.

Nishimura, K., Taketani, S. and Inokuchi, H. (1995b). Cloning of a human cDNA for protoporphyrinogen oxidase by complementation in vivo of a *hemG* mutant of *Escherichia coli*. *J. Biol. Chem.* **270:** 8076 – 8080.

Nishiya, Y., and Imanaka, T. (1996) Analysis of interaction between the Arthrobacter sarcosine oxidase and the coenzyme flavin adenine dinucleotide by site-directed mutagenesis. *Appl. environ. Microbiol.* **62:** 2405 – 2410.

Nordmann, Y. and Deybach, J-C. (1990). Human Hereditary Porphyria. In: Biosynthesis of heme and chlorophylls. (H.A. Dailey, ed), McGraw-Hill, New York, pp. 491 – 542.

Nordmann, Y., de Verneuil, H., Deybach, J-C., et al. (1990). Molecular genetics of the porphyrias. *Ann. Med.* **22:** 387 – 391.

Norris, P.G., Elder, G.H. and Hawk, J.L.M. (1990). Homozygous variegate porphyria: a case report. *Br. J. Dermatol.* **122:** 253 – 257.

O'Donnell, V.B., Smith, G.C.M. and Jones, O.T.G. (1994). Involvement of phenyl radicals in iodonium inhibition of flavoenzymes. *Mol. Pharmacol.* **46:** 778 – 785.

Ohashi, and Kikuchi, G. (1978). Purification and some properties of two forms of delta-aminolevulinate synthase from rat liver cytosol. *J. Biochem.* **85:** 239 – 247.

Onuchic, J.N., Nymeyer, H., Garcia A.E., et al. (2000). The energy landscape theory of protein folding: insights into folding mechanisms and scenarios. *Adv. Protein. Chem.* **53:** 87 – 152.

Oshio, H., Shibata, H., Mito, N., et al. (1993). Isolation and characterization of a *Chlamydomonas reinhardtii* mutant resistant to photobleaching herbicides. *Z. Naturforsch* **48c:** 339 – 344.

Pai, E.F., Krengel, U., Petsko, G., et al. (1990). Refined crystal structure of the triphosphate conformation of H-ras p21 at 1.35Å resolution implications for the mechanism of GTP hydrolysis. *EMBO J.* **9:** 2351 – 2359.

Palmer, R.A, Elder, G.H., Barrett, D.F. et al. (2001). Homozygous variegate porphyria: a compound heterozygote with novel mutations in the protoporphyrinogen oxidase gene. *Br. J. Dermatol.* **144:** 866 – 869.

Patton, G.M. and Beattie, D.S. (1973). Studies on hepatic δ-aminolevulinic acid synthetase. *J. Biol. Chem.* **248:** 4467 – 4474.

Pauling, L., Corey, R.B., and Branson, H.R. (1951). The structure of proteins: two hydrogen-bonded helical configurations of the polypeptide chain. *Proc. Natl. Acad. Sci. U.S.A.* **37:** 205 – 211.

Perutz, M.F. (1989). Myoglobin and haemoglobin: role of distal residues in reactions with haem ligands. *Trends. Biochem. Sci.* **14:** 42 – 44.

Phillips, J.D., Whitby, F.G., Kushner, J.P. et al. (1997). Characterization and crystallization of human uroporphyrinogen decarboxylase. *Protein. Sci.* **6:** 1343 – 1346.

Plewinska, M., Thunell, S., Holmberg, L., et al. (1991). δ-aminolevulinate dehydratase deficient porphyria: identification of the molecular lesions in a severely affected homozygote. *Am. J. Genet.* **49:** 167 – 174.

Poh-Fitzpatrick, M.B. (1980). A plasma porphyrin fluorescence marker for variegate porphyria *Arch. Dermatol.* **116:** 543 – 547.

Poh-Fitzpatrick, M.B. (1985). Porphyrin-sensitized cutaneous photosensitivity: pathogenesis and treatment. *Clin. Dermatol.* **3:** 41 – 82.

Ponka, P. (1997). Tissue-specific regulation of iron metabolism and heme synthesis: Distinct control mechanisms in erythroid cells. *Blood* **89:** 1 – 25.

Pornprom, T., Matsumoto, H., Usui, K. et al. (1994). Characterization of oxyfluorfen tolerance in selected soybean line. *Pestic. Biochem. Physiol.* **50:** 107 – 114.

Porra, R.J. (1976). A rapid spectrophotometric assay for ferrochelatase (EC4.99.1.1) in preparations containing high concentrations of haemoglobin. In: Porphyrins in human disease. (M. Doss, ed), S. Karger, Basel, pp. 123 – 130.

Porra, R.J. and Falk, J.E. (1964). The enzymic conversion of coproporphyrinogen III into protoporphyrin IX. *Biochem. J.* **90:** 69 – 75.

Poulson, R. (1976). The enzymic conversion of protoporphyrinogen IX to protopoprphyrin IX in mammalian mitochondria. *J. Biol. Chem.* **251:** 3730 – 3733.

Poulson, R. and Polglase, W.J. (1975). The enzymic conversion of protoporphyrinogen IX to protoporphyrin IX. Protoporphyrinogen oxidase activity in mitochondrial extracts of *Saccharomyces cerevisiae*. *J. Biol. Chem.* **250:** 1269 – 1274.

Prasad A.R.K., and Dailey, H.A. (1995). Generation of resistance to the diphenyl ether herbicide acifluorfen by MEL cells. *Biochem. Biophys. Res. Commun* **215:** 186 – 191.

Privalov, P.L. (1979). Stability of proteins: small globular proteins. *Adv Protein Chem.* **33:** 167 – 241.

Privalov, P.L. and Gill, S.J. (1988). Stability of protein structure and hydrophobic interactions. *Adv. Protein Chem.* **39:** 191 – 234.

Proulx, K.L. and Dailey, H.A. (1992). Characteristics of murine protoporphyrinogen. *Prot. Sci.* **1:** 801 – 809.

Puy, H., Robreau, A.M., Rosipal, R., et al. (1996). Protoporphyrinogen oxidase: Complete genomic sequence and polymorphisms in the human gene. *Biochem. Biophys. Res. Commun.* **226:** 226 – 230.

Puy, H., Deybach, J. C., Lamoril, J., et al. (1997). Molecular epidemiology and diagnosis of acute intermittent porphyria. *Am. J. Hum. Genet.* **60:** 1373 – 1383.

Ragan, C.I. and Bloxham, D.P. (1977). Specific labelling of a constituent polypeptide of bovine heart mitochondrial reduced nicotinamide-adenine dinucleotide-ubiquinone reductase by the inhibitor diphenyleneiodonium. *Biochem. J.* **163:** 605 – 615.

Raich, N., Romeo, P.H., Dubart, A., et al. (1986). Molecular cloning and complete primary sequence of human erythrocyte porphobilinogen deaminase. *Nucleic. Acid. Res.* **14:** 5955 – 5968.

Rank, J.M., Pascual-Leone, A., Payne, W., et al. (1991). Hematin therapy for the neurologic crisis of tyrosinemia. *Proc. Natl. Acad. Sci. USA* **91:** 283 – 297.

Ranking, J.E. and Pardington, G.L. (1890). Two cases of haematoporphyrin in the urine. *Lancet* **2:** 607 – 609.

Reddy, K.N., Dayan, F.E. and Duke, S.O. (1997). QSAR analysis of protoporphyrinogen oxidase inhibitors. *Pestic. Biochem. Biophys.* **43:** 193 – 211.

Reddy, K.N., Nandihalli, U.B., Lee, H.J., et al. (1995). Predicting activity of protoporphyrinogen oxidase inhibitors by computer-aided molecular modeling. *Am. Chem. Soc. Symposium Series* **589:** 221 – 224.

Rege, V.D., Kredich, N.M., Tai, C.H., et al. (1996). A change in the internal aldimine lysine (K42) in O-acetylserine sulfhydrylase to alanine indicates its importance in transimination and as a general base catalyst. *Biochem.* **35:** 13485 – 13493.

Retzlaff, K. and Boger, P. (1996). An endoplasmicreticulum plant enzyme has protoporphyrinogen oxidase activity. *Pestic. Biochem. Physiol.* **54:** 105 – 114.

Riddle, R.D., Yamamoto, M. and Engel, J.D. (1989). Expression of delta-aminolevulinate synthase in avian cells: separate genes encode erythroid-specific and nonspecific isozymes. *Proc. Natl. Acad. Sci. USA*, **86:** 792 – 796.

Rimington, C. (1985). A review of the enzymic errors in the various porphyrias. *Scand. J. Clin. Lab. Invest.* **45:** 291 – 301.

Rimington, C., Magnus, I.A., Ryan, E.A. et al. (1967). Porphyria and photosensitivity. *Q.J. Med.* **36:** 29 – 57.

Rio, B., Parrent-Massin, D. and Hoellinger, H. (1997). Effects of a diphenyl-ether herbicide, oxyfluorfen, on human BFU-E/CU-E development and haemoglobin synthesis. *Hum. Exper. Toxicol.* **16:** 115 – 122.

Roberts, A.G. and Elder, G.H. (1997). Purification and properties of uroporphyrinogen decarboxylase from human erythrocytes. *Methods Enzymol.* **281:** 349 – 355.

Roberts, A.G., Elder, G.H., De Salamanca, R.E., et al. (1995a). A mutation (G281E) of the human uroporphyrinogen decarboxylase gene causes both hepatoerythropoietic porphyria and familial porphyria cutanea tarda. *J. Invest. Dermatol.* **104:** 500 – 502.

Roberts, A.G., Whatley, S.D., Daniels, J., et al. (1995b). Partial characterisation and assignment of the gene for protoporphyrinogen oxidase and variegate porphyria to human chromosome 1q23. *Hum. Mol. Genet.* **4:** 2387 – 2390.

Roberts, D.L., Frerman, F.E., and Kim, J.P. (1996). Three dimensional structure of human electron transfer flavoprotein to 2.1-Å resolution. *Proc. Natl. Acad. Sci.* **93:** 14355 – 14360.

Roberts, A.G., Whatley, S.D., Morgan, R.R., et al. (1997). Increased frequency of the haemochromatosis Cys282Tyr mutation in sporadic porphyria cutanea tarda. *Lancet* **349:** 321 – 323.

Roberts, A.G., Puy, H., Dailey, T.A., et al. (1998). Molecular characterization of homozygous variegate porphyria. *Hum. Mol. Genet.* **7:** 1921 – 1925.

Rocci, E., Gibertini, P., Cassanelli, M., et al. (1986). Iron removal therapy in porphyria tutanea tarda: phlebotomy versus slow subcutaneous desferrioxamine infusion. *Br. J. dermatol.* **114:** 621 – 629.

Romana, M., Le Boulch, R. and Romeo P.H. (1987a). Rat uroporphyrinogen decarboxylase cDNA: nucleotide sequence and comparison to human uroporphyrinogen decarboxylase. *Nucl. Acid. Res.* **15:** 7211.

Romana, M., Dubart, A., Beaupain, D., et al. (1987b). Structure of the gene for human uroporphyrinogen decarboxylase. *Nucl. Acid Res.* **15:** 7343 – 7355.

Romeo, R.H., Raich, N., Dubart, A., et al. (1986). Molecular cloning and nucleotide sequence of a complete human uroporphyrinogen decarboxylase cDNA. *J. Biol. Chem.* **261:** 9825 – 9830.

Rosipal, R., Lamoril, J., Puy, H., et al. (1999). Systematic analysis of coproporphyrinogen oxidase gene defects in hereditary coproporphyria and mutation update. *Hum. Mutat.* **13:** 44 – 53.

Rossi, E., Attwood, P.V. and Garcia-Webb, P. (1992). Inhibition of human lymphocyte coproporphyrinogen oxidase activity by metals, bilirubin and haemin. *Biochem. Biophys. Acta.* **1135:** 262 – 268.

Roth, J.A. and McCormick, D.B. (1967). Complexing of ribloflavin and its 2-substituted analogs with adenosine and other 6-substituted purine derivatives. *Photochem. Photobiol.* **6:** 657.

Rumbly, J., Hoang, L., Mayne, L. et al. (2001). An amino acid code for protein folding. *Proc. Natl. Acad. Sci. USA* **98:** 105 – 112.

Runge, W. and Watson, C.J. (1962). Experimental production of skin lesions in human cutaneous porphyria. *Proc. Sci. Exp. Biol. Med.* **109:** 809 – 811.

Saillet, H. (1896). De 1' urospectrine (ou urohematoporphyrine urinale normale). *Rev. Med.* **10:** 1123 – 1125.

Sancovich, H.A., Batlle, A.M. del C. et al. (1969). Porphyrin synthesis. VI. Separation and purification of porphobilinogen deaminase and uroporphyrinogen isomerase from cow liver. Porphobilinogenase an allosteric enzyme. *Biochim. Biophys. Acta.* **191:** 130 – 143.

Sano, S. and Granick, S. (1961). Mitochondrial coproporphyrinogen oxidase and protoporphyrin formation. *J. Biol. Chem.* **236:** 1173 – 1180.

Saraste, M., Sibbald, P.R. and Wittinghofer, A.. (1990). The P-loop--a common motif in ATP- and GTP-binding proteins. *Trends Biochem. Sci..* **15:** 430 – 434.

Sarkany, R.P.E., Alexander, G.J.M.A. et al. (1994). Recessive inheritance of erythropoietic protoporphyria with liver failure. *Lancet* **343:** 1394 – 1396.

Sasarman, A., Letowski, J., Czaika, G., et al. (1993). Nucleotide sequence of the *hemG* gene in the protoporphyrinogen oxidase activity of *Escherichia coli* K12. Can. *J. Microbiol.* **39:** 1155 – 1161.

Sassa, S. (1982). Delta-aminolevulinic acid dehydratase assay. *Enzyme* **28:** 133 – 145.

Sassa, S. (1998). ALAD porphyria. *Semin. Liv. Dis.* **18:** 95 – 101.

Sassa, S., Zalar, G. L. and Kappas, A. (1978). Studies in porphyria VII. Induction of uroporphyrinogen I synthase and expression of the gene defect of acute intermittent porphyria in mitogen stimulated human lymphocytes. *J. Clin. Invest.* **61:** 499 – 508.

Sassa, S., Fujita, H., Doss, M., et al. (1991). Hereditary hepatic porphyria due to homozygous delta-aminolevulinic acid dehydratase deficiency: studies in lymphocytes and erythrocytes. *Eur. J. Clin. Invest.* **21:** 244 – 248.

Sassa, S., Kondo, M., Taketani, S., et al. (1997). Molecular defects of the coproporphyrinogen oxidase gene in hereditary coproporphyria. *Cell. Mol. Biol.* **43:** 59 – 66.

Sawada, H., Takeshita, M., Sugita, Y. et al. (1969). Effect of lipid on protoheme ferro-lyase *Biochim. Biophys. Acta.***482:** 461 – 469.

Scalla, R. and Matringe, M. (1994). Inhibitors of protoporphyrinogen oxidase as herbicides: diphenyl ethers and related photobleaching molecules. *Rev. Weed Sci.* **6:** 103 – 132.

Scalla, R., Matringe, M., Camadro, J.M. et al. (1990). Recent advance in the mode of action of diphenyl ether and related herbicides. *Z. Naturforsch* **45c:** 503 – 511.

Scherer, J. (1841). Untersuchungen Liebigs. *Ann. Chem. Pharm.* **40:** 1 – 64.

Schneider-Yin, X., Schäfer, B.W., Tönz, O., et al. (1995). Human ferrochelatase: A novel mutation in patients with erythropoietic protoporphyria and an isoform caused by alternative splicing. *Hum. Genet.* **95:** 391 – 396.

Schultz, J.H. (1874). Ein Fall von Pemphigus Leprosus, kompliziert durch lepra visceralis. Inagural dissetation, Griefswald.

Scott, A.W., Chang, L.F. and Beattie, D.S. (1983). The characterisation and sub-mitochondrial localisation of delta-aminolevulinic acid synthase and an associated amidase in rat liver mitochondria using an improved assay for both enzymes. *J. Biol. Chem.* **258:** 81 – 90.

Seehra, J.S., Jordan, P.M. and Akhtar, M. (1982). Anaerobic and aerobic coproporphyrinogen III oxidases of *Rhodopseudomonas spheroides*. Mechanism and stereochemistry of vinyl group formation. *Biochem J.* **269:** 709 – 718.

Seki, Y., Kawanishi, S. and Sano, S. (1986). Uroporphyrinogen decarboxylase purification from chicken erythrocytes. *Methods Enzymol.* **123:** 415 – 421.

Sellers, V.M., Johnson, M.K. and Dailey, H.A. (1996). Function of the [2Fe-2S] cluster in mammalian ferrochelatase: a possible role as a nitric oxide sensor. *Biochem.* **35:** 2699 – 2704.

Sellers, V.M., Wang, K.F., Johnson, M.K. et al. (1998). Evidence that the fourth ligand to the [2Fe-2S] cluster in animal ferrochelatase is a cysteine. Characterization of the enzyme from *Drosophila melanogaster*. *J. Biol. Chem.* **273:** 22311 – 22316.

Senior, N.M., Brockenhurst, K., Cooper, J.B., et al. (1996). Comparative studies on the 5-aminolaevulinic acid dehydratases from *Pisum sativum*, *Escherichia coli* and *Saccharomyces cerevisiae*. *Biochem. J.* **320:** 401 – 412.

Senior, N.M., Siligardi, G., Drake, A., et al. (1997). Structural studies on 5-aminolaevulinic acid dehydratase from Saccharomyces cerevisiae. *Biochem. Soc. Trans.* **25:** 78S.

Seubert, S., Seubert, A., Rumpf, K.W. et al. (1985). A porphyria cutanea tarda-like distribution pattern of porphyrins in plasma, hemodialysate, hemofiltrate, and urine of patients on chronic hemodialysis. *J. Invest. Dermatol.* **85:** 107 – 109.

Shemin, D. (1976). 5-Aminolaevulinic acid dehydratase: structure, function, and mechanism. *Phil. Trans. R. Soc. Lond. Biol. Sci.* **273:** 109 – 115.

Shemin, D. and Rittenberg, D. (1946). The biological utilisation of glycine for the synthesis of the protoporphyrin of hemoglobin. *J. Biol. Chem.* **166:** 621 – 625.

Shemin, D. and Wittenberg, J. (1951). The mechanism of porphyrin formation-The role of tricarboxylic acid cycle. *J. Biol. Chem.* **192:** 315.

Shemin, D. and Russell, C.S. (1953). Succinate glycine cycle. *J. Am. Chem. Soc.* **75:** 4873 – 4875.

Shemin, D., Russell, C.S. and Abramsky, T. (1955). The succinate glycine cycle. I. The mechanism of pyrrole synthesis. *J. Biol. Chem.* **215:** 613 – 620.

Sherman, T.D., Becerril, J.M., Matsumoto, H., et al. (1991). Physiological basis for differential sensitivities of plant species protoporphyrinogen oxidase-inhibiting herbicides. *Plant physiol.* **97:** 280 – 287.

Shibuya, H., Nonneman, D., Tamassia, M., et al. (1995). The coding sequence of the bovine ferrochelatase gene. *Biochem. Biophys. Acta.* **1231:** 117 – 120.

Shoolingin-Jordan, P.M. (1995). Porphobilinogen deaminase and uroporphyrinogen III synthase: structure, molecular biology, and mechanism. *J. Bioenerg. Biomembr.* **27:** 181 – 195.

Shoolingin-Jordan, P.M. (1998). Structure and mechanism of enzymes involved in the assembly of the tetrapyrrole macrocycle. *Biochem. Soc. Trans.* **26:** 326 – 336.

Shoolingin-Jordan, P.M., Warren, M.J. and Awan, S.J. (1996). Discovery that the assembly of the dipyrromethane cofactor of porphobilinogen deaminase holoenzyme proceeds initially by the reaction of preuroporphyrinogen with the apoenzyme. *Biochem. J.* **316:** 373 – 376.

Shoolingin-Jordan, P.M., Warren, M.J. and Awan, S.J. (1997). Dipyrromethane cofactor assembly of porphobilinogen deaminase: formation of apoenzyme and preparation of holoenzyme. *Methods Enzymol.* **281:** 317 – 327.

Siepker, L.J., Ford, M., de Kock, R., and Kramer, S. (1987). Purification of bovine protoporphyrinogen oxidase: immunological cross-reactivity and structural relationship to ferrochelatase. *Biochim. Biophys. Acta.* **913:** 349 – 358.

Smith, K. M. eds (1975). *Porphyrins and metalloporphyrins*, Elsevier, Amsterdam, 1 – 754.

Smith, A.G. and Francis, J.E. (1981). Investigation of rat liver urporphyrinogen decarboxylase - Comparisons of porphyrinogens I and III as substrates and the inhibition by porphyrins. *Biochem J.* **195:** 241 – 250.

Smith, A.G. and Francis, J.E. (1983). Synergism of iron and hexachlorobenzene inhibits hepatic uroporphyrinogen decarboxylase in inbred mice. *Biochem. J.* **13:** 135 – 142.

Smith, A.G., Santana, M.A., Wallace-Cook, et al. (1994). Isolation of cDNA encoding chloroplast ferrochelatase from Arabidopsis thaliana by functional complementation of yeast mutant. *J. Biol. Chem.* **265:** 19377 – 19380.

Smythe, E. and Williams, D.C. (1988). Rat liver uroporphyrinogen III synthase has similar properties to the enzyme from *Euglena gracilis* including absence of a requirement for reversibly bound cofactor. *Biochem. J.* **253:** 275 – 279.

Soret, J.L. (1883). Réchèrches sur l' absoprtion des rayons ultraviolets par diverses substances. *Arch. Sci. Phys. Nat.* **10:** 430 – 485.

Sorkin, L., Mendez, M., Rosseti, M.V., et al (1996). Identification of six new mutations in the uroporphyrinogen decarboxylase gene. *Am. J. Hum. Genet.* **59:** A285.

Spencer, P. and Jordan, P.M. (1993). Purification and charactarization of 5-aminolaevulinic acid dehydratase from *Escherichia coli* and a study of the reactive thiols at the metal-binding domain. *Biochem. J.* **290:** 279 – 287.

Spencer, P. and Jordan, P.M. (1995). Characterization of the two 5-aminolaevulinic acid binding sites, the A- and P-sites, of 5-aminolaevulinic acid dehydratase from *Escherichia coli. Biochem. J.* **305:** 151 – 158.

Spivey, A.C., Capretta, A., Frampton, C.S., et al. (1996). Biosynthesis of porphyrins and related macrocycles. Part 45. Determination by a novel X-ray method of the absolute configuration of the spiro lactam which inhibits uroporphyrinogen III synthase (cosynthase). *J. Chem. Soc. Perkin. Trans.* **1:** 2091 – 2102.

Srivastava, G., Borthwick, I.A., Brooker, J.D., et al. (1983). Hemin inhibits transfer of pre-5-aminolaevulinate synthase into chick liver mitochondria. *Biochem. Biophys. Res. Commun.* **117:** 344 – 349.

Srivasata G, Borthwick I.A., Macguire, D.J., et al. (1988). Regulation of 5-aminolevulinate acid synthase mRNA in different rat tissues. *J. Biol. Chem.* **263:** 5202 – 5209.

Stamford, N.P., Capretta, A. and Battersby, A.R. (1995). Expression, purification and characterization of the product from the *Bacillus hemD* gene, uroporphyrinogen III synthase. *Eur. J. Biochem.* **231:** 236 – 241.

Stokvis, B.J. (1889). Over twee zeldsame kleurstoffen in urine van Zicken. *Nederlands tijdschr. Geneeskunde, Amsterdam* **13:** 409 – 417.

Stoltz, M. And Dornemann, D. (1996). Purification, metal cofactor, N-terminal sequence and subunit composition of a 5-aminolevulinic acid dehydratase from the unicellular green alga *Scenedesmus obiquus*, mutant C-2A`. *Eur. J. Biochem.* **236:** 600 – 608.

Straka, J.G. and Kushner, J.P. (1983). Purification and characterization of bovine hepatic uroporphyrinogen decarboxylase. *Biochem.* **22:** 4664 – 4672.

Straka, J.D., Kushner, J.P. and Pryor, M. (1982). Uroporphyrinogen decarboxylase, a method for measuring enzyme activity. *Enzyme* **28:** 170 – 185.

Strand, L.J., Meyer, U.A., Felsher, B.F., et al. (1972). Decreased red cell uroporphyrin-I synthetase activity in intermittent acute porphyria. *J. Clin. Invest.* **51:** 2530 – 2536.

Strierle, A., Upadhyay, R. and Strobel, G. (1991). Cyperin, a phytotoxin produced by *Aschochyta cypericola*, a fungal pathogen of *Cyperus rotundus*. *Phytochem.* **30:** 2191 – 2192.

Stuart, R.A. and Neupert, W. (1996). Topogenesis of inner membrane proteins of mitochondria. *Trends Biochem. Sci.* **21:** 261 – 267.

Stuart, K.A., Busfield, F., Jazwinska, E.C., et al. (1998). The C282Y mutation in the haemochromatosis gene (HFE) and hepatitis C virus infection are independent cofactors for porphyria cutanea tarda in Australian patients. *J. Hepatol.* **28:** 404 – 409.

Sturrock, E.D., Meissner, P.N., Maeder, D.L. et al. (1989). Uroporphyrinogen decarboxylase and protoporphyrinogen oxidase in dual porphyria. *S. Afr. Med. J.* **76:** 405 – 408.

Sutherland, G.R., Baker, E., Callen, D.F., et al. (1988). 5-aminolevulinate synthase is at 3p21 and thus not the primary defect in X-linked sideroblastic anemia. *Am. J. Hum. Genet.* **43:** 331 – 335.

Sweeney, G.D. (1986). Porphyria cutanea tarda, or the uroporphyrinogen decarboxylase deficiency diseases. *Clin. Biochem.* **19:** 3 – 14.

Swindells, M.B., Orengo, C.A., Jones, D.T., et al. (1993). Recurrence of a binding motif? *Nature.* **362:** 299.

Taketani, S. and Tokunaga, R. (1981). Rat liver ferrochelatase. Purification, properties, and stimulation by fatty acids. *J. Biol. Chem.* **256:** 12748 – 12753.

Taketani, S. and Tokunaga, R. (1982). Purification and substrate specificity of bovine liver ferrochelatase. *Eur. J. Biochem.* **127:** 443 – 447.

Taketani, S., Nakahashi, Y., Osumi, T. et al. (1990). Molecular cloning, sequencing and expression of mouse ferrochelatase. *J. Biol. Chem.* **265:** 19377 – 19380.

Taketani, S., Yoshinaga, T., Furukawa, T., et al. (1995a). Induction of terminal enzymes for heme biosynthesis during differentiation of mouse erythroleukemia cells. *Eur. J. Biochem.* **230:** 760 – 765.

Taketani, S., Inazawa, J., Abe, T., et al. (1995b). The human protoporphyrinogen oxidase gene (*PPOX*): organisation and localisation to chromosome1. *Genomics* **29:** 698 – 703.

Taketani, S., Inazawa, J., Nakahashi, Y., et al. (1992). Structure of the human ferrochelatase gene. Exon/intron gene organisation and location of the gene to chromosome18. *Eur. J. Biochem.* **205:** 217 – 222.

Taketani, S., Kohno, H., Furukawa, T., et al. (1994). Molecular cloning, sequencing and expression of cDNA encoding human coproporphyrinogen oxidase. *Biochem. Biophys. Acta* **1183:** 547 – 549.

Tan, D., Barber, M.J. and Ferreira, G.C. (1998). The role of tyrosine 121 in aminolevulinate synthase. *Prot. Sci.* **7:** 1208 –1213.

Tanigawa, K., Bensidhoum, M., Takahura, N., et al. (1996). A novel point mutation in congenital erythropoietic porphyria in two members of a Japanese family. *Hum. Genet.* **97:** 557 – 560.

Te Velde, K., Noordhoek, K.H.N., Wilson, J.H.P. et al. (1989). Een familie-onderzoek bij de eerste Nederlandse patiëten met porfyrie. *Ned. Tijdschr. Geneeskd.* **133:** 2547 – 2552.

The QIAexpressionist (2001). High-level expression and purification of 6 X His-tagged proteins. 2nd ed, Qiagen Ltd, Germany, pp. 48 – 62.

Thudicum, J.L.W. (1867). Report on researches intended to promote an improved chemical identification of disease. Tenth report of the medical officer, Privy Council, appendix 7, H.M.S.O. London. 152 – 195, 200, 227 – 233.

Thunell, S., Holmberg, L. and Lundgren, J. (1987). Aminolaevulinate dehydratase porphyria in infancy. A clinical and biochemical study. *J. Clin. Chem. Clin. Biochem.* **25:** 5 – 14.

Tian, H., Yu, L., Mather., M.W., and Yu, C.A (1998). The flexibility of the neck region of the rieske iron sulfur protein is functionally important in the cytochrome bc1 complex. *J. Biol. Chem.* **273:** 27953 – 27959.

Tio, T.H. (1958). Porphyria cutanea tarda. *Arch. Dermatol.* **77:** 568 – 575.

Todd, D.J., Hughes, E.A., Ennis, K.T., et al. (1993). Identification of single base pair deletion (40 del g) in exon 1 of the ferrochelatase gene in patients with erythropoietic protoporphyria. *Hum. Mol. Genet.* **2:** 1495 – 1496.

Trudgill, P.W., DuBus, R. and Gunsalus, I.C. (1966). Mixed function oxidation. VI. Purification of a tightly coupled electron transport complex in camphor lactonization. *J. Biol. Chem.* **241:** 4288 – 4290.

Tsai, S.F., Bishop, D.F. and Desnick, R.J. (1987). Purification and properties of uroporphyrinogen III synthase from human erythrocytes. *J. Biol. Chem.* **262:** 1268 – 1273.

Tsai, S-F., Bishop, D.and Desnick, R. (1988). Human uroporphyrinogen III synthase: molecular cloning, nucleotide sequence, and expression of a full-length cDNA. *Proc. Natl. Acad. Sci. USA* **85:** 7049 – 7053.

Tsai, S.F., Martin, D.I., Zon, L.I., et al. (1989). Cloning of cDNA for the major DNA-binding protein of the erythroid lineage through expression in mammalian cells. *Nature* **339:** 446 – 451.

Tschudy, D.P. Hess, R.A. and Frykholm, B.D. (1981). Inhibition of δ-aminolevulinic acid dehydratase by 4,6-dioxoheptanoic acid. *J. Biol. Chem.* **256:** 9915 – 9923.

Tsukamoto, I., Yoshinaga, T. and Sano S. (1979). The role of zinc with special reference to the essential thiol groups in delta-aminolevulinic acid dehydratase of bovine liver. *Biochim. Biophys. Acta.* **570:**167 – 178.

Tu, J.B.; Blackwell, R.Q.; Feng, Y.S. (1971). Clinical and biochemical studies of hereditary hepatic porphyria in Chinese subjects in Taiwan. *Metabolism* **20:** 629 – 641.

Tugores, A., Magness, S.T. and Brenner, D.A. (1994). A single promoter directs both housekeeping and erythroid preferential expression of the human ferrochelatase gene. *J. Biol. Chem.* **269:** 30789 – 30797.

Urban-Grimal, D., Volland, C., Garnier, T., et al. (1986). The nucleotide sequence of the *HEM1* gene and evidence for a precursor form of the mitochondrial 5-aminolevulinate synthase in *Saccharomyces cerevisiae*. *Eur. J. Biochem.* **156:** 511 – 519.

Van der Sar, A. and Den Ouden, A. (1976). Porphyria variegata in a curacao Negroid female. *Neth. J. Med.* **19:** 19 – 23.

Venkatasubbaiah, P., Van Dyke, C.G. Chilton, W.S. (1992). Phytotoxic metabolites of *Phoma sorghina*, a new foliar pathogen of pokeweed. *Mycologia* **84:** 715 – 723.

Versano, R., Matringe, M., Magnin, N., et al. (1990). Competetive interaction of three peroxidizing herbicides with the binding of [^{3}H]acifluorfen to corn etioplast membrane. *FEBS Lett.* **272:** 106 – 108.

Volland, C. and Felix, F. (1984). Isolation and properties of 5-aminolevulinate synthase from the yeast *Saccharomyces cerevisiae*. *Eur. J. Biochem.* **142:** 551 – 557.

Vrielink, A., Lloyd, L.F., and Blow, D.M. (1991) Crystal structure of cholesterol oxidase from *Brevibacterium sterolicum* refined at 1.8 Å resolution. *J. Mol. Biol.* **219:** 533 – 554.

Waldenström, J. (1937).Studien über porphyrie. *Acta. Med. Scand.* **92:** (Suppl.) 1 – 254.

Waldenström, J. (1957). The porphyrias as inborn errors of metabolism. *Am. J. Med.* **22:** 758 – 773.

Wang, A.L., Arredondo-Vega, F.X., Giampietro, P.F., et al. (1981). Regional gene assignment of human porphobilinogen deaminase and esterase A4 to chromosome 11q23 leads to 11qter. *Proc. Natl. Acad. Sci. USA* **78:** 5734 – 5738.

Wang, X., Poh-Fitpatrick, M., Taketani, S., et al. (1994). Screening for ferrochelatase mutations: Molecular heterogeneity of erythropoietic protoporphyria. *Biochim. Biophys. Acta.* **1225:** 187 – 190.

Warner, C.A., Yoo, H-W., Tsai, S-F., et al. (1990). Congenital erythropoietic porphyria: characterization of the genomic structure and identification of mutations in the uroporphyrinogen III synthase gene. *Am. J. Hum. Genet.* **47:** 83.

Warnich, L., Kotze, M.J., Groenewald, I.M., et al. (1996a). Identification of three mutations and associated haplotypes in the protoporphyrinogen oxidase gene in South African families with variegate porphyria. *Hum. Mol. Genet.* **5:** 981 – 984.

Warnich, L., Meissner, P.N., Hift, R.J., et al. (1996b). Mapping of the variegate porphyria (VP) gene: contradictory evidence for linkage between VP and microsatellite markers at chromosome 14q32. *Hum. Genet.* **97:** 690 – 692.

Warnick, G.R. and Burnham, B.F. (1971). Regulation of porphyrin biosynthesis. Purification and characterization of 5-aminolevulinic acid synthase. *J. Biol. Chem.* **246:** 6880 – 6885.

Watanabe, N., Che, F., Iwano, M., et al. (1998). molecular characterization of photomixotrophic tobacco cells resistant to protoporphyrinogen oxidase-inhibiting herbicides. *Plant Physiol.* **118:** 751 – 758.

Watanabe, N., Che, F., Terashima, K., et al. (2000). Purification and properties of protoporphyrinogen oxidase from spinac chloroplasts. *Plant cell physiol.* **41:** 889 – 892.

Watson, C.J. (1960). The problem of porphyria-some facts and questions. *N. Engl. J. Med.* **293:** 1205 – 1215.

Watson, C.J. (1975). Hematin and porphyria. *N. Engl. J Med.* **293:** 605 – 607.

Watson, C.J., Cardinal, R.A., Bossenmaier, I. et al. (1975) Porphyria variegata and porphyria cutanea tarda in siblings: chemical and genetic aspects. *Proc. Natl. Acad. Sci. U S A* **72:** 5126 – 5129.

Weber, H.A. and Gloer, J.B. (1988). Interference competition among natural fungal competitors: An antifungal metabolite from the coprophilus fungus *Preussia fleishhakii*. *J. Natural Products* **51:** 879 – 883.

Wells, G.C. and Rimington, C. (1953). Studies on a case of porphyria cutanea tarda. *Br. J. Dermatol.* **65:** 337 – 351.

Westall, R.G. (1952). Isolation of porphobilinogen from a urine of a patient with acute porphyria. *Nature* **170:** 614.

Wetmur, J.G., Bishop, D., Cantelmo, C. et al. (1986). Human δ-aminolevulinate dehydratase: nucleotide sequence of a full-length cDNA clone. *Proc. Natl. Acad. Sci. USA* **83:** 7703 – 7707.

Whatley, S.D., Roberts, A.G. and Elder, G.H. (1995). De-novo mutation and sporadic presentation of acute intermittent porphyria. *Lancet.* **346:** 1007 – 1008.

Whatley, S.D., Puy, H., Morgan, R.R., et al. (1999). Variegate porphyria in Western Europe: Identification of *PPOX* gene mutation in 104 families, extent of allelic heterogeneity, and absence of correlation between phenotype and type of mutation. *Am. J. Hum. Genet.* **65**, 984 – 994.

Whitby, F.G., Phillips, J.D., Kushner, J.P. et al. (1998). Crystal structure of human uroporphyrinogen decarboxylase. *EMBO. J.* **17:** 2463 – 2471.

Whiting, M.J. and Elliott, W.H. (1972). Purification and properties of solubilized mitochondrial δ-aminolevulinic acid synthetase and comparison with the cytosol enzyme. *J. Biol. Chem.* **247:** 6818 – 6826.

Wierenga, R.K., Tepstra, P. and Hol, W.J.J. (1986). Prediction of the occurrence of the ADP-binding βαβ-fold in proteins, using an amino acid sequence fingerprint. *J. Mol. Biol.* **187:** 101 – 107.

Windebank, A.J. and Bonkovsky, H.I. (1992). Porphyric neuropathy. In: Peripheric neuropathy. (R.J. Dyck, and S.K. Thomas, eds), Saunders, Philadelphia.

Wingfield, P.T., Palmer, I. and Liang, S.-M. (1995).Folding and purification of insoluble (inclusion-body) proteins from *Escherichia coli.* In: Current protocols in protein science, Vol. 1. (J.E. Coligan, B.M. Dunn, H.L. Ploegh, D.W. Speicher and P.T. Wingfield, eds), Wiley and Sons, New York, pp. 6.2.1 – 6.2.15.

Witkowski, D.A. and Halling, B.P. (1988). Accumulation of photodynamic tetrapyrroles induced by acifluorfen-methyl. *Plant Physiol.* **87:** 632 – 637.

Wu, C., Xu, W., Kozak, C.A. and Desnick, R.J. (1996). Mouse uroporphyrinogen decarboxylase: cDNA cloning, expression, and mapping. *Mammalian Genome* **7:** 349 – 352.

Wyckoff, E.E., and Kushner, J.P (1994). In: The porphyrias. (I.M. Arias, J.L. Boyer, N. Fausto, W.B. Jakoby, D.A. Schachter, D.A. Shafritz, eds). *The Liver: Biology and Pathobiology*, 3rd ed. Raven Press, New York, pp. 505 – 527.

Wyckoff, E.E., Phillips, J.D., Sowa, A.M., et al. (1996). Mutational analysis of human uroporphyrinogen decarboxylase. *Biochim. Biophys. Acta* **1298:** 294-304.

Xu, K. and Elliot, T. (1993). An oxygen-dependent coproporphyrinogen oxidase encoded by the *hemF* gene of *Salmonella typhimurium*. *J. Bacteriol.* **175:** 4990 – 4999.

Xu, W., Kozak, C.A. and Desnick, R.J. (1995). Uroporphyrinogen III synthase: molecular cloning, nucleotide sequence, expression of a mouse full-length cDNA, and its localisation on mouse chromosome 7. *Genomics* **26:** 556 – 562.

Xu, W., Astrin, K.H., Desnick, R.J., et al. (1996). Molecular basis of congenital erythropoietic porphyria: Mutations in the human uroporphyrinogen III synthase gene. *Hum. Mutat.* **7:** 187 – 192.

Yamamoto M., Kure S., Engel J.D. (1988). Structure, turnover, and heme-mediated suppression of the level of mRNA encoding rat liver delta-aminolevulinate synthase. *J. Biol. Chem.* **263:** 15973 – 15979.

Yamauchi, K., Hayashi, N. and Kikuchi, G. (1980). Translocation of δ-aminolevulinate synthetase from the cytosol to the mitochondria and its regulation by hemin in the rat liver. *J. Biol. Chem.* **255:** 1746 – 1751.

Yeung-Laiwah, A.C., Macphee, G., Boyle, P., et al. (1987). Autonomic neuropathy in acute intermittent porphyria. *J. Neurol. Neurosurg. Psychiatry.* **48:** 1025 – 1030.

Yoshimura, T., Bhatia, M.B., Manning, J.M., et al. (1992). Partial reactions of bacterial D-amino acid transaminase with asparagine substituted for the lysine that binds coenzyme pyridoxal 5'-phosphate. *Biochem.* **31:** 11748 – 11754.

Yoshinaga, T. and Sano, S. (1980). Coproporphyrinogen oxidase. II. Reaction mechanism and role of tyrosine residues on the activity. *J. Biol. Chem.* **255:** 4727 – 4731.

Zaleski, J. (1903). Untersuchungen über das Mesoporphyrin. *Hoppe-Seyler's physiol. Chem.* **37:** 54 – 74.

APPENDIX 1

TRANSFORMATION OF *E.COLI* JM109 CELLS WITH HUMAN PPOX RECOMBINANT PLASMID

Materials

Equipment

- Heating block (Techne dri-block DB-2D, Laboratory and Scientific Equipment Co. Cape Town, SA)
- Sterile 50ml graduated (polypropylene) centrifuge tubes (Greiner Labortechnik, Frickenhausen, Germany)
- Centrifuge (Centrikon T-324, Kontron Instruments, A.G. Zurich, Switzerland)
- Ice bath

Reagents

- Recombinant plasmid vector (pTrcHis)
- Calcium Chloride solution, pH 8.0
  0.05M $CaCl_2$
  0.01M Tris/HCl
  Sterilise by autoclaving
- LB agar plates with ampicillin
  2g Tryptone
  1g Yeast extract
  1g NaCl
  3g Agar Noble (Difco Laboratories, Detroit, Michigan, USA)

Make up to 200ml with deionised water and autoclave. Cool the media to 40°C, add 100μg/ml (final concentration) of ampicillin and immediately pour into sterile petri plates under sterile hood before agar solidifies.

Procedure

- Transfer 1ml of 10ml overnight culture of *E. coli* JM109 cells into 100ml of sterile LB broth in a 500ml flask.
- Allow culture to grow (with shaking, 225rpm) at 37°C until an OD_{600nm} of 0.5 – 0.7 is achieved.
- Decant the culture into pre-chilled sterile 50ml capped tubes and chill on ice for 10min.
- Centrifuge the cell suspension at 4000 g for 5min at 4°C.
- Resuspend pellet in half of the original culture volume in ice-cold sterile $CaCl_2$ solution and place in ice bath for 15min.
- Centrifuge at 4000 g for 5min at 4°C.
- Resuspend cells in 1/15 of the original volume of culture media in ice-cold sterile $CaCl_2$ solution and dispense 200µl aliquots into pre-chilled sterile Eppendorf tubes.
- Store at 4°C for 12–24h to increase competence.
- Add recombinant plasmid DNA (approximately 40ng in a maximum of 100µl TE buffer) to an aliquot of the cell suspension, mix and store on ice for 30min.
- Heat at 42°C for 2min.
- Add 1ml of sterile LB broth and incubate at 37°C for 1h without shaking. This allows the bacteria to recover and begin expressing antibiotic resistance.
- Use a sterile glass spreader to spread 100, 200, and 500µl of transformed cell suspension over LB plates, containing ampicillin (100µg/ml).
- Allow the medium to absorb the cell suspension then incubate the plates at 37°C for 12–16h until colonies appear. Re-plate apparent single colonies onto fresh plates.
- Once single colonies have appeared, inoculate 100ml of LB broth containing ampicillin (100µg/ml) with a single colony.
- After overnight growth, transfer 700µl aliquots of the culture into 2ml cryotubes containing 300µl sterile glycerol. Mix and store at -70°C as stocks.

APPENDIX 2

EXPRESSION OF WILD TYPE PPOX

Materials

Equipment

- Orbital shaker incubator (Yih der LM-510, Taiwan)
- Centrifuge (Centrikon T-324, Kontron Instruments, A.G. Zurich, Switzerland)
- Autoclave Huxley, Speedy (Laboratory and Scientific, Pty, Ltd, Cape Town, SA)

Reagents

- Luria-Broth (LB)
  5g NaCl
  5g Yeast
  10g Tryptone

Make up to 1 L with deionised water and autoclave (121°C for 30min). Cool to room temperature (~ 40°C) before adding 100μg/ml ampicillin.

Procedure

- Innoculate 500μl of JM109 cells (of a 30% glycerol stock) containing wild type PPOX into 1 L Luria broth containing 100μg/ml ampicillin (final concentration).
- Incubate for 18h at 30°C on a rotary shaker (225rpm).
- Harvest by centrifugation (3000 g) for 30min at 4°C and perform plasmid miniprep (see Appendix 3).

APPENDIX 3

DNA PURIFICATION

Materials

Equipment

- Labnet force 14 microcentrifuge (Denver Instruments, Laboratory and Scientific Pty, Ltd, Cape Town)
- 1.5ml microcentrifuge tubes (Quality Scientific plastics, Porex Bio Product Group, Whitehead Scientific, Brackenfell, SA)
- GeneQuant Spectrophotometer (Pharmacia Biotech. Cambridge, UK)

Reagents

- Wizard® Plus SV Minipreps DNA purification system (Promega Corporation, Madison, WI, USA)

Procedure

Plasmid miniprep

- Pellet 5ml of bacterial culture by centrifugation for 5min at 10000g in a table top microcentrifuge and discard supernatant.
- Add 250µl of Wizard® Plus SV Minipreps cell lysis solution and mix by inverting the tube eight times.
- Allow to stand for 3.5min.
- Add 350µl of Wizard® Plus SV Minipreps neutralisation solution and mix by inverting the tube eight times.
- Centrifuge lysate at 14000g in microcentrifuge for 10min at room temperature.
- Decant clear lysate into Wizard® Plus SV Minipreps spin column inserted into a 2ml collection tube.
- Centrifuge the cleared lysate at 14000g in a microcentrifuge for 2min.

- Remove Wizard® Plus SV Minipreps spin columns from the tubes and discard the flow through.
- Return column to the collecting tube and add 750µl of Wizard® Plus SV Minipreps column wash solution.
- Centrifuge at 14000g for 1min.
- Remove the Wizard® Plus SV Minipreps spin column from the tubes and discard flow through.
- Add 250µl of Wizard® Plus SV Minipreps spin column wash solution to the Wizard® Plus SV Minipreps spin column.
- Centrifuge at 14000g for 2min.
- Transfer spin column to a clean sterile 1.5ml microcentrifuge tube.
- Elute plasmid DNA by adding 100µl of nuclease free water to the spin column.
- Centrifuge at 14000g for 1min and quantify DNA on a GeneQuant spectrophotometer.

APPENDIX 4

HUMAN PPOX cDNA SEQUENCE

(Nishimura et al., 1995; Accesion number: D38537)

Table 4.1: The sequence complementary to the forward oligonucleotide in the study is denoted by a single underline (PF), and that complimentary to the reverse oligonucleotide is denoted by double underline (PR). codons are single underlined, with mutated bp(s) printed in blue or red colour (—— naturally occurring mutants, —— self-designed mutants). The relative mutant names appear in the right column. The ATG start site and TGA termination codons are shown in bold type.

cDNA sequence	Mutants/start and stop codons
1 GAATTCGGGG GGAGAACAGA GTGGACGGAG AGTAGGAGAG ACCGAAAAGG CTGGGGGTGG	
61 GAGTAGCGGA TTTGAAGCAC TTGTTGGCCT ACAGAGGTGT GGCAAGCAGA GCACCTCAGA	
121 ACTCAGGCGT ACTGCCCGCC GCCCGAGCCC TGCGAGGGCC GATAGCGAGG GTGTGGCCCT	
181 TATCTGCACC CAGCAGAGCG CCGGCGGGGT ACGGTCTTAG GACCTCGATC TCCTTCTCCC CATCATGGT ATGGCTAGTC C (PF1)*	
241 TCATTTTCTC TCATCCCTAC CTATTGTGGG TTTCCGCATG GGCCGGACCG TGGTCGTGCT	Start codon
301 GGGCGGAGGC ATCAGCGGCT TGGCCGCCAG TTACCACCTG AGCCGGGCCC CCTGCCCCCC	G9A, G11A, G14A, H20P
361 TAAGGTGGTC CTAGTGGAGA GCAGTGAGCG TCTGGGAGGC TGGATTCGCT CCGTTCGAGG	
421 CCCTAATGGT GCTATCTTTG AGCTTGGACC TCGGGGAATT AGGCCAGCGG GAGCCCTAGG	R59W (R59K, R59S, R59I)
481 GGCCCGGACC TTGCTCCTGG TTTCTGAGCT TGGCTTGGAT TCAGAAGTGC TGCCTGTCCG	
541 GGGAGACCAC CCAGCTGCCC AGAACAGGTT CCTCTACGTG GGCGGTGCCC TGCATGCCCT PF2	
601 ACCCACTGGC CTCAGGGGGC TACTCCGCCC TTCACCCCCC TTCTCCAAAC CTCTGTTTTG	
661 GGCTGGGCTG AGGGAGCTGA CCAAGCCCCG GGGCAAAGAG CCTGATGAGA CTGTGCACAG	
721 TTTTGCCCAG CGCCGCCTTG GACCTGAGGT GGCGTCTCTA GCCATGGACA GTCTCTGCCG PR1	R168C
781 TGGAGTGTTT GCAGGCAACA GCCGTGAGCT CAGCATCAGG TCCTGCTTTC CCAGTCTCTT	
841 CCAAGCTGAG CAAACCCATC GTTCCATATT ACTGGGCCTG TTGCTGGGGG CAGGGCGGAC	
901 CCCACAGCCA GACTCAGCAC TCATTCGCCA GGCCTTGGCT GAGCGCTGGA GCCAGTGGTC	
961 ACTTCGTGGA GGTCTAGAGA TGTTGCCTCA GGCCCTTGAA ACCCACCTGA CTAGTAGGGG PF3 PR2	
1021 GGTCAGTGTT CTCAGAGGCC AGCCGGTCTG TGGGCTCAGC CTCCAGGCAG AAGGGCGCTG	
1081 GAAGGTATCT CTAAGGGACA GCAGTCTGGA GGCTGACCAC GTTATTAGTG CCATTCCAGC	
1141 TTCAGTGCTC AGTGAGCTGC TCCCTGCTGA GGCTGCCCCT CTGGCTCGTG CCCTGAGTGC	

Table continues to the next page

Table 4.1: Continued

1201 CATCACTGCA GTGTCTGTAG CTGTGGTGAA TCTGCAGTAC CAAGGAGCCC ATCTGCCTGT	
1261 CCAGGGATTT GGACATTTGG TGCCATCTTC AGAAGATCCA GGAGTCCTGG GAATCGTGTA (PF4)	Y348C
1321 TGACTCAGTT GCTTTCCCTG AGCAGGACGG (PR3) GAGCCCCCCT GGCCTCAGAG TGACTGTGAT	
1381 GCTGGGAGGT TCCTGGTTAC AGACACTGGA GGCTAGTGGC TGTGTCTTAT CTCAGGAGCT	
1441 GTTTCAACAG CGGGCCCAGG AAGCAGCTGC TACACAATTA GGACTGAAGG AGATGCCGAG	
1501 CCACTGCTTG GTCCATCTAC ACAAGAACTG CATTCCCCAG TATACACTAG GTCACTGGCA	
1561 AAAACTAGAG TCAGCTAGGC AATTCCTGAC TGCTCACAGG TTGCCCCTGA CTCTGGCTGG	
1621 AGCCTCCTAT GAGGGAGTTG CTGTTAATGA CTGTATAGAG AGTGGGCGCC AGGCAGCAGT	
1681 CAGTGTCCTG GGCACAGAAC CTAACAGCTG A (PR4) TCCCCAACT CTCATTCATG AAAATAAAAA	Termination codon
1741 TTGCTGGAGC TCCCGAATCC CGAATTC	

* The primer incorporates the last two histidines of the six histidine tag as well as the first part of inserted Bgl 1I restriction enzyme specific cassette which allows one easy release of the PPOX sequence for future cloning using Bgl II and Hind III.

APPENDIX 5

SITE-DIRECTED MUTAGENESIS

Materials

- *In vitro* site-directed mutagenesis system (GeneEditor™ kit, Promega Corporation, Madison, WI, USA)
- Phosphorylated mutagenic oligonucleotides (Integrated DNA Technologies, Inc. Coralville, IA, USA)

Table 5.1 **Designed Oligonucleotides used in site-directed mutagenesis. In each case the mutated DNA bp(s) is/are underlined. The amino acids encoded by the sequences are shown above and the altered amino acids shown in bold. The direction of the oligonucleotide and the annealing temperatures are shown on the right.**

PPOX	Mutation oligonucleotides (5' → 3')	Direction of oligonucleotide	Annealing temperature (°C)
Wild type	S Y H L S R CG GCT CAG GTG GTA ACT GGC		
H20P	S Y **P** L S R 5' Phos-CG GCT CAG GG̲G GTA ACT GGC	Reverse	53
Wild type	I V Y D S GA ATC GTG TAT GAC TCA G		
Y348C	I V **C** D S 5' Phos-GA ATC GTG TG̲T GAC TCA G	Forward	50
Wild type	E L G P R G I R P T GAG CTT GGA CCT CGG GGA ATT AGG CCA G		
R59W	L G P **W** G I 5' Phos-CTT GGA CCT T̲GG GGA ATT AG	Forward	57
R59K	E L G P **K** G I R P 5' Phos-T GAG CTT GGA CCT A̲AG GGA ATT AGG CCA G	Forward	51
R59S	E L G P **S** G I R P 5' Phos-T GAG CTT GGA CCT A̲GT̲ GGA ATT AGG CCA G	Forward	51
R59I	E L G P **I** G I R P 5' Phos-T GAG CTT GGA CCT A̲TT̲ GGA ATT AGG CCA G	Forward	51
Wild type	V V L G_9 G G_{11} I S G_{14} L A A GTC GTG CTG GGC GGA GGC ATC AGC GGC TTG GCC GCC AG		
G9A	V V L **A** G G I 5' Phos-GTC GTG CTG G̲C̲C GGA GGC ATC	Forward	57
G11A	G G **A** I S 5' Phos-TG GGC GGA G̲C̲C ATC AGC GG	Forward	57
G14A	G I S **A** L A A 5' Phos-GA GGC ATC AGC G̲C̲C TTG GCC GCC AG	Forward	59

5.1 Determination of optimal annealing temperature

Materials

Equipment

- Sterile microcentrifuge tubes (Quality Scientific plastics, Porex Bio Product Group, Whitehead Scientific, Brackenfell, SA)
- Robocycler gradient thermal cycler, Teddington, UK.

Reagents

- Wild type DNA
- Mutagenic oligonucleotide
- Appropriate oligonucleotide of the relevant cDNA fragment
- Reagents for PCR (see Appendix 6.1)

Procedure

- Determine appropriate annealing temperature by performing the polymerase chain reaction (PCR) on the relevant cDNA fragment that includes the bps requiring mutagenesis using DNA extracted from wild type PPOX (see Appendices 3 and 6.1).
- Where a forward mutagenic oligonucleotide is utilised, use the reverse oligonucleotide of the relevant cDNA fragment.
- The reverse should apply for a reverse mutagenic oligonucleotide.

5.2 DNA template preparation

Materials

Equipment

- Labnet force 14 microcentrifuge (Denver Instruments, Laboratory and Scientific Pty, Ltd, Cape Town)
- GeneQuant Spectrophotometer (Pharmacia Biotech. Cambridge, UK)

Reagents

- Wild type HPPOX DNA (extracted as described in Appendix 3)
- Primers (Integrated DNA Technologies Inc. Coralville IA, USA) were designed with Primer Designer for Windows software package (Soft Packaging version 2, Scientific and Education Software).
- Freshly prepared 2M ammonium acetate, pH 4.6
- Freshly prepared 2M NaOH, 2mM EDTA
- 100% Ethanol
- Sterile water

Procedure

Alkaline denaturation (dsDNA)

- Prepare the following alkaline denaturation reaction:

dsDNA template	0.5pmol
2M NaOH, 2mM EDTA	2µl
Sterile deionised water to final volume of	20µl

- Incubate at room temperature for 5min.
- Add 2µl of 2M ammonium acetate (pH 4.6) and 75µl of 100% ethanol.
- Incubate for 30min at -70°C.
- Microcentrifuge at 14000g for 15min at 4°C.
- Drain and wash the pellet with 200µl of 70% ethanol.
- Centrifuge at 14000g for 1min, pour off supernatant, and allow inverted tube to drain for 30min.
- Resuspend the pellet in 50µl sterile water and leave for 5min.
- Quantify by measuring the optical density on a GeneQuant spectrophotometer.

5.3 Hybridisation reaction

Materials

Equipment

- Hybaid Omnigene thermal cycler, Teddington, UK.

Reagents

- Template DNA (dsDNA)
- Selection oligonucleotide
- Mutagenic oligonucleotide
- Annealing 10 x buffer
  200mM Tris/HCl (pH 7.5)
  100mM $MgCl_2$
  500mM NaCl
- Sterile deionised water

Procedure

Mutagenesis reaction

Template DNA (dsDNA) (alkaline denatured)	10µl (0.05pmol)
Appropriate phosphorylated selection oligonucleotide	1µl (0.25pmol)
Phosphorylated mutagenic oligonucleotide	2µl (1.25pmol)
Annealing 10 X buffer	2µl
Sterile deionised water (to final volume)	20µl

- Heat the reaction for 5min at appropriate hybridisation temperature (see table 5.1) and allow 1.5°C per min stepwise cooling to 37°C.

5.4 Mutant strand synthesis and ligation

Materials

Equipment

- Techni dry block BD-2D (Laboratory & Scientific, Cape Town, SA).
- Labnet force 14 microcentrifuge (Denver Instruments, Laboratory & Scientific, Cape Town, SA).

Reagents

- T4 DNA polymerase
- T4 DNA ligase
- Synthesis 10 X buffer
  100mM Tris/HCl (pH 7.5)
  5mM dNTPs
  10mM ATP
  20mM DTT
- Sterile deionised water

Procedure

- After the annealing reaction has cooled to 37°C, spin briefly in microcentrifuge to collect contents at the bottom of the tube and add the following:

Sterile deionised water	5.0µl
Synthesis 10 X buffer	3.0µl
T4 DNA polymerase	1.0µl
T4 DNA ligase	1.0µl
Final volume	30µl

- Incubate the reaction for 90min at 37°C to perform mutant strand synthesis and ligation.

5.5 Transformation of BMH 71-18 *mut*S competent cells

Materials

Equipment

- Orbital shaker incubator (Yih der LM-510, Taiwan)
- Sterile 17 x 100mm polypropylene tubes (Laboratory and Scientific Equipment Company Pty, Ltd, Cape Town, SA)
- Heating block (Techne dri-block DB-2D, Laboratory and Scientific Equipment)
- Water bath (37°C) Memmert, Laboratory and Scientific, Cape Town, SA

Reagents

- BMH 71-18 *mutS* competent cells.
- LB (Luria-Bertani) medium
  10g Tryptone
  5g Yeast extract
  5g NaCl, in 1L deionised water

Procedure

- Pre-chill sterile 17 x 100mm propylene culture tubes on ice (one for each annealing reaction).
- Remove frozen competent cells from -70°C and place on ice for 5min or until just thawed.
- Mix cells gently by flicking the tube and then transfer 100µl of the thawed BMH 71-18 *mut*S cells to each of the pre-chilled culture tubes.
- Add 1.5µl (≈ 5 – 10ng) of each mutagenesis reaction to 100µl of BMH 71-18 *mut*S competent cells.
- Move the pipette tip through the cells while dispensing and quickly flick the tube several times.
- Immediately place tubes on ice for 10min.
- Heat-shock the cells for 50s in a water bath at exactly 42°C without shaking.
- Immediately place tubes on ice for 2min.
- Add 900µl of room temperature LB broth (without antibiotic) to each transformation reaction and incubate for 60min at 37°C with shaking (225rpm).

- Prepare an overnight culture by adding 4ml of LB containing 50µl of the GeneEditor™ Antibiotic Selection Mix to each of transformation reaction.
- Incubate for 18h at 37°C with shaking (225rpm).
- Check overnight growth by measuring absorption at 600nm. Absorption at 600nm must be >0.200, if not, allow growth to continue.
- Purify plasmid DNA (Appendix 3) from the overnight culture of *MutS* and quantify on a GeneQuant spectrophotometer.

5.6 Transformation into JM109

Materials

Equipment

- Sterile 17 x 100mm polypropylene culture tubes
- Orbital shaker incubator (Yih der LM-510, Taiwan)
- Autoclave (Laboratory and Scientific, Pty, Ltd, Cape Town, SA)
- Water bath (37°C) (Memmert, Laboratory and Scientific, Cape Town, SA)

Reagents

- JM109 cells
- Sterile glycerol
- LB medium
- LB agar plates + ampicillin

Add 15g agar to 1 litre of LB medium to pH 7.0 and autoclave. Allow medium to cool to 55°C and add ampicillin to final concentration of 125µg/ml. Pour 20–25ml of medium into 85mm petri dishes and flame the surface of the medium with a Bunsen burner to eliminate bubbles (if present). Allow to set and store at 4°C for up to one month.

- SOC medium, pH 7.0
  2.0g Tryptone
  0.5g Yeast extract
  1ml 1M NaCl
  0.25ml 1M KCl
  1ml 2M Mg^{2+} stock (1M $MgCl_2.6H_2O$, 1M $MgSO_4$.7H2O) (filter sterilised).
  1ml 2M glucose (filter sterilised)

Add tryptone, yeast extract, NaCl, KCl, to 97ml deionised water. Stir to dissolve, autoclave and cool to room temperature. Add 2M Mg^{2+} stock and 2M glucose stock, each to final concentration of 20mM. Filter medium through a 0.2μm filter unit.

Procedure

- Prepare plates by evenly spreading 100μl of the GeneEditor Antibiotic Selection Mix onto 20–25ml LB agar plates containing 125μg/ml ampicillin.
- Allow GeneEditor™Antibiotic Selection Mix to soak into the plate for at least 20min but no longer than 2 h before spreading the transformed cells.
- Chill sterile 17 x 100mm polypropylene culture tubes on ice.
- Remove frozen JM109 from -70°C storage and place on ice for 5min, or until just thawed.
- Mix the cells gently by flicking the tube and transfer 100μl of the thawed JM109 cells to each of the pre-chilled tubes.
- Perform two transformations by adding 2.5ng or 5ng of plasmid DNA ex *mut*S cells (Appendix 3) to each of 100μl of JM109 cells.
- Move pipette tip through the cells while dispensing and quickly flick the tube several times.
- Immediately place the tube on ice for 30min.
- Heat-shock cells for 50s in a water bath at exactly 42°C without shaking.
- Add 900μl of room temperature SOC medium to each transformation reaction and incubate for 1h at 37°C with shaking (225rpm).
- For each transformation reaction plate, plate 75μl and 100μl of cells and incubate at 37°C for 12 – 14h.
- Innoculate 6 single colonies from plates into 10 ml LB medium containing 100μg/ml ampicillin in 50ml screw capped tube (screw capped tube is loosely fitted to allow aeration).
- Grow culture overnight with shaking (225rpm) at 37°C.
- Prepare glycerol stock solution (0.3ml glycerol and 0.7ml culture) for each culture and store at -70°C.
- From the remaining culture (approximately 6ml), perform DNA purification/plasmid miniprep (Wizard® Plus SV Minipreps DNA purification system) and quantify DNA.

APPENDIX 6

MUTATIONAL ANALYSIS

Materials

Reagents

- Primers (Integrated DNA Technologies Inc. Coralville IA, USA) were designed with Primer Designer for Windows software package (Soft Packaging version 2, Scientific and Education Software).

Table 6.1 Oligonucleotides used for PCR of cDNA fragments

Fragments	Fragment size (bp)	Oligonucleotides (5'-3')
1	533	PF_1 CATCATGGTATGGCTAGTCC
		PR_1 AGACTGTCCATGGCTAGAGA
2	411	PF_2 CTGCATGCCCTACCCACTG
		PR_2 TTCAAGGCCTGAGGCAACA
3	390	PF_3 ACTTCGTGGAGGTCTAGAGA
		PR_3 CCGTCCTGCTCAGGGAAAGCAAC
4	432	PF_4 GTGCCATCTTCAGAAGATCC
		PR_4 TCAGCTGTTAGGTTCTGTGC

PF = Forward oligonucleotides

PR = Reverse oligonucleotides

Procedure

- Amplify the relevant HPPOX cDNA fragment that includes the mutated base pair(s) using fragment specific primers.

6.1 Polymerase chain reaction (PCR) of cDNA fragments

Materials

Equipment

- Sterile microcentrifuge tubes (Quality Scientific plastics, Porex Bio Product Group, Whitehead Scientific, Brackenfell, SA)
- Sterile filter tips (Quality Scientific plastics, Porex Bio Product Group, Whitehead Scientific, Brackenfell, SA)
- Robocycler gradient (temperature cycler), Stratagene, Cambridge, UK.
- Hybaid Omnigene thermal cycler, Teddington, UK.
- Force 14 microcentrifuge (Denver Instruments, Laboratory & Scientific, Cape Town, SA)

Reagents

- Deoxynucleotide Triphosphates (dNTP's), Promega Corporation, Southampton, UK.
- dNTP stock solution
- Take 100mM equal volumes of dATP, dCTP, dGTP and dTTP. Dilute and combine to make stock solution containing 2.5mM of each dNTP.
- 25μM forward and reverse oligonucleotides
- Taq DNA polymerase (5 units/μl) (Promega Corporation, Southampton, UK)
- Thermophilic DNA polymerase 10 x buffer, magnesium free
- 25mM magnesium chloride solution
- Mineral oil

Procedure

- Prepare the following reaction mixture in a sterile 1.5ml microcentrifuge tube on ice, using sterile filter tips.

Table 6.2 Preparation of PCR reaction

Reaction mixture	Volume (µl)	Final concentration
Thermophilic poly 10 x buffer	5	1 x
25mM $MgCl_2$ solution	5	1 x
2.5mM dNTP stock	2	100µM
Forward oligonucleotide	1	1µM
Reverse oligonucleotide	1	1µM
Taq DNA polymerase	0.2	1unit
Sterile water	30.8	

- Scale up these volumes to make sufficient mixture to allow for 45µl for each PCR required, in addition to sufficient volume for a blank (i.e. no DNA).
- Aliquot 45µl of the mixture into a 0.6ml microcentrifuge tube on ice.
- Add 5µl of DNA (± 250ng) (5µl of water to the blank).
- Vortex tube and centrifuge briefly.
- Overlay with drop of mineral oil.
- Place in thermocycler and start PCR reaction.
- When optimal annealing temperature needs to be determined, perform gradient PCR on the robocycler using one or more of the below gradients:
- 37 – 44°C, 42 – 56°C, 51 – 65°C.
- Use the following temperature profiles for the four PPOX fragments.

Fragments 1 and 4

	Temperature (°C)	Time (min)	No. of cycles
Initial denaturation	95	1	1
Denaturation	95		
Annealing	53	0.5	45
Extension	72		
Final extension	72	7	1

Fragment 2

	Temperature (°C)	Time (min)	No. of cycles
Initial denaturation	95	1	1
Denaturation	95		
Annealing	56	0.5	35
Extension	72		
Final extension	72	7	1

Fragment 3

	Temperature (°C)	Time (min)	No. of cycles
Initial denaturation	95	1	1
Denaturation	94	1	
Annealing	65	0.5	32
Extension	72	1	
Final extension	72	1	1

- Analyse PCR products by 6% polyacrylamide gel electrophoresis (see Appendix 7.2).
- When required for sequencing, run PCR product on MS8 agarose (see Appendix 8) and extract by the Qiaex II agarose gel extraction protocol described below (see Appendix 9).

APPENDIX 7

RESTRICTION ANALYSIS

7.1 Digestion of DNA fragment

Materials

Equipment

- Techni dry block BD-2D (Laboratory & Scientific, Cape Town, SA).
- Force 14 microcentrifuge (Denver Instruments, Laboratory & Scientific, Cape Town, SA).

Reagents

- *Ava I* (Promega Corporation, Madison, USA) is used for identification of R59W, R59K, R59S, and R59I mutations in fragment 1 and recognises the following sequence:
  5' C↓(T/C)CG(A/G) G 3'
  3' G (A/G)GC(T/C)↑C 5'
- *Mae III* (Roche Diagnostics Pty Ltd, Randburg, SA) is used for identification of Y348C mutant in fragment 3 (390 bp) and recognises the following sequence:
  5' ↓GTNAC 3'
  3' CANTG ↑5'
- *Xcm I* (New England Biolabs, Laboratory Specialist Services, Cape Town, SA) is used for identification of G11A mutant in fragment 1 (533 bp) and recognises the following sequence:
  5' CCANNNNN↓NNNNTGG 3' N = Purine or Pyrimidine
  3' GGTNNNN↑NNNNNACC 5'
- *Msp A1 I* (Promega Corporation, Southampton, UK) is used for identification of G14A mutant in fragment 1 (533 bp) and recognises the following sequence:

  5' C(A/C)G↓C(G/T)G 3'
  3' G(T/G)C↑G(C/A)C 5'

Procedure

- Scale up the volumes for single digestion to allow for the number of digests required.
- Analyse digestion products on 6% polyacrylamide gel electrophoresis (see Appendix 7.2).

Ava1

Wild type has 2 cutting sites

Digestion products = 237 + 209 + 87 bp

R59W, R59K, R59S, and R59I mutations abolish 1 cutting site.

Digestion products = 446 + 87 bp.

- Prepare digestion as follows:

10 x buffer B	2.0µl
10 mg/ml Bovine serum albumin (BSA)	0.2µl
Deionised water	7.3µl
10 units/µl of *Ava I*	0.5µl
Total	10µl

- Mix and centrifuge briefly in microcentrifuge.
- To 10µl of the above mixture add 10µl of PCR products (1 – 1.5µg).
- Mix, layer mineral oil on top of the mixture and centrifuge briefly in microcentrifuge.
- Incubate at 37°C for 3h.

Mae III

Wild type has no cutting site.

Fragment remains 390 bp.

Y348C mutant creates one cutting site

Digestion products = 359 + 31bp

- Prepare digestion as follows:

2 x incubation buffer	10µl
Deionised water	1.75µl
2 units/µl of *Mae III*	0.75µl
Total	12.5µl

- Add 75µl of the above mixture to 7.5µl of the PCR product (±1µg).
- Mix, layer mineral oil on top of the mixture and centrifuge briefly in microcentrifuge.
- Incubate at 55°C for 3h.

Xcm I

Wild type has 1 cutting site.

Digestion products = 493 + 40 bp

G11A mutation creates an additional cutting site

Digestion products = 75 + 418 + 40 bp

- Prepare digestion as follows:

NE Buffer 2	2µl
Deionised water	7.7µl
10 units/µl of *Xcm I*	0.3µl
Total	10µl

- Mix and centrifuge in microcentrifuge.
- Incubate at 37°C for 3h.

Msp A1 I

Wild type has 3 cutting sites.

Digestion products = 74 + 152+ 87 + 220 bp

G14A mutation abolishes 1 cutting site

Digestion products = 226 + 87 + 220 bp

- Prepare digestion as follows:

Buffer C 10 x	2µl
BSA 10mg/ml	0.2µl
Deionised water	7.5µl
10 units/µl of *Msp A1 I*	0.3µl
Total	10µl

- Mix and centrifuge briefly in microcentrifuge. In a 0.6ml of microcentrifuge tube, add 10µl of the mixture and 10µl of PCR product (±1µg).
- Mix, layer mineral oil on top of mixture and centrifuge briefly in microcentrifuge.
- Incubate at 37°C for 3h.

6% non-denaturing polyacrylamide gel electrophoresis

Materials

Equipment

- SE600 vertical slab gel electrophoresis unit, (Hoefer Scientific Instruments Pharmacia Biotech, Cambridge, UK)
- PS1200 DC power supply, (Hoefer Scientific Instruments Pharmacia Biotech, Cambridge, UK)
- Uvitec gel documentation system, (Uvitec, Cambridge, UK).

Reagents

- 1L of 10 x TBE (Tris/Borate/EDTA)
  890mM Tris base
  890mM boric acid
  20mM EDTA, pH 8.0
- Ethidium Bromide (prepare stock solution of 1mg/ml and store in the dark. Add 200µl of stock to 200ml water for use)
- Sucrose sample solution
  30g sucrose
  10mg bromophenol blue
  5ml 0.5M Na_2EDTA
  make up to 50ml with water
- 100bp DNA ladder (Promega Corporation, Southampton, UK)

Procedure

- To 100ml beaker add the following:
  5ml 10 x TBE
  10ml A-Bis-A solution (30% acrylamide, 0.8% bisacrylamide)
  500µl of 10% ammonium persulphate
  50µl TEMED
  Make up to 50ml with deionised water.

- Pour this solution into the space between the clamped two glass gel plates (1.5mm spacers) mounted in the gel casting stand.
- Insert 20 sample spacer comb and allow to set.
- Assemble upper buffer chamber on top of gel plate and fill with 500ml of 1 x TBE buffer.
- Fill lower buffer chamber with 2L of 1 x TBE.
- Dilute PCR products with sucrose sample solution (1:1) and load into sample bays using Hamilton syringe.
- Load 10µl of DNA markers (diluted 1:1 with sucrose sample solution) into a bay (100bp DNA ladder).
- Run at 150V for ± 2h.
- Stain gel in ethidium bromide for 10min, rinse in deionised water and then visualise under UV light.
- Photograph using gel documentation system.

APPENDIX 8

AGAROSE GEL ELECTROPHORESIS

Materials

Equipment

- Horizontal mini-gel system (Mgu-202T), (CBS Scientific Company Inc., Del Mar, USA).
- HIS PS1500DC power supply (Hoefer/Pharmacia Biotech, Cambridge, UK).
- Electronic UV Transilluminator (Ultralum, Whitehead Scientific, Brackenfell, Cape Town)
- Water bath (37°C) (Memmert, Laboratory and Scientific, Cape Town, SA)

Reagents

- MS-8 Agarose (Whitehead Scientific, Brackenfell, SA)
- Ethidium Bromide (Roche Diagnostics, Pty Ltd, Randburg, SA)
- Bromophenol blue (Associated Chemical Enterprises, South dale, SA)
  0.025g bromophenol blue
  3ml sterile glycerol
  Make up to 10ml with sterile water

Procedure

- Insert gel tray between tapered baffles.
- Add 50ml 1 x TBE to 0.75g agarose in 100ml glass flask. Fill the neck of glass with paper towel and heat in microwave for 1–2min.
- Once agarose has dissolved completely, mix well and add 20µl ethidium bromide.
- Mix and pour into gel tray before inserting comb.
- Allow to set for 1h.
- Remove comb and tapered baffles.

- Fill both reservoirs of gel tank with 250ml 1 x TBE so that the surface of the gel is covered by approximately 3mm.
- Prepare PCR products by diluting with sucrose sample solution 1: 0.5.
- Load into bays and run for 90min at 100 volts.
- Visualise the gel under UV light.
- Excise DNA band from the gel using sterile scalpel blade (minimise exposure of DNA to UV light to prevent DNA shearing).
- Minimise size of the gel slice by removing excess of agarose.

APPENDIX 9

QIAEX II AGAROSE GEL EXTRACTION PROTOCOL

Materials

Equipment

- Force 14 microfuge (Denver Instruments, Laboratory and Scientific, Cape Town, SA)
- Microcentrifuge tubes (1.5ml) (Quality Scientific plastics, Porex Bio Product Group, Whitehead Scientific, Brackenfell, SA)

Reagents

- Qiaex II Gel extraction kit (Qiagen Ltd, Crawley, West Sussex, UK)

Procedure

- Place excised gel slice in 1.5ml microcentrifuge tube.
- Add 3 volumes of buffer QX1 to 1 volume of gel.
- Resuspend the Qiaex II silica particles by vortexing for 30 s.
- Add 10µl Qiaex II suspension to tube.
- Incubate in water bath at 50°C for 30min with vortexing every 2min to keep Qiaex in suspension.
- Centrifuge for 1min in microcentrifuge (14000g) and remove supernatant.
- Wash pellet with 500µl of buffer QX1. Vortex to resuspend pellet.
- Microcentrifuge for 1min at 14000 g.
- Wash pellet twice with 500µl of PE buffer (vortex the suspended pellet and centrifuge for 1min at 14000 g).
- Remove supernatant after each wash.
- Air dry pellet for ± 15min.
- Add 20µl of sterile water, vortex to resuspend and incubate at 50°C for 10min to elute DNA.
- Centrifuge at 14000 g for 1min. Carefully, remove supernatant and quantify on GeneQuant spectrophotometer.

APPENDIX 10

OPTIMISATION OF PPOX EXPRESSION

Materials

Equipment

- Orbital shaker incubator (Yih der LM-510, Taiwan).
- Jouan KR 422 centrifuge (Saint Herblain , France).
- Sonicator Ultrasonic Processor XL (Heat systems Inc, Farmingdale, New York, USA).
- Beckman L 7-65 Ultracentrifuge Ti 50 Rotor (Beckman Instruments, Inc., Palo Alto. California, USA).

Reagents

- LB medium with 100μg/ml ampicillin.
- Phenyl-methyl-sulphonyl fluoride (PMSF)
  Use at 1μg/ml final concentration
- Isopropyl-1-thio-β-D-galactoside (IPTG) 1M stock solution

Procedure

Effect of temperature on expression

- Inoculate 1L of LB medium containing 100μg/ml ampicillin with 500μl of *E. coli* cells containing pHPPO-X plasmid expressing recombinant human wild type/mutant PPOX stock solution (in 30% (v/v) glycerol) in 2L flask. Mix thoroughly and aliquot 7 x 100ml of the inoculated medium.
- Incubate at 25°C with rotary shaking at 225rpm.
- Remove first aliquot after 12 h and the remainder at two hourly intervals.
- Repeat the procedure for 30°C and 37°C.
- Harvest the cells, sonicate in assay buffer (see Appendix 13.4 for assay buffer) and determine enzyme activity (see Appendix 13).
- Determine time and temperature that gives maximum activity of PPOX/mg protein.

Effect of IPTG induction on PPOX expression

- Inoculate a flask of 10 ml LB medium, containing 100μg/ml ampicillin, with 10μl of *E. coli* cells containing pHPPO-X plasmid expressing recombinant human wild type/mutant PPOX stock solution in a 50ml flask.
- Incubate overnight (±16h) at 37°C with rotary shaking (225rpm).
- Inoculate 2 x 1 L media (with 100μg/ml ampicillin) with 1 ml of the overnight culture and grow with shaking (225rpm) until OD_{600nm} is 0.5 – 0.7.
- In one flask induce expression by adding IPTG to a final concentration of 1mM (the other one serves as a control).
- Mix thoroughly and aliquot 5 x 100ml of the induced and non-induced cultures and allow to grow removing a 100ml aliquot every hour.
- Harvest the cells by centrifugation (3000g at 4°C for 30min) and discard the supernatant.
- Resuspend the cells in 5ml lysis buffer (0.02M Tris/HCl, 0.3M NaCl, 0.01M imidazole, 1% (w/v) *n*-octyl-β-D-glucopyranoside, pH 8.0) and sonicate (3 x 30s).
- Centrifuge at 100 000 g at 4°C for 30min and retain supernatant.
- Determine enzyme activity and protein concentration (see Appendices 13.4 and 14).

APPENDIX 11

NATIVE PURIFICATION OF WILD TYPE AND MUTANT PPOX BY METAL AFFINITY CHROMATOGRAPHY (TALON RESIN)

Materials

Equipment

- Talon resin (Clontech Laboratories, Palo Alto, USA).
- Orbital shaker incubator (Yih der LM-510, Taiwan)
- Ultracentrifuge Ti 50 Rotor (Beckman L7-65, Beckman Instruments, Palo Alto, Califonia, USA)
- Pump (Gilson minipuls 3) (Laboratory & Scientific, Cape Town, SA)

Reagents

- Phenyl-methyl-sulfonyl fluoride (PMSF), (100mg/ml stock solution)
- *n*-octyl-β-D-glucopyranoside (Sigma Chemical Co. St. Louis, Mo, USA)
- Lysis buffer, pH 8.0
  20mM Tris/HCl
  300mM NaCl
  10mM imidazole
  1% *n*-octyl-β-D-glucopyranoside
- Equilibration buffer, pH 8.0
  20mM Tris/HCl
  300mM NaCl
  10mM imidazole
  0.2% *n*-octyl-β-D-glucopyranoside
- Wash buffer, pH 8.0
  20mM Tris/HCl
  300mM NaCl
  20mM imidazole
  0.2% *n*-octyl-β-D-glucopyranoside

- Elution buffer, pH 8.0
  20mM Tris/HCl
  300mM NaCl
  200mM imidazole
  0.2% *n*-octyl-β-D-glucopyranoside

Procedures

Preparation of Talon column

- Invert bottle containing TALON resin to achieve a homogeneous suspension of resin in the storage solution.
- Immediately transfer 1ml of resin suspension to a 1cm diameter column (clamped in a retort stand) to give 0.5ml of resin bed volume.
- Equilibrate with 10ml equilibration buffer.
- Transfer column to 4°C cold room 30min prior to purification.

Enzyme preparation and purification

- Inoculate 1L LB media with 500µl PPOX stock solution (30% glycerol).
- Shake on orbital shaker for 18h at 30°C.
- Harvest the cells by centrifugation at 3000g for 30min.
- Resuspend the cell in cold sonication buffer.
- Sonicate in tube submerged in iced water (3 x 30s with 5min cooling between).
- Centrifuge at 100 000g at 4°C for 30min.
- Load the supernatant from 30 ml sonicate onto a pre-equilibrated Talon column (equilibration buffer) at 0.25ml/min.
- Collect the flow through for further analysis.
- Wash the column at 0.5ml/min with 10ml equilibration buffer followed by 10ml wash buffer.
- Elute the enzyme with elution buffer at 0.5ml/min.
- Collect 0.5ml fractions, analyse on SDS-PAGE, and determine enzyme activity.

APPENDIX 12

SODIUM DODECYL SULPHATE POLYACRYLAMIDE GEL ELECTROPHORESIS (SDS-PAGE) (Laemmli, 1979)

12.1 Gradient gel preparation

Materials

Equipment

- S.E. 600 vertical slab gel electrophoresis unit (Hoefer Scientific Instruments/ Pharmacia Biotech, Cambridge, UK).
- 30ml gradient mixer (Hoefer Scientific Instruments Pharmacia Biotech, Cambridge, UK)

Reagents

- *Spacer buffer,* pH 6.8
  0.125M Tris/HCl
- *"Low buffer",* pH 8.8
  1M Tris/HCl
  7.5% glycerol
- *"High buffer",* pH 8.8
  1M Tris/HCl
  30% glycerol
- *A-Bis-A solution*
  30g acrylamide
  0.8g bisacrylamide
  Add deionised water to final volume of 100ml. Filter and store in dark bottle.
- *Spacer solution*
  To a 50ml beaker add:
  1.2ml A-Bis-A solution
  8.6ml spacer buffer
  0.1ml 10% SDS.

0.1ml ammonium persulphate (150mg/ml)
0.01ml N,N,N',N'-Tetramethyl-ethelenediamine (TEMED) (immediately before pouring).
Mix well.

- *7.5% resolving solution*
  To a 50ml beaker add:
  7ml of "low buffer"
  5ml A-Bis-A solution
  0.3ml of 10% SDS
  7ml of deionised water and mix well
  0.1ml ammonium persulphate (50mg/ml)
  0.01ml TEMED (immediately before pouring)
  Mix well.

- *17.5% resolving solution*
  To a 50ml beaker add:
  7ml "high buffer"
  12ml A-Bis-A solution
  0.3ml of 10% of SDS
  0.7ml of water and mix well
  0.1ml ammonium persulphate
  0.01ml TEMED (add just before pouring)
  Mix well.

Procedure

Gradient Gel Preparation

- Ensure tap between left and right chamber of gradient mixer is closed.
- Pour 15ml of 7.5% solution into the left chamber of the gradient mixture and 15ml of 17.5% solution into right hand chamber.
- Ensure the solution in the right hand chamber is mixed continuously.
- Simultaneously, open the tap between the two chambers and turn on the pump which pumps the solution from the right hand chamber into the space between the two glass plates, mounted in the gel pouring stand.

- Stop the pump when the solution is approximately 2cm from top of the plate.
- Layer water on top of the gel and allow to set for approximately 1h.
- Once set, pour off water, add spacer solution and immediately thereafter insert comb.
- Allow to set for approximately 15min.

12.2 Preparation of Samples for SDS-PAGE (Maizel, 1971)

Materials

Reagents

- Sample Application Buffer
  20% glycerol
  0.125M Tris/HCl pH 6.8
  2% SDS
  0.002% bromophenol blue
  0.2% β-mercaptoethanol

Procedure

- Add equal volumes of sample application buffer and samples.
- Boil for 3min.

10.3 Gel Electrophoresis

Materials

Equipment

- Hamilton syringe
- PS 1200 DC power supply. (Hoefer Scientific instruments/Pharmacia Biotech, Cambridge, UK).
- Orbital shaker (Yih der LM-510, Taiwan)

Reagents

- Tank Buffer
  0.025M Tris/HCl pH 8.8
  0.2M glycine
  0.1% SDS
- Stain
  0.1% Coomassie Brilliant Blue R250 (w/v)
  30% methanol (v/v)
  10% trichloroacetic acid (v/v)
- Destain
  20% methanol (v/v)
  20% glacial Acetic acid (v/v)

Procedure

- Fill tank with buffer.
- Using Hamilton syringe introduce the samples into the sample bays.
- Run gel at constant voltage of 70V for approximately 16h or until the tracker dye has advanced to approximately 1cm from the bottom of the plates.
- Remove gel from between the plates and stain with constant shaking for 2h.
- Destain and photograph.

APPENDIX 13

PROTOPORPHYRINOGEN OXIDASE ASSAY

(Meissner et al., 1986)

13.1 Preparation of substrate (protoporphyrinogen)

Materials

Equipment

- 50ml boiling tube with stopper
- Hitachi U-1100 UV/VIS spectrophotometer (Koki Co. Ltd, Tokyo, Japan)

Reagents

- Protoporphyrin-IX (Porphyrin Products, Logan, UT. USA).
- 20% ethanol
- 10mM KOH
- 2.7N HCl

Procedure

- Dissolve 12mg protoporphyrin in 30ml freshly prepared 10mM KOH in 20% ethanol.
- Cover the flask with tin foil (to protect from light) and stir on magnetic stirrer at room temperature for approximately 1h.
- Filter 5ml protoporphyrin stock solution through a 0,45μM filter and dilute to ± 250μM in 10mM KOH.
- Place in boiling tube (covered in tin foil) with stopper.
- Determine concentration of protoporphyrin by measuring absorption of 1/100 dilution of protoporphyrin in 2.7N HCl at 408nm, using the extinction coefficient, 262.
- $[\text{Protoporphyrin}]\mu M = \frac{OD_{408nm}}{262 \times 10^5}$

13.2 Preparation of 4% Na-Hg amalgam for protoporphyrin IX reduction

Prepare the substrate protoporphyrinogen IX by reduction of protoporphyrin IX with 4% (w/v) sodium amalgam in low light. The preparation must be performed in the dark as it can readily undergo auto-oxidation.

Materials

Equipment

- Round bottomed glass flask with side arm
- Bunsen burner
- Mortar and pestle

Reagents

- 1.8g Sodium
- 43.2g mercury

Procedure

- Weigh out 1.8g of Na metal (keep under paraffin oil to prevent spontaneous combustion).
- Weigh out 43.2g of Hg in fume hood.
- Pour the mercury into round bottom flask with side arm attached to nitrogen.
- Heat flask over the Bunsen burner in the fume hood.
- When mercury is hot, add sodium (in about four pieces) piece by piece.
- A spontaneous reaction may occur, if not continue heating gently over the Bunsen burner.
- Continue heating until amalgam is completely liquid and glass sides clear.
- Pour into mortar dish and immediately chop until it solidifies into small granules.
- Grind further if necessary.

13.3 Reduction of protoporphyrin IX to protoporphyrinogen IX

Materials

Equipment

- 0.45μM biological filter (Millex-HV Millipore, Millipore Corporation, Bedford, MA, USA)
- 10ml syringe
- pH Meter (Crison Basic 20 pH-meter, Laboratory and Scientific, Cape Town, SA)
- UV light

Reagent

- 2M MOPS

Procedure

- Perform this procedure in as low light as possible.
- Add freshly prepared amalgam in approximately 3 additions to the protoporphyrin solution in the 50ml boiling tube (see Appendix 13.2).
- Stopper and shake vigorously in the dark under fume hood.
- Allow the gas to escape from time to time and check fluorescence under UV light.
- Keep on shaking until reduction is complete.
- Pour into 10ml syringe and filter slowly through 45μM filter.
- Immediately adjust pH appropriately (i.e to pH optimum of enzyme/mutant being studied) by addition of 2M MOPS drop-wise.
- Utilise immediately in assay reaction.

13.4 PPOX assay

Materials

Equipment

- Water bath (37°C) (Memmert, Laboratory and Scientific, Cape Town, SA)
- Hitachi 650-10S Fluorescence Spectrophotometer (Koki Co. Ltd, Tokyo, Japan)

Reagents

- Assay buffer
  - 100mM Tris/HCl pH 7.8/8.1
  - 1mM EDTA
  - 3mM DTT
  - 0.1% Tween 20
- Cuvette buffer
  - 100mM Tris/HCl pH 7.8/8.1
  - 1mM EDTA
  - 3mM DTT

Procedure

Calibration of fluorimeter

- Make a 1/250 dilution of the ±250µM protoporphyrin IX solution and prepare standards as below:

Cuvette buffer (µl)	1/250 dilution (µl)
800	200
600	400
400	600
200	800
0	1000

- Calibrate fluorimeter such that the highest protoporphyrin concentration read at approximately 1000 relative fluorescence units (RFU).

Preparation of assay and cuvette tubes

- Prepare cuvette tubes by adding 1ml cuvette buffer at room temperature to the appropriate number of tubes required.
- To assay tubes add 880µl assay buffer, 20µl of PPOX sample (or blank), mix and place in a water bath at 37°C.

- Prepare amalgam and substrate
- Immediately add substrate (100µl) to the assay tubes to start the reaction, and mix by vortexing.
- Incubate the reaction tubes at 37°C for 10min.
- At each time point (e.g. 10, 20, 30, 40min) transfer 100µl from assay tube to 1ml of cuvette buffer and read fluorescence.

Determination of activity (to calculate kinetic activity from RFUs)

- Use a customised spread sheet (Lotus 123).
- This subtracts the rates of auto-oxidation measured by the change in the fluorescence in the blank tubes from the rate of oxidation observed in each sample, corrects for the dilution factor and converts values to nmol/ml/h.

APPENDIX 14

PROTEIN CONCENTRATION DETERMINATION BY BIO-RAD MICROASSAY PROCEDURE

(Bradford 1976)

Materials

Equipment

- Hitachi U-3200 UV/VIS Spectrophotometer (Koki Co. Ltd, Tokyo, Japan)
- 1cm path length glass cuvettes

Reagents

- Bovine serum albumin (BSA)
- Bio-Rad dye reagent

Procedure

- Prepare triplicate of both standards and PPOX samples.
- Add appropriate dilutions of BSA standards (1 – 7μg) in deionised water (0.8ml final volume), to test tubes.
- Add appropriate dilution of protein sample (0.8ml volume) to tubes.
- Prepare blank for samples and standard by adding 0.8ml of water/appropriate dilution buffer per tube.
- Add 200μl of Bio-Rad dye reagent to all tubes and vortex carefully avoiding excessive foaming.
- Allow to stand for 10min at room temperature before reading at 595nm against appropriate blank.
- Plot BSA concentration against its absorbance at 595nm and calculate the best line fit by linear regression.
- Calculate unknown concentrations from absorbance values extrapolated from standard curve.

APPENDIX 15

ANALYSIS OF FLAVIN COFACTOR

(Cerletti and Giordano, 1971; Koziol, 1971; Faeder and Siegel, 1973)

Materials

Equipment

- Hitachi U-3200 UV/VIS Spectrophotometer (Koki Co. Ltd, Tokyo, Japan)
- Hitachi 650-10S Fluorescence Spectrophotometer (Koki Co. Ltd, Tokyo, Japan)
- Beckman L7-65 Ultracentrifuge, Ti 50 Rotor (Beckman Instrument Inc. Palo Alto, California, USA)

Reagents

- Flavin adenine dinucleotide (FAD) standard (97% purity) (Sigma Chemical Co. Louis, Mo, USA)

Procedure

Fluorimetric analysis

- To purified wild type PPOX in elution buffer (0.02M Tris/HCl, 0.3M NaCl, 0.2M imidazole, 0.2% (w/v) *n*-octyl-β-D-glucopyranoside, pH 8.0), add ice cold TCA to a final concentration of 10% (as a blank treat elution buffer in identical manner).
- Protect from light and immerse in ice water for 10min.
- Centrifuge at 105 000 g for 20min at 4°C.
- Divide supernatant in half and immediately adjust one aliquot to pH 3.5 and other to 7.4 with 2M Tris.
- Prepare appropriate dilutions of FAD standard at pH 3.5 and 7.4.
- Record the fluorescence emmision spectra of sample and standard between wavelengths 480 and 600nm at excitation wavelength of 450nm to identify the flavin.

Spectrophotometric analysis of purified PPOX and FAD

- Measure optical density of purified PPOX at wavelength of 450nm, using elution buffer as a reference solution.
- Determine the protein concentration of PPOX.
- Express the absorption at the above wavelengths per mg protein/ml.
- Record UV/VIS spectrum (250 – 550nm) of purified wild type and mutants.
- Record UV/VIS spectrum of FAD standard (10μM) and FAD extracted from purified PPOX.

APPENDIX 16

INHIBITION OF PPOX

(Corrigall et al. 1994)

16.1 Kinetic Inhibition

Materials

Equipment

- Water bath (37°C) Memmert, Laboratory and Scientific, Cape Town, SA
- Hitachi 650-10S Fluorescence Spectrophotometer (Koki Co. Ltd, Tokyo, Japan)

Reagents

- Inhibitors: Acifluorfen (AF), Acifluorfen-methyl (AFM) (Chem. Services West Chester, PA, USA)
- Biliverdin IX hydrochloride (BV) and Bilirubin IX (BR) (Porphyrin products, Logan USA)
- Solvent: Dimethylsulfoxide (DMSO) (final concentration of 2.5% was utilised as solvent for the inhibitors in all cases).

Procedures

- Perform inhibition assay as per PPOX assay (Appendix 13.4) in the following manner:

PPOX	20µl
Inhibitor	25µl
Substrate	100µl
Assay buffer	855µl
Total	1000µl

- Determine IC_{50} values for the above inhibitors by measuring PPOX activity over a range of inhibitor concentration 0-100µM at single substrate concentration of 15µM.
- Determine the kinetic constants K_i, K_s and α by performing PPOX assay at 4 different inhibitor concentrations (0 – 10µM) for 8 different substrate concentrations (0.5 – 20µM).
- Determine kinetic constants from secondary replots of K_m/V_{max} vs [I] and $1/V_{max}$ vs [I].

16.2 Determination of inhibition kinetic constants

Kinetic constants, K_i, K_s and α and model discriminations were determined from secondary replots of K_m/V_{max} vs [I] and $1/V_{max}$ vs [I] where [I] represents the inhibitor concentration.

Observed K_i was determined from the secondary replot of K_m/V_{max} vs [AF], using the equation:

$$1/K_i = \frac{\text{slope}}{\text{y- intercept}}$$

Calculated K_i was obtained by applying the relationship below, which exists for competitive inhibition between K_i, K_m, and IC_{50} at any saturating substrate concentration, S:

$$K_i = \frac{IC_{50}}{(S/K_m) + 1}$$

K_i is equivalent to that inhibitor concentration required to double the slope of the double reciprocal enzyme velocity vs substrate concentration plot. Thus the lower the K_i the more effective the inhibitor.

Observed K_s was determined from equation:

$$K_s = \frac{\text{Y-intercept of (} K_m/V_{max} \text{ vs [I])}}{\text{Y-intercept of (} 1/V_{max} \text{ vs [I]).}}$$

K_s is the dissociation constant of the enzyme-inhibitor complex.

The α value was determined from both secondary replots using equation:

$$\frac{1}{(K_i)(\alpha)} = \frac{\text{Slope}}{\text{Y-intercept of } 1/V_{max} \text{ vs [I]}}$$

where slope/Y-intercept were obtained from the plot $1/V_{max}$ vs [I].

α is the factor by which K_s changes when the inhibitor occupies the active site of the enzyme.

APPENDIX 17

EFFECT OF TEMPERATURE ON PPOX ACTIVITY AND STABILITY

17.1 Temperature induced unfolding

Materials

Equipment

- Pye-Unicam SP 1800 spectrophotometer with custom-made heating block interfaced to an IBM PC through an Oasis digital converter
- 1cm quartz cuvette

Procedure

- Add 0.5ml of the PPOX (0.15mg/ml) into the cuvette and insert it into the heating chamber.
- Close tightly and allow nitrogen gas to run through.
- Increase heating at a rate of 1°C/min, recording the absorbance value at 0.3°C from 15 – 75°C.
- Once heating is complete, cool the instrument by circulating ice-cold water, turn off the nitrogen gas, and remove the heated sample.
- Process data obtained on Microsoft excel software.
- Extract melting temperature from the melting curves using method as described by Marky and Breslauer (1987).

17.2 Effect of temperature on PPOX activity

Materials

Equipment

- Microcentrifuge tubes
- Hybaid Omnigene thermal cycler, Teddington, UK.
- Water bath (37°C) (Memmert, Laboratory and Scientific, Cape Town, SA)

Procedure

- Heat an aliquot (~200µl) of the PPOX at 90°C for 5min to use as blank.
- Aliquot 9 x 50µl of the remaining PPOX and keep one aliquot at 4°C.
- Heat each of the remaining 8 aliquots at one of the following temperatures: 30, 35, 40, 45, 50, 55, 60, and 65°C in Hybaid Omnigene Thermocycler, for 3min, then place on ice.
- Assay for PPOX activity and plot residual activity vs temperature for $T_{1/2}$ determination.

Data evaluation

Calculating transition enthalpy (ΔH)

ΔH was determined by analysing the shape of an integral curve using the following equations that assume the validity of a two-state model:

$$\Delta H = - (2 + 2n)RT_m^2 (\partial\alpha/\partial T)_{T = Tm}, \quad (1)$$

$$= - 4RT_m^2 (1/\Delta T) \text{ for } n = 1 \quad (2)$$

Where n = molecularity (number of chains),

R = gas constant.

T_m = melting temperature expressed in Kelvin.

$\partial\alpha$ = 1, for complete unfolding of PPOX.

$\partial T = \Delta T$, change in absolute temperature, expressed in Kelvin (at the transition region of melting curve).

ΔH was determined from 1/ΔT of equation (2), in the transition region. Since a small change in T_m does not cause any significant change to ΔH, the value $4RT_m^2$ was regarded as a constant.

Calculating change in entropy (ΔS) and change in free energy (ΔG)

ΔS that corresponds to ΔH was determined from equation (3):

$$\Delta S = \frac{\Delta H}{T_m} \quad (3)$$

Free energy change ΔG at T_m was calculated from ΔH_{vH}, and ΔS, and extrapolated to 25°C (for free energy of folding), and from 25°C to 70°C (for free energy of unfolding). The following equations were utilised,

$$\Delta G = \Delta H - T\Delta S \quad (4)$$

Substitution of equation (3) into equation (4) yielded the following equation (5):

$$\Delta G = -\Delta H - T(\Delta H/T_m)$$

$$= -\Delta H(1 - T/T_m) \quad (5)$$

This equation was used to calculate the change in free energy of folding and unfolding, where T can be freely chosen.

Calculating change in melting temperature (ΔT_m) and free energy for folding $\Delta(\Delta G_{25°C})$

Change in melting temperature was calculated from equations:

$$\Delta T_m = T_m^{mut} - T_m^{wt} \quad (6)$$

T_m^{mut} and T_m^{wt} = melting temperatures of mutants and wild type respectively.

Change in free energy of folding was calculated from equation:

$$\Delta(\Delta G_{25°C}) = \Delta G_{25°C}^{wt} - \Delta G_{25°C}^{mut} \quad (7)$$

$\Delta G_{25°C}^{wt}$ and $\Delta G_{25°C}^{mut}$ = change in free energy of wild type and mutants at 25°C respectively.

APPENDIX 18

CIRCULAR DICHROISM (CD) SPECTROSCOPY

(Hennessey and Johnson, 1981)

Materials

Equipment

- Jasco J-810 spectropolarimeter (Jasco Corporation, ISHIKAWA-Cho, Hachioji-Shi, Tokyo 192, Japan)
- 0.1cm path length circular quartz cuvette
- 0.1ml micro syringe

Procedure

Scanning of CD spectrum

- Calibrate the instrument by running CD spectrum of deionised water followed by buffer in which the PPOX is resuspended (0.01 M Tris-acetate, *n*-octyl-β-D-glucopyranoside pH 7.2)
- Analyse all spectra on 10 spectra accumulation to obtain an optimal signal-to-noise ratio.
- Place the 100μl sample into the cuvette and allow 10 – 15min for thermal equilibration at the desired temperature.
- Record the CD spectrum of both PPOX sample and blank buffer under identical instrumental settings.

Data evaluation

- Data are recorded on the CD instrument as the difference in absorbance of the right- and left–handed circularly polarised light ($\Delta A = A_L - A_R$) or as ellipticity (Θ) expressed in degrees.
- The differential absorbance is measured by the instrument using the equation:

$$\Delta\varepsilon = \varepsilon_L - \varepsilon_R = \frac{A_L - A_R}{(c)(d)}$$

$\Delta\varepsilon$, has units of 1(mol residues)$^{-1}$1(cm^{-1})

A_L-A_R, measure differential CD absorbance

c, is the concentration in mol/l

d, is the path length in cm.

- The molar ellipticity, [Θ] is calculated from the measured ellipticity Θ (in degrees) using the equations:

- Multiplication factor = $\frac{51\ 000}{(10)(c)(d)}$

$$[\Theta] = \frac{(\Theta)(\text{multiplication factor})}{477}$$

Where:

51 000, is the molecular weight of PPOX

c, is the concentration of the PPOX in mg/ml

d, is the path length in cm

Θ, is the measured ellipticity in degrees

10, is the conversion factor from molar concentration to the **dmol/cm^3** concentration unit.

477, is the number of amino acids of PPOX

- Analyse data using Microsoft excel.
- Analyse further using progrmme by Deléage and Roux (1987).

APPENDIX 19

UV MELTING CURVES SHOWING THE EFFECT OF ACIFLUORFEN ON T_m OF R59 MUTANT PPOXs

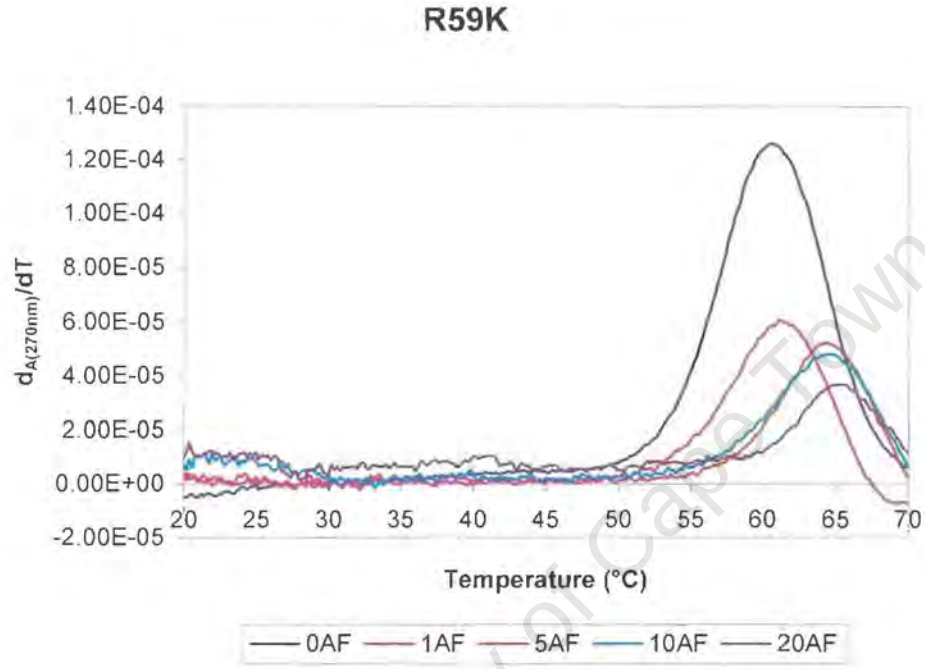

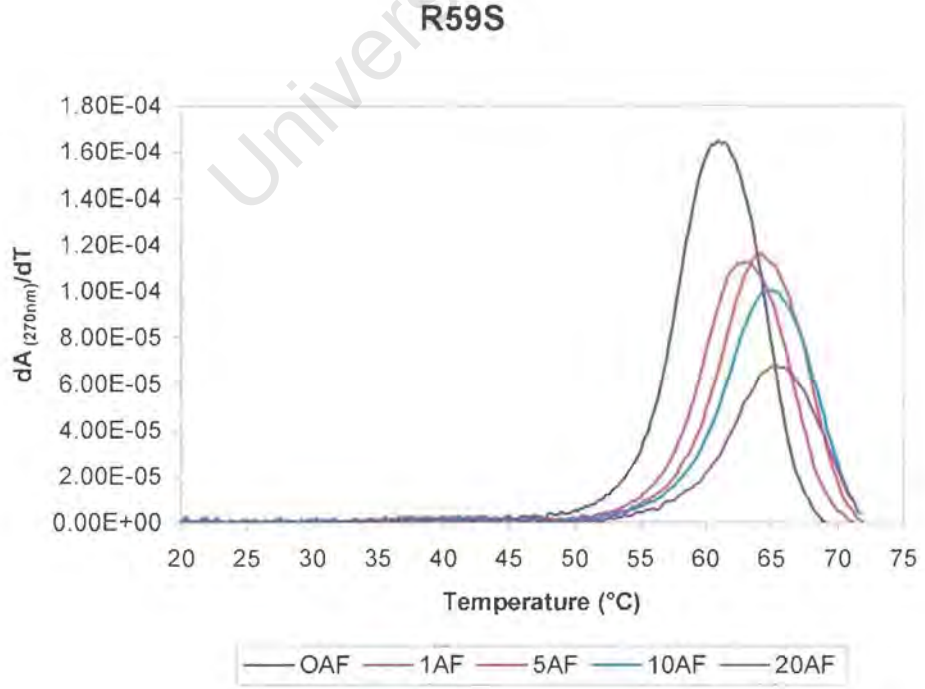

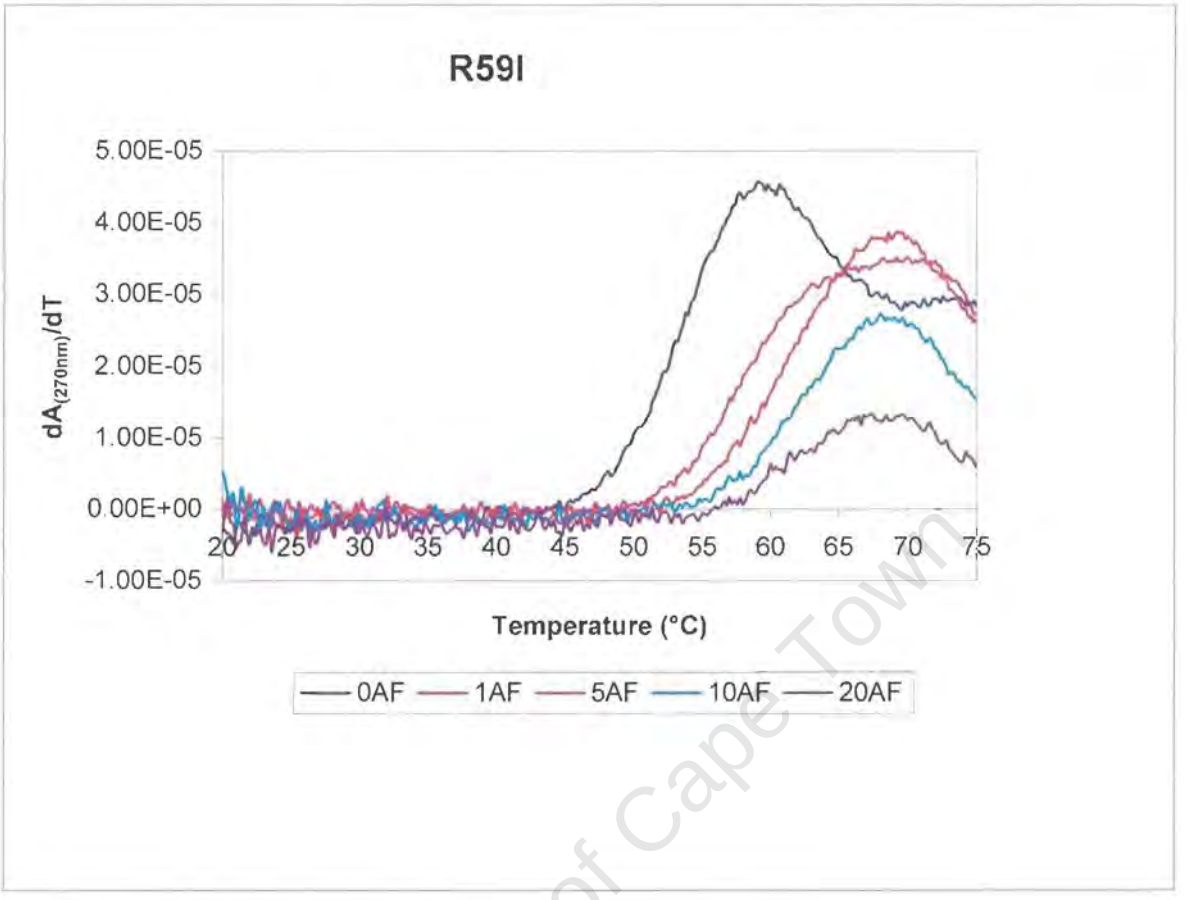

APPENDIX 20

CD SCANS OF MUTANT PPOXs

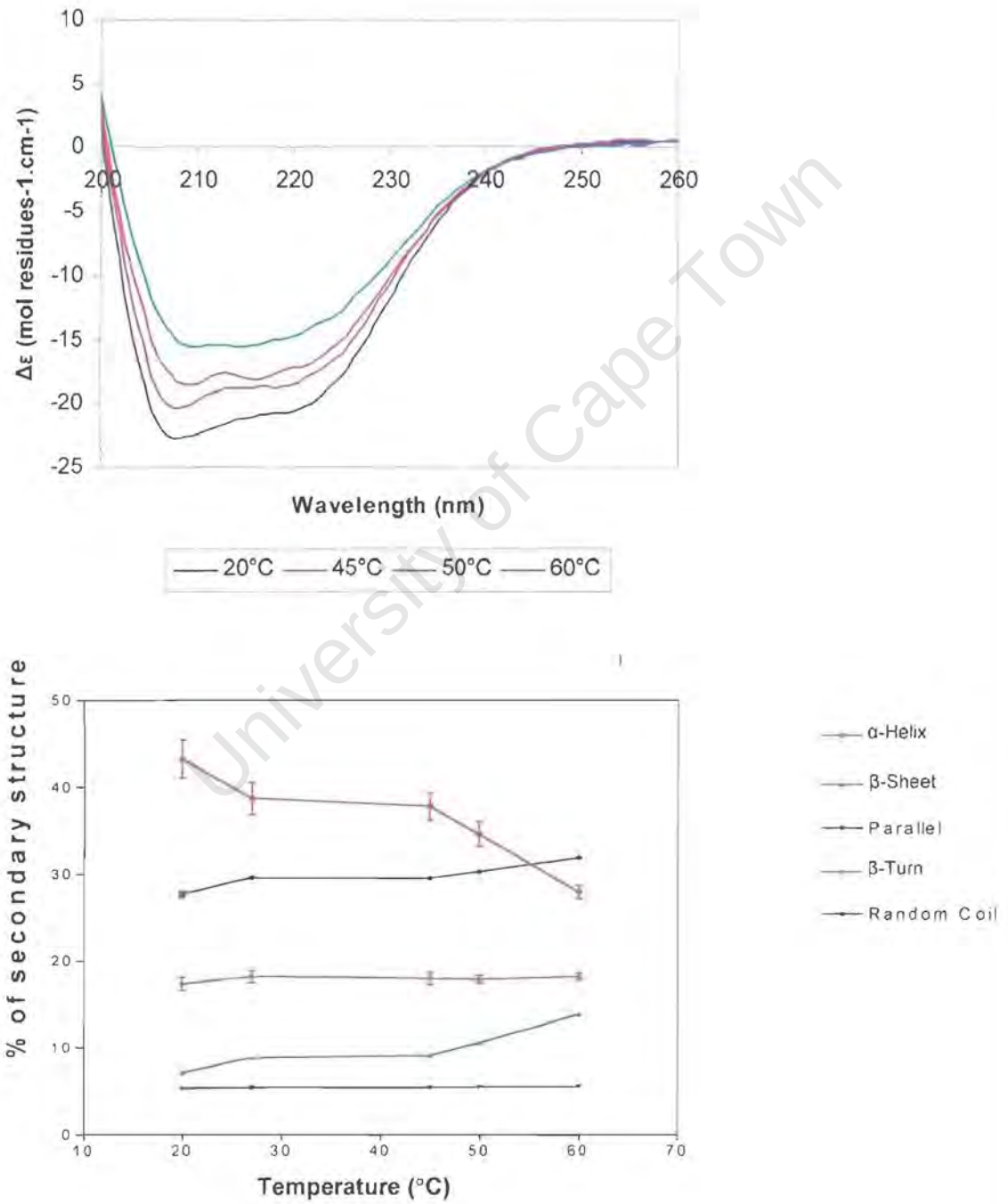

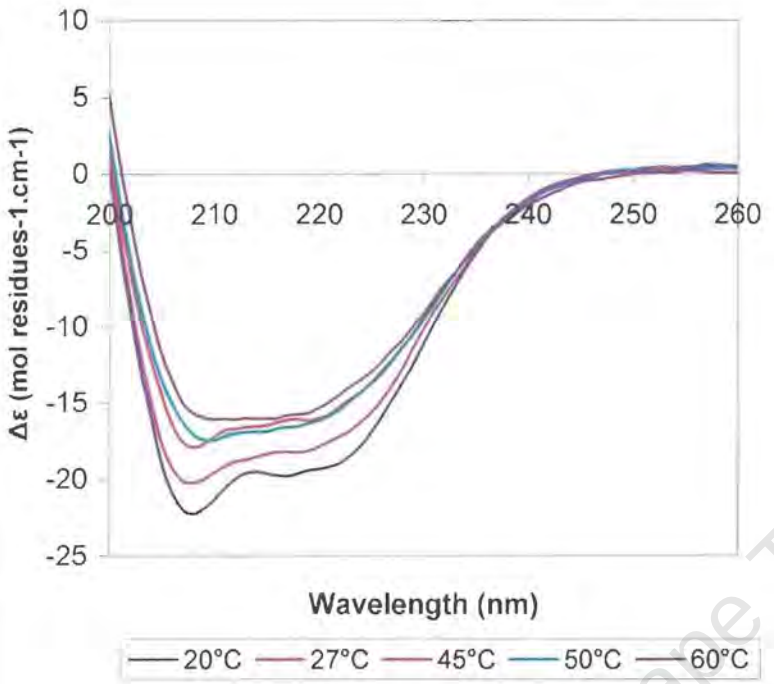

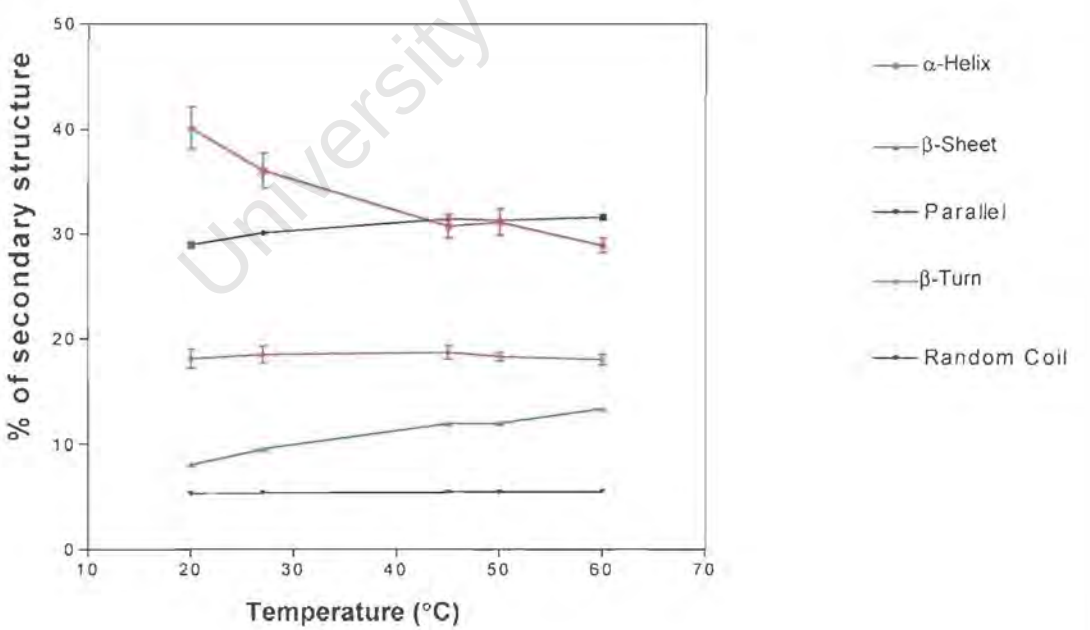

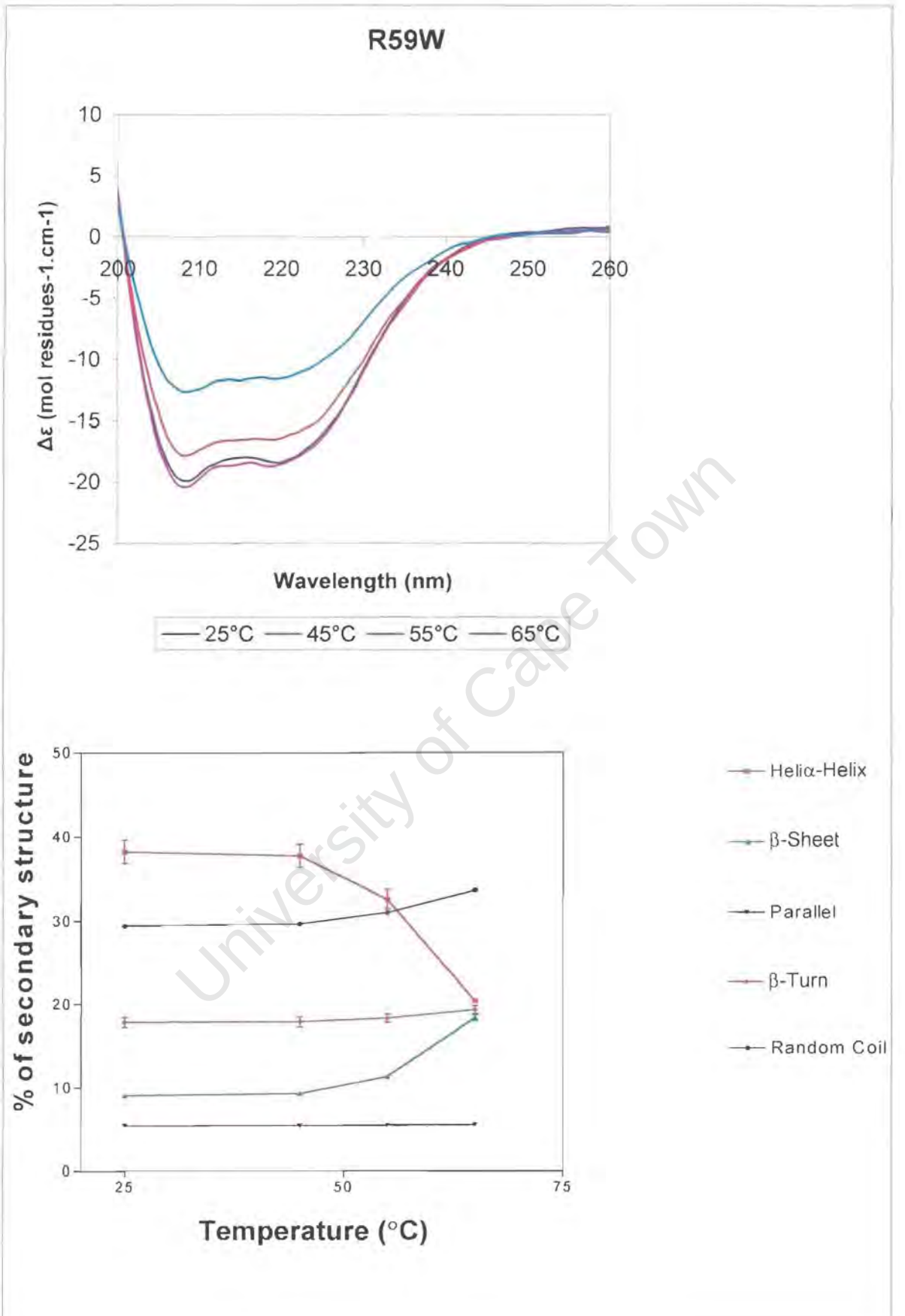

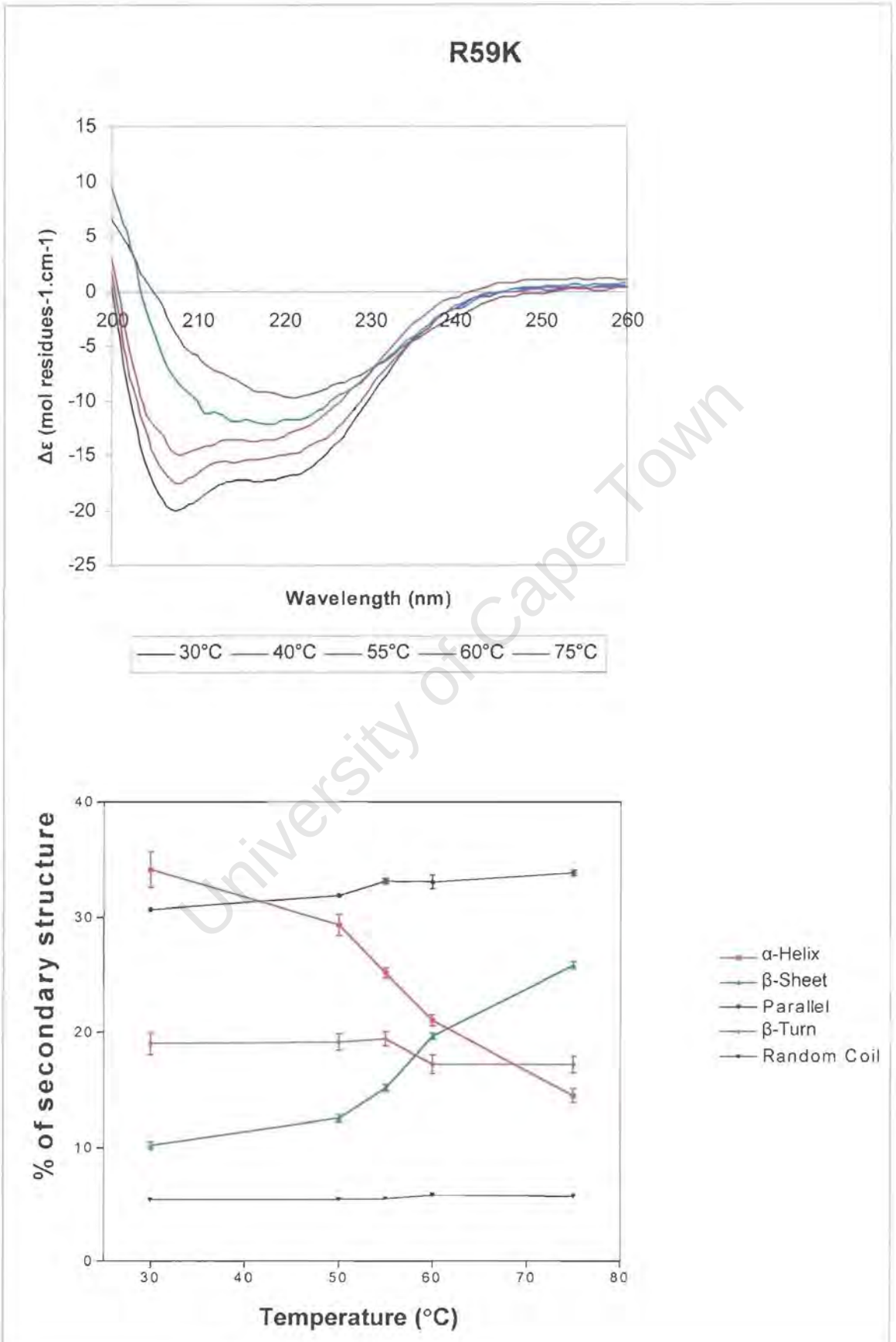

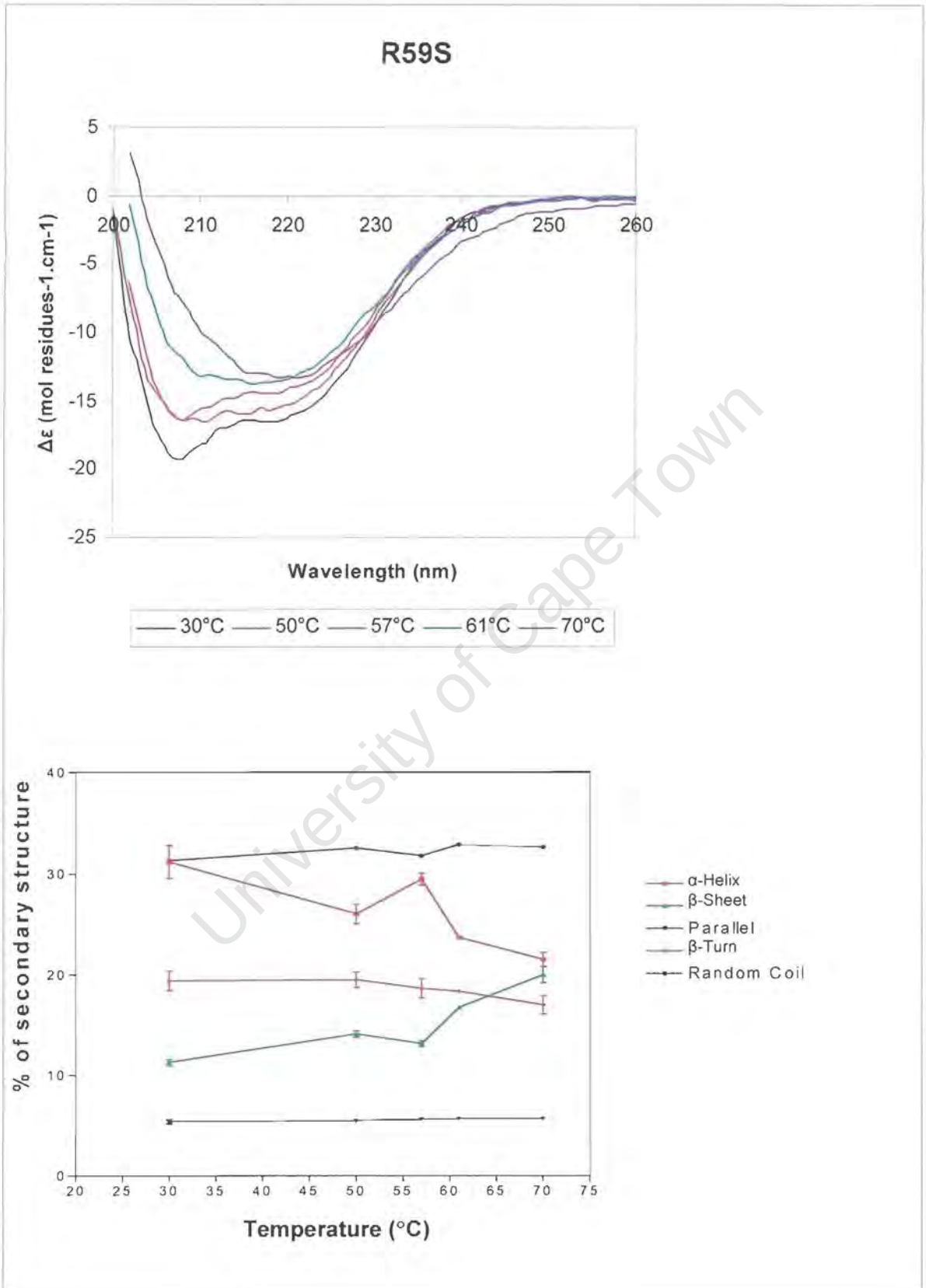

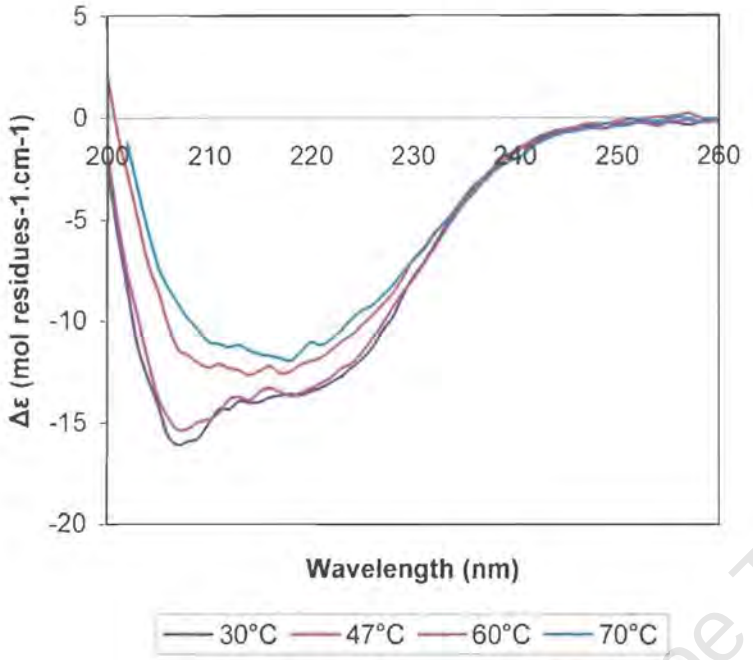

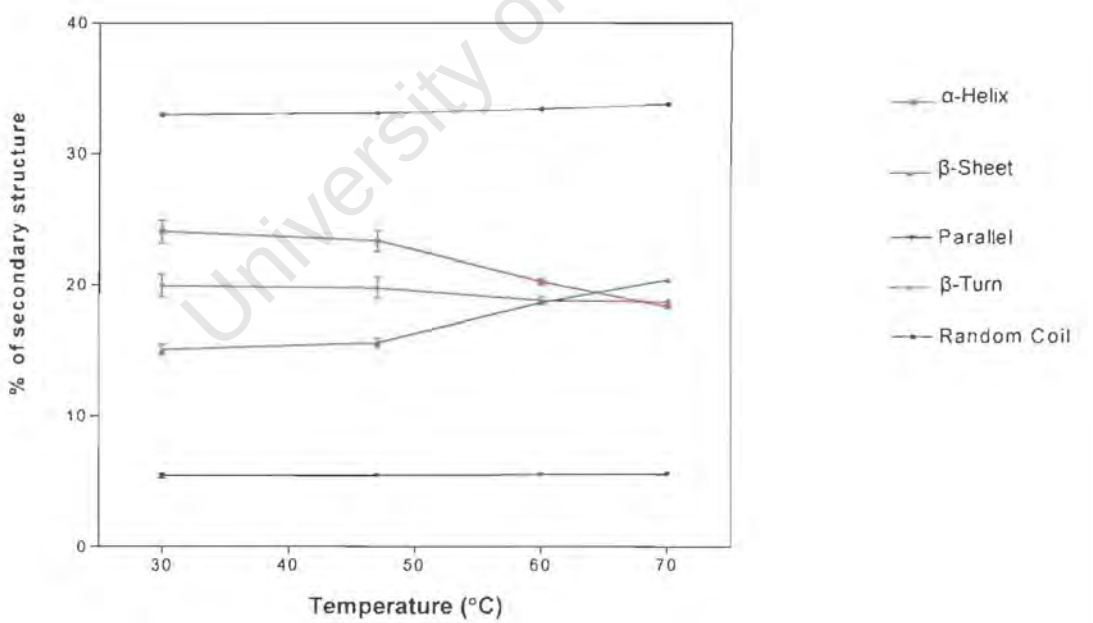

APPENDIX 21

Observed data for determination of means and standard deviations

Table 21.1: Actual data points of specific activities of wild type and mutants, from which averaged data in table 5.1 is derived.

PPOX	Specific activity (nmol//mg/min)
Wild type	7243 7274 7263 6818
Y348C	628 626 610 605
R168C	1240 1217 1314
H20P	10.33 11.46 12.16
R59W	21.37 19.87 19.00 18.67
R59K	2596 2734 2740
R59S	164.5 189.4 186.2 192.4
R59I	108.3 108.0 113.8 94.10
G9A	33.13 40.20 37.22
G11A	1.76 1.47 1.47
G14A	2956 3120 3054

Table 21.2: **Actual data points of substrate binding affinity and catalytic efficiency of wild type and mutant PPOXs, from which averaged data in table 5.2 is derived.**

PPOX	K_m (μM)	k_{cat} (s^{-1})
Wild type	0.91	5.72
	0.93	5.49
	0.91	5.96
	0.68	5.56
	0.84	6.20
	0.81	6.77
Y348C	1.07	0.52
	1.25	0.65
	1.03	0.58
	0.94	0.45
	1.08	0.50
	1.03	0.46
R168C	1.08	0.98
	0.99	1.02
	1.00	1.00
	0.92	1.07
R59W	1.32	0.036
	1.38	0.045
	1.26	0.038
	1.20	0.050
	1.13	0.051
R59K	0.91	2.58
	0.70	2.71
	0.88	2.41
R59S	1.49	0.16
	2.11	0.16
	1.60	0.17
	1.59	0.18
R59I	2.16	0.16
	2.02	0.14
	2.08	0.17
G14A	0.89	4.09
	0.82	3.73
	0.84	3.88

Table 21.3: **Actual data points of FAD absorption at 450nm for wild type and mutant PPOXs, from which averaged data in figure 5.6 is derived.**

PPOX	$OD450_{nm/mg/ml}$
Wild type	0.19
	0.19
	0.20
Y348C	0.20
	0.16
	0.17
R168C	0.33
	0.29
	0.30
R59W	0.032
	0.031
	0.30
R59K	0.29
	0.30
	0.29
R59S	0.25
	0.23
	0.24
R59I	0.33
	0.27
	0.26
G14A	0.33
	0.31
	0.30

Table 21.4: **Actual data points of IC_{50} of the wild type and mutant PPOXs, from which averaged data in table 6.1 is derived.**

PPOX	IC_{50} (μM)			
	AF	MEAF	BV	BR
Wild type	3.9 3.8 4.6 4.2 4.5	0.17 0.20 0.17 0.17	38 41 43 41	No inhibition
Y348C	75.0 65.5 70.0 64.4 75.0 73.0	59.3 53.5 54.0	2.60 3.30 2.90 3.50 3.10	30.4 30.5 37.0 39.0
R168C	39.5 46.5 51.6 48.0	1.20 1.00 1.00 1.10	0.43 0.40 0.38	No inhibition
R59W	4.00 4.20 4.80 4.00	0.16 0.25 0.20 0.20	22.0 22.5 22.0 20.0	No inhibition
R59K	3.55 3.45 3.00	ND	ND	ND
R59S	2.40 2.80 2.80	ND	ND	ND
R59I	0.88 0.91 0.89	ND	ND	ND
G14A	5.8 5.9 5.4	ND	ND	ND

ND = not determined

Table 21.5: **Actual data points of kinetic parameters (K_i, K_s and α) of wild type and mutant PPOXs for inhibitor AF, from which averaged data in table 6.3 is derived.**

PPOX	Calculated K_i (μM)	Observed K_i (μM)	Observed K_s (μM)
Wild type	0.20 0.25 0.23 0.24	0.20 0.19 0.20	0.50 0.51 0.53
Y348C	5.00 4.40 4.70 4.30 5.00 4.90	ND	ND
R168C	2.47 2.91 3.20 3.00	2.50 3.80 3.10	0.33 0.38 0.42
R59W	0.31 0.32 0.37 0.31	ND	ND
R50K	0.19 0.18 0.16	ND	ND
R59S	0.24 0.28 0.28	ND	ND
R59I	0.107 0.110 0.108	ND	ND
G14A	0.31 0.32 0.29	ND	ND

ND = not determined

Table 21.6: Actual data points of $T_{1/2}$s of wild type and mutant PPOXs, from which averaged data in table 7.1 is derived.

PPOX	$T_{1/2}$ (°C)
R59S	60.5
	60.5
	59.8
Wild type	**57.0**
	56.0
	57.0
	57.2
G14A	**55.5**
	56.5
	57.0
R59K	**57.0**
	56.0
	56.0
R59I	54.5
	54.0
	54.0
R59W	53.0
	52.0
	53.0
	54.0
Y348C	51.0
	50.0
	50.0
	50.0
R168C	46.8
	47.8
	48.2
	47.5